REPORT NO. CENC 1139
SUBJECT CATEGORY:
"ANALYTICAL REPORT"

1979-308-1

COMBUSTION ENGINEERING, INC.
NUCLEAR COMPONENTS DEPARTMENT

C.E. CONTRACT 21466

G.E. APED PURCHASE ORDER 205-B1171

ANALYTICAL REPORT
FOR
PILGRIM REACTOR VESSEL

CERTIFIED
by VENDOR
APPROVED
By DB Dewhurst
Date 3/9/71
FOR
BECHTEL CORPORATION
ATOMIC POWER ENGR. DEPT.
SAN JOSE, CALIFORNIA
ENGINEERING PLANNING
ENGINEERING SECTION

T. M. Pierson
B. W. Kinyon
G. G. Chen

9805180275 980505
PDR ADOCK 05000293
P PDR

ABSTRACT

This report contains the results of the detailed structural and thermal analyses necessary to establish the structural integrity of the Pilgrim Reactor Vessel for requirements of General Electric Specification 21A1110AB, Rev. 3, dated August 19, 1970, and compliance with rules of Section III, ASME Boiler and Pressure Vessel Code, 1965 Edition, June 30, 1966 Addenda, and Interpretations to ASME Boiler and Pressure Vessel Code, Numbers 1332-4 1335-2, 1336, and 1339-2.

PREPARED BY

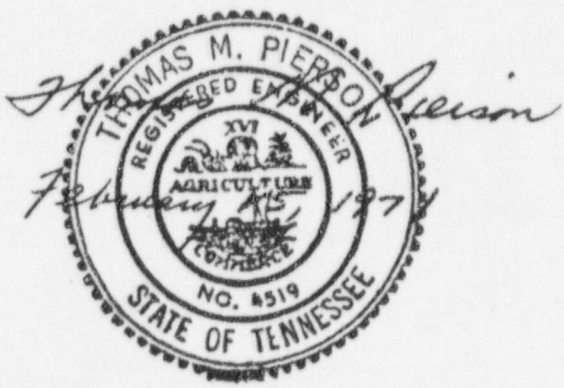
T. M. Pierson
Lead Structural Engineer

G. G. Chen
Lead Thermal Engineer

APPROVED BY

F. P. Hill, Jr.
Supervisor
Project Analytical Group

H. W. Dolfi
Supervisor
Contract Engineering Section



This document is the property of Combustion Engineering, Inc., Windsor, Connecticut, and is not to be reproduced or used to furnish any information for making of drawings or apparatus except where provided for by agreement with said Company.

ACKNOWLEDGEMENT

Structural Analysis

J. Clem
M. Goodwin
A. Fife
D. Massey
J. Bass
E. Wilson

Thermal Analysis

M. Bairagdar

Design

G. St. Cin
R. Lumpkin
D. Howard

DISTRIBUTION LIST

Ewbank/Sher/Dolfi/Alden/Halvorsen	1
F. P. Hill, Jr.	1
J. L. Pyle	1
G. E. St. Cin	1
General Electric - APED	10
Hartford Inspector	1
NCD Library	1
Met Lab Library	1

TABLE OF CONTENTS

ABSTRACT 1

1.000 INTRODUCTION 3

2.000 DESIGN CRITERIA 3

3.000 VESSEL GEOMETRY 6

4.000 SUMMARY OF DETAILED ANALYSIS 8

4.100 Closure Region 8

4.200 Vessel Shell 10

4.300 Bottom Head - Support Skirt 11

4.400 Nozzles 13

4.500 Internal Brackets 21

4.600 Shroud Support and Attachments 24

4.700 Basin Seal Skirt 27

4.800 External Attachments 28

5.000 REFERENCES 32

Appendix A - Detailed Structural Analysis

Appendix B - Detailed Thermal Analysis

Appendix C - Design Drawings

1.000 INTRODUCTION

The Pilgrim Reactor Vessel, designed and fabricated by Combustion Engineering, Inc., in accordance with General Electric APED Specification 21A1110AB, provides the pressure retaining boundary and support structure for the reactor core of a boiling water type nuclear energy steam generating system.

The vessel consists of a 224 inch I.D. cylindrical shell closed at the bottom with a hemispherical head and at the top with a bolted closure. The unit is supported by a cylindrical skirt welded to the bottom head. Openings required for system operation and control are provided throughout the length of the cylindrical shell and in both heads.

This report consists of a summary of the results of detailed structural and thermal analyses, shown in Appendices A and B, necessary to show compliance with rules of Section III, ASME Boiler and Pressure Vessel Code for a Class A vessel.

2.000 DESIGN CRITERIA

Ability of the structure, as shown by the drawings of Appendix C, to comply with the rules of Article 4, Section III, ASME Boiler and Pressure Vessel Code for stress and cyclic life shows adequacy of the structure for the required design and operating parameters defined by General Electric - APED Specification 21A1110AB.

2.100 DESIGN PARAMETERS

Design loading conditions defined by GE-APED Specification 21A1110AB include:

System Design Temperature	575°F
System Design Pressure	1250 psig
Feedwater Design Pressure	1475 psig
Recirculation Design Pressure	1370 psig
Design Pressure Drop Across Shroud	100 psig
Water Level (Normal)	520 inches
Water Level (Refueling)	958 inches
Water Weight (Normal)	506 kips
Water Weight (Refueling)	899 kips
Seismic Load Factor (Vertical)	0.06 g's
Seismic Load Factor (Horizontal)	0.40 g's
Design Life Objective	40 years

2.000 DESIGN CRITERIA

2.100 DESIGN PARAMETERS (Cont'd)

Pipe reactions are defined for the Recirculation Inlet and Outlet Nozzles, the Steam Outlet Nozzle, Feedwater Nozzle, and the Core Spray Nozzle. Since reactions for other nozzles have not been defined, they are assumed to not be significant.

2.200 OPERATING PARAMETERS

System operating transients are shown by GE Specification 21A1110AB, GE Drawing 730E941, and include the following.

Transient Condition	Occurrences
Normal Startup (100°F/Hr)	120
50% Power Operation	14,600
Rod Worth Tests	400
Loss of Feedwater Heaters	
Turbine Trip at 25% Power	10
Feedwater Heater Bypass	70
Loss of Feedwater Pumps	10
Turbine Generator Trip	40
Reactor Overpressure	1
Safety Valve Blowdown	2
All other Scrams	147
Improper Start of Cold Recirc. Loop	5
Sudden Start of Cold Recirc. Loop	5
Normal Shutdown	
100°F/hr Cooldown (546-375°F)	
Shutdown Flooding (375-330°F)	
100°F/hr Cooldown (330-100°F)	118

In addition, the vessel is expected to be subjected to 133 cycles of hydrostatic pressure tests, three of which will be at 125% of design pressure, and 130 at design pressure.

2.300 MATERIAL PARAMETERS

In accordance with Article 4, Section III, ASME Code, materials are evaluated with respect to Allowable Design Stress Intensity. Values of Design Stress Intensity (S_m) for materials used are:

2.300 MATERIAL PARAMETERS (Cont'd)

Material		S_m at 100°F	S_m at 575°F	Reference
SA 515-70	Plate	23.3 ksi	19.15 ksi	ASME III, Summer '66
SA 516-70		23.3	19.15	ASME III, Summer '66
ASTM A533 B-1		26.7	26.7	Code Case 1339-2
SA 302B		26.7	26.7	ASME III (1965)
SA 240 TP-304		20.0	15.8	ASME III (1965)
SB 168		23.3	23.3	Code Case 1336
ASTM A508-64 I	Forging	30.0	18.2	Code Case 1332-4
ASTM A508-64 II		26.7	26.7	Code Case 1332-4
SA 336 F-1		26.7	26.7	Code Case 1332-4
SA 182F304		20.0	15.8	ASME III (1965)
SB 166		23.3	23.3	Code Case 1336
SA 312 TP304	Pipe	20.0	15.8	ASME III (1965)
SB 167		23.3	23.3	Code Case 1336
ASTM A540 B23(3)	Bolting	43.3	36.3	Code Case 1335-2
SA 193 B-7		35.0	28.0	ASME III (1965)

3.000 VESSEL GEOMETRY

The Pilgrim Reacto .essel consists of a 224 inch minimum I.D. cylindrical shell closed at the bottom with a hemispherical head and at the top with a bolted closure shell.

The cylindrical shell consists of four courses of formed plates. The upper and lower courses are 6-1/2" thick and the two intermediate courses are 5-17/32" thick. The bottom head is welded to the lower shell course and is 112" minimum inner radius. The upper segment is 3-1/4" thick and the lower, or dome, segment

3.000 VESSEL GEOMETRY (Cont'd)

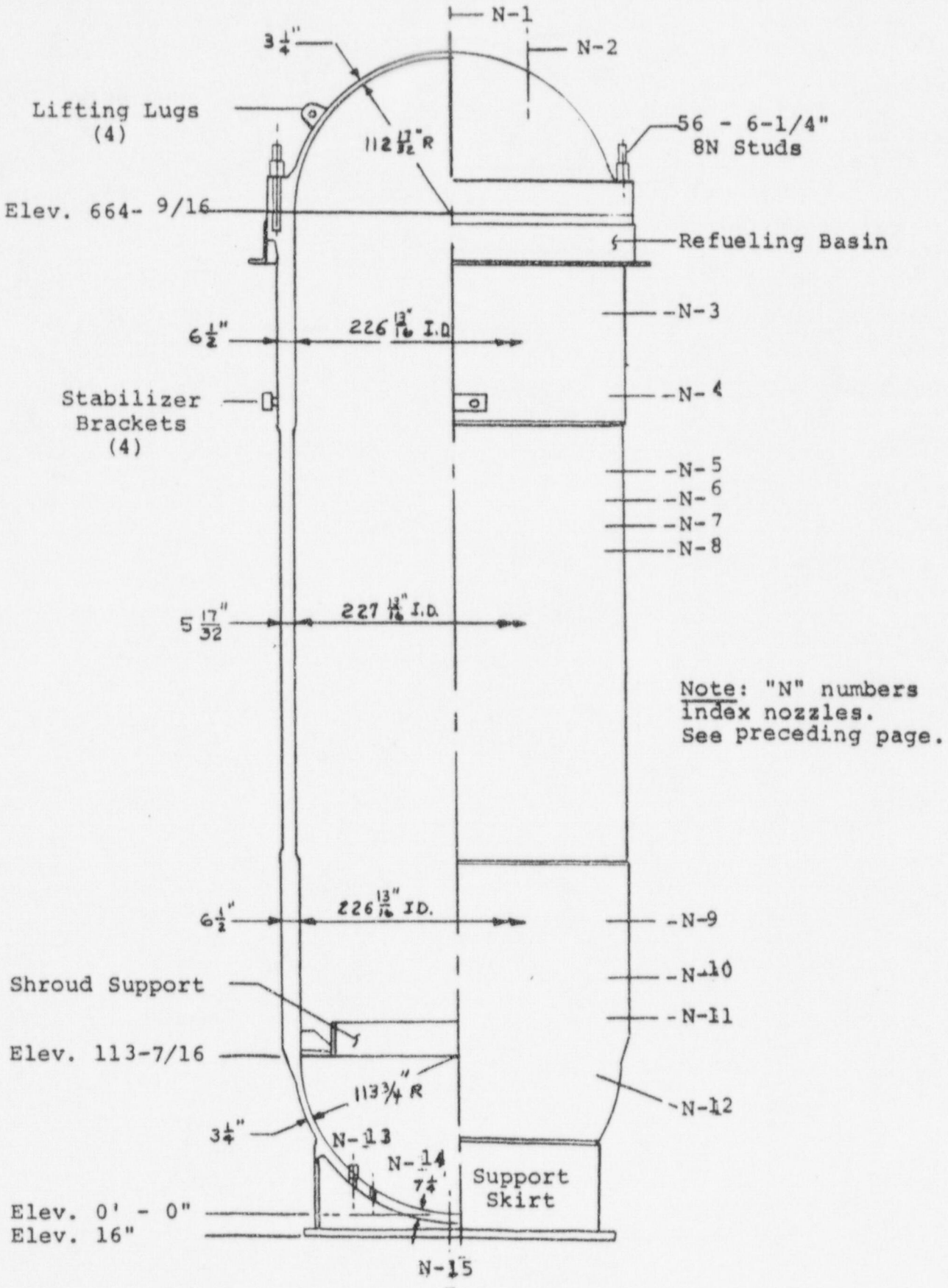
is 7-1/4" minimum thickness. The support skirt, consisting of a tapered forging and a 2 inch thick by 198 inch O.D. cylinder is welded to the transition between the bottom head segments.

The vessel flange is 250-1/2" O.D. and is drilled for fifty-six bushed studs. A 1/4 inch thick skirt is attached to the flange O.D. to support the Refueling Basin.

The closure head is 3-1/4" thick with a 250-1/2" O.D. flange at the mating edge. Holes are provided in the flange for the fifty-six (56) 6-1/4" closure studs. Two grooves are machined in the flange mating surface for the main closure O-ring seals.

Openings required for system operation, control, and instrumentation are provided along the length of the vessel and in both heads. Location and description of these openings are listed below and indexed to the drawing shown on the following page.

Index	Description	Location
N-1	1 - 4" Vent Nozzle (Flanged)	Top Head
N-2	2 - 6" Spray/Instrument Nozzles (Flanged)	Top Head
N-3	4 - 20" Steam Outlet Nozzles	604-1/2"
N-4	2 - 2" Instrument Nozzles	547"
N-5	4 - 12" Feedwater Nozzles (Liner)	468-1/4"
N-6	2 - 10" Core Spray Nozzles (Liner)	454-3/4"
N-7	1 - 3" CRD Return Nozzle (Liner)	440"
N-8	2 - 2" Instrument Nozzles	425-1/2"
N-9	10 - 12" Recirculation Inlet Nozzles (Liner)	200"
N-10	2 - 28/36" Recirculation Outlet Nozzles	145"
N-11	2 - 4" Jet Pump Instrument Nozzles	134"
N-12	1 - 2" Core ΔP Nozzle	Bottom Head
N-13	145 - 6" Control Rod Drive Nozzles	Bottom Head
N-14	42 - 2" Flux Monitor Nozzles	Bottom Head
N-15	1 - 2" Drain Nozzle	Bottom Head


N-1
N-2
3 1/4"
Lifting Lugs (4)
112 17/32" R
56 - 6-1/4" 8N Studs
Elev. 664- 9/16
Refueling Basin
N-3
6 1/2"
226 13/16" I.D.
Stabilizer Brackets (4)
N-4
N-5
N-6
N-7
N-8
5 17/32"
227 13/16" I.D.
Note: "N" numbers index nozzles. See preceding page.
6 1/2"
226 13/16" I.D.
N-9
N-10
Shroud Support
N-11
Elev. 113-7/16
113 3/4" R
N-12
3 1/4"
N-13
N-14
7 1/4"
Support Skirt
Elev. 0' - 0"
Elev. 16"
N-15

4.000 SUMMARY OF DETAILED ANALYSES

Results of detailed analyses required to comply with rules of Article 4, Section III, ASME Boiler and Pressure Vessel Code for a Class A vessel are presented on the following pages. The detailed analyses are shown in Appendix A.

4.100 CLOSURE REGION

4.110 Abstract

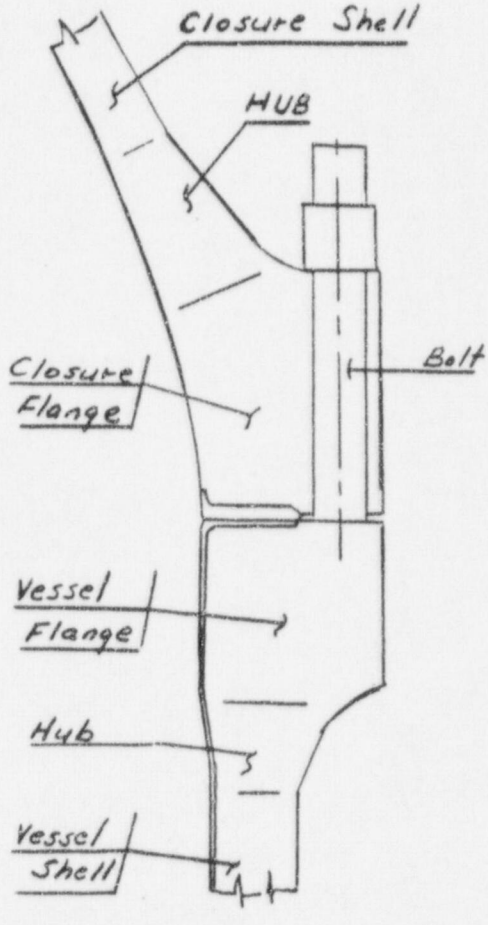
Ability of the design of the closure region to comply with rules of Article 4, Section III, ASME Code (1965 Edition with addenda through Winter 1966) is shown by calculations presented in this report.

4.120 Geometry

The structure included in the closure region consists of the vessel and closure flanges with their hubs and adjacent shell sections, the closure bolts, and the O-ring seals.

4.130 Significant Results

Ability of the vessel shell design to comply with rules of Article 4, Section III, ASME Code is shown by the detailed analysis.



Maximum primary membrane stresses calculated for the closure and vessel shells are 21.9 and 21.8 (26.7 ksi allowable), respectively. Primary local plus bending stress calculations show maximum stress intensities of 33.8 ksi at the Closure Shell-Hub junction and 29.8 ksi at the Vessel Shell-Hub junction. For both locations, the calculated stress intensity is less than the 40 ksi allowable for the material at design temperature.

4.100 CLOSURE REGION

4.130 Significant Results (Cont'd)

Primary plus secondary stress intensity ranges of 67.8 ksi at the closure shell-hub junction and 74.4 ksi at the vessel shell-hub junction are less than the 80.1 ksi allowable for the material.

Results of calculation of bolt stresses shows:

Average Design Stress	= 34.4 ksi	< 36.3 ksi	allow. at	575°F
Average Service Stress	= 59.2 ksi	< 86.6 ksi	allow. at	100°F
	= 41.2 ksi	< 73.6 ksi	allow. at	546°F
Maximum Service Stress	= 121.8 ksi	< 129.9 ksi	allow. at	100°F
	= 91.7 ksi	< 108.9 ksi	allow. at	546°F

Evaluation of cyclic life of the structure shows maximum usage factors of 0.21 in the closure shell, 0.77 in the vessel shell and 0.786 in the bolts. For each of these parts, the calculated values are less than the allowable usage factor of 1.0.

4.140 Discussion of Analysis

Although Article I-12, Section III, ASME Code does not require a minimum seal load for O-rings, a load of 1000#/inch was used in the analysis of the closure region. Continuity loads at gross changes in geometry were determined from the set of simultaneous equations obtained by equating free edge deformations of adjacent sections. Deformations of the bolt at the top of the closure flange were calculated by treating the bolt as a cantilever beam subject to an end shear and moment. A friction load is applied to the mating surface. The friction factor used is based on results of observations made during hydro test of similar vessels.

The evaluation of stresses and cyclic life of the bolts is in accordance with rules of Par. N-416, Section III, ASME Boiler and Pressure Vessel Code, except that the allowable number of load cycles is determined by the equation defined by ASME Code Case 1336. It should be noted that the required number of bolt-up operations for the bolts is 80 times even though the required cycles for the shell structure is 130.

4.200 VESSEL SHELL

4.210 Abstract

Ability of the vessel shell design to comply with rules of Article 4, Section III, ASME Code is shown by the detailed analysis.

4.220 Geometry

The vessel shell consists of four cylindrical shell courses. The upper and lower shell courses are 6-1/2" thick. The two middle courses are 5-17/32" minimum thickness. The mid-radius of the shell courses is constant for the full length of the vessel.

Stresses at attachments to the vessel shell are included in analysis of the attachments, so are not considered in this analysis.

4.230 Significant Results

The magnitude of stresses and effect on the cyclic life of the cylindrical shell sections due to mechanical loadings, operating transients, internal heat generation, and the thermal discontinuity at the water-steam interface are evaluated in this analysis. These loadings are superimposed on the structural discontinuity formed by the junction of shells of different thickness so as to give the maximum possible magnitude of stress. Rules of Article 4, Section III, ASME Code are satisfied for all categories of stress and for cyclic life of the structure.

Maximum primary membrane stress intensity is 26.3 ksi which is less than the allowable value of 26.7 ksi. Since there are no primary local or bending loads on the structure, the maximum primary stress intensity across the wall section is equal to the primary membrane stress intensity. This maximum primary membrane stress intensity is 26.3 ksi which is less than the 40.05 ksi allowable for the material.

Maximum primary plus secondary stress intensity range of 32.8 ksi is less than three times the allowable design stress intensity value of 80.1 ksi.

4.200 VESSEL SHELL

4.230 Significant Results (Cont'd)

Maximum usage factor is calculated as 0.4353 which is less than the 1.0 allowable value.

4.240 Discussion of Analysis

Analysis of the vessel shell has been conservatively simplified by assuming the maximum stresses due to gravity and seismic loads, internal heat generation, and thermal discontinuity (water-steam interface) occur at the change in wall sections. Stresses due to the gross structural discontinuity at the change in wall section are determined from solution of a continuity analysis of the structure.

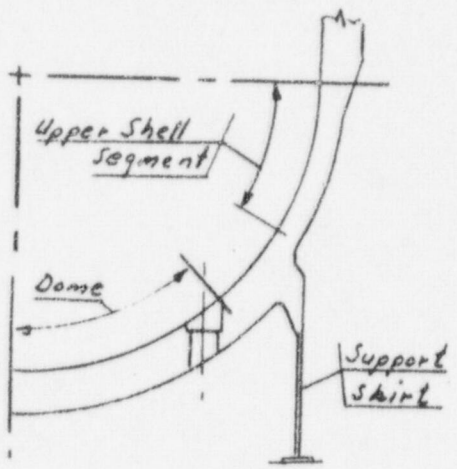
4.300 BOTTOM HEAD - SUPPORT SKIRT

4.310 Abstract

Comparison of the magnitudes of stress intensity and usage factors calculated for the structure with allowable values shows compliance with the rules of Article 4, Section III, ASME Code.

4.320 Geometry

Included in the analysis of the bottom head - support skirt region are the bottom head dome segment, upper segment, support skirt forging, and support skirt cylinder. The support skirt cylinder is assumed fixed at the base plate.



4.300 BOTTOM HEAD - SUPPORT SKIRT

4.330 Significant Results

Ability of the bottom head-support skirt structure to satisfy rules of Article 4, Section III, ASME Code is shown by the detailed analysis presented in Appendix A of this report.

Primary membrane stress intensity calculations result in maximum values of 24.8 ksi in the upper shell segment and 26.6 ksi in the dome segment. Both of these values are less than the allowable stress of 26.7 ksi. The primary membrane stress intensity of 10.3 ksi in the skirt is less than the 19.1 ksi allowable stress. Since primary local plus bending stresses are equal to primary membrane stress intensities for all parts, these stress intensities are less than the allowable values of 150% of the allowable membrane stress intensities.

Maximum values of primary plus secondary stress intensity range at each significant location are:

Upper segment at transition taper:
SI = 36.5 ksi < 80.1 ksi allow.
Dome segment at edge of penetrations:
SI = 71.9 ksi < 80.1 ksi allow.
Support skirt forging at attachment to head:
SI = 36.9 ksi < 80.1 ksi allow.
Support skirt forging at bottom of taper:
SI = 70.4 ksi < 80.1 ksi allow.
Support skirt at base plate:
SI = 54.8 ksi < 56.1 ksi allow.

Results of the cyclic life evaluation of the structure shows the following usage factors:

Upper segment at transition taper	U = 0.309 < 1.0
Dome segment at edge of penetrations	U = 0.222 < 1.0
Support skirt forging at attachment to head	U = 0.265 < 1.0
Support skirt forging at bottom of taper	U = 0.079 < 1.0
Support skirt at base plate	U = 0.079 < 1.0

4.300 BOTTOM HEAD - SUPPORT SKIRT

4.340 Discussion of Analysis

For analysis of the bottom head-support skirt region, deformations of the upper shell section, the dome segment, and the support skirt are determined by use of the Seal-Shell-2 Computer Program. These three elements are connected by a ring element at their point of intersection. Continuity loads at the junctions of each of the elements with the ring are determined by equating deformations of each of the elements with those of the ring, and solving the resulting simultaneous equations.

Particular assumptions and methods used to represent the structure as a model for the Seal-Shell solution were as follows:

1. The stiffness of the bottom head dome segment was adjusted to compensate for the penetrations by modifying the elastic moduli per equations for a flat plate with a rectangular array of holes as described in Welding Research Council Bulletin No. 80 (Reference 12).

2. The support skirt was assumed fixed at its attachment to the support plate.

Stresses in the perforated dome region were adjusted from the isotropic segment stresses obtained from the Seal-Shell Solution by applying factors from Volume 19, Journal of Applied Mechanics (Reference 13).

Stresses in the attachment region of the support skirt were calculated directly from loads obtained from the Seal-Shell Solution using classical methods.

4.400 NOZZLES

Since nozzles provided in the vessel for system operation and control have been designed in accordance with the rules of Par. N-450, Section III, ASME Code, analytical requirements for each nozzle are dependent upon the necessity of a fatigue analysis as determined by requirements of Par. N-415.1, Section III, ASME Code.

4.400 NOZZLES

The Feedwater, Core Spray, CRD Return, Recirculation Inlet, and Recirculation Outlet Nozzles are subjected to flow conditions of such severity as to require a fatigue analysis. Although the CRD Nozzles are also in this category, their geometry is so different that they are discussed separately.

Nozzles subjected to vessel coolant only, and shown by satisfaction of requirements of Par. N-415.1, Section III, ASME Code to not require a fatigue analysis include the Vent, 6" Spray/Instrument, Steam Outlet, 2" Instrument, Jet Pump Instrument, Core ΔP, In-Core Instrument, and Drain Nozzles.

4.410 Abstract

Results of analyses presented in Appendix A of this report, and summarized in Figures 4.431 and 4.432 show ability of the nozzle designs to satisfy rules of Article 4, Section III, ASME Code.

4.420 Geometry

The geometry of the nozzles can be separated into three basic design configurations. The first, designated as Type A in this report, consists of a reinforced nozzle attached to the vessel shell with a full penetration weld. A tapered transition is provided for the change from the reinforced section to the connecting pipe geometry. This nozzle configuration is used for most of the nozzles in the vessel. Variations in the basic configuration includes provisions for the thermal liners required for the Feedwater, Core Spray, CRD Hydraulic Return, and Recirculation Inlet Nozzles, and the flanged ends provided for the nozzles in the closure head.

The second design configuration, designated as Type B, consists of nozzles of uniform section attached to the vessel with a partial penetration weld. This design is used for the small instrument nozzles that are not subjected to significant pipe reactions.

The nozzles designated as Type C consists of the CRD Nozzles that are attached to the vessel with a partial penetration weld and extend into the vessel.

4.400 NOZZLES

4.430 Significant Results

Satisfaction of the rules of Article 4, Section III, ASME Code for the design of all nozzles in the vessel is shown by the detailed analyses of Appendix A.

Design of all nozzles in the vessel comply with rules of Paragraph N-450, Section III, ASME Code for opening compensation. Therefore, as provided by Par. N-451, Section III, requirements of primary stress limits are satisfied by the designs used.

Results of the detailed analysis of the Feedwater, Core Spray, CRD Hydraulic Return, Recirculation Inlet, and Recirculation Outlet nozzles as shown in Figure 4.431.

As stated in Paragraph N-451(a) Section III, ASME Code, compliance with the rules of Paragraphs N-415.1 and N-450 shows ability of nozzles to satisfy stress and cyclic life limits of Article 4 of the Code. Thus analysis of the Vent, 6" Instrument/Head Spray, Steam Outlet, 2" Instrument, Jet Pump Instrument, Core ΔP, In-Core Instrument, and Drain Nozzles is limited area reinforcement calculations and evaluation of primary stresses outside of the limits of reinforcement. Results of these calculations are shown in Figure 4.432.

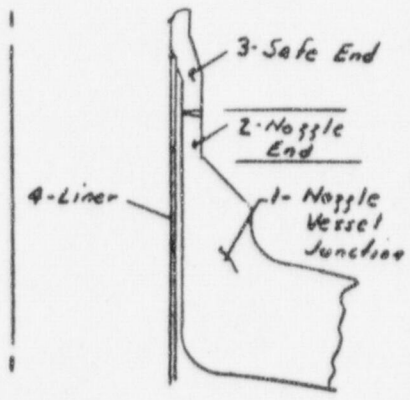
In addition to the analyses summarized in Figure 4.432, stress and cyclic life of the bolts and flanges for the Vent Nozzle and the 6" Instrument/Head Spray Nozzle were determined from a detailed analysis based on continuity requirements of the structure. Results of the analyses were:

a) Bolt Area calculation per Article I-12, Section III, ASME Code shows 2.159 in^2 required versus 7.55 in^2 available for the Vent Nozzles and 2.920 in^2 required versus 14.014 in^2 available for the Instrument/Spray Nozzle.

FIGURE 4.431

NOZZLES REQUIRING FATIGUE ANALYSIS

Opening Compensation		
Nozzle	Reinf. Area	
	Req'd.	Avail.
Feedwater	79.646	82.980
Core Spray	73.846	78.626
CRD Hyd. Return	25.698	26.374
Recirc. Inlet	72.220	82.830
Recirc. Outlet	193.08	207.38



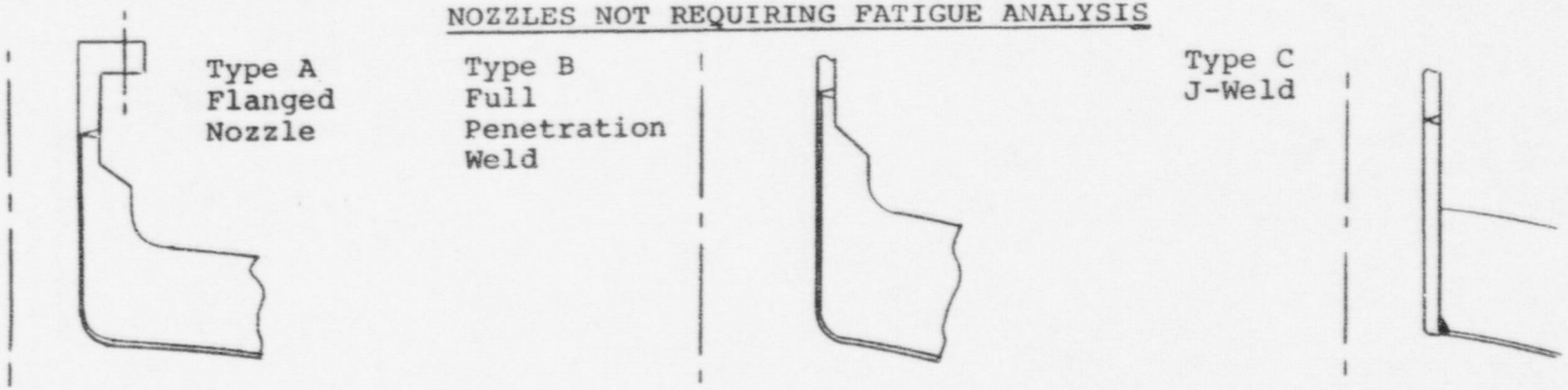
Typical Nozzle

Type A

Stress and Cyclic Life Summary							
Nozzle	Section	Primary Stress Intensity (Ksi)		P + S Stress Intensity Range (Ksi)		Usage Factor	
		Max.	Allow.	Max.	Allow.	Max.	Allow.
Feedwater	1	< 26.7	26.7	77.0	80.1	0.372	1.000
	2	12.7	26.7	37.7	80.1	0.367	1.000
	3	12.7	17.7	20.4	53.3	0.195	1.000
	4	7.6	15.8	<20.4	48.0	<0.195	1.000
Core Spray	1	< 26.7	26.7	57.5	80.1	0.377	1.00
	2	14.0	26.7	36.2	80.1	0.274	1.00
	3	14.0	15.8	36.6	48.0	0.437	1.00
	4	10.5	15.8	<36.6	48.0	<0.205	1.00
CRD Hyd. Return	1	< 26.7	26.7	66.9	80.1	0.096	1.00
	2	10.2	26.7	16.4	80.1	Neg.	1.00
	3	10.2	15.8	27.0	48.0	0.613	1.00
	4	Neg.		Neg.		0.613	1.00
Recirc. Inlet	1	< 26.7	26.7	33.1	80.1	0.281	1.00
	2	13.3	26.7	34.5	80.1	0.085	1.00
	3	13.3	15.8	34.2	48.0	0.104	1.00
	4	13.2	15.8	(Ref.	24)	0.970	1.00
Recirc Outlet	1	< 26.7	26.7	29.6	80.1	0.751	1.00
	2	13.5	26.7	33.4	80.1	0.563	1.00
	3	13.5	15.8	20.4	48.0	0.469	1.00
	4	LINER NOT REQUIRED					

FIGURE 4.432

NOZZLES NOT REQUIRING FATIGUE ANALYSIS



Primary Stress Evaluation							
Nozzle	Type	Reinforcement Area (In^2)		Primary Membrane Stress Intensity (Ksi)			
				Nozzle End		Safe End	
		Req'd.	Avail.	Max.	Allow.	Max.	Allow.
Vent	A	11.600	12.160	3.1	26.7	3.1	15.8
6" Inst./Head Spray	A	18.696	31.948	3.5	26.7	3.5	15.8
Steam Outlet	B	102.06	112.12	16.9	26.7	16.9	18.2
2" Inst. (Upper)	C	13.820	20.763	6.4	23.3	8.5	15.8
2" Inst. (Lower)	C	13.880	13.898	6.4	23.3	8.5	15.8
Isolation Condenser	B	———	———	Deleted	———	———	———
Jet Pump Inst.	B	23.429	24.367	8.0	26.7	9.6	15.8
Core ΔP	C	7.062	7.575	6.4	23.3	8.5	15.8
In-Core Inst.	C	9.147	16.707	--	--	--	--
Drain	B	4.757	12.8	2.7	18.1	--	--

4.400 NOZZLES

4.430 Significant Results (Cont'd)

b) Bolt stress and cyclic life calculations show:

Eval. Category	Vent	Inst/Spray	Allow.
Avg. Oprn. Stress (Ksi)	19.4	29.3	$2S_m = 56.0$
Max. Oprn. Stress (Ksi)	43.8	35.2	$3S_m = 84.0$
Usage Factor (U)	0.493	0.493	1.0

c) Results of analysis of flange-safe end junction were:

Eval. Category	Vent	Inst/Spray	Allow.
Primary Stress Int.(Ksi)	2.3	2.9	$S_m = 15.8$
Usage Factor	0.0268	0.0115	1.0

Analysis of the Control Rod Drive Nozzles was accomplished by an interaction solution based on continuity of deformations.

Satisfaction of primary stress requirements for the bottom head in the region of the nozzles was shown by complying with the rules for area compensation, as defined by Paragraph N-450, Section III, ASME Code. These calculations showed the available opening reinforcement area to be 35.911 in^2 which is greater than the required area of 28.566 in^2.

Maximum primary stress intensities calculated for the drive housing and stub tube were 6.0 ksi (23.3 ksi allow.) and -5.7 ksi (12.0 ksi compressive allow.), respectively. Maximum primary plus secondary stress intensity ranges were 36.4 ksi (47.4 ksi allow.) for the housing and 54.7 ksi (69.9 ksi allow.) for the stub tube.

The maximum usage factor calculated was 0.6000, which is less than the 1.0.

4.400 NOZZLES

4.440 Discussion of Analyses

The method of analysis used for the Feedwater, Core Spray, CRD Hydraulic Return, Recirculation Inlet, and Recirculation Outlet Nozzles was as follows:

1. Satisfaction of primary stress requirements for the reinforced region of each nozzle is shown by calculations verifying adequacy of opening compensation in accordance with the rules of Par. N-450, Section III, ASME Code.

2. Satisfaction of primary stress requirements for the nozzle outside of the reinforced section, the safe end, and the liner is shown by treating each of the components as a long cylinder subject to the action of design operating conditions and applicable nozzle and liner reactions.

3. Primary plus secondary and peak stresses in each nozzle were determined from detailed solutions obtained by use of the Seal-Shell-2 Computer Program (Reference 10).

4. Evaluation of primary plus secondary stresses and cyclic life for each nozzle was in accordance with requirements of Par. N-414.4 and N-415.2, Section III, ASME Code.

Use of the Seal-Shell-2 Computer Program (Reference 10) for analysis of the subject nozzles required that the nozzle structure be represented as a symmetrical model. This was accomplished by treating the vessel as a spherical shell of radius equal to 1.5 times the actual cylindrical vessel radius. Stresses obtained from the Seal-Shell solution were then adjusted for the actual cylindrical vessel loads and deformations. A detailed description of the procedure, and derivation of the adjustment factors are presented in Appendix A.

Validity of the method of detailed analysis used is shown in Appendix A where calculated stresses are compared to test data for a photo-elastic model and stresses calculated for each nozzle are compared to data for similar photo-elastic nozzle models.

4.400 NOZZLES

4.440 Discussion of Analyses (Cont'd)

Cyclic life of the Recirculation Inlet Nozzle Liner is determined by the methods defined by S. W. Tagart in Reference 24 and shown in the Nuclear Piping Code (B31.7).

Analysis of the Vent and 6" Instrument/Head Spray Nozzles considered the nozzles to be in a steam atmosphere for all operating conditions. Bolt loads and continuity loads at the flange-safe end junction were determined from an interaction analysis in which the mating flanges were assumed to be of the same geometry as the nozzle flanges. The bimetal joint was assumed to be at the nozzle end-reinforced section junction.

Stresses in the safe end of the Steam Outlet Nozzle are calculated by applying attenuation factors from Reference 3 to loads determined from the nozzle end-reinforced section junction.

Since the nozzle-safe end junctions of the 2" Instrument Nozzles consists of two cylinders of equal thickness and radius, and of approximately the same conductivity, stresses are limited to those due to different thermal expansion coefficients.

Length of the Jet Pump Instrument and Core ΔP Nozzles are sufficient to allow attenuation of continuity loads. Thus, analysis of these nozzles was accomplished by interaction solutions of two cylinders of constant thickness and radius but different elastic moduli.

Requirements for the In-Core Instrument nozzle are limited to provision of the required opening for installation of the nozzles by others. Thus, consideration of the nozzle in the analysis was limited to requirements for complying with the rules of Paragraph N-415.1, Section III, ASME Code, for cyclic life.

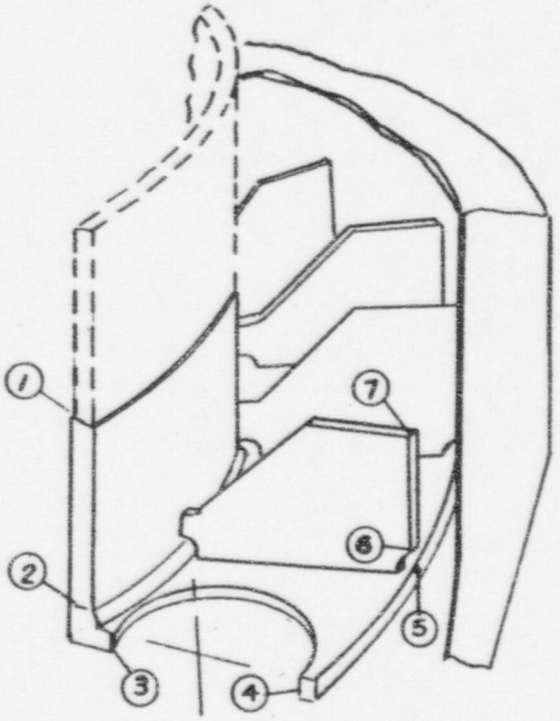
Since nozzle and piping material of the Drain Nozzle are the same, analysis of this structure was limited to evaluation of the nozzle-vessel intersection region.

FIGURE 4.630

SHROUD SUPPORT AND ATTACHMENTS

	Primary Stress Intensity				Primary Plus Secondary Stress Intensity Range (Ksi)		Usage Factor	
	Membrane (Ksi)		Local Plus Bending (Ksi)					
	Calc.	Allow	Calc.	Allow	Calc.	Allow	Calc.	Allow
1	5.7	15.8	5.0	23.7	23.3	48.0	0.374	1.0
2	> 5.0	23.3 Ksi	> 5.0	35.0 Ksi	69.9	69.9 Ksi	0.062	
3	*		3.1		Ref.24		0.160	
4	7.9		12.5		43.9		0.43	
5	*		7.8		40.5		0.330	
6	*		22.0		5.1		0.330	
7	*		22.0		28.3		0.112	

*Negligible



4.600 SHROUD SUPPORT AND ATTACHMENTS

4.640 Discussion of Analyses (Cont'd)

Cyclic life evaluation of the Shroud Support Plate at its junction with the Shroud Cylinder is accomplished by use of the method defined by S. W. Tagart in Reference 24 and shown in the Nuclear Piping Code, ASA-B31.7.

4.700 BASIN SEAL SKIRT

4.710 Abstract

Ability of the Basin Seal Skirt design to comply with rules of Article 4, Section III, ASME Code, is shown by the detailed analysis of Appendix A.

4.720 Geometry

The Basin Seal Skirt is attached to the vessel flange and furnishes the support and seal for the refueling basin. Analysis of this component includes consideration of the skirt cylinder and plate.

4.730 Significant Results

Location of maximum stresses and cyclic usage factor was calculated in the skirt cylinder at its attachment to the flange. Maximum primary stress intensities at this location were 8.2 ksi membrane (19.1 ksi allow.) and 8.2 ksi local plus bending (28.7 ksi allow.). The maximum calculated primary plus secondary stress intensity range was 52.9 ksi (58.8 ksi allow.). The resulting usage factor was 0.859 which is less than the 1.0 allowable. Rotation of the plate was determined as 0.003 degrees which is less than the 0.3 degrees allowed by specification.

4.740 Discussion of Analysis

The effect of vessel flange deformations on the basin skirt cylinder attachment was minimized by attachment of the cylinder at the flange centroid. Flange deformations were taken from Calculation S-101, "Closure Study."

4.800 EXTERNAL ATTACHMENTS

External attachments to the vessel include the Stabilizer Brackets, Insulation Brackets, and Head Lifting Lugs.

4.810 Abstract

Results of analyses, shown in Appendix A, of the Stabilizer Brackets, Insulation Brackets, and Head Lifting Lugs show stresses and cyclic life of all parts to be within limits defined by Article 4, Section III, ASME Code.

4.820 Geometry

Four equally spaced stabilizer brackets are welded to the vessel shell for resistance to horizontal seismic and jet thrust loads. Each bracket consists of a lug welded to the vessel shell and two plate sections, welded to the lug and with pin holes for attachment to supporting structure.

Two rows of brackets are attached to the vessel cylinder for support of insulation. Each bracket consists of an "L" shaped lug with the bottom leg welded to the vessel shell and a plate attached to the top of the vertical leg.

Four lugs are equally spaced around the closure head for use in handling of the closure head.

4.830 Significant Results

Ability of the Stabilizer Bracket to comply with rules of Article 4, Section III, ASME Code for stress and cyclic life were shown by the analysis. Results of the analysis were as follows:

1. Maximum primary shear stresses are 15.7 ksi in the bracket and 2.6 ksi in the vessel. Allowable is 16.0 ksi.

2. Maximum torsion stresses are 1.9 ksi in the bracket and 0.5 ksi in the vessel. Allowable is 21.4 ksi.

3. Maximum primary membrane stress intensities are 21.2 ksi for the bracket and 22.2 ksi for the vessel. Allowable value is 26.7 ksi.

4.800 EXTERNAL ATTACHMENTS

4.830 Significant Results (Cont'd)

4. Maximum primary local plus bending stress intensities are 27.4 ksi in the bracket and 27.6 ksi in the vessel. The allowable value is 40.0 ksi.

5. Maximum primary plus secondary stress intensity ranges are 27.4 ksi in the bracket and 31.1 ksi in the vessel. The allowable value is 80.1 ksi.

6. Cyclic capability of the bracket structure is shown by complying with the rules of Paragraph N-415.1, Section III, ASME Code.

Compliance with rules of Article 4, Section III, ASME Code for stress and cyclic life capability of the Insulation Brackets was shown by analysis of this region. Specific results included:

1. Maximum primary shear stresses were calculated as 1.5 ksi in the bracket (11.2 ksi allow.) and 0.1 ksi in the vessel shell (16.0 ksi allow.).

2. Maximum primary membrane stress intensities were negligible in the bracket and 24.4 ksi in the vessel shell (26.7 ksi allow.).

3. Maximum primary local plus bending stress intensities were calculated as 6.3 ksi in the bracket (28.1 ksi allow.) and 24.4 ksi in the vessel shell (40.0 ksi allow.).

4. Maximum calculated primary plus secondary stress intensity ranges were 6.3 ksi in the bracket (56.1 ksi allow.) and 24.4 ksi (80.0 ksi allow.) in the vessel shell.

5. Cyclic capability of the structure was shown by complying with rules of Paragraph N-415.1, Section III, ASME Code.

Analysis of the Head Lifting Lugs showed that the design complies with rules of Article 4, Section III, ASME Code for stress and cyclic life capability.

4.800 EXTERNAL ATTACHMENTS

4.830 Significant Results (Cont'd)

Maximum stresses were calculated as follows:

1. Maximum shear stress at the lug hole was 12.3 ksi (16.0 ksi allow.).

2. Maximum bearing stress on the lug hole was 16.4 ksi (40 ksi allows.).

3. Maximum primary membrane stress intensities were 12.3 ksi (26.7 ksi allow.) and 17.5 ksi (26.7 ksi allow.) in the lug and shell, respectively.

4. Maximum primary local plus bending stress intensities were 32.8 ksi (40.0 ksi allow.) in the lug and 23.0 ksi (40.0 ksi allow.) in the head shell.

5. Maximum primary plus secondary stress intensity ranges were 31.6 ksi (80.1 ksi allow.) and 23.0 ksi (80.0 ksi allow.) in the lug and head shell, respectively.

6. Adequacy of the structure for cyclic operation was shown by complying with rules of Paragraph N-415.1, Section III, ASME Code.

4.840 Discussion of Analysis

Analysis of the Stabilizer Brackets includes evaluation of shear tear and bearing stresses at the pin holes, primary stresses in the bracket, lug, and vessel wall, and cyclic stresses in each of the components. Stresses in the bracket and lug were determined from standard equations found in most structures text books. Stresses in the vessel wall were calculated by methods developed by P. P. Bijlaard and presented in Welding Research Council Bulletin No. 107, Reference 14.

Stresses in the Insulation Bracket plate and lug were determined from equations available in most text books on structural analysis. Stresses in the vessel shell were determined by methods developed by P. P. Bijlaard and shown

4.840 Discussion of Analyses (Cont'd)

in Welding Research Council Bulletin No. 107 (Reference 14). Half of the bracket loads were assumed to act as a concentrated load at the centerline of the outer edge of each plate.

The Head Lifting Lugs were designed for a load equal to the total head weight applied to one lug at any angle in the plane of the lug and with a maximum angle of 10° lateral to the plane of the lug. For analysis of stresses in the head, the lug was taken as an attachment of radius equal to the width of the lug plus two-thirds of the fillet welds.

5.000 REFERENCES

1. General Electric-APED Specifications 21A1110 AB, Revision 13, dated August 19, 1970.
2. "Nuclear Vessels" ASME Boiler and Pressure Vessel Code, Section III, 1965, including:
   a. Summer 1966 Addenda, dated June 30, 1966.
   b. Interpretation of ASME Boiler and Pressure Vessel Code Numbers 1332-4, 1335-1, 1336, 1339-2 and 1366.
3. Timoshenko, Theory of Plates and Shells, McGraw-Hill Book Co., New York, 1940.
4. Timoshenko, Advanced Strength of Materials, Parts I and II, D. Van Nostrand Co., New York, 1965.
5. Timoshenko, Theory of Elasticity, McGraw Hill Book Co., New York, 1951.
6. W. J. O'Donnell, "The Effect of Local Flexibilities on Stresses in a Structure," Westinghouse Report Number WAPD-X(CE)-170, March 27, 1961.
7. W. J. O'Donnell, "The Additional Deflection of a Cantilever Due to the Elasticity of the Support," ASME Paper 60-APMW-3, January 5, 1960.
8. W. J. O'Donnell, "Stresses and Deflections in Built-in Beams," ASME Paper 62WA-16, September 11, 1961.
9. Matusz, O'Donnell, and Erdlac, "Local Flexibility Coefficients for the Built-in Ends of Beams and Plates," ASME Paper Number 68-WA/PVP-6, August 1, 1968.
10. "Seal-Shell-2, A Computer Program for the Stress Analysis of a Thick Shell of Revolution with Axisymmetric Pressures, Temperatures and Distributed Loads," AEC Research and Development Report WAPD-TM-398, 1963.
11. "Tentative Structural Design Basis for Reactor Vessels and Directly Associated Components," Office of Technical Service, U. S. Department of Commerce Publication PB151987, December, 1958.
12. Mahoney, Salerno and Goldberg, "Analysis of a Perforated Circular Plate Containing a Rectangular Array of Holes," Welding Research Council Bulletin No. 80, August, 1962.
13. Horvay, "The Plane Stress Problem of Perforated Plates," Journal of Applied Mechanics, Vol. 19, September, 1952, (KAPL Report No. P769).
14. Wichman, Hopper, and Mershon, "Local Stresses in Spherical and Cylindrical Shells Due to External Loadings," Welding Research Council Bulletin No. 107, August, 1965.
15. Taylor and Lind, "Photoelastic Study of the Stresses Near Openings in Pressure Vessels," Welding Research Council Bulletin Number 113, April 1966.

5.000 REFERENCES (Cont'd)

16. Galletly, "Analysis of Discontinuity Stresses Adjacent to a Central Circular Opening of a Hemispherical Shell," Department of the Navy, David W. Taylor Model Basin Report No. 870.
17. Mahoney and Salerno, "Stress Analysis of a Circular Plate Containing a Rectangular Array of Holes," Welding Research Council Bulletin No. 106, July, 1965.
18. Roark, Formulas for Stress and Strain, McGraw-Hill Book Co., New York, 4th Ed.
19. Peterson, Stress Concentration Design Factors, John Wiley and Sons, New York, 1962.
20. Den Hartog, Advanced Strength of Materials, McGraw-Hill Book Co., New York.
21. Seely and Smith, Advanced Mechanics of Materials, John Wiley and Sons, 2nd Edition.
22. Peery, Aircraft Structures, McGraw-Hill Book Co., New York, 1950.
23. Biach, "Instruction and Maintenance Manual, 1,680,000# Tensioner," Biach Order #973.
24. Tagart, S. W., "Plastic Fatigue Analysis of Pressure Components," ASME Paper #68-PVP-3.

APPENDIX A

DETAILED STRUCTURAL ANALYSIS

APPENDIX A

DETAILED STRUCTURAL ANALYSIS

A.100 ABSTRACT A-4

A.200 DISCUSSION A-4

A.300 NOMENCLATURE A-4

A.400 REFERENCES A-5

S-101 Closure Region A-6

S-102 Vessel Shell A-100

S-103 Bottom Head/Support Skirt A-118

S-200 General Nozzle Solution A-160

S-201 Vent Nozzle A-186

S-202 6" Instrument/Head Spray Nozzle A-205

S-211 Steam Outlet Nozzle A-227

S-212 Feedwater Nozzle A-254

S-213 Core Spray Nozzle A-291

S-214 CRD Return Nozzle A-327

S-215 2" Instrument Nozzle (Upper) A-365

S-216 2" Instrument Nozzle (Lower) A-379

S-221 Recirculation Outlet Nozzle A-393

S-222 Recirculation Inlet Nozzle A-421

S-223 Jet Pump Instrument Nozzle A-472

S-231 Core ΔP Nozzle A-489

S-232 In-Core Instrument Nozzle A-503

S-233 Drain Nozzle A-511

S-234	CRD Nozzle	A-527
S-301	Stabilizer Bracket	A-597
S-302	Basin Seal Skirt	A-613
S-303	Insulation Bracket	A-639
S-304	Head Lifting Lug	A-647
S-401	Dryer Hold Down Brackets	A-655
S-402	Guide Rod Brackets	A-663
S-403	Steam Dryer Bracket	A-675
S-404	Feedwater Sparger Bracket	A-690
S-405	Core Spray Bracket	A-700
S-406	Jet Pump Support Pads	A-708
S-407	Shroud Support	A-720
S-408	Jet Pump Adapter	A-781
S-409	Surveillance Bracket	A-794

APPENDIX A

DETAILED STRUCTURAL ANALYSES

A.100 ABSTRACT

Ability of the design of the Pilgrim Reactor Vessel to satisfy requirements of Article 4, Section III, ASME Boiler and Pressure Vessel Code is shown by the detailed structural analyses presented herein.

A.200 DISCUSSION

Analysis of each of the structural components shown in the Pilgrim Reactor Vessel Design Drawings presented in Appendix C for the design and operating parameters defined by General Electric - APED Specifications is presented in this appendix.

Evaluation of the structure is accomplished by complying with the rules of Article 4, Section III, ASME Boiler and Pressure Vessel Code. Temperature data used in the calculations is taken from Appendix B.

A.300 NOMENCLATURE

Unless otherwise indicated in the specific calculation, the following nomenclature has been used.

A - Area of section (in^2)

B - Bearing load (kips or kips/inch)

D - Flexural rigidity of section (in-lbs)

E - Elastic modulus (lbs/in^2)

F - Load (kips/inch)

H - Radial shear load (kips/inch)

I - Moment of inertia of section (in^4)

M - Moment (inch-kips/inch)

N - Axial load (kips/inch)

P - Pressure (ksi)

A.300 NOMENCLATURE (Cont'd)

R - Mid-radius of section (inches)

S - Stress intensity (ksi)

V or W - Vertical load (kips)

a - Outer radius of section (inches)

e - Eccentricity (inches)

h - Height of section (inches)

l - Length of section (inches)

t - Thickness of section (inches)

α - Coefficient of thermal expansion (in/in/^{o}F)

Δ or δ - Radial deflection (in)

Δ^* or δ^* - Rotation (radians)

μ - Poisson's ratio (0.3)

σ - Normal stress (ksi)

τ - Shear stress (ksi)

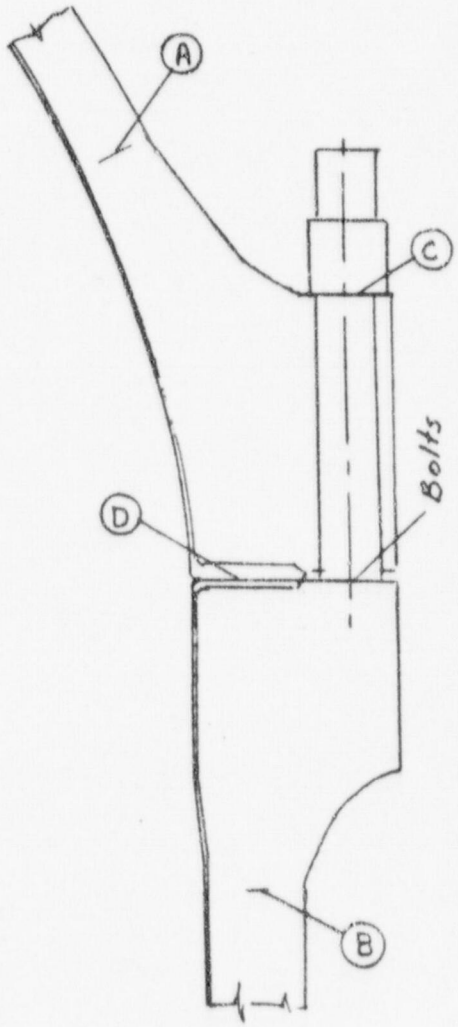
A.400 REFERENCES

References indicated in the analysis of this appendix are shown in Part 5.00 of the report.

ABSTRACT

Ability of the design of the closure region to comply with rules of Article 4, Section III, ASME Code (1965 Edition with Addenda through Summer 1966) is shown by calculations presented in this report.

The structure included in the closure region consists of the vessel and closure flanges with their hubs and adjacent shell sections, the closure bolts, and the O-ring seals. Loading conditions considered are as defined by General Electric APED Specification (Ref. 1).



SIGNIFICANT RESULTS

Stresses calculated for each significant location are listed in the summary on the following page. Maximum calculated stresses and cyclic life for the shell structure are:

Primary Membrane Stress Intensity:	21.9 ksi < 26.7 ksi allow.
Pri. + Sec. Stress Intensity Rg.:	74.4 ksi < 80.0 ksi allow.
Usage Factor:	0.77 < 1.0 allow.

For the bolts, maximum service stress and usage factor are calculated as:

Maximum Service Stress:	121.8 ksi < 129.9 ksi
Maximum Usage Factor:	0.786 < 1.0 allow.

Significant Results

Maximum stresses calculated for each significant location, as indexed in the sketch on the preceeding page, are:

Stress Category	Location	Load Condition	Stress (ksi) Calculated	Stress (ksi) Allowable	Evaluation Basis
Bearing Stress	C	Design Preload	43.6	50.0	(σ_y) base metal @ 100°F
	D		46.6		
General Primary Membrane Stress Intensity	A	Design Oprn.	21.9	26.7	Sm @ 575°F
		Code Hydro	27.4	45.0	0.9 σ_y @ 100°F
	B	Design Oprn.	21.8	26.7	Sm @ 575°F
		Code Hydro	27.3	45.0	Sm @ 100°F
Primary Local plus Bending Stress Intensity	A	Design Oprn	33.8	40.0	1.5 Sm @ 575°F
		Code Hydro	41.3	67.5	1.35 σ_{yp} @ 100°F
	B	Design Oprn	29.8	40.0	1.5 Sm @ 575°F
		Code Hydro	37.0	67.5	1.35 σ_{yp} @ 100°F
Primary plus Secondary Stress Intensity Range	A	Code Hydro → 0	67.8	80.0	3Sm @ 100°F
		Vessel O.P. → 0	59.2	80.0	3Sm @ 546°F
	B	Hydro Bolt Tensioning → 0	74.4	80.0	3Sm @ 100°F
		Startup → 0	38.4	80.0	3Sm @ 546°F
Average Design	Bolts	Design Oprn.	34.4	36.3	Sm @ 575°F
Average Service		Hydro Bolt Tensioning	59.2 ✓	86.6	2Sm @ 100°F
		End Startup	41.2 ✓	73.6	2Sm @ 546°F
Maximum Service		Hydro Bolt Preload	121.8	129.9	3Sm @ 100°F
		Shutdown Flood.	91.7	108.9	3Sm @ 546°F

Maximum calculated usage factors are:

Location	Usage Factor Calculated	Usage Factor Allowable
A	0.17	1.0
B	0.64	
Bolts	0.786	

General Discussion

Design requirements defined by GE Specifications (Ref. 1) are listed in Part A.0 of this report. Bolt sizing requirements of Article I-12, Section III, ASME Code (Ref. 2) are shown by calculations presented in Part B.0. Part C.0 includes the detailed analysis needed to show compliance of the design with stress and cyclic load requirements of Article 4, Section III, ASME Code (Ref. 2)

The methods of analysis used are discussed in detail in the introduction to Parts B.0 and C.0.

COMBUSTION ENGINEERING, INC.
ENGINEERING DEPARTMENT, CHATTANOOGA, TENN.

NUMBER S101 | CENO 59
SHEET B | A-8
CHARGE NO. 224" BWC
DATE 1-30-70 BY Piron
DESCRIPTION Closure Region
CHECK DATE 1-30-70 BY BC

A.0 Design Requirements

A.1 Design Data

Design Pressure			P	1250 #/in²
Design Temperature			T	575°F
Corrosion Allowance			C.A.	1/16"
Closure Radius (inside clad)			R_c	112.34375*
Vessel Radius (inside clad)			R_v	113.3125*
Gasket Description				5/8" x .0625" O-RINGS
Gasket Sealing Load			F_1	1000 #/in ⓐ
Gasket Seating Load			F_2	2950 #/in ⓐ
Inner Gasket Diameter			G_i	228"
Outer Gasket Diameter			G_o	231"
Material	Shells			ASTM-A 533 B(1) ⓑ
	Flanges			ASTM-A 508(2) ⓒ
	Bolting			A 540 B23(3) ⓓ ⓔ
	Gaskets			Inconel 718 - Silver ℞
	Clad			304 S.S.
Design Stress Intensity	Shells	Design Temp.	S_{so}	26700 #/in²
		Atm. Temp.	S_{sa}	26700 #/in²
	Flanges	Design Temp.	S_{fo}	26700 #/in²
		Atm. Temp.	S_{fa}	26700 #/in²
	Bolting	Design Temp.	S_b	36300 #/in²
		Atm. Temp.	S_a	43300 #/in²
Allow. Bearing Stress	Flanges	Design Temp.	S_B	42300 #/in²
		Atm. Temp.	S_A	50000 #/in²

Notes ⓐ Gasket Loads not required by Section III for o-rings. Loads F_1 & F_2 from C-E test data.

ⓑ ASME Code Case 1339-2

ⓒ ASME Code Case 1332-4

ⓓ ASME Code Case 1335-2

* Radii include maximum fabrication tolerance but do not include out-of-round allowances

ⓔ Material may be either B 23 or B-24 provided requirements of Note 1, Table 2, ASTM 1540 are satisfied.

COMBUSTION ENGINEERING, INC.
ENGINEERING DEPARTMENT, CHATTANOOGA, TENN.

CHARGE NO. 224" PWR

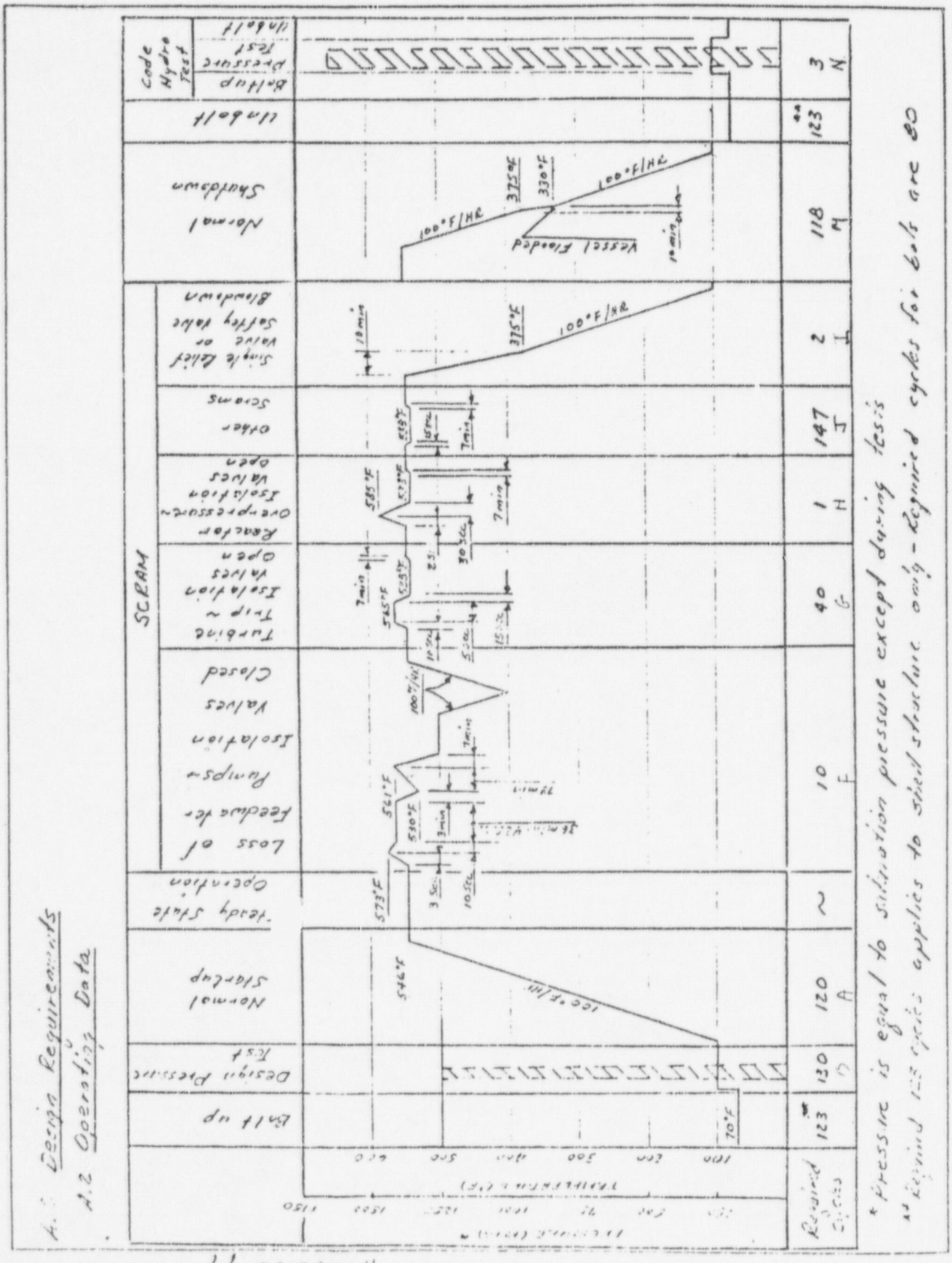
DESCRIPTION Closure Region

NUMBER S-101 | CENC 1139

SHEET 1-9

DATE 1-30-70 BY TP

CHECK DATE 1-30-70 BY EW



* Pressure is equal to saturation pressure except during tests
** Required test cycles applies to steel structure only - Expansion cycles for bolt are 80

A. Design Requirements
B. Operating Data

(2) reqd

B.0 Sizing Calculations

Per Par. N-416, Section III, ASME Code, the total bolt area required to resist internal pressure is determined by methods of Article I-12, Section III, ASME Code. Thus, using geometry and load data from Part A.1,

$G_o = 231"$
$G_i = 228"$

$P = 1250\ \#/in^2$
$F_1 = 1000\ \#/in$
$F_2 = 2950\ \#/in$

From Table I 1220(a), Section III, ASME Code (Summer '66 Addenda), for metal O-rings,

$m = y = 0$

$$\therefore \quad W_{m1} = 0.785 P G_o^2 + F_1 \pi (G_i + G_o)$$
$$= 52387 + 1442 = 53829 \text{ lbs}$$

W_{m2} = larger of $F_2 \pi (G_i + G_o) = 4254$ lbs
or $1.15\, W_{m1} = 61903$ lbs

where sealing load (W_{m2}) is arbitrarily increased 15% to allow for changes in material properties between atmosphere and design temperatures.

Required bolt area is larger of

$$(A_B)_r = \frac{W_{m1}}{S_b} = \frac{53829}{36.3} = 1482.2\ in^2$$
$$\text{or } (A_B)_r = \frac{W_{m2}}{S_a} = \frac{61903}{43.3} = 1429.6\ in^2$$

Using 56 - 6¼" BN studs with 6" shank and 1⅛" center hole gives

$$A_B = 56 \left(\frac{\pi}{4}\right)\left(6^2 - 1\tfrac{1}{8}^2\right) = 1527.7\ in^2 > (A_B)_r = 1482.2\ in^2$$

C.0 DETAILED ANALYSIS

C.1 Method of Analysis

The detailed structural analysis of the closure region is accomplished by calculation of loads and stresses in an analytical model consisting of structural elements that represent the actual geometry as closely as possible. The analytical model consists of:

1) Closure Shell and Hub - Axisymmetric Shell of Revolution as defined for use of the Seal-Shell-2 Computer Program (Ref. 10)

2) Closure Flange - Ring

3) Vessel Flange and Bolt - Ring with Beam Appendage

4) Vessel Hub and Shell - Axisymmetric Shell of Revolution as defined for use of the Seal-Shell-2 Computer Program (Ref. 10).

External loads applied to the structure include internal pressure, bolt load, seal leakage load, bearing load between the flanges, friction load between the flanges, and thermal loads resulting from temperature distributions in the structure.

Internal pressure (P) is taken as a uniform load acting on the surfaces of all parts within the pressure boundary. The pressure boundary is taken as the inner surface of the shells and flanges and the inner O-ring at the mating surface.

In addition to the bolt operating loads, use of stud tensioners for preloading requires that the bolt be elongated more than required for the preload. From tests by Biach, results of which are shown in the stud tensioner manual, (Ref. 23) the required overload is 1.33 times the required preload. Thus, the bolt tensioning load is:

$$F_{PT} = 1.33\ F_P\ ;$$

however, since the effective length, and stiffness of the idealized beam, and the distribution of the bolt end loads around the circumference are all changed, the continuity load equations derived for operating conditions are not applicable.

Therefore, for the preloading operation, it is assumed that flange deformations are not affected by end loads on the bolt, that the length of the bolt is to the spherical seat on the tensioner, and that the bolt and tensioner parts included in the assumed beam are of constant section equal to the bolt section. End loads on the bolt are then determined as direct functions of the mismatch in flange rotation.

The seal leakage load (P_o) is included to enable evaluation of the structure in the event of leakage of the inner seal. The load is applied at the midpoint and is taken as a vertical load applied at the midpoint between the O-rings and equal to the pressure load acting on the area between the O-rings, or

$$P_o = P(R_{o_2} - R_{o_1}).$$

The bearing load (B) acting between the flanges, is assumed at the mid-radius between the O-rings. This load is expressed in terms of pressure and bolt load by applying the requirement for equilibrium of vertical loads, or

$$B = (1/R_F)(FR_F - \frac{1}{2} P R_{o_1}^2) - P_o .$$

The friction load between the flanges is equal to the friction factor times the bearing load, or

$$H_B = fB .$$

The friction factor is determined from hydro test results on a similar vessel (Millstone 224" BWR) where initial flange slippage, evidenced by the loud noise common to this condition, occurred at 500 psi. Calculation of the friction factor was accomplished by requiring continuity of the flanges at the 500 psi pressure and the bolt load determined from the preload, and substitution of the resulting bolt load into the above equation.

Thermal loads in the structure were derived from the coolant temperatures defined by specifications (Ref. 1) by combining the defined operating conditions into composite conditions as follows:

a) Temperature of the structure during steady state operation is taken as equal to coolant temperature.

b) Heatup rates of 100°F/hr or less are assumed to have the same range and rate of temperature change as the normal startup condition. The temperature distribution in the structure is determined from a finite difference solution programed for the IBM 360 Computer and described in Calculation T-101. This condition is called "startup" and the required cycles are equal to the sum of the included cycles.

c) Due to lack of similarity with any other condition, the shutdown flooding condition is treated as a separate condition. Temperature distribution in the structure for this condition is determined from the finite difference solution of (b) above.

d) Cooldown rates of 100°F/hr or less are assumed to result in the same temperature distribution as occurs at the end of shutdown. This temperature distribution, obtained from the same finite difference program as (b) above, is called "shutdown," and has a required number of cycles equal to the sum of the included cycles.

e) Heatup rates of greater than 100°F/hr are assumed to be step temperature changes and are combined into a composite condition called "rapid heating." The structure is assumed to be at the minimum temperature of any of the included cycles, the surface in contact with the coolant is taken as the maximum temperature of the included conditions, and the required cycles are defined as the sum of the included cycles.

f) "Rapid cooldown" is used to define conditions with cooldown rates greater than 100°F/hr. These temperature changes are treated as step changes with the structure assumed at the maximum temperature of the included conditions, the surface in contact with the coolant at the minimum temperature of the included cycles, and the required cycles equal to the sum of the included cycles.

Geometry of the structure is defined by the design drawings. Actual dimensions used are based on the following considerations.

1) For the continuity analysis, thickness of the closure shell is taken as the machined thickness at the shell-hub junction rather than the minimum drawing dimension, thus more nearly representing the actual stiffness of part. The minimum drawing dimension is used for calculation of stresses.

2) Thickness of the vessel shell used in the continuity analysis is taken as 1/2" greater than the minimum drawing dimension so as to more accurately represent the actual stiffness of the part. This is justified by material ordering practices where plate thickness, after forming, is 1" greater than the minimum required wall section so as to allow for possible machining needed to satisfy code out-of-roundness tolerances. Since the added thickness is divided equally on each side of the wall centerline, the maximum machining cut would be 1/2" thereby leaving 1/2" added thickness except in possible local areas. Conservatism is assured by using the minimum drawing dimension for calculation of stresses.

3) Geometry of the closure and vessel hubs are obtained from full scale layouts of these sections.

4) In accordance with known thread loading patterns and with tests performed by Biach (Ref. 23), the effective length of the bolt is assumed to extend into the vessel flange and the hub a distance equal to the shank radius.

5) The bearing load at the flange mating surfaces is treated as a point load acting at the midpoint between the O-rings. Although the actual radius of the bearing load centroid changes with load changes, past attempts to include these radius changes have resulted in large increases in complexity of the analysis without significant improvement in the accuracy of the results. In evaluating this assumption, it should be noted that the difference between the assumed dimension and the radius calculated for similar vessels is very small for most operating conditions.

6) The basin seal skirt is neglected in analysis of the closure region since comparison of the seal skirt stiffness with that of the closure parts shows the effect of the skirt on flange deformations to be insignificant.

Continuity loads in the structure resulting from either self-constraint or constraint of adjacent parts are determined by equating deformations of adjacent elements. Basis of this solution are requirements for continuity of the structure at every point and equilibrium of internal and external forces. Loads required to maintain structural continuity are determined by equating edge deformations of adjacent elements when each element is treated as a free body subjected to the action of applied loads and the unknown edge, or continuity, loads.

The Seal-Shell-2 Computer Program (Ref. 10) is used to determine load-deformation relations for the element formed by the closure shell and hub. For this solution, the continuity loads, consisting of a radial shear (H_1 #/in) and moment (M_1 in-#/in) are represented by a dummy shear ($G_{RN} = 2\pi R H_1 = 10^6$#) and moment ($G_{MN} = 2\pi R\, M_1 = 10^6$ in-#) applied at the bottom edge of the element. The internal pressure load is applied as a uniform internal load ($p_1 = 10^3$ #/in^2) and a blowoff load ($G_{ZN} = p_1 \pi a^2$ #) applied at the bottom edge. Deformation coefficients for both general (axial gradient effects) and local (radial gradient effects) temperature gradients are included by entering temperatures at the surfaces, quarter points, and midpoints of each node. Influence coefficients for each load are calculated by multiplying the deformations obtained from the Seal-Shell solution by the ratio of actual load to the input load.

Deformations of the closure flange are calculated by use of standard equations (Ref. 4) for deformations of rings. Local deformations at the flange-hub junction are included as (Ref. 9)

$$EK_1 = \frac{\delta_H}{H} = f\,(R/\bar{t})(1-\mu^2)$$

$$EK_2 = \frac{\delta_M}{M} = \frac{\theta_H}{H} = 2.76\,(1-\mu-2\mu^2)/\bar{t}$$

$$EK_3 = \frac{\theta_M}{M} = 7.6\,(1-\mu^2)/(\bar{t})^2$$

where $\bar{t} = t + 0.75r$ and $f(R/\bar{t})$ is from Figure 5, Ref. 9. Although the threaded joint between the nut and bolt, and the bearing junctions between the nut and washer and the washer and flange do not conform to normal requirements for a fixed

joint, the structure is conservatively assumed fixed at this point. However, this conservatism is reduced by including the local flexibility effect for moment rotation, or

$$EK_B = \frac{I\theta}{M} = \frac{5.306\ I}{bh^2} = 9.0077\ I/d^3$$

where $Z = bh^2/6 = \pi d^3/32$; $bh^2 = 3\ d^3/16$ to convert from the rectangular section of the reference to the actual round section. Radial deflection of the flange centroid due to temperature is calculated by using the nodal block average temperature. Rotations of the flange are determined from the mean vertical temperature gradient through the centroid. Slope of the top surface of the flange is taken as that resulting from the difference in axial growth between the bearing radius and bolt radius divided by the distance between the radii.

Vessel flange deformations are calculated in the same manner as for the closure flange. Total deformations of the bolts at the top of the closure flange are obtained by adding bolt deformations to those of the flange where the bolt is treated as a beam cantilevered from the vessel flange and subjected to the action of combined axial and transverse loads. Deformation coefficients for the bolt are obtained from Table VI, page 148, Ref. 18 as follows:

1. Case 13 is used for combined tensile and shear loads.

2. Case 8 is used for combined tensile load and moment by assuming the beam length to be twice the effective bolt length and converting the compression load of the reference to a tensile load by use of relations on page 147 of the reference.

Since deformations of a beam subjected to combined axial and transverse loads are a function of the axial load, exact solution of the bolt deformations would require an iteration solution. However, evaluation of the coefficients for the range of bolt load normally expected for designs of this type shows a maximum variation of approximately 6 % from the average value, or:

F_T (assumed)	50 kips/in	70 kips/in	90 kips/in
$G_{11} = \frac{E}{F_T}(l_B - \frac{1}{k}\tanh U)$	2253.8	2140.5	2032.8
$G_{12} = \frac{E}{F_T}(\frac{\cosh U - 1}{\cosh U})$	100.71	95.299	90.275
$G_{22} = \frac{E}{F_T}(k \tanh U)$	6.2529	5.9804	5.3372

where

$$k = \sqrt{F_T/EI} \qquad U = l_B k$$

Thus, using the load required to maintain sealing at design conditions (F_T) allows direct solution of the bolt deformation relations within the accuracy of the analysis. In evaluating bolt deformations with respect to assumptions made regarding local flexibility effects and bolt load, it is interesting to compare the coefficients obtained from the equations used herein to those for a cantilever beam subjected to transverse loading only.

Loading Equations	G_{11}	G_{12}	G_{22}
Axial plus transverse	2140.5	95.299	5.9804
Axial plus transverse plus local effects	2768.8	114.13	7.1096
Transverse loading only	2628.6	118.4	7.0796

From this it can be seen that even though including axial load and local flexibility effects is more theoretically correct, accuracy of the solution is not significantly effected.

Equating edge deformations of adjacent elements gives a set of six simultaneous equations in terms of the applied loads and the unknown edge (continuity) shears and moments. For this analysis, these equations are solved by matrix algebra using the IBM 360 Computer.

In addition to the normal operating conditions considered in the preceding continuity solution, the special condition of non-uniform bolt load, and change in load path, for the bolt tensioning operation must be included. Since the added flexibility of the bolt and tensioner eliminate requirements for radial continuity between the bolt and closure flange, continuity loads in the structure are calculated by setting the shear load (H_2) and moment (M_2) at this joint equal to zero and solving the resulting two sets of two simultaneous equations. This solution conservatively assumes the tensioning load to be applied uniformly around the circumference rather than to only four bolts at a time.

In determining the loads needed for continuity of radial displacements and rotations, the bolt load is treated as an applied load. However, the bolt load actually consists of the bolt preload (F_P) and the bolt load needed to maintain vertical continuity between the top of the closure flange and the bolt (Cut II), or

$$F = F_P \left(\frac{E_{oprn}}{E_{atm}}\right) + V$$

where V is calculated by equating vertical deflections

$$EY_{22} = EY_{32}$$

Thus, the continuity bolt load is expressed as a function of the applied loads and includes deflections due to flange rotations, compression of the nut and flanges, tension of the bolt, and thermal growth of the flanges and bolts.

For the bolt tensioning operation, the load is applied directly to the bolt so the bolt continuity load is zero. Also, since the overpressure condition exceeds design pressure, separation of the flanges may occur so continuity bolt load is taken as zero for this condition.

Continuity loads at the junctions of the shells and hubs are calculated by rationing the Seal-Shell 2 Solution Output Loads at these points by the ratios of the actual applied loads to the dummy loads used in the solution. For convenience, the part of the calculated load at the closure nub edge due to the radial component of the pressure load is removed from the continuity load.

As previously noted, operating bolt load consists of the bolt preload, adjusted for temperature effects, plus the continuity bolt load, or

$$F = F_P \left(\frac{E_{oprn}}{E_{atm}}\right) + V$$

where the bolt preload is defined as the load needed to maintain sealing at design conditions. Thus, where the required seal load is F_o = 1000 #/in from CE experience, the design bolt load can be calculated directly from requirements for equilibrium of vertical forces. Then, solving for the preload where the operating bolt load is known gives the magnitude of preload for operation and hydro test. Loads applied to the bolts during tensioning are determined directly from graphs included in the tensioner instruction manual (Ref. 23). Operating bolt loads are calculated by substituting applied loads into the equation for the continuity bolt load.

Vessel stresses were calculated at the four cuts indicated in Part C.8. Minimum thicknesses were used in all cases even though the nominal dimensions indicated on CE drawings reflect the more general values at critical cuts.

Primary local + bending loads for this area are equal to General Primary loads as defined in Section III ASME Code (Ref. 2). However, stresses due to discontinuities were included to check for yielding at any point, thus guaranteeing the elastic action of the structure under Design Operation and Code Hydro Test conditions. These stresses were compared to the minimum yield point for tensile test specimens of the material.

The following stress categories are evaluated for the vessel and bolts as specified in Section III, ASME Code and customer specifications:

Vessel

1) General Primary Membrane Stress Intensity.
2) Primary Local + Bending Stress Intensity.
3) Primary + Secondary Stress Intensity Range.
4) Peak Stress Evaluation.

Bolts

1) Maximum Average Bolt Service Stress.
2) Maximum Bolt Service Stress.
3) Maximum Primary + Secondary Bolt Service Stress.
4) Peak Stress Evaluation.

Primary + Secondary + Radial Thermal Stresses are also calculated. Bearing stresses are evaluated for the washer and mating surface. O-Ring separation is calculated as required by customer specification.

Finally, a comparison is made between the above conditions and ASME Code and customer limits.

C.0 Detailed Analysis

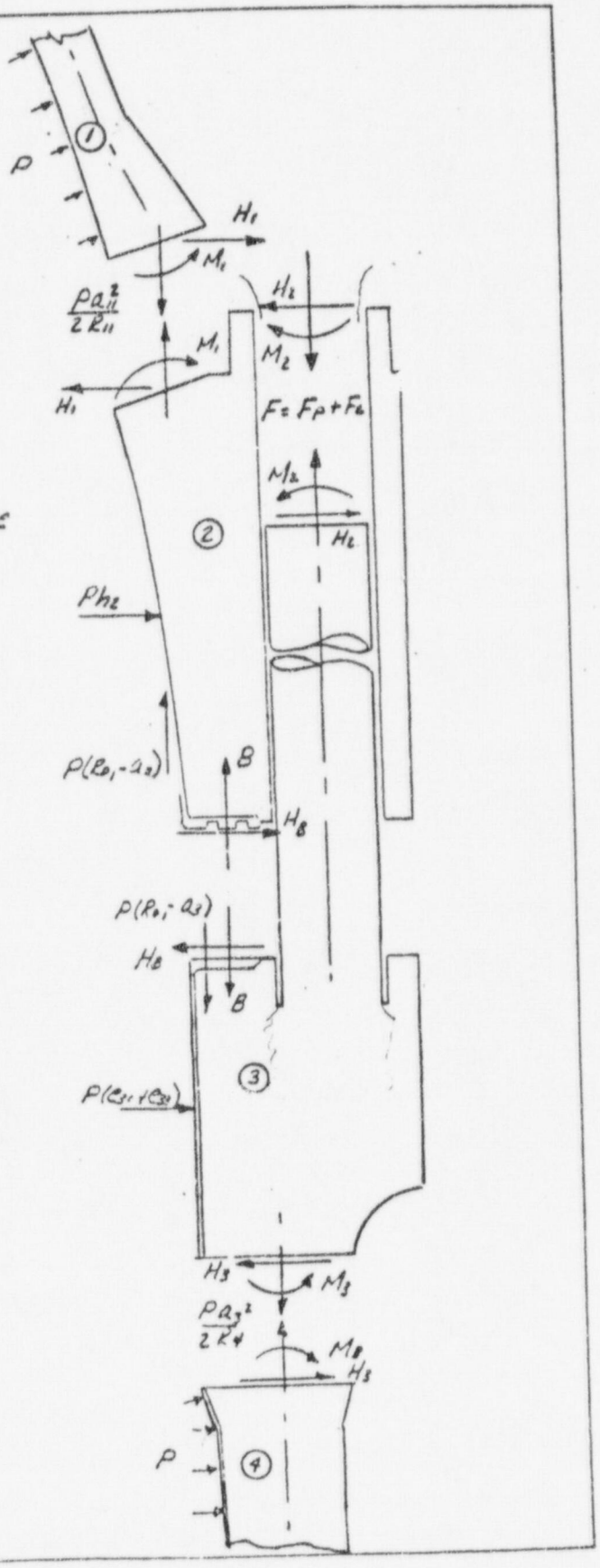
C.1 Method of Analysis

The analytical model used is shown at the right and consists of the following structural elements.

① Axisymmetric shell of revolution
② Ring
③ Ring with beam appendage
④ Axisymmetric shell of revolution

Applied loads are:
Internal pressure (P #/in²)
Bolt preload (Fp #/in)
Bearing load (B #/in)
Friction load (Hb #/in)
Thermal loads

Continuity loads include
Edge Radial Loads (H_j #/in)
Edge Moments (M_j in-#/in)
Variable Bolt Load (Fc #/in)



C.0 Detailed Analysis

C.2 Applied Loads

External loads applied to the structure are derived from the design and operating conditions defined by specifications and shown in Part A.0 of this report.

C.2.1 Design Conditions

Ambient	P = 0	T = 100°F
Design Operation	P = 1250 psi	T = 575°F

C.2.2 Operating Conditions

Data shown in Part A.2 is combined into the following composite cycles. Derivation of the cycles is shown on the next page.

Description of Composite Condition		Coolant Temperature (°F)		Coolant Pressure (psi)		Time Duration of Transient	No. of Cycles Occurrences
		$T_{initial}$	T_{final}	$P_{initial}$	P_{final}	τ (hrs)	n
Bolt Tensioning		100	100	0	0	—	246/160 *
Bolts Preloaded		100	100	0	0	—	123/80
Design Pressure Test		100	100	0	1250	—	130
Steady State Operation		546	546	1000	1000	—	—
Inner Seal Leakage		546	546	1000	1000	—	123
Start up		100	546	0	1000	4.46	323
Shutdown	Flooding	546	100	1000	0	4.18	118
	End						130
Vessel Overpressure		546→585→558		1000→1375→1000		≈ 0	1
Rapid Heating		546	573	1000	1250	0	50
Rapid Cooling		573	375	1250	185	0	219
Code Hydro Test	Bolt Tensioning	100	100	0	0	—	6 *
	Bolts Preloaded	100	100	0	0	—	3
	Pressure Test	100	100	0	1565	—	3

Note: Assumed 2 load applications on each bolt and 4 on bolt

C.0 Detailed Analysis

C.2 Applied Loads

C.2.2 Operating Conditions

Composite transients are defined by the following category:

Transient – Rate – Transient

Rapid Heating < +100°F ≡ Startup

Rapid Cooling < -100°F < Shutdown

Maximum temperature is taken as the maximum of the included transients. Minimum temperature is taken as the minimum of the included transients. Pressure range is saturation pressure difference for max. and min. temp. Required cycles are equal to the sum of cycles of included conditions.

Composite Cycle					Included Cycles						
Title	Temp. Range	Pres. Range	Transient Time	Req'd Cycles	Title		Coolant Temp. (°F) Tinitial	Tfinal	Range	Time Δ (min)	Cycles in
Startup	100°F → 546°F	0psi → 1000psi	4.46 hrs	328 cycles	Normal Startup		100	546	+446	4.46	120
					Loss of Feedflow		530	561	+31	1.22	10
							400	546	+146	1.46	10
					Turbine Trip		528	546	+8	0.117	90
					Vessel Overpressure		538	546	+8	0.117	1
					Other Scrams		538	546	+8	0.117	147
End Shutdown	546°F → 100°F	1000psi → 0psi	6.46hrs	130 cycles	Normal Shutdown	Initial Cooling	546	375	-171	1.71	118
						Flooding	375	330	-45	0.17	
						End Cooling	330	100	-230	2.30	
					Loss of Feedflow		500	400	-100	1.00	10
					Blowdown		375	100	-275	2.75	2
RAPID HEATING 546°F → 573°F		1000 → 1250psi	0	50 cycles	Loss of Feedflow		546	573	+27	(3sec.)	10
					Turbine Trip		546	565	+19	(2sec.)	40
Rapid Cooling 573°F → 375°F		1250psi → 135psi	0	219 cycles	Loss of Feedflow		573	561	-12	(10sec)	10
							561	530	-31	(3min)	10
							561	500	-61	(7min)	10
					Turbine Trip		565	538	-27	(55sec)	40
					Blowdown		546	375	-171	(40min)	2
					Other Scrams		546	538	-8	(15sec)	147

C.0 Detailed Analysis

C.2 Applied Loads

C.2.3 Load Derivations

Application of loads derived from operating data is as follows:

Pressure: Pressure from operating data is applied to pressure boundary as a load per unit area.

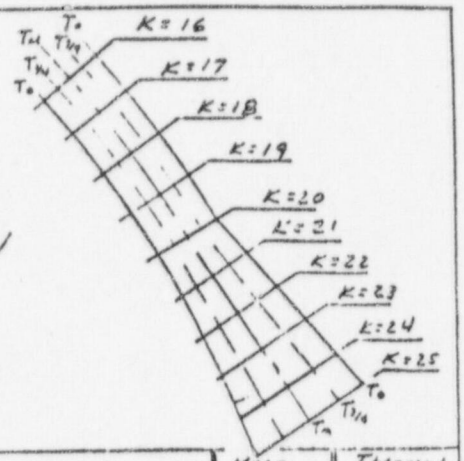
Temperature: Temperature distribution in the structure is taken as:

1. Structure assumed isothermal at ambient temperature for bolt tensioning, bolts preloaded, and design & hydro tests.
2. Structure assumed isothermal at steady state operating temperature for steady state and seal leakage conditions
3. Temperature distributions in the structure for startup, shutdown heating and end of shutdown are determined from a finite difference solution programmed for the SEAL 220 computer and described in CE Calc T-101. For the vessel and closure shells, this data is provided as temperatures at the inner surface $(T_i)_x$, quarter thickness $(T_{\frac{1}{4}})_x$, mid-surface $(T_m)_x$, three quarter thickness $(T_{\frac{3}{4}})_x$, and outer surface $(T_o)_x$ for each node (x) as required for the Seal-Shell-2 computer program (Ref. 10). In addition, mean temperature $(\bar{T})_x$ and thermal moment $(MT)_x$ are determined. For the flanges, data is expressed as mean temperature (T_j), average slope (m_j), and mean axial temperatures from the C.G. to the top and bottom surfaces $(\bar{T}_{\bar{U}})$.
4. For rapid heating, rapid cooling, and vessel overpressure conditions, structure is assumed isothermal at the initial temperature but with the surfaces in contact with the coolant at final coolant temperature.

Resulting temperature data is shown on the following pages.

C.0 Detailed Analysis
C.2 Applied Loads
C.2.3 Load Derivations

Temperature data for the closure shell and hub is as follows:



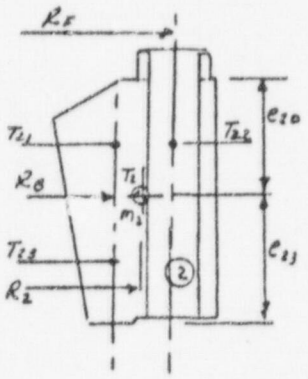
Condition	Node (K)	Temperature (°F) $(T_c)_K$	$(T_{H})_K$	$(T_m)_K$	$(T_{1/4})_K$	$(T_o)_K$	Mean Temp. $(T_H)_K$	Thermal Moment $(M_T)_K$
Ambient: Bolt Tensioning; Bolts Preloaded; Design Pressure Test; Hydro Test: Bolt Tensioning; Bolts Preloaded; Pressure Test	0→25	100°F					100°F	0
Design Condition	0→25	575°F					575°F	0
Steam Flow Cond. Inner Seal Leakage	0→25	546°F					546°F	0
Start up (4.46 hrs)	0→19	542.5	539.0	534.5	533.5	532.0	536.1	Not required for Sol 1 Shell Sol 2 Hub
	20	541.8	536.6	531.4	530.1	528.8	533.4	
	23	539.3	527.8	516.2	512.5	508.8	520.1	
	25	535.3	503.6	480.7	457.3	409.6	478.5	
Shutdown Flooding (1.81 hr.)	0→19	461.0	463.9	467.7	468.5	469.3	466.3	
	20	466.2	470.0	473.7	474.6	475.5	472.3	
	23	476.1	481.3	486.5	488.0	489.4	484.6	
	25	485.6	495.3	501.8	507.8	517.0	501.6	
End of Shutdown (4.98 hrs)	0→19	103.1	106.6	111.1	112.1	113.1	109.5	
	20	103.8	109.1	114.4	115.7	117.1	112.4	
	23	106.5	118.7	130.8	134.7	138.6	126.7	
	25	111.0	145.0	164.7	195.2	246.6	172.2	
Rapid Heating	0→25	573F	546F				546F	0
Rapid Cooling	0→25	375°F	573°F				573°F	0
Vessel Overpressure	0→25	585°F	546°F				546°F	0

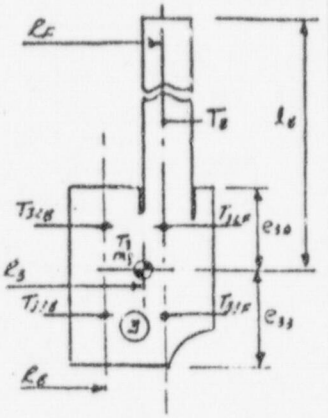
C.0 Detailed Analysis

C.2 Applied Loads

C.2.3 Load Derivations

Temperature data for the flanges is as follows:





Element	Index	Ambient: Bolt Tensioning	Ambient: Joint Preloaded	Ambient: Design Pressure Test	Ambient: HYDRO: Bolt Tensioning	Ambient: HYDRO: Joint Preloaded	Ambient: HYDRO: Pressure Test	Design Operation	Steady State operation	Steady State: Inner Seal Leakage	Startup (4.96 hr.)	Shutdown Flooding (6.81 hr.)	End of Shutdown (4.18 hr.)	Rapid Heating	Rapid Cooling	Vessel Overpressure
Element ②	T_2 (°F)										422.9	517.4	235.0			
	T_{21} (°F)										450.0	511.9	204.2			
	T_{22} (°F)			100°F				575°F	546°F		354.0	530.4	309.8	546°F	573°F	542°F
	T_{23} (°F)										483.0	506	168.6			
	T_{2i} (°F)										546°F		100°F	573°F	375°F	515°F
	m_2 (°F/in.)			0				0	0		1.271	-0.0871	-1.320	0	0	0
Element ③	T_3 (°F)										453.9	513.7	198.4			
	T_{32B} (°F)										476.9	508.1	173.5			
	T_{32F} (°F)										420.0	523.1	235.0			
	T_{31B} (°F)			100°F				575°F	546°F		496.9	502.6	151.7	546°F	573°F	546°F
	T_{31F} (°F)										441.7	518.9	211.3			
	T_B (°F)	Bolt T									290.5	536.0	353.0			
	T_{3i} (°F)										546°F		100°F	573°F	375°F	515°F
	m_3 (°F/in.)			0				0	0		1.83	-0.347	-1.985?	0	0	0

where

$$T_2 = \frac{\int T\,dV}{\int dV}$$

$$T_{21} = \left[\frac{\int_0^{e_{20}} T\,dy}{\int_0^{e_{20}} dy}\right]_{r=R_B}$$

$$T_{22} = \left[\frac{\int_0^{e_{21}} T\,dy}{\int_0^{e_{21}} dy}\right]_{r=R_F}$$

$$T_{23} = \left[\frac{\int_0^{e_{21}} T\,dy}{\int_0^{e_{21}} dy}\right]_{r=R_B}$$

$$m_2 = \frac{\int_{e_{21}}^{e_{20}} (T_y - T_i)\, y\, dr\, \frac{\pi}{4} r_i\, dy}{\int_{e_{21}}^{e_{20}} y\, dr\, \frac{\pi}{4} r_i\, dy}$$

T_{2i} = coolant temperature

$$T_3 = \frac{\int T\,dV}{\int dV}$$

$$T_{32B} = \left[\frac{\int_0^{e_{30}} T\,dy}{\int_0^{e_{30}} dy}\right]_{r=R_B}$$

$$T_{32F} = \left[\frac{\int_0^{e_{31}} T\,dy}{\int_0^{e_{31}} dy}\right]_{r=R_F}$$

$$T_{31B} = \left[\frac{\int_0^{e_{31}} T\,dy}{\int_0^{e_{31}} dy}\right]_{r=R_B}$$

$$T_{34} = \left[\frac{\int_0^{e_{31}} T\,dy}{\int_0^{e_{31}} dy}\right]_{r=R_3}$$

$$m_3 = \frac{\int_{e_{31}}^{e_{30}} (T_y - T_3)\, y\, dr\, \frac{\pi}{4} R_3\, dy}{\int_{e_{31}}^{e_{30}} y\, dr\, \frac{\pi}{4} r_3\, dy}$$

$$T_B = \frac{\int_0^{l_B} T\,dy}{\int_0^{l_B} dy}$$

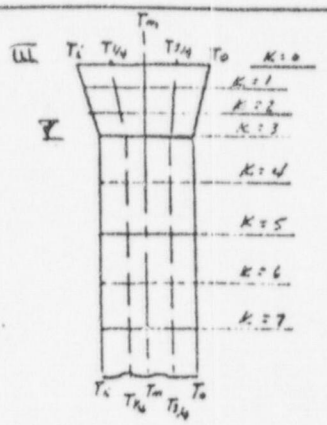
T_{3i} = coolant temperature

C.0 Detailed Analysis

C.2 Applied Loads

C.2.3 Load Derivations

Temperature data for the vessel shell and hub is as follows:



Condition		Node K	Temperature (°F) $(T_i)_K$	$(T_{1/4})_K$	$(T_m)_K$	$(T_{3/4})_K$	$(T_o)_K$	Mean Temp. $\bar{T}$	Thermal Moment M_T
Auxiliary	Bolt Tensioning / Bolts Preloaded / Design Pressure Test / Bolt Tensioning / Bolts Preloaded / Pressure Test	0 → 25	100 °F					100 °F	0
Design Condition		0 → 25	575 °F					575 °F	0
Steady State	Steady State Cond. / Inner Seal Leakage	0 → 25	546 °F					546 °F	0
Start up (4.46 hr)		1a 0	536.8	505.2	481.3	465.1	458.3	487.3	
		3b 3	537.1	508.3	486.9	472.9	467.8	492.6	
		5a 5	537.6	512.9	494.4	482.3	478.3	499.4	
		6→25	538.7	513.6	494.5	480.1	472.0	498.3	
Shutdown Flooding (1.81 hr)		0	488.3	500.0	508.1	513.1	515.1	505.7	
		3	487.8	498.9	506.4	511.0	512.6	504.1	
		5	487.0	497.0	503.9	508.1	509.4	501.8	
		6→25	484.5	494.2	500.7	504.5	505.4	498.6	
End of Shutdown (4.18 hr)		0	109.3	142.6	168.0	185.4	192.7	161.8	
		3	108.9	139.1	161.7	176.6	182.0	155.7	
		5	108.3	133.1	152.9	168.0	170.0	148.0	
		6→25	107.0	128.1	143.3	152.5	154.5	138.7	
Rapid Heating		0→25	573 °F	546 °F				546 °F	0
Rapid Cooling		0→25	375 °F	573 °F				573 °F	0
Vessel Overpressure		0→25	585 °F	546 °F				546 °F	0

Not required for Seal Study

C.0 Detailed Analysis

C.2 Applied Loads

C.2.3 Load Derivations

Bolt Load: The bolt load (F) for normal operating conditions consists of the bolt preload (F_P) plus the variable portion of the bolt load (V) required to maintain continuity between the top of the closure flange and the bolt. The continuity bolt load (V) is calculated as part of the continuity solution shown in Part C.5. The bolt preload (F_P) is determined from requirements for sealing at design operating conditions. Thus, required bolt preload is

$$F_P = \frac{E_{actual}}{E_{design}} (F_o - V_o)$$

where $E_o = (\frac{1}{2} P R_{S1}^2 + 2F_o R_B) / R_F = 54.094\ P + 1,9105\ ^{lb}/_{in}$

$F_o = 1000\ ^{lb}/_{in}$ required for o-ring seating as determined from CE experience.

V_o is determined from equations of Part C.5.

In the same manner, required bolt preload for hydro test is determined as

$$F_{PH} = (F_o - V_o) \qquad \text{where} \quad \frac{E_{actual}}{E_{design}} = 1.0$$

For bolt tensioning, curves of test data by Enerpac included in the stud tensioner instruction manual (Ref. 23) shows the bolt tensioning load required for a defined preload. In addition, experience at C.E. on hydro tests of similar units has shown that stud tensioner pump pressure must be increased by 10% (above that required for the defined load) to loosen the nuts for unseating. Thus, the procedure used here is to determine the bolt tensioning load is

C.0 Detailed Analysis
C.2 Applied Loads
C.2.3 Load Derivations

Bolt Load (Cont'd)

as follows:

1. Express the required bolt preload (F_P lb/in) as a total load/bolt, or $F_B = \frac{2\pi R_E}{N} F_P$.
2. From curve in the stud tensioner manual (Ref. 23), read tensioner pump pressure required for the load F_B.
3. Increase pump pressure of 2. above by 10% (rounded off to the nearest 100psi).
4. From curve, read "tensioned" load ($\bar{F}_B$) for the pump pressure of 3. above.
5. Convert tensioning load to load/inch of bolt circle, or $F_T = \frac{N'}{2\pi R_E} \bar{F}_B$.

During vessel overpressure condition, the pressure blowoff load exceeds the design load used to determine preload. Thus, elongation of the bolt is increased and the bolt load is equal to the overpressure blow-off load, or

$$F_{OP} = (P)_{o.p.} R_{oi}^2 / 2R_F = 74.339 \text{ lb/in}$$

Seal Leakage Load: The seal leakage load is defined as the pressure load that would exist if the pressure boundary were extended outward to the outer o-ring. This load is expressed as a unit load/inch of circumference, or,

$$P_3 = P(R_{o2} - R_{o1}) = 1.5P$$

and is assumed to occur at steady state conditions for a number of cycles equal to the required startup cycles.

C.0 Detailed Analysis

C.2 Applied Loads

C.2.3 Loc' Derivation

Bearing Load: The bearing load acting on the mating surface at each operating condition is determined from requirements for equilibrium of vertical forces, or

$$B = \frac{1}{R_B}(FR_F - \frac{1}{2}PR_{oi}^2) - P_o = 1.0468F - 56.627P - P_o$$

Friction Load: The friction load acting between the mating surfaces is calculated as a function of the bearing load where the friction factor (f) has been determined as 0.15 (See Part C.1). Thus,

$$H_B = fB$$
$$= fFR_F/R_B - fPR_{oi}^2/2R_B - fP_o$$
$$= 0.15702F - 8.4941P - 0.15P_o$$

COMBUSTION ENGINEERING, INC.
ENGINEERING DEPARTMENT, CHATTANOOGA, TENN.

CHARGE NO. 224" BWR

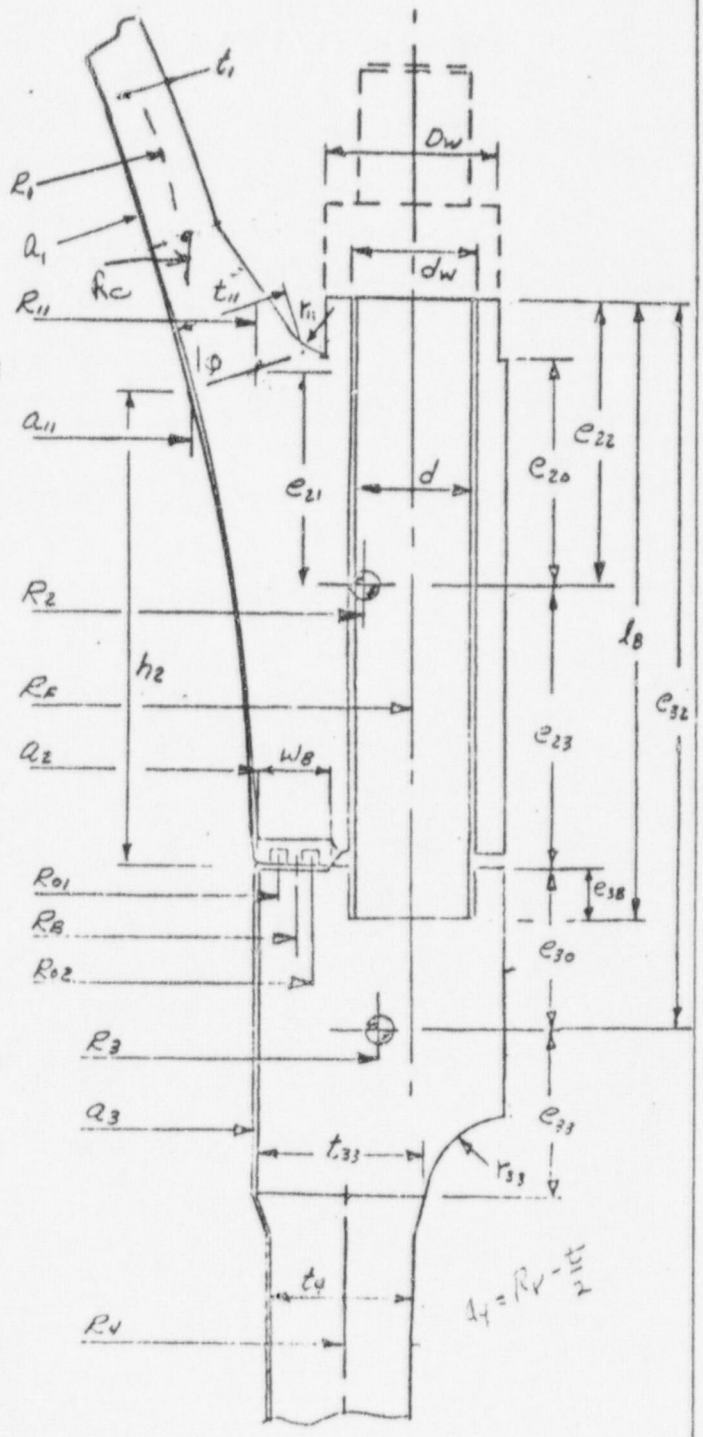
DESCRIPTION Closure Region

NUMBER S-101 | CENC 1139
SHEET 38 | A-31
DATE 10-30-70 BY TP
CHECK DATE 10-30-70 BY EW

C.0 Detailed Analysis

C.3 Geometry

R_1 = 114.28	a_{11} = 108.30		
R_{11} = 111.20	a_2 = 112.10		
R_2 = 117.36	a_3 = 112.34		
R_3 = 118.48	a_1 = 112.44		
R_4 = 116.75	t_1 = 3.500 **		
R_{01} = 114.00	t_{11} = 6.250		
R_{02} = 115.50	t_{33} = 8.375		
R_B = 114.75	t_4 = 7.000 **		
R_F = 120.125	t_c = 3/32" nominal		
R_c = 106.86	d = 6.000		
A_2 = 319.33	N = 56		
I_2 = 17184	ℓ_B = 33.375		
e_{20} = 12.542	A_B = 27.280		
e_{21} = 11.192	I_B = 63.539		
e_{22} = 16.542	F_T = 69.528	*	
e_{23} = 13.771	k = 22.541	*	
h_2 = 23.6125	U = 0.75397	*	
A_3 = 185.41	$\cosh U$ = 1.2980	*	
I_3 = 4248.9	$\tanh U$ = 0.63748	*	
e_{30} = 8.819	K_B = 0.5647	*	
e_{32} = 39.122	d_w = 6.375		
e_{33} = 8.618	D_w = 8.750		
e_{3B} = 3.062	A_w = 26.213		
φ = 64.25°			
$\sin\varphi$ = 0.90070	W_B = 3.4875		
$\cos\varphi$ = 0.43444	w_2 = 9.5078	*	
r_{11} = 3.000			
r_{33} = 5.000	f = 0.1500	*	

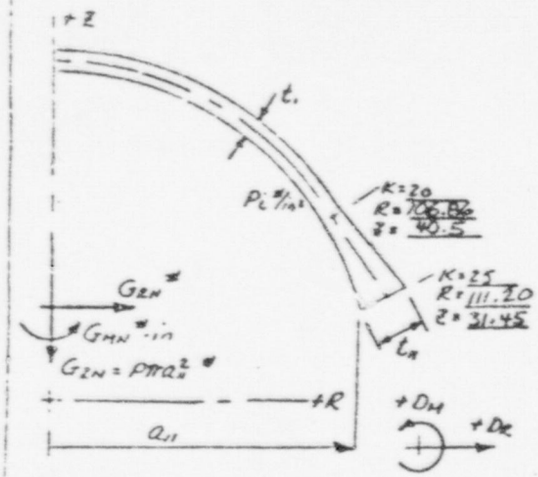


K_{11} = 5.8240 *	K_{31} = 626.31 *	K_{41} = 5.096 *	E = 28.9 x 10^6
K_{12} = 0.16884 *	K_{32} = 18.826 *	K_{42} = 0.11856 *	α = 6.66 x 10^{-6}
K_{13} = 0.09572 *	K_{33} = 0.56407 *	K_{43} = 0.04704 *	

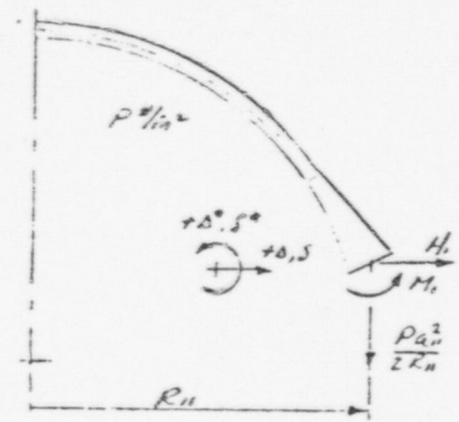
Note * See Part C.1; ** Thickness used for continuity analysis only

C.0 Detailed Analysis

C.4 Load - Deformation Relations (P+S)



Seal Shell Model



Analytical Model

Element ① Shell of Revolution

Deformations of Element ① are determined by use of the Seal-Shell-2 Computer Program (Ref. 10). Radial deflections $(D_R)_K$ and rotations $(D_M)_K$ at the edge are:

Description of Applied Load		Deformations (K=25) $(D_R) \times 10^3$	Deformations (K=25) $(D_M) \times 10^3$
Radial Edge Load	$G_{EN} = 10^6$ #	+15.686	+1.0222
Edge Moment	$G_{HN} = 10^6$ in.-#	+1.0222	+0.12350
Internal Pressure	$P_i = 10^3$ #/in²	+ 95.582	-1.0826
Pressure Blowoff	$G_{ZN} = 36.915 \times 10^6$ #	- 269.02	-14.783
Normal 100°F/hr Startup ②	(4.46 hr)	+378.44	- .99633
Normal Shutdown Flooding ②	(1.81 hr)	+360.67	+0.76026
Normal Shutdown ②	(4.33 hr)	+101.24	+1.0209

Converting Seal-Shell Data to nomenclature used in this calculation gives:

$$E\begin{bmatrix}\Delta_{11}\\ \Delta_{11}^*\end{bmatrix} = 2\pi E \begin{bmatrix}\frac{(D_R)_{GEN}}{G_{EN}} & \frac{(D_R)_{GHN}}{G_{HN}}\\ \frac{(D_M)_{GEN}}{G_{EN}} & \frac{(D_M)_{GHN}}{G_{HN}}\end{bmatrix}\begin{bmatrix}H_1 R_{11}\\ M_1 R_{11}\end{bmatrix} = \begin{bmatrix}+2.8480 & +0.18559\\ +0.18559 & +0.02242\end{bmatrix}\begin{bmatrix}H_1 R_{11}\\ M_1 R_{11}\end{bmatrix}$$

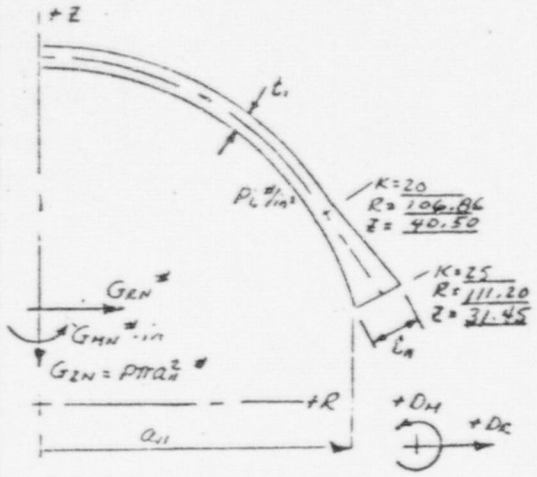
$$E\begin{bmatrix}S_{11}\\ S_{11}^*\end{bmatrix} = PE\begin{bmatrix}\frac{(D_R)_{Pi}}{P_i} + \frac{(D_R)_{GEN}}{P_i}\\ \frac{(D_M)_{Pi}}{P_i} + \frac{(D_M)_{GEN}}{P_i}\end{bmatrix} + E\begin{bmatrix}\frac{(D_R)_{THERMAL}}{(D_M)_{THERMAL}}\end{bmatrix} = P\begin{bmatrix}-5012.4\\ -458.2\end{bmatrix} + \left\{\begin{bmatrix}+10937\\ -28.794\end{bmatrix}\text{ or }\begin{bmatrix}+10923.\\ +21.972\end{bmatrix}\text{ or }\begin{bmatrix}+7925.8\\ +31.238\end{bmatrix}\right. = 0$$

Startup; Shutdn. Flood; Shutdn

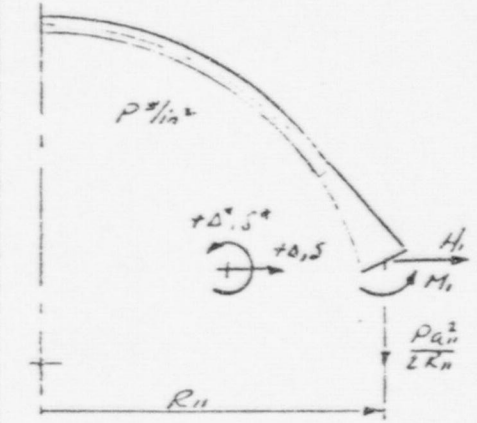
Note ② Thermal only

C.0 Detailed Analysis

C.4 Load - Deformation Relations (PEAK)



Sc. 1 Shell Model



$G_{EN} = 2\pi R_{11} H_1$ $\quad D_R = \Delta_{11} + \delta_{11}$

$G_{HN} = 2\pi R_{11} M_1$ $\quad D_H = L_{11}^* + S_{11}^*$

Analytical Model

Element ① Shell of Revolution

Deformations of Element ① are determined by use of the Seal-Shell-2 Computer Program (Ref. 10). Radial deflections $(D_R)_K$ and rotations $(D_H)_K$ at the edge are:

Description of Applied Load		Deformations (K=25) $(D_R) \times 10^3$	Deformations (K=25) $(D_H) \times 10^3$
Radial Edge Load	$G_{EN} = 10^6$ #	+15.686	+1.0222
Edge Moment	$G_{HN} = 10^6$ in.#	+1.0222	+0.12350
Internal Pressure	$P_i = 10^3$ #/in²	+95.582	-1.0826
Pressure Blowoff	$G_{EN} = 36.915 \times 10^6$ #	-269.02	-14.783
Normal 100°F/hr Startup ④	(4.46 hr)	+382.48	-0.12973
Normal Shutdown Flooding ④	(1.81 hr)	+358.38	+0.37545
Normal Shutdown ④	(4.33 hr)	+97.102	+0.1727

Converting Seal-Shell Data to nomenclature used in this calculation gives:

$$E\begin{bmatrix}\Delta_{11}\\ \Delta_{11}^*\end{bmatrix} = 2\pi E \begin{bmatrix} \frac{(D_R)_{GEN}}{G_{EN}} & \frac{(D_R)_{GHN}}{G_{HN}} \\ \frac{(D_H)_{GEN}}{G_{EN}} & \frac{(D_H)_{GHN}}{G_{HN}} \end{bmatrix} \begin{bmatrix} H_1 R_{11} \\ M_1 R_{11} \end{bmatrix} = \begin{bmatrix} +2.8480 & +0.18559 \\ +0.18559 & +0.02242 \end{bmatrix} \begin{bmatrix} H_1 R_{11} \\ M_1 R_{11} \end{bmatrix}$$

$$E\begin{bmatrix}S_{11}\\ S_{11}^*\end{bmatrix} = PE \begin{bmatrix} \frac{(D_R)_{Pi}}{P_i} + \frac{(D_R)_{GEN}}{P_i} \\ \frac{(D_H)_{Pi}}{P_i} + \frac{(D_H)_{GEN}}{P_i} \end{bmatrix} + E \begin{bmatrix} (D_R)_{THERMAL} \\ (D_H)_{THERMAL} \end{bmatrix} = P \begin{bmatrix} -5012.4 \\ -458.2 \end{bmatrix} + \left\{ \begin{bmatrix} +11054 \\ -3.7492 \end{bmatrix}_{\text{startup}} \text{ OR } \begin{bmatrix} +10357 \\ +10.851 \end{bmatrix}_{\text{shutdn. Flood}} \text{ OR } \begin{bmatrix} +2806.2 \\ +4.9910 \end{bmatrix}_{\text{shutdn}} \right\} 10^3$$

Note ④ Thermal only

C.0 Detailed Analysis

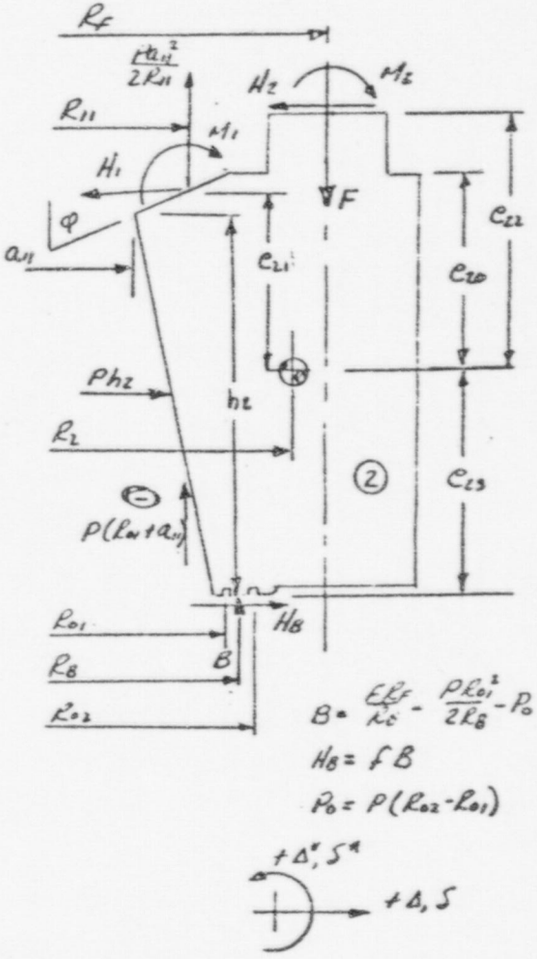
C.4 Load - Deformation Relations (P+S & Peak)

Element ② - Ring

Using ring theory defined in References 4 and 6 and described in Part C.2 gives:

$$E \begin{bmatrix} \Delta_{21} \\ \Delta'_{21} \\ \Delta_{22} \\ \Delta'_{23} \end{bmatrix} = \begin{bmatrix} -0.36754 - \frac{R_2}{A_2} - \frac{R_2 c_{21}^2}{I_2} - 0.85417 - 0.04248 - \frac{K_{11}}{R_{11}} \sin^2\varphi & +0.07633 + \frac{R_2 c_{21}}{I_2} + 0.00136 + \frac{K_{12}}{R_{11}} \sin\varphi & -0.36754 - \frac{R_2}{A_2} - 1.2625 - \frac{R_2 c_{21} c_{22}}{I_2} & +0.07633 + \frac{R_2 c_{21}}{I_2} \\ +0.07633 + 0.00136 + \frac{R_2 c_{21}}{I_2} + \frac{K_{12}}{R_{11}} \sin\varphi & -0.00682 - 0.00682 - \frac{R_2}{I_2} - \frac{K_{13}}{R_{11}} & +0.11282 + \frac{R_2 c_{22}}{I_2} & -0.00682 - \frac{R_2}{I_2} \\ -0.36754 - 1.2625 - \frac{R_2}{A_2} - \frac{R_2 c_{21} c_{22}}{I_2} & +0.11282 + \frac{R_2 c_{22}}{I_2} & -0.36754 - 1.8119 - \frac{R_2}{A_2} - \frac{R_2 c_{22}}{I_2} & +0.11282 + \frac{R_2 c_{22}}{I_2} \\ +0.07633 + \frac{R_2 c_{21}}{I_2} & -0.00682 - \frac{R_2}{I_2} & +0.11282 + \frac{R_2 c_{22}}{I_2} & -0.00682 - 0.00469 - \frac{R_2}{I_2} - \frac{K_R}{K_F} \end{bmatrix} \begin{bmatrix} H_1 R_{11} \\ M_1 R_{11} \\ H_2 R_F \\ M_2 R_F \end{bmatrix}$$

$$= \begin{bmatrix} -1.2642 & +0.07769 & -1.6300 & +0.07633 \\ +0.07769 & -0.00768 & +0.11282 & -0.00682 \\ -1.6300 & +0.11282 & -2.2336 & +0.11282 \\ +0.07633 & -0.00682 & +0.11282 & -0.01151 \end{bmatrix} \begin{bmatrix} H_1 R_{11} \\ M_1 R_{11} \\ H_2 R_F \\ M_2 R_F \end{bmatrix}$$



C.0 Detailed Analysis

C.4 Load-Deformation Relations (P+S & Peak)

Element ② - Ring (Cont'd).

$$\begin{bmatrix} \delta_{21} \\ \delta_{21}^{q} \\ \delta_{22} \\ \delta_{22}^{q} \end{bmatrix} = E \begin{bmatrix} \frac{a_{11}^2 R_2 c_{21}}{2I_2}(R_2-R_{11}) + \frac{a_{11}^2}{2R_{11}} K_{11}\sin\phi\cos\phi + \frac{R_2 h_2}{2A_2}(a_{11}+a_2) - \frac{R_2 h_2 c_{21}}{2I_2}(c_{23}-\frac{h_2}{2})(a_{11}+a_2) \\ \quad + \frac{R_2 c_{21}}{2I_2}(R_{01}^2-a_{11}^2)(R_2-\frac{R_{01}+a_{11}}{2}) - \frac{R_{01}^2 R_2 c_{21}}{2I_2}(R_2-R_E) - \frac{f R_{01}^2 R_2}{2I_2} + \frac{f R_{01}^2 R_2 c_{21} c_{23}}{2I_2} \\ -\frac{a_{11}^2 R_2}{2I_2}(R_2-R_{11}) - \frac{a_{11}^2}{2R_{11}}(K_{12}\cos\phi) + \frac{R_2 h_2}{2I_2}(c_{23}-\frac{h_2}{2})(a_{11}+a_2) - \frac{R_2}{2I_2}(R_{01}^2-a_{11}^2)(R_2-\frac{R_{01}+a_{11}}{2}) \\ \quad + \frac{R_{01}^2 R_2}{2I_2}(R_2-R_E) - \frac{f R_{01}^2 R_2 c_{23}}{2I_2} \\ + \frac{a_{11}^2 R_2 c_{22}}{2I_2}(R_2-R_{11}) + \frac{R_2 h_2}{2A_2}(a_{11}+a_2) - \frac{R_2 h_2 c_{22}}{2I_2}(c_{23}-\frac{h_2}{2})(a_{11}+a_2) + \frac{R_2 c_{23}}{2I_2}(R_{01}^2-a_{11}^2)(R_2-\frac{R_{01}+a_{11}}{2}) \\ \quad - \frac{R_{01}^2 R_2 c_{22}}{2I_2}(R_2-R_E) - \frac{f R_{01}^2 R_2}{2A_2} + \frac{f R_{01}^2 R_2 c_{22} c_{23}}{2I_2} \\ -\frac{a_{11}^2 R_2}{2I_2}(R_2-R_{11}) + \frac{R_2 h_2}{2I_2}(c_{23}-\frac{h_2}{2})(a_{11}+a_2) - \frac{R_2}{2I_2}(R_{01}^2-a_{11}^2)(R_2-\frac{R_{01}+a_{11}}{2}) + \frac{R_{01}^2 R_2}{2I_2}(R_2-R_E) \\ \quad - \frac{f R_{01}^2 R_2 c_{23}}{2I_2} \end{bmatrix} = P \begin{bmatrix} \frac{R_F R_2 c_{21}}{I_2}(R_F-R_E) + \frac{f R_2 R_F}{A_2} - \frac{f R_2 R_F c_{21} c_{23}}{I_2} \\ \quad - \frac{R_E R_2}{I_2}(R_F-R_E) + \frac{f R_F R_2 c_{23}}{I_2} \\ \frac{R_F R_2 c_{22}}{I_2}(R_F-R_E) + \frac{f R_2 R_F}{A_2} - \frac{f R_2 R_F c_{22} c_{23}}{I_2} \\ \quad - \frac{R_F R_2}{I_2}(R_F-R_E) + \frac{f R_2 R_2 c_{23}}{I_2} \end{bmatrix} + F \begin{bmatrix} +6.6213 \\ -4.4097 \\ +1.6938 \\ \end{bmatrix} + P_0 \begin{bmatrix} -\frac{R_E R_2 c_{21}}{I_2}(R_2-R_E) - \frac{f R_2 R_E}{A_2} + \frac{f R_2 R_E c_{21} c_{23}}{I_2} \\ \quad + \frac{R_E R_2}{I_2}(R_2-R_E) - \frac{f R_2 R_E c_{23}}{I_2} \\ -\frac{R_E R_2 c_{22}}{I_2}(R_2-R_E) - \frac{f R_2 R_E}{A_2} + \frac{f R_2 R_E c_{22} c_{23}}{I_2} \\ \quad + \frac{R_E R_2}{I_2}(R_2-R_E) - \frac{f R_2 R_E c_{23}}{I_2} \end{bmatrix} + E\alpha \begin{bmatrix} +R_{11}T_2 - R_{11}c_{21}m_2 \\ +R_{11}m_2 - \frac{c_{20}}{R_E-R_E}(T_{21}-T_{22}) \\ +R_E T_2 - R_E c_{21} m_2 \\ +R_E m_2 - \frac{c_{20}}{R_E-R_E}(T_{21}-T_{22}) \end{bmatrix}$$

$$= P \begin{bmatrix} +3118.5 \\ -218.53 \\ +4145.7 \\ -214.46 \end{bmatrix} + F \begin{bmatrix} +37.017 \\ -2.7159 \\ +51.548 \\ -2.7159 \end{bmatrix} + P_0 \begin{bmatrix} -11.109 \\ +0.42750 \\ -13.398 \\ +0.42750 \end{bmatrix} + \left\{ \begin{bmatrix} +8746.9 \\ -15.912 \\ +9283.7 \\ -13.729 \end{bmatrix} \text{or} \begin{bmatrix} +11095 \\ +6.4272 \\ +11981 \\ +6.2778 \end{bmatrix} \text{or} \begin{bmatrix} +5345.9 \\ +19.174 \\ +5933.8 \\ +16.934 \end{bmatrix} \right\} 10^3$$

C.0 Detailed Analysis

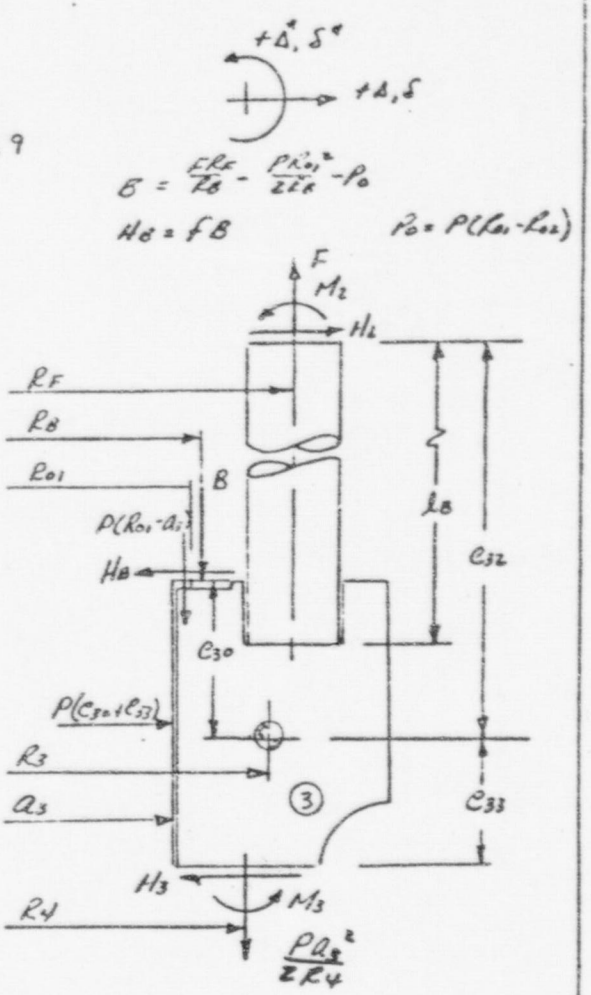
C.4 Load-Deformation Relations (P+S & Peak)

Element ③ – Ring with Beam Appendage

Using ring and beam theory defined in References 4, 6, 8, 9 and 18 and described in Part C.2 gives:

$$\begin{bmatrix} \Delta_{32} \\ \Delta^*_{32} \\ \Delta_{33} \\ \Delta^*_{33} \end{bmatrix} = \begin{bmatrix} +0.63901 + 42.203 + 5.2305 + \frac{R_3}{A_3} + \frac{R_3 C_{32}^2}{I_3} + \frac{K_{21}}{R_F} + 17.844 + \frac{E}{F_T R_F}\left(k_B - \frac{1}{k_B}\tanh U\right) & -1.0785 - 0.15672 - \frac{R_3 C_{32}}{I_3} - \frac{K_{22}}{R_F} - 0.79459 - \frac{E}{F_T R_F}\left(\frac{\cosh U - 1}{\cosh U}\right) & -0.63901 - \frac{R_3}{A_3} + 9.2943 + \frac{R_3 C_{32} C_{33}}{I_3} & -1.0785 - \frac{R_3 C_{32}}{I_3} \\ -1.0785 - 0.13672 - \frac{R_3 C_{32}}{I_3} - \frac{K_{32}}{R_F} - 0.70439 - \frac{E}{F_T R_F}\left(\frac{\cosh U - 1}{\cosh U}\right) & +0.03786 + 2.00470 + \frac{R_3}{I_3} + \frac{K_{33}}{R_F} + 0.04983 + \frac{E}{F_T R_F}\left(k_B \tanh U\right) & -0.23751 - \frac{R_3 C_{33}}{I_3} & +0.02756 + \frac{R_3}{I_3} \\ +0.63901 + \frac{R_3}{A_3} - 9.2943 - \frac{R_3 C_{32} C_{33}}{I_3} & +0.23751 + \frac{R_3 C_{33}}{I_3} & -0.63901 - 2.0449 - \frac{R_3}{A_3} - \frac{R_3 C_{33}}{I_3} - 0.04345 - \frac{K_{41}}{R_4} & +0.23751 + \frac{R_3 C_{33}}{I_3} + 0.00101 + \frac{K_{42}}{R_4} \\ -1.0785 - \frac{R_3 C_{32}}{I_3} & +0.02756 + \frac{R_3}{I_3} & -0.23751 - 0.00101 - \frac{R_3 C_{33}}{I_3} - \frac{K_{43}}{R_4} & +0.02756 + 0.00101 + \frac{R_3}{I_3} + \frac{K_{43}}{R_4} \end{bmatrix} \begin{bmatrix} H_2 R_F \\ M_2 R_F \\ H_3 R_4 \\ M_3 R_4 \end{bmatrix}$$

$$= \begin{bmatrix} +65.917 & -2.0296 & +8.6553 & -1.0785 \\ -2.0296 & +0.08209 & -0.23751 & +0.02756 \\ -8.6553 & +0.23751 & -2.7296 & +0.23852 \\ -1.0785 & +0.02756 & -0.23852 & +0.02797 \end{bmatrix} \begin{bmatrix} H_2 R_F \\ M_2 R_F \\ H_3 R_4 \\ M_3 R_4 \end{bmatrix}$$



COMBUSTION ENGINEERING, INC.
ENGINEERING DEPARTMENT, CHATTANOOGA, TENN.

CHARGE NO. 224" BWR
DESCRIPTION Closure Region

NUMBER S-101 | CENC-1139
SHEET 43 | A-36
DATE 1-30-70 BY TP
CHECK DATE 1-30-70 BY EN

C.0 Detailed Analysis

C.4 Load-Deformation Relations (P+S & Peak)

Element ③ - Ring with Beam Appendage (Cont'd)

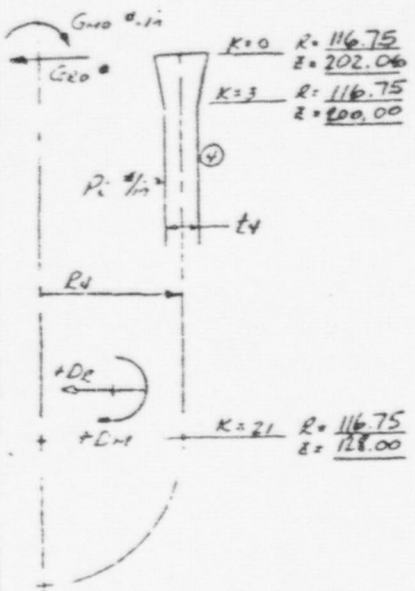
$$\begin{bmatrix} S_{32} \\ - \\ S_{32}^{*} \\ - \\ S_{33} \\ - \\ S_{33}^{*} \end{bmatrix} E = P \begin{bmatrix} \frac{R_{01}^2 R_3 c_{32}}{2I_3}(R_3-R_B) + \frac{fR_3R_{01}^2}{2A_3} + \frac{fR_3R_B^2 c_{30}c_{32}}{2I_3} - \frac{R_3 c_{32}}{2I_3}(R_{01}^2-a_3^2)(R_3-\frac{R_{01}+a_3}{2}) \\ + \frac{R_3 a_3}{A_3}(c_{30}+c_{32}) + \frac{R_3 a_3 c_{32}}{2I_3}(c_{30}^2-c_{33}^2) - \frac{a_3^2 R_3 c_{32}}{2I_3}(R_3-R_4) \\ - \frac{R_{01}^2 R_3}{2I_3}(R_3-R_B) - \frac{fR_3R_{01}^2 c_{30}}{2I_3} + \frac{R_3}{2I_3}(R_{01}^2-a_3^2)(R_3-\frac{R_{01}+a_3}{2}) - \frac{R_3 a_3}{2I_3}(c_{30}^2-c_{33}^2) + \frac{a_3^2 R_3}{2I_3}(R_3-R_4) \\ - \frac{R_{01}^2 R_3 c_{33}}{2I_3}(R_3-R_B) + \frac{fR_3R_{01}^2}{2A_3} - \frac{fR_3R_B^2 c_{30}c_{33}}{2I_3} + \frac{R_3 c_{33}}{2I_3}(R_{01}^2-a_3^2)(R_3-\frac{R_{01}+a_3}{2}) \\ + \frac{R_3 a_3}{A_3}(c_{30}+c_{33}) - \frac{R_3 a_3 c_{33}}{2I_3}(c_{30}^2-c_{33}^2) + \frac{a_3^2 R_3 c_{33}}{2I_3}(R_3-R_4) \\ - \frac{R_{01}^2 R_3}{2I_3}(R_3-R_B) - \frac{fR_3R_{01}^2 c_{30}}{2I_3} + \frac{R_3}{2I_3}(R_{01}^2-a_3^2)(R_3-\frac{R_{01}+a_3}{2}) - \frac{R_3 a_3}{2I_3}(c_{30}^2-c_{33}^2) + \frac{a_3^2 R_3}{2I_3}(R_3-R_4) \end{bmatrix}$$

$$+F \begin{bmatrix} -\frac{R_F R_3 c_{32}}{I_3}(R_F-R_B) \\ -\frac{fR_3R_F}{A_3} - \frac{fR_3R_F c_{30}c_{32}}{I_3} \\ + \frac{R_F R_3}{I_3}(R_F-R_B) \\ + \frac{fR_F R_3 c_{30}}{I_3} \\ + \frac{R_F R_3 c_{33}}{I_3}(R_F-R_4) \\ - \frac{fR_3R_F}{A_3} + \frac{fR_3R_F c_{30}c_{33}}{I_3} \\ + \frac{R_F R_3^2}{I_3}(R_F-R_4) \\ + \frac{fR_F R_3 c_{30}}{I_3} \end{bmatrix} + P_0 \begin{bmatrix} + \frac{R_3R_B c_{32}}{I_3}(R_3-R_B) \\ + \frac{fR_3R_B}{A_3} + \frac{fR_3R_B c_{30}c_{32}}{I_3} \\ - \frac{R_B R_3}{I_3}(R_3-R_B) \\ - \frac{fR_3R_B c_{30}}{I_3} \\ - \frac{R_3R_B c_{33}}{I_3}(R_3-R_4) \\ + \frac{fR_3R_B}{A_3} - \frac{fR_3R_B c_{30}c_{33}}{I_3} \\ - \frac{R_B R_3}{I_3}(R_3-R_4) \\ - \frac{fR_3R_B c_{30}}{I_3} \end{bmatrix} + E\alpha \begin{bmatrix} + R_F T_3 - R_F c_{32} m_3 \\ + \frac{k_B(c_{32}-R_B)}{(R_F-R_B)}(T_{32B}-T_{32F}) \\ + R_F m_3 \\ - \frac{(c_{32}-R_B)}{(R_F-R_B)}(T_{32B}-T_{32F}) \\ + R_4 T_4 - R_4 T_3 \\ + R_4 c_{33} m_3 \\ + R_4 m_3 \\ - \frac{c_{33}}{(R_F-R_4)}(T_{33B}-T_{33F}) \end{bmatrix}$$

$$= P \begin{bmatrix} +24646. \\ -581.91 \\ -3140.3 \\ -581.91 \end{bmatrix} + F \begin{bmatrix} -879.22 \\ +22.174 \\ +179.58 \\ +22.174 \end{bmatrix} + P_0 \begin{bmatrix} +636.29 \\ -15.979 \\ -126.71 \\ -15.979 \end{bmatrix} + \left\{ \begin{bmatrix} +9229.8 \\ +30.580 \\ +10554 \\ +24.087 \end{bmatrix} \text{Start-up} \text{ OR } \begin{bmatrix} +12088 \\ -4.9303 \\ +11476 \\ -2.7672 \end{bmatrix} \text{Shutdn Flood.} \text{ OR } \begin{bmatrix} +5960.4 \\ -33.231 \\ +4073.7 \\ -26.228 \end{bmatrix} \text{Shutdown} \right\} 10^3$$

C.0 Detailed Analysis

C.4 Load-Deformation Relations (P+S)



Seal-Shell Model

Element ④ Shell of Revolution

Deformations of Element ④ are determined by use of the Seal-Shell-2 Computer Program (Ref. 10). Radial deflections $(D_R)_0$ and rotations $(D_M)_0$ at the edge are:

Description of Applied Load		Deformations (K=0) $(D_R) \times 10^2$	Deformations (K=0) $(D_M) \times 10^3$
Radial Edge Load	$G_{R0} = 10^6$ #	+8.1857	-0.36086
Edge Moment	$G_{M0} = 10^6$ in-#	-0.36086	+0.03271
Internal Pressure	$P_i = 10^3$ #/in²	-56.066	+.10403
Normal 100°F/hr Start-up @	(4.96 hr.)	-386.61	-0.27790
Normal Shutdown Flooding @	(1.81 hr.)	-390.62	+0.09751
Normal Shutdown @	(4.33 hr.)	-117.00	+0.30981

Converting

$$E\begin{bmatrix}\Delta_{43}\\ \Delta^{\circ}_{43}\end{bmatrix} = 2\pi E\begin{bmatrix}-\frac{(D_R)_{G_{R0}}}{G_{R0}} & -\frac{(D_R)_{G_{M0}}}{G_{M0}}\\ -\frac{(D_M)_{G_{R0}}}{G_{R0}} & -\frac{(D_M)_{G_{M0}}}{G_{M0}}\end{bmatrix}\begin{bmatrix}H_3R_4\\ M_3R_4\end{bmatrix} = \begin{bmatrix}+1.4862 & +0.06552\\ -0.06552 & -0.00594\end{bmatrix}\begin{bmatrix}H_3R_4\\ M_3R_4\end{bmatrix}$$

$$E\begin{bmatrix}S_{43}\\ S^{\circ}_{43}\end{bmatrix} = PE\begin{bmatrix}-\frac{(D_R)_{P_i}}{P_i}\\ -\frac{(D_M)_{P_i}}{P_i}\end{bmatrix} + \begin{bmatrix}\frac{(D_R)_{THERMAL}}{-(D_M)_{THERMAL}}\end{bmatrix} = P\begin{bmatrix}+1620.3\\ -0.11647\end{bmatrix} + \left\{\begin{bmatrix}+11173.\\ +8.0313\end{bmatrix}\text{OR}\begin{bmatrix}+11289.\\ -28758\end{bmatrix}\text{OR}\begin{bmatrix}+3381.2\\ -8.9535\end{bmatrix}\right\}\begin{matrix}\text{m}\\ \text{o}\end{matrix}$$

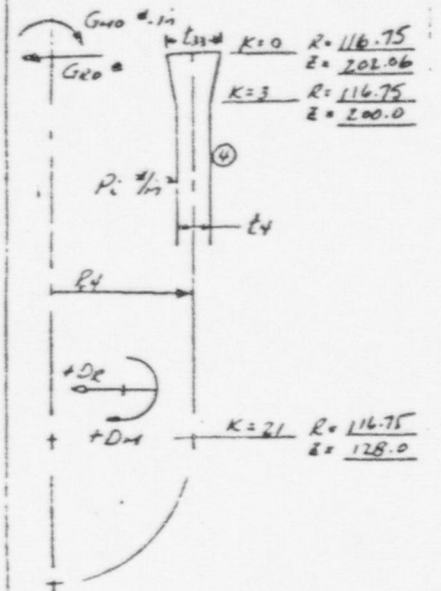
START-UP SHUTDOWN FLOOD SHUTDOWN

Note @ Thermal only.

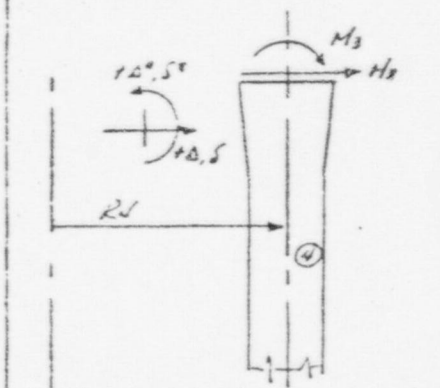
Analytical Model
$G_{R0} = -2\pi R_4 H_3$ $D_R = \Delta_{43} - S_{43}$
$G_{M0} = +2\pi R_4 M_3$ $D_M = \Delta^{\circ}_{43} - S^{\circ}_{43}$

C.0 Detailed Analysis

C.4 Load-Deformation Relations (PEAK)



Seal-Shell Model



Analytical Model

Element ④ Shell of Revolution

Deformations of Element ④ are determined by use of the Seal-Shell-2 Computer Program (Ref. 10). Radial deflections $(D_R)_0$ and rotations $(D_M)_0$ at the edge are:

Description of Applied Load		Deformations (K=0) $(D_R) \times 10^3$	Deformations (K=0) $(D_M) \times 10^3$
Radial Edge Load	$G_{R0} = 10^6$ #	+8.1857	-0.36086
Edge Moment	$G_{M3} = 10^6$ in-#	-0.36086	+0.03271
Internal Pressure	$P_i = 10^3$ #/in²	-56.066	+0.00403
Normal 100°F/hr Start-up ④	(4.46 hr.)	-401.86	+1.2957
Normal Shutdown Flooding ④	(1.81 hr.)	-384.26	-0.50679
Normal Shutdown ④	(4.33 hr.)	-101.24	-1.3275

Converting

$$E\begin{bmatrix}\Delta_{43}\\ \delta_{43}^*\end{bmatrix} = 2\pi E\begin{bmatrix}-\frac{(D_R)_{G_{R0}}}{-G_{R0}} & -\frac{(D_R)_{G_{M0}}}{G_{M0}}\\ -\frac{(D_M)_{G_{R0}}}{-G_{R0}} & -\frac{(D_M)_{G_{M0}}}{G_{M0}}\end{bmatrix}\begin{bmatrix}H_3R_4\\ M_3R_4\end{bmatrix} = \begin{bmatrix}+1.4862 & +0.06552\\ -0.06552 & -0.00594\end{bmatrix}\begin{bmatrix}H_3R_4\\ M_3R_4\end{bmatrix}$$

$$E\begin{bmatrix}S_{43}\\ S_{43}^*\end{bmatrix} = P\bar{E}\begin{bmatrix}-\frac{(D_R)_{P_i}}{P_i}\\ -\frac{(D_M)_{P_i}}{P_i}\end{bmatrix} + \begin{bmatrix}-(D_R)_{THERMAL}\\ -(D_M)_{THERMAL}\end{bmatrix} = P\begin{bmatrix}+1620.3\\ -0.11647\end{bmatrix} + \left\{\begin{bmatrix}+11614\\ -37.446\end{bmatrix}\text{OR}\begin{bmatrix}+11105\\ +14.646\end{bmatrix}\text{OR}\begin{bmatrix}+2925.8\\ +38.365\end{bmatrix}\right\}10^3$$

STARTUP SHUTDOWN FLOOD SHUTDOWN

Note ④ Thermal only

C.0 Detailed Analysis

C.5 Continuity Load Solution (P+S + PEAK)

Equating edge deformations of adjacent elements gives a set of simoultaneous equations in terms of the continuity loads H_j and M_j.

$$E\begin{bmatrix} \Delta_{11} \\ -\Delta_{21} \\ \hline \Delta^*_{11} \\ -\Delta^*_{21} \\ \hline \Delta_{22} \\ -\Delta_{32} \\ \hline \Delta^*_{22} \\ -\Delta^*_{32} \\ \hline \Delta_{33} \\ -\Delta_{43} \\ \hline \Delta^*_{33} \\ -\Delta^*_{43} \end{bmatrix} = \left[\begin{array}{cccccc} +2.8480 & +0.18559 & & & 0 & 0 \\ +1.2642 & -0.07769 & +1.6300 & -0.07633 & & \\ \hline +0.18559 & +0.02242 & & & 0 & 0 \\ -0.07769 & +0.00768 & -0.11282 & +0.00682 & & \\ \hline -1.6300 & +0.11282 & -2.2336 & +0.11282 & & \\ & & -65.917 & +2.0296 & 8.6553 & +1.0785 \\ \hline +0.07633 & -0.00682 & +0.11282 & -0.01151 & & \\ & & +2.0296 & -0.08209 & +0.23751 & -0.02756 \\ \hline & & -8.6553 & +0.23751 & -2.7296 & +0.23852 \\ 0 & 0 & & & -1.4862 & -0.06552 \\ \hline & & -1.0758 & +0.02756 & -0.23852 & +0.02797 \\ 0 & 0 & & & +0.06552 & +0.00594 \end{array}\right] \begin{bmatrix} H_1 R_{11} \\ \hline M_1 R_{11} \\ \hline H_2 R_F \\ \hline H_2 L_F \\ \hline H_3 R_4 \\ \hline M_3 R_4 \end{bmatrix}$$

$$= \left[\begin{array}{cccccc} +4.1122 & +0.10790 & +1.6300 & -0.07633 & 0 & 0 \\ +0.10790 & +0.03010 & -0.11282 & +0.00682 & 0 & 0 \\ -1.6300 & +0.11282 & -68.151 & +2.1424 & -8.6553 & +1.0785 \\ +0.07633 & -0.00682 & +2.1424 & -0.09360 & +0.23751 & -0.02756 \\ 0 & 0 & -8.6553 & +0.23751 & -4.2158 & +0.17300 \\ 0 & 0 & -1.0785 & +0.02756 & -0.17300 & +0.03391 \end{array}\right] \begin{bmatrix} H_1 R_{11} \\ M_1 R_{11} \\ H_2 R_F \\ M_2 R_F \\ H_3 R_4 \\ M_3 L_4 \end{bmatrix}$$

COMBUSTION ENGINEERING, INC.
ENGINEERING DEPARTMENT, CHATTANOOGA, TENN.

CHARGE NO. 224" EVIL

DESCRIPTION Closure Region

NUMBER 2701 | CENC 427
SHEET 98 | A-41
DATE 1/30/70 BY TP
CHECK DATE 1/30/70 BY JB

C.0 Detailed Analysis

C.5 Continuity Load Solution (Prim + Sec)

$$
\begin{bmatrix} \delta_{21} \\ -\delta_{11} \\ \delta_{21}^{*} \\ -\delta_{11}^{*} \\ \delta_{32} \\ -\delta_{22} \\ \delta_{32}^{*} \\ -\delta_{22}^{*} \\ \delta_{43} \\ -\delta_{33} \\ -\delta_{43}^{*} \\ -\delta_{33}^{*} \end{bmatrix} E = P \begin{bmatrix} +3118.5 \\ +5012.4 \\ -218.33 \\ +458.2 \\ 24646 \\ -4145.7 \\ -581.91 \\ +214.4 \\ +1620.3 \\ +3140.3 \\ -0.11647 \\ +581.91 \end{bmatrix} + F \begin{bmatrix} +37.017 \\ 0 \\ -2.7159 \\ 0 \\ -879.22 \\ -51.548 \\ +22.174 \\ +2.7159 \\ 0 \\ -179.58 \\ 0 \\ -22.174 \end{bmatrix} + P_o \begin{bmatrix} -11.109 \\ 0 \\ +0.42750 \\ 0 \\ +636.29 \\ +13.398 \\ -5.979 \\ -0.42750 \\ 0 \\ +126.71 \\ 0 \\ +15.979 \end{bmatrix} + \left\{ \begin{bmatrix} +8746.9 \\ -10937 \\ -15.912 \\ +28.794 \\ +9229.8 \\ -9283.7 \\ +30.580 \\ +15.729 \\ +11173. \\ -10554. \\ +8.0313 \\ -24.087 \end{bmatrix} \text{STARTUP} \text{ OR } \begin{bmatrix} +11095. \\ -10423 \\ +6.4272 \\ -21.972 \\ +12088. \\ -11981. \\ -4.9303 \\ -6.2778 \\ +11289. \\ -11476. \\ -2.8758 \\ +2.7672 \end{bmatrix} \text{SHUTDOWN FLOOD} \text{ OR } \begin{bmatrix} +5345.9 \\ -2925.8 \\ +19.174 \\ -31.238 \\ +5980.4 \\ -5933.8 \\ -33.231 \\ -16.931 \\ +3381.3 \\ -4073.7 \\ -8.9535 \\ +26.228 \end{bmatrix} \text{SHUTDOWN} \right\} 10^{3}
$$

$$
= P \begin{bmatrix} +8131.0 \\ +240.19 \\ +20501. \\ -367.45 \\ +4760.6 \\ +581.79 \end{bmatrix} + F \begin{bmatrix} +37.017 \\ -2.7159 \\ -930.77 \\ +24.890 \\ -179.58 \\ -22.174 \end{bmatrix} + P_o \begin{bmatrix} -11.109 \\ +0.42750 \\ +649.69 \\ -16.406 \\ +126.71 \\ +15.979 \end{bmatrix} + \left\{ \begin{bmatrix} -2191.0 \\ +12.882 \\ -53.900 \\ +44.309 \\ +619.00 \\ -16.056 \end{bmatrix} \text{STARTUP} \text{ OR } \begin{bmatrix} +672.00 \\ -15.545 \\ +107.00 \\ -11.208 \\ -187.00 \\ -0.1086 \end{bmatrix} \text{SHUTDOWN FLOOD} \text{ OR } \begin{bmatrix} +2920.1 \\ -12.064 \\ +86.600 \\ -50.162 \\ -692.40 \\ +17.274 \end{bmatrix} \text{SHUTDOWN} \right\} 10^{3}
$$

$$
\begin{bmatrix} H_1 R_{11} \\ H_1 R_{21} \\ H_1 R_{22} \\ H_1 R_{32} \\ H_1 R_{33} \\ H_1 R_{43} \end{bmatrix} = \begin{bmatrix} +0.28051 & -1.1002 & +0.00793 & -0.28671 & -0.01584 & -0.40438 \\ -1.1002 & +38.308 & -0.01749 & +4.7482 & +0.15459 & +3.6267 \\ -0.00793 & +0.01749 & -0.09364 & -1.5973 & +0.04214 & +1.4651 \\ +0.28671 & -4.7482 & -1.5973 & -42.844 & +0.26539 & +14.627 \\ +0.01584 & -0.15459 & +0.04214 & +0.26539 & -0.33216 & +0.56994 \\ -0.40438 & +3.6267 & 1.4651 & -14.627 & -0.56994 & +67.106 \end{bmatrix} E \begin{bmatrix} \delta_{21} - \delta_{11} \\ \delta_{21}^{*} - \delta_{11}^{*} \\ \delta_{32} - \delta_{22} \\ \delta_{32}^{*} - \delta_{22}^{*} \\ \delta_{43} - \delta_{33} \\ \delta_{43}^{*} - \delta_{33}^{*} \end{bmatrix}
$$

$$
\begin{bmatrix} H_1 \\ H_1 \\ H_2 \\ H_2 \\ H_3 \\ H_3 \end{bmatrix} = P \begin{bmatrix} +17.750 \\ +8.9730 \\ -2.8312 \\ -50.275 \\ -3.3544 \\ +79.234 \end{bmatrix} + F \begin{bmatrix} +0.09592 \\ -1.0655 \\ +0.05833 \\ +0.59812 \\ +0.13189 \\ -3.5195 \end{bmatrix} + P \begin{bmatrix} -0.01978 \\ +0.15175 \\ -0.04813 \\ -0.60535 \\ -0.08734 \\ +2.5202 \end{bmatrix} + \left\{ \begin{bmatrix} -5802.3 \\ 128353. \\ -379.34 \\ -21412. \\ -2072.4 \\ -9136.3 \end{bmatrix} \text{STARTUP} \text{ OR } \begin{bmatrix} +1912.5 \\ -12763. \\ -4792.2 \\ +4366.6 \\ +65637 \\ -1898.5 \end{bmatrix} \text{SHUTDOWN} \text{ OR } \begin{bmatrix} +6391.3 \\ -30646. \\ +452.55 \\ +24369. \\ +2294.1 \\ +10502. \end{bmatrix} \text{SHUTDOWN} \right\}
$$

COMBUSTION ENGINEERING, INC.
ENGINEERING DEPARTMENT, CHATTANOOGA, TENN.
CHARGE NO. 224 BWR

NUMBER S-101 | CENC 1139
SHEET 49 | A-42
DATE 11-1-30-70 BY TP
CHECK DATE 11-30-70 BY JB

DESCRIPTION Closure Region

C.0 Detailed Analysis
C.5 Continuity Load Solution (Peak)

$$\begin{bmatrix} \delta_{21} \\ -\delta_{11} \\ \delta_{21}^{a} \\ -\delta_{11}^{a} \\ \delta_{12} \\ -\delta_{22} \\ \delta_{32}^{a} \\ -\delta_{22}^{a} \\ \delta_{V3} \\ -\delta_{33} \\ \delta_{V3}^{a} \\ -\delta_{33}^{a} \end{bmatrix} E = P \begin{bmatrix} +3118.5 \\ +5012.4 \\ -218.33 \\ +458.52 \\ +24646 \\ -4145.7 \\ -581.91 \\ +214.46 \\ +1620.3 \\ +3140.3 \\ -0.11647 \\ +581.91 \end{bmatrix} + F \begin{bmatrix} +37.017 \\ 0 \\ -2.7159 \\ 0 \\ -879.22 \\ -51.548 \\ +22.174 \\ +2.7159 \\ 0 \\ -179.58 \\ 0 \\ -22.174 \end{bmatrix} + P_o \begin{bmatrix} -11.109 \\ 0 \\ +0.42750 \\ 0 \\ +636.29 \\ +13.398 \\ -15.979 \\ -0.42750 \\ 0 \\ +126.71 \\ 0 \\ +15.979 \end{bmatrix} + \left\{ \begin{bmatrix} +8746.9 \\ -11054 \\ -15.912 \\ +3.7492 \\ +9229.8 \\ -9283.7 \\ +30.580 \\ +13.729 \\ +11614. \\ -10554 \\ -37.446 \\ -24.087 \end{bmatrix}_{\text{STARTUP}} \text{OR} \begin{bmatrix} +11095 \\ -10357 \\ +6.4272 \\ -10.851 \\ +12088 \\ -11981 \\ -4.9303 \\ -6.2778 \\ +11105 \\ -11476 \\ +14.646 \\ +2.7672 \end{bmatrix}_{\text{SHUTON FLUID}} \text{OR} \begin{bmatrix} +5345.9 \\ -2806.2 \\ +19.174 \\ -4.9910 \\ +5960.4 \\ -5933.8 \\ -33.231 \\ -16.931 \\ +2925.8 \\ -4073.7 \\ +38.365 \\ +26.228 \end{bmatrix}_{\text{SHUTDOWN}} \right\} 10^3$$

$$= P \begin{bmatrix} +8131.0 \\ +240.19 \\ +20501 \\ -367.45 \\ +4760.6 \\ +581.77 \end{bmatrix} + F \begin{bmatrix} +37.017 \\ -2.7159 \\ -930.77 \\ +24.890 \\ -179.58 \\ -22.174 \end{bmatrix} + P_o \begin{bmatrix} -11.109 \\ +0.4275 \\ +649.69 \\ -16.406 \\ +126.71 \\ +15.979 \end{bmatrix} + \left\{ \begin{bmatrix} -2307.1 \\ -12.163 \\ -53.900 \\ +44.309 \\ +1060.0 \\ -61.533 \end{bmatrix}_{\text{STARTUP}} \text{OR} \begin{bmatrix} +738.00 \\ -4.4238 \\ +107.00 \\ -11.208 \\ -371.00 \\ +17.413 \end{bmatrix}_{\text{SHUTON FLUID}} \text{OR} \begin{bmatrix} +2539.7 \\ +14.183 \\ +26.600 \\ -50.162 \\ -1147.9 \\ +64.593 \end{bmatrix}_{\text{SHUTDOWN}} \right\} 10^3$$

$$\begin{bmatrix} H_1 R_{11} \\ M_1 R_{11} \\ H_1 R_{12} \\ M_1 R_{12} \\ H_1 R_{14} \\ M_1 R_{14} \end{bmatrix} = \begin{bmatrix} +0.28051 & -1.1002 & +0.00793 & -0.28671 & -0.01584 & -0.40438 \\ -1.1002 & +38.308 & -0.01749 & +4.7482 & +0.15459 & +3.6267 \\ -0.007928 & +0.01749 & -0.09364 & -1.5973 & +0.04214 & +1.4651 \\ +0.28671 & -4.7482 & -1.5973 & -42.844 & +0.26539 & +14.627 \\ +0.015835 & -0.15459 & +0.04214 & +0.26539 & -0.33216 & +0.56994 \\ -0.40438 & +3.6267 & -1.4651 & -14.627 & -0.56994 & +67.106 \end{bmatrix} E \begin{bmatrix} \delta_{21} - \delta_{11} \\ \delta_{21}^{a} - \delta_{11}^{a} \\ \delta_{12} - \delta_{22} \\ \delta_{32}^{a} - \delta_{22}^{a} \\ \delta_{V3} - \delta_{33} \\ \delta_{V3}^{a} - \delta_{33}^{a} \end{bmatrix}$$

$$\begin{bmatrix} H_1 \\ M_1 \\ H_2 \\ M_2 \\ H_3 \\ M_3 \end{bmatrix} = P \begin{bmatrix} +17.750 \\ +8.1730 \\ -2.8312 \\ -50.275 \\ -3.3544 \\ +79.234 \end{bmatrix} + F \begin{bmatrix} +0.09592 \\ -1.0655 \\ +0.05833 \\ +0.51812 \\ +0.13189 \\ -3.5195 \end{bmatrix} + P_o \begin{bmatrix} -0.01978 \\ +0.15175 \\ -0.04818 \\ -0.60535 \\ -0.08734 \\ +2.5202 \end{bmatrix} + \left\{ \begin{bmatrix} -5744.8 \\ +20004. \\ -775.25 \\ -25263. \\ -3531.7 \\ -37804. \end{bmatrix}_{\text{STARTUP}} \text{OR} \begin{bmatrix} +1931.5 \\ -9269.2 \\ +98.486 \\ +5811.6 \\ +1259.6 \\ +9187.6 \end{bmatrix}_{\text{SHUTON FLUID}} \text{OR} \begin{bmatrix} +6326.1 \\ -21878. \\ +865.79 \\ +28367. \\ +3802.4 \\ +40325. \end{bmatrix}_{\text{SHUTDOWN}} \right\}$$

C.0 Detailed Analysis

C.5 Continuity Load solution (P+S & Peak)

The preceding solution is applicable where continuity of radial deflections and rotations are required at the junction of the closure flange and bolt. However, during bolt tensioning, the additional flexibility of the bolt due to the added length of the assumed "beam", threaded joints in the tensioner, and clearances between the tensioner piston and cylinder makes these requirements negligible. Thus, for the bolt tensioning condition, solution of continuity loads reduces to a separate solution for the closure shell-flange and the vessel shell-flange. Using equations from Part C.4 where H_2 and M_2 are zero gives:

$$E\begin{bmatrix}\Delta_{11}-\Delta_{21}\\ \Delta'_{11}-\Delta'_{21}\end{bmatrix} = \begin{bmatrix}+4.1122 & +0.10790\\ +0.1079 & +0.03010\end{bmatrix}\begin{bmatrix}H_1K_{11}\\ M_1K_{11}\end{bmatrix} \qquad E\begin{bmatrix}\delta_{21}-\delta_{11}\\ \delta'_{21}-\delta'_{11}\end{bmatrix} = F_T\begin{bmatrix}37.017\\ -2.7159\end{bmatrix}$$

$$E\begin{bmatrix}\Delta_{33}-\Delta_{43}\\ \Delta'_{33}-\Delta'_{43}\end{bmatrix} = \begin{bmatrix}-4.2158 & +0.1730\\ -0.1730 & +0.03391\end{bmatrix}\begin{bmatrix}H_3K_4\\ M_3K_4\end{bmatrix} \qquad E\begin{bmatrix}\delta_{43}-\delta_{33}\\ \delta'_{43}-\delta'_{33}\end{bmatrix} = F_T\begin{bmatrix}-179.58\\ -22.174\end{bmatrix}$$

Solving the above equations, and including H_2 and M_2, gives

$$\begin{bmatrix}H_1\\ M_1\\ H_2\\ M_2\\ H_3\\ M_3\end{bmatrix} = F_T\begin{bmatrix}+0.11285\\ -1.2159\\ 0\\ 0\\ +0.17073\\ -4.7299\end{bmatrix}$$

Note that above solution assumes the tensioning load (F_T) to be applied uniformly around the circumference rather than to only four bolts at a time.

C.0 Detailed Analysis

C.5 Continuity Load Solution P+S

4. Elongation of the bolt, $E(Y_{32})_B = [2\pi R_F L_B / N A_B] V \frac{E}{E_B}$
5. Compression of the vessel flange, $E(Y_{32})_F = -B\, e_{33}/w_B$
6. Thermal growth of the closure flange, $E(Y_{22})_T = E_L(T_{32}e_{22} + T_{33}e_{23})$
7. Thermal growth of vessel flange & bolt, $E(Y_{32})_T = -E_L T_{32} e_{33} + E_L \lambda_B T_B$

Thus, where $E\theta_2 = E(\Delta_2^\circ + S_2^\circ)$ and $E\theta_3 = E(\Delta_3^\circ + S_3^\circ)$

$$E\begin{bmatrix} Y_{22} \\ Y_{32} \\ Y_{22} - Y_{32} \end{bmatrix} = (E_F - E_B)\begin{bmatrix} E\theta_2 \\ E\theta_3 \\ E\theta_2 - E\theta_3 \end{bmatrix} + 2\pi R_F V \frac{E}{E_B}\begin{bmatrix} -\frac{e_{22}-e_{20}}{NA_B} \\ +\frac{\ell_B/NA_B}{-[e_{22}-e_{20}/NA_B]} \\ -\ell_B/NA_B \end{bmatrix} + B\begin{bmatrix} -\frac{2R_B(e_{20}+e_{23})}{w_2(R_F+R_B)} \\ -\frac{e_{33}}{w_B} \\ -\frac{2R_y(e_{20}+e_{23})}{w_2(R_F+R_B)} + \frac{e_{3F}}{w_2} \end{bmatrix} + \begin{bmatrix} E_L(T_{32}e_{22} + T_{33}e_{23}) \\ -E_L T_{32} e_{33} + E_L \lambda_B T_B \\ E_L(T_{32}e_{22} + T_{33}e_{23}) \\ +E_L T_{32} e_{33} - E_L \lambda_B T_B \end{bmatrix}$$

$$= (5.375)\begin{bmatrix} E\theta_2 \\ E\theta_3 \\ E\theta_2 - E\theta_3 \end{bmatrix} + V\frac{E}{E_B}\begin{bmatrix} -1.9109 \\ +16.489 \\ -18.400 \end{bmatrix} + B\begin{bmatrix} -2.7042 \\ -.83037 \\ -1.8738 \end{bmatrix} + \left\{ \begin{bmatrix} +1881.5 \\ 976.53 \\ 904.97 \end{bmatrix}_{\text{Start-up}} \text{ or } \begin{bmatrix} 2592.7 \\ 2727.7 \\ -135.0 \end{bmatrix}_{\text{Shutdn Flood.}} \text{ or } \begin{bmatrix} 835.97 \\ 1596.4 \\ -760.43 \end{bmatrix}_{\text{Shutdown}} \right\} 10^3$$

From Part C.4

$$E\begin{bmatrix} \theta_2 \\ \theta_3 \\ \theta_2 - \theta_3 \end{bmatrix} = \left[\begin{array}{cc|cc|cc} 0.07633 & -0.00682 & +0.11282 & -0.00682 & 0 & 0 \\ 0 & 0 & -1.0785 & +0.02756 & -0.23751 & +0.02756 \\ \hline 0.07633 & -0.00682 & +1.1913 & -0.03438 & +0.23751 & -0.02756 \end{array}\right]\begin{bmatrix} H_1 R_{11} \\ M_1 R_{11} \\ H_2 R_F \\ M_2 R_F \\ H_3 F_4 \\ M_3 F_4 \end{bmatrix}$$

$$+P\begin{bmatrix} -214.46 \\ -581.91 \\ +367.45 \end{bmatrix} + V\begin{bmatrix} -2.7159 \\ +22.174 \\ -24.890 \end{bmatrix} + P_o\begin{bmatrix} +0.4275 \\ -15.979 \\ +16.407 \end{bmatrix} + \left\{ \begin{bmatrix} -13.729 \\ +24.087 \\ -37.816 \end{bmatrix}_{\text{Start-up}} \text{ or } \begin{bmatrix} +6.2778 \\ -2.7672 \\ +9.0450 \end{bmatrix}_{\text{Shutdn Flood}} \text{ or } \begin{bmatrix} +16.931 \\ -26.228 \\ +43.159 \end{bmatrix}_{\text{Shutdown}} \right\} 10^3$$

$$= P\begin{bmatrix} -67.790 \\ -33.590 \\ -34.200 \end{bmatrix} + V\begin{bmatrix} -0.7886 \\ +1.5880 \\ -2.3950 \end{bmatrix} + P_o\begin{bmatrix} -0.01250 \\ -1.2100 \\ +1.1990 \end{bmatrix} + \left\{ \begin{bmatrix} -72.080 \\ +30.412 \\ -102.49 \end{bmatrix}_{\text{Start-up}} \text{ or } \begin{bmatrix} +27.963 \\ -6.4092 \\ +34.375 \end{bmatrix}_{\text{Shutdn Flood}} \text{ or } \begin{bmatrix} +80.594 \\ -34.021 \\ +114.61 \end{bmatrix}_{\text{Shutdown}} \right\} 10^3$$

From Part C.4

$$B = \frac{1}{w_B}\left(-\tfrac{1}{2}PH_{31}^2 + VK_1\right) = -56.627\, P + 1.0468\, V - P_o$$

C.0 Detailed Analysis

C.5 Continuity Load Solution (Peak)

4. Elongation of the bolt, $E(Y_{32})_B = [2\pi R_F L_B/NA_B]\, V \frac{E}{E_B}$
5. Compression of the vessel flange, $E(Y_{32})_F = -B' c_{33}/w_B$
6. Thermal growth of the closure flange, $E(Y_{22})_T = E_L(T_{32}c_{22} + T_{23}c_{23})$
7. Thermal growth of vessel flange & bolt, $E(Y_{32})_T = -E_L T_{32} c_{33} + E_{L_B} L_B T_B$

Thus, where $E\Theta_2 = E(\delta_2^* + \delta_2^*)$ and $E\Theta_3 = E(\delta_3^* + \delta_3^*)$

$$E\begin{bmatrix} Y_{22} \\ Y_{32} \\ Y_{22} \\ -Y_{32} \end{bmatrix} = (R_F - L_R)\begin{bmatrix} E\Theta_2 \\ E\Theta_3 \\ E\Theta_2 \\ -E\Theta_3 \end{bmatrix} + 2\pi R_F \frac{E}{E_B}\begin{bmatrix} -\frac{c_{22}-c_{20}}{NA_B} \\ +\frac{L_B}{NA_B} \\ -[c_{22}-c_{20}/NA_B] \\ -L_B/NA_B \end{bmatrix} + B'\begin{bmatrix} -\frac{2L_B(c_{20}+c_{23})}{w_2(R_F+R_B)} \\ -\frac{c_{33}}{w_B} \\ -\frac{2L_B(c_{20}+c_{23})}{w_2(R_F+R_B)} + \frac{c_{33}}{w_B} \end{bmatrix} + \begin{bmatrix} E_L(T_{22}c_{22}+T_{23}c_{23}) \\ -E_L T_{32} c_{33} + E_{L_B} L_B T_B \\ E_L(T_{22}c_{22}+T_{23}c_{23}) \\ +E_L T_{32} c_{33} - E_{L_B} L_B T_B \end{bmatrix}$$

$$= (5.375)\begin{bmatrix} E\Theta_2 \\ E\Theta_3 \\ E\Theta_2 \\ -E\Theta_3 \end{bmatrix} + V\frac{E}{E_B}\begin{bmatrix} -1.9109 \\ +16.489 \\ -18.400 \end{bmatrix} + B'\begin{bmatrix} -2.7042 \\ -0.83037 \\ -1.8738 \end{bmatrix} + \left\{ \begin{bmatrix} 1881.5 \\ 976.53 \\ 904.97 \end{bmatrix}_{\text{Start up}} \text{ or } \begin{bmatrix} 2592.7 \\ 2727.7 \\ -135.0 \end{bmatrix}_{\text{Shutdn Flood.}} \text{ or } \begin{bmatrix} 835.97 \\ 1596.4 \\ -760.43 \end{bmatrix}_{\text{Shutdown}} \right\} 10^3$$

From Part C.4

$$E\begin{bmatrix} \Theta_2 \\ \Theta_3 \\ \Theta_2 - \Theta_3 \end{bmatrix} = \left[\begin{array}{cc|c|cc|cc} 0.07633 & -0.00682 & +0.11282 & -0.00682 & 0 & 0 \\ 0 & 0 & -1.0785 & +0.02756 & -0.23751 & +0.02756 \\ 0.07633 & -0.00682 & +1.1913 & -0.03438 & -0.23751 & -0.0275 \end{array}\right] \begin{bmatrix} H_1R_{11} \\ M_1R_{11} \\ H_2K_2 \\ M_2P_2 \\ H_3L_4 \\ M_3P_4 \end{bmatrix}$$

$$+P\begin{bmatrix} -214.46 \\ -581.91 \\ +367.45 \end{bmatrix} + V\begin{bmatrix} -2.7159 \\ +22.174 \\ -24.890 \end{bmatrix} + P_o\begin{bmatrix} +4.42750 \\ -15.979 \\ +16.407 \end{bmatrix} + \left\{ \begin{bmatrix} -15.912 \\ +24.087 \\ -39.999 \end{bmatrix}_{\text{Start up}} \text{ or } \begin{bmatrix} +6.4272 \\ -2.7672 \\ +9.1944 \end{bmatrix}_{\text{Shutdn Flood}} \text{ or } \begin{bmatrix} +19.174 \\ -26.228 \\ 45.402 \end{bmatrix}_{\text{Shutdown}} \right\} 10^3$$

$$=P\begin{bmatrix} -67.790 \\ -33.590 \\ -34.200 \end{bmatrix} + V\begin{bmatrix} -0.7866 \\ +1.5880 \\ -2.3750 \end{bmatrix} + P_o\begin{bmatrix} -0.0125 \\ -1.2100 \\ +1.1990 \end{bmatrix} + \left\{ \begin{bmatrix} -69.653 \\ +17.181 \\ -86.832 \end{bmatrix}_{\text{Start up}} \text{ or } \begin{bmatrix} +26.424 \\ -1.6541 \\ +28.078 \end{bmatrix}_{\text{Shutdn Flood}} \text{ or } \begin{bmatrix} +77.954 \\ -20.167 \\ +98.119 \end{bmatrix}_{\text{Shutdown}} \right\} 10^3$$

From Part C.4

$B' = \frac{1}{w_B}(-\frac{1}{2}\pi R_F^2 P + VW_{12}) - P_o = -56.627P + 1.0468V - P_o$

where B' is bearing load change due to variable portion of the TOTAL bolt load

C.0 Detailed Analysis

C.5 Continuity Load Solution P+S

Substitution of expressions for EO and B into deflection eqns. gives:

$$E\begin{bmatrix} Y_{22} \\ Y_{32} \\ Y_{22}-Y_{32} \end{bmatrix} = +(5.375)\left\| P\begin{bmatrix} -67.790 \\ -33.590 \\ -34.200 \end{bmatrix} + V\begin{bmatrix} -0.7866 \\ +1.5880 \\ -2.3750 \end{bmatrix} + P_o\begin{bmatrix} -0.01250 \\ -1.2100 \\ +1.1990 \end{bmatrix} + \left\{ \begin{bmatrix} -72.080 \\ +30.412 \\ -102.49 \end{bmatrix}_{\text{startup}} \text{or} \begin{bmatrix} -27.963 \\ -6.4092 \\ +34.375 \end{bmatrix}_{\text{shutdn Flood}} \text{or} \begin{bmatrix} +80.594 \\ -34.021 \\ +114.61 \end{bmatrix}_{\text{shutdown}} \right\} \right\|$$

$$+V\frac{E}{E_B}\begin{bmatrix} -1.9109 \\ +16.489 \\ -18.400 \end{bmatrix} + \left\| +P\begin{bmatrix} 153.13 \\ 47.021 \\ 106.11 \end{bmatrix} + V\begin{bmatrix} -2.8308 \\ -0.86923 \\ -1.9615 \end{bmatrix} + P_o\begin{bmatrix} +2.7042 \\ +0.83037 \\ +1.8738 \end{bmatrix} \right\| + \left\{ \begin{bmatrix} +1881.5 \\ +976.53 \\ +904.97 \end{bmatrix}_{\text{start-up}} \text{or} \begin{bmatrix} +2592.7 \\ +2727.7 \\ -135.0 \end{bmatrix}_{\text{shutdn Flood}} \text{or} \begin{bmatrix} +835.97 \\ +1596.4 \\ -760.43 \end{bmatrix}_{\text{shutdown}} \right\} 10^3$$

$$= P\begin{bmatrix} -211.24 \\ -183.53 \\ -77.710 \end{bmatrix} + V\begin{bmatrix} -7.0588 - 1.9109\frac{E}{E_B} \\ +7.6663 + 16.489\frac{E}{E_B} \\ -14.729 - 18.400\frac{E}{E_B} \end{bmatrix} + P_o\begin{bmatrix} +2.6370 \\ -5.6734 \\ +8.3183 \end{bmatrix} + \left\{ \begin{bmatrix} +1484.1 \\ +1140.0 \\ +354.09 \end{bmatrix}_{\text{Startup}} \begin{bmatrix} +2743.0 \\ +2693.2 \\ +49.770 \end{bmatrix}_{\text{Shutdn Flood}} \begin{bmatrix} +1269.2 \\ +1413.5 \\ -144.40 \end{bmatrix}_{\text{Shutdown}} \right\} 10^3$$

Thus, where $E Y_{32} - E Y_{32} = 0$,

$$V = \frac{-77.710\,P + 8.3183\,P_o + \left\{ (+354.09)_{\text{or}} (+49.770)_{\text{or}} (-144.40) \right\}_{\text{su}}^{\text{fl}}\ 10^3}{+14.728 + 18.40\,E/E_B}$$

As discussed in Part C.2, the bolt load (F) for vessel over-pressure and bolt tensioning operations is equal to the applied load. Thus, for these conditions, $V = 0$.

The solution of continuity loads used in the preceding calculations includes the horizontal component of the pressure membrane load as part of the radial continuity load H_1. For convenience in further calculations, this pressure component is removed and

$$\overline{H_1} = P\left(+17.750 - \frac{\pi a_i^2 \cos\theta}{2\pi a_i \cos\theta}\right) = -7.6880\,P$$

C.0 Detailed Analysis

C.5 Continuity Load Solution (Peak)

Substitution of expressions for EΘ and Θ into deflection gens. gives:

$$E\begin{bmatrix} Y_{12} \\ Y_{31} \\ Y_{22}-Y_{12} \end{bmatrix} = +(.5375)\left\| P\begin{bmatrix} -67.790 \\ -33.590 \\ -34.200 \end{bmatrix} + V\begin{bmatrix} -0.7866 \\ +1.5880 \\ -2.3750 \end{bmatrix} + P_o\begin{bmatrix} -0.01250 \\ -1.2100 \\ +1.1990 \end{bmatrix} + \left\{ \begin{bmatrix} -69.653 \\ +17.181 \\ -86.832 \end{bmatrix}_{\text{Startup}} \text{or} \begin{bmatrix} +26.424 \\ -1.6541 \\ +28.078 \end{bmatrix}_{\text{Shutdn Flood}} \text{or} \begin{bmatrix} +77.954 \\ -20.167 \\ +98.119 \end{bmatrix}_{\text{Shutdown}} \right\} 10^3 \right\|$$

$$+V\frac{E}{E_B}\begin{bmatrix} -1.9109 \\ +16.489 \\ -18.400 \end{bmatrix} + \left\| +P\begin{bmatrix} +153.13 \\ +47.021 \\ +106.11 \end{bmatrix} + V\begin{bmatrix} -28308 \\ -0.86923 \\ -1.9615 \end{bmatrix} + P_o\begin{bmatrix} +2.7042 \\ +0.83037 \\ +1.8738 \end{bmatrix} + \left\{ \begin{bmatrix} +1881.5 \\ +976.53 \\ +904.97 \end{bmatrix}_{\text{Startup}} \text{or} \begin{bmatrix} 2592.7 \\ 2727.7 \\ -135.0 \end{bmatrix}_{\text{Shutdn Flood}} \text{or} \begin{bmatrix} 835.97 \\ 1596.4 \\ -760.43 \end{bmatrix}_{\text{Shutdown}} \right\} 10^3$$

$$E\begin{bmatrix} Y_{22} \\ Y_{32} \\ Y_{22}-Y_{32} \end{bmatrix} = P\begin{bmatrix} -211.24 \\ -133.53 \\ -77.71 \end{bmatrix} + V\begin{bmatrix} -7.0588 - 1.9109\frac{E}{E_B} \\ +7.6663 + 16.489\frac{E}{E_B} \\ -14.728 - 18.400\frac{E}{E_B} \end{bmatrix} + P_o\begin{bmatrix} +2.6270 \\ -5.6734 \\ +8.3183 \end{bmatrix} + \left\{ \begin{bmatrix} +1507.1 \\ +993.71 \\ +438.25 \end{bmatrix}_{\text{Startup}} \begin{bmatrix} 2734.7 \\ +2718.8 \\ +15.92 \end{bmatrix}_{\text{Shutdn Flood}} \begin{bmatrix} 1254.97 \\ +1488.0 \\ -233.04 \end{bmatrix}_{\text{Shutdown}} \right\} 10^3$$

Thus, where $EY_{22} - EY_{32} = 0$,

$$V = \frac{-77.710\ P + 8.3183\ P_o + \left\{ (+438.25)_{SS} \text{ or } (+15.920)_{SDE} \text{ or } (-233.04)_{SD} \right\} 10^3}{+14.728 \quad + 18.400\ E/E_B}$$

As discussed in Part C.2, the bolt load (F) for vessel over-pressure and bolt tensioning operations is equal to the applied load. Thus, for these conditions, $V = 0$.

The solution of continuity loads used in the preceding calculations includes the horizontal component of the pressure membrane load as part of the radial continuity load H_1. For convenience in further calculations, this pressure component is removed and

$$H_1 = P\left(17.750 - \frac{-23.458}{\text{Shell area}}\right) = -7.6880\ P$$

C.0 Detailed Analysis

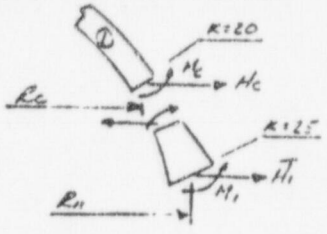
C.5 Continuity Loads P+S

Although the continuity load solution is used to determine loads at the junctions of the hubs with their flanges, the locations of maximum interest in the structure are at the junctions of the shells and hubs. To determine the continuity loads at these locations, the Seal-Shell 2 Computer Solutions (Ref. 10) are used as follows:

The Seal-Shell-2 output data includes loads F_R and F_M due to applied edge loads G_R and G_M. For the solutions for elements ① and ② these loads are:

Component	Description of Applied Load		Loads at junctions of shells & hubs	
			$F_R)_K \times 10^6$	$F_M)_K \times 10^4$
Element ① Closure Shell K = 20	Edge Radial Load	$G_{RN} = 10^6$ #	5.4794	+378.26
	Edge Moment	$G_{MN} = 10^6$ IN-#	-4.5527	70.309
Element ② Vessel Shell K = 3	Edge Radial load	$G_{RO} = 10^6$ #	80.722	-185.50
	Edge Moment	$G_{MO} = 10^6$ IN-#	0.82050	99.101

Converting to the convention of the analysis gives:

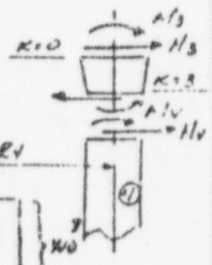


$$\begin{bmatrix} H_c \\ M_c \end{bmatrix} = \begin{bmatrix} (F_R)_{GRN}/G_{RN} & (F_R)_{GMN}/G_{MN} \\ (F_M)_{GRN}/G_{RN} & (F_M)_{GMN}/G_{MN} \end{bmatrix} \begin{bmatrix} \bar{H}_1 \\ M_1 \end{bmatrix} = \begin{bmatrix} .05702 & -.04783 \\ 3.9362 & .73164 \end{bmatrix} \begin{bmatrix} \bar{H}_1 \\ M_1 \end{bmatrix}$$

$$= P \begin{bmatrix} -.86351 \\ -23.696 \end{bmatrix} + F \begin{bmatrix} 10.05595 \\ -0.4020 \end{bmatrix} + F_0 \begin{bmatrix} -.00832 \\ 10.03317 \end{bmatrix} + \left\{ \begin{bmatrix} -1.6745 \\ -2.1145 \end{bmatrix} \text{ or } \begin{bmatrix} .71376 \\ -1.8099 \end{bmatrix} \text{ or } \begin{bmatrix} 1.8164 \\ 2.7356 \end{bmatrix} \right\} \times 10^3$$

(Startup; Shutdown Flnd; Shutdown)

$$\begin{bmatrix} H_V \\ M_V \end{bmatrix} = \begin{bmatrix} (F_R)_{GRO}/G_{RO} & (F_R)_{GMO}/G_{MO} \\ (F_M)_{GRO}/G_{RO} & (F_M)_{GMO}/G_{MO} \end{bmatrix} \begin{bmatrix} H_3 \\ M_3 \end{bmatrix} = \begin{bmatrix} 0.80722 & -.00821 \\ 1.8.50 & 0.99101 \end{bmatrix} \begin{bmatrix} H_3 \\ M_2 \end{bmatrix}$$



$$= P \begin{bmatrix} -.33582 \\ 77.211 \end{bmatrix} + V \begin{bmatrix} -.13535 \\ -3.2432 \end{bmatrix} + P_0 \begin{bmatrix} -.0119 \\ 12.3356 \end{bmatrix} + \left\{ \begin{bmatrix} -1.5979 \\ -12.898 \end{bmatrix} \text{ or } \begin{bmatrix} 0.54512 \\ -0.66287 \end{bmatrix} \text{ or } \begin{bmatrix} 1.7656 \\ 14.663 \end{bmatrix} \right\} \times 10^3$$

(Start-up; Shutdown Flnd; Shutdown)

C.0 Detailed Analysis

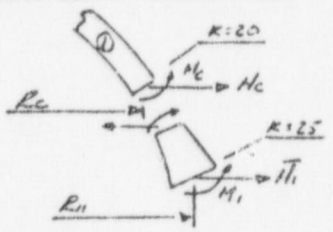
C.5 Continuity Loads - Peak

Although the continuity load solution is used to determine loads at the junctions of the hubs with their flanges, the locations of maximum interest in the structure are at the junctions of the shells and hubs. To determine the continuity loads at these locations, the Seal-Shell 2 Computer Solutions (Ref. 10) are used as follows:

The Seal-Shell-2 output data includes loads F_R and F_M due to applied edge loads G_R and G_M. For the solutions for elements ① and ② these loads are:

Component	Description of Applied Load		Loads at junctions of shells & hubs	
			$F_R)_K \times 10^6$	$F_M)_K \times 10^4$
Element ① Closure Shell K = 20	Edge Radial Load	$G_{RN} = 10^6$ #	5.4794	4378.26
	Edge Moment	$G_{MN} = 10^6$ in-#	-4.5527	70.309
Element ④ Vessel Shell K = 3	Edge Radial load	$G_{RO} = 10^6$ #	80.722	-185.50
	Edge Moment	$G_{MO} = 10^6$ in-#	0.82050	99.101

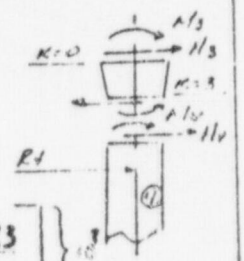
Converting to the convention of the analysis gives:



$$\begin{bmatrix} H_c \\ M_c \end{bmatrix} = \frac{R_3}{R_2} \begin{bmatrix} \frac{(F_R)_{GRN}}{G_{RN}} & \frac{(F_R)_{GMN}}{G_{MN}} \\ \frac{(F_M)_{GRN}}{G_{RN}} & \frac{(F_M)_{GMN}}{G_{MN}} \end{bmatrix} \begin{bmatrix} \bar{H}_1 \\ M_1 \end{bmatrix} = \begin{bmatrix} .05702 & -.04733 \\ 3.9362 & .73164 \end{bmatrix} \begin{bmatrix} \bar{H}_1 \\ M_1 \end{bmatrix}$$

$$= P \begin{bmatrix} -.86351 \\ -23.696 \end{bmatrix} + F \begin{bmatrix} +0.05545 \\ -0.4020 \end{bmatrix} + P_0 \begin{bmatrix} -.00832 \\ +0.03317 \end{bmatrix} + \left\{ \begin{bmatrix} -1.2754 \\ -7.977 \end{bmatrix}_{\text{Start-up}} \text{ or } \begin{bmatrix} .5.4931 \\ .8206 \end{bmatrix}_{\text{Shutdn Fluid}} \text{ or } \begin{bmatrix} 1.3973 \\ 8.894 \end{bmatrix}_{\text{Shutdown}} \right\} \times 10^3$$

$$\begin{bmatrix} H_v \\ M_v \end{bmatrix} = \begin{bmatrix} \frac{(F_R)_{GMO}}{G_{MO}} & \frac{(F_R)_{GMO}}{G_{MO}} \\ \frac{(F_M)_{GMO}}{G_{MO}} & \frac{(F_M)_{GMO}}{G_{MO}} \end{bmatrix} \begin{bmatrix} H_3 \\ M_3 \end{bmatrix} = \begin{bmatrix} 0.85722 & -.00321 \\ 1.3550 & 0.99101 \end{bmatrix} \begin{bmatrix} H_3 \\ M_3 \end{bmatrix}$$



$$= P \begin{bmatrix} -.33582 \\ 72.211 \end{bmatrix} + V \begin{bmatrix} -.13535 \\ -3.2432 \end{bmatrix} + P_0 \begin{bmatrix} -.01117 \\ +2.8355 \end{bmatrix} + \left\{ \begin{bmatrix} -2.5405 \\ -44.015 \end{bmatrix}_{\text{Start-up}} \text{ or } \begin{bmatrix} 0.94134 \\ 11.441 \end{bmatrix}_{\text{Shutdown}} \text{ or } \begin{bmatrix} 2.7583 \\ 47.016 \end{bmatrix}_{\text{Shutdown}} \right\} \times 10^3$$

C.0 Detailed Analysis

C.5 Continuity Load Solution (P+S)

Continuity loads are summarized as follows:

Normal Operations

$$\begin{bmatrix} H_c \\ M_c \\ \bar{H}_1 \\ M_1 \\ H_2 \\ M_2 \\ H_3 \\ M_3 \\ H_v \\ M_v \end{bmatrix} = P \begin{bmatrix} -0.86351 \\ -23.696 \\ -7.6880 \\ +8.9730 \\ -2.8312 \\ -50.275 \\ -3.3544 \\ +79.234 \\ -3.3582 \\ 72.299 \end{bmatrix} + F \begin{bmatrix} +0.05595 \\ -0.40200 \\ +0.09592 \\ -1.0655 \\ +0.05833 \\ +0.59812 \\ +0.13189 \\ -3.5195 \\ -0.13536 \\ -3.2432 \end{bmatrix} + P_o \begin{bmatrix} -0.00832 \\ +0.03317 \\ -0.01978 \\ +0.15175 \\ -0.04818 \\ -0.60535 \\ -0.08734 \\ +2.5202 \\ -0.09119 \\ 2.3355 \end{bmatrix} + \left\{ \begin{bmatrix} -1674.2 \\ -294.8 \\ -5802.3 \\ +28353. \\ -37934 \\ -21412. \\ -2072.4 \\ -9136.3 \\ -1597.9 \\ -12898. \end{bmatrix}_{\text{Start-up}} \text{or} \begin{bmatrix} +713.76 \\ -1809.9 \\ +1912.5 \\ -12763. \\ -4792.2 \\ +4366.6 \\ +656.37 \\ -1898.5 \\ 54542 \\ -663.87 \end{bmatrix}_{\text{Shutdn Fluid}} \text{or} \begin{bmatrix} +1816.4 \\ +2735.6 \\ +6391.3 \\ -30646 \\ +452.55 \\ +24364 \\ +2294.1 \\ +10502. \\ 1765.6 \\ +8466.3 \end{bmatrix}_{\text{Shutdown}} \right\}$$

$$V = \frac{-77.710\,P + 8.3183\,P_o + \left[(+354.09)_{SU} \text{ or } (+49.770)_{SDF} \text{ or } (-144.40)_{SD} \right] 10^{-3}}{14.728 + 18.400\,E/E_B}$$

Bolt Tensioning

$$\begin{bmatrix} M_c \\ M'_c \\ \bar{H}_1 \\ M_1 \\ H_2 \\ M'_2 \\ H_3 \\ M'_3 \\ H_v \\ M'_v \\ V \end{bmatrix} = F \begin{bmatrix} +0.06404 \\ -0.44540 \\ +0.11285 \\ -1.2159 \\ 0 \\ 0 \\ +0.17073 \\ -4.7299 \\ +0.17665 \\ -4.3707 \\ 0 \end{bmatrix}$$

Vessel Overpressure

$$\begin{bmatrix} H_c \\ M_c \\ \bar{H}_1 \\ M_1 \\ H_2 \\ M_2 \\ H_3 \\ M_3 \\ H_v \\ M_v \\ V \end{bmatrix} = P \begin{bmatrix} -0.86351 \\ -23.696 \\ -7.6880 \\ +8.9730 \\ -2.8312 \\ -50.275 \\ -3.3544 \\ +79.234 \\ -3.3582 \\ +72.299 \\ 0 \end{bmatrix} + F \begin{bmatrix} +0.05595 \\ -0.40200 \\ +0.09592 \\ -0.6655 \\ +0.05833 \\ +0.59812 \\ +0.13189 \\ -3.5195 \\ -0.13536 \\ -3.2432 \\ 0 \end{bmatrix} + P_i \begin{bmatrix} -0.00832 \\ +0.03317 \\ -0.01978 \\ +0.15175 \\ -0.04818 \\ -0.60535 \\ -0.08734 \\ +2.5202 \\ -0.09119 \\ 2.3355 \\ 0 \end{bmatrix}$$

C.0 Detailed Analysis

C.5 Continuity Load Solution (Peak)

Continuity loads are summarized as follows:

Normal Operations

$$\begin{bmatrix} H_c \\ H_c \\ \bar{H}_1 \\ H_1 \\ H_2 \\ H_3 \\ H_3 \\ H_4 \\ H_4 \end{bmatrix} = P \begin{bmatrix} -0.86351 \\ -23.696 \\ -7.6880 \\ +8.9730 \\ -2.8312 \\ -50.275 \\ -3.3544 \\ +79.234 \\ +3.3582 \\ +72.299 \end{bmatrix} + F \begin{bmatrix} +0.05595 \\ -0.40200 \\ +0.09592 \\ -1.0655 \\ +0.0583 \\ +0.59812 \\ +0.13189 \\ -3.5195 \\ -0.13536 \\ -3.2432 \end{bmatrix} + P_o \begin{bmatrix} -0.00832 \\ +0.03317 \\ -0.01978 \\ +0.15175 \\ -0.04818 \\ -0.60535 \\ -0.08734 \\ +2.5202 \\ +0.09119 \\ +2.3355 \end{bmatrix} + \left\{ \begin{bmatrix} -1275.4 \\ -7977.0 \\ -5744.8 \\ +20004. \\ -775.25 \\ -25263. \\ -3531.7 \\ -37804. \\ +2540.5 \\ -44015 \end{bmatrix}_{\text{Start-up}} \text{or} \begin{bmatrix} +549.31 \\ +821.05 \\ +1931.5 \\ -9269.2 \\ +98.486 \\ +5811.6 \\ +1259.6 \\ +9187.6 \\ +941.34 \\ +11442 \end{bmatrix}_{\text{Shutdn Fluid}} \text{or} \begin{bmatrix} 1397.3 \\ 8894.0 \\ +6326.1 \\ -21878 \\ +865.79 \\ +28367. \\ +3802.4 \\ +40825 \\ 2738.3 \\ 49016 \end{bmatrix}_{\text{Shutdown}} \right\}$$

$$V = \frac{-77.710\,P + 83183\,P_o + \{(+438.25)_{14} \text{ or } (+15.920)_{300} \text{ or } (-233.04)_{10}\}\,10^3}{+14.728 \qquad +18.400\ E/E_B}$$

Unit Tensioning

$$\begin{bmatrix} H_c \\ H_c \\ \bar{H}_1 \\ H_1 \\ H_2 \\ H_2 \\ H_3 \\ H_3 \\ H_4 \\ V \end{bmatrix} = F_T \begin{bmatrix} +0.06404 \\ -0.44540 \\ +0.11285 \\ -1.2159 \\ 0 \\ 0 \\ +0.17073 \\ -4.7299 \\ +0.17665 \\ -4.3707 \\ 0 \end{bmatrix}$$

Vessel Overpressure

$$\begin{bmatrix} H_c \\ H_c \\ \bar{H}_1 \\ H_1 \\ H_2 \\ H_2 \\ H_3 \\ H_3 \\ H_4 \\ V \end{bmatrix} = P \begin{bmatrix} -0.86351 \\ -23.696 \\ -7.6880 \\ +8.9730 \\ -2.8312 \\ -50.275 \\ -3.3544 \\ +79.234 \\ +3.3582 \\ 72.299 \\ 0 \end{bmatrix} + 1F \begin{bmatrix} +0.05595 \\ -0.4020 \\ +0.09592 \\ -1.0655 \\ +0.0583 \\ +0.59812 \\ +0.13189 \\ -3.5195 \\ -0.13536 \\ -3.2432 \\ 0 \end{bmatrix} + 1P_o \begin{bmatrix} -0.00832 \\ +0.03317 \\ -0.01978 \\ +0.15175 \\ -0.04818 \\ -0.60535 \\ -0.08734 \\ +2.5202 \\ +0.09119 \\ +2.3355 \\ 0 \end{bmatrix}$$

C.0 Detailed Analysis

C.6 Operating Loads P+S & Peak

Combining applied loads (Ref C.2) with continuity loads (Ref C.5) gives the total loads at any operating condition. First, it is necessary to determine the continuity bolt load (V), bolt preload, and the resulting total bolt load for normal operating conditions, the bolt preload (F_c) is determined as a function of the required sealing load at design conditions. Thus, where

$$F_{design} = \frac{1}{R_F}\left(\frac{1}{2}PR_{oi}^2 + 2F_oR_B\right) = \underline{69.528}$$

$$V_{design} = \frac{-77.710\,P}{14.728 + 18.400\,E_{design}/E_B} = -2.9321$$

$$F_p = \frac{E_{atm}}{E_{design}}(F - V) = 1.0653(72.460) = \underline{78.641}\ \#/in$$

$F_o = 1000\ \#/in$
$P = 1250$ psi
$E_{atm} = 27.9 \times 10^6$
$E_{design} = 27.55 \times 10^6$
$E_B = 27.55 \times 10^6$

and for hydro preload,

$$F_{HYDRO} = \frac{1}{R_F}\left(\frac{1}{2}PR_{oi}^2 + 2F_oR_B\right) = \underline{86.432}$$

$$V_{Hydro} = \frac{-77.71\,P}{33.128} = -3.6710$$

$$F_{PH} = (F - V) = \underline{90.103}$$

$F_o = 1000\ \#/in$
$P = 1562.5$ psi
$E_{atm} = 27.9 \times 10^6$
$E_{hydro} = 27.9 \times 10^6$
$E_B = 27.9 \times 10^6$

From Part C.2, bolt tensioning loads are obtained from Birch graphs (Ref. 23) as

$F_{DT} = \underline{104.59}$ Normal Conditions
$F_{HT} = \underline{119.84}$ Hydro Test

From Part C.2, vessel compressive loads are

$$F_{OP} = P_{OP}\left(\frac{R_{oi}^2}{2R_i}\right) = 1.375\left[\frac{114.00^2}{2(120.125)}\right] = \underline{74.379}$$

C.0 Detailed Analysis

C.6 Operating Loads (P+S)

With bolt preloads known, operating bolt loads for normal conditions and hydro pressure test are calculated.

$$F = F_P \frac{E_{OT}}{E_{AM}} + V \quad ; \quad V = \frac{-77.710p + 8.3183 P_o + \{(+354.09^{SU})\alpha_{SU}(+49.770^{SDC})\alpha_{SD}(-144.40^{SD})\}}{14.728 + 18.40 E_{OT}/E_B} = \frac{-77.710P + 8.3183 R_i E_T}{14.728 + 18.40 E_{OT}/E_{AM}}$$

Equation	Condition	Design Pressure Test	Steady State Operation	Startup	Shutdown Flooding	Shutdown	Rapid Heating	Rapid Cooling	Inner Seal Leakage	Hydro Pressure Test
T_F	Ref. Flange Temp. (°F)	100	546	422.9	517.4	235.0	546	573	546	100
T_B	Ref. Bolt Temp. (°F)	100	546	290.5	536.0	353.0	546	573	546	100
E_{AM}	$(E \times 10^{-6})_{100°F}$	29.9	29.9	29.9	29.9	29.9	29.9	29.9	29.9	29.9
E_{OT}	$(E \times 10^{-6})_{T_F}$	29.9	27.72	28.46	27.90	29.32	27.72	27.55	27.72	29.9
E_B	$(E \times 10^{-6})_{T_B}$	29.9	27.72	29.05	27.78	28.79	27.72	27.55	27.72	29.9
P	Pressure (psi)	1.25	1.00	1.00	0.185	0	1.25	0.185	1.00	1.565
P_o	Seal leakage Load (#/in)	0	0	0	0	0	0	0	1.5	0
$E\alpha_T$	Temp. Ref. $\times 10^{-3}$	0	0	+354.09	+49.770	-144.40	0	0	0	0
D_T	$14.728 + 18.40 \frac{E_{OT}}{E_B}$	33.128	33.128	32.755	33.207	33.467	33.128	33.128	33.128	33.128
N_T	$-77.710P + 8.3183 P_o + E\alpha_T$	-97.138	-77.710	+276.38	+35.394	-144.40	-97.138	-14.376	-65.232	-121.62
V	N_T/D_T (#/in)	-2.9322	-2.3457	+8.438	+1.0658	-4.3147	-2.9322	-0.43395	-1.9691	-3.6712
F_P	Preload (#/in)	78.641	78.641	78.641	78.641	78.641	78.641	78.641	78.641	90.103
F	$F_P \frac{E_{OT}}{E_{AM}} + V$ (#/in)	75.709	70.567	83.291	74.446	72.800	69.975	72.026	70.938	86.431

COMBUSTION ENGINEERING, INC.
ENGINEERING DEPARTMENT, CHATTANOOGA, TENN.
CHARGE NO 224" HWK
DESCRIPTION Closure Region
NUMBER C-ENG 1131
SHEET 61 OF 61
DATE 11-30-70 BY TP
CHECK DATE 11-30-70 BY TB

C.0 Detailed Analysis

C.6 Operating Loads (PEAK)

With bolt preloads known, operating bolt loads for normal conditions and hydro pressure test are calculated.

$$F = F_P \frac{E_{OPT}}{E_{ARM}} + V \quad ; \quad V = \frac{-77.710\,P + 8.3183\,P_O + \{(+438.25^{ST}) or (+15.920^{SDF}) or (-233.04^{SD})\}^{10^3}}{14.728 + 18.400\,E_{OPT}/E_B} = \frac{-77.710\,P + 8.3183\,B_1 E_T}{14.728 + 18.400\,E_{OPT}/E_B}$$

Factor	Condition	Design Pressure Test	Steady State Operation	Startup	Shutdown Flooding	Shutdown	Rapid Heating	Rapid Cooling	Inner-Seal Leakage	Hydro Pressure Test
T_F	Ref. Flange Temp. (°F)	100	546	422.9	517.4	235.0	546	573	546	100
T_B	Ref. Bolt Temp. (°F)	100	546	290.5	536.0	353.0	546	573	546	100
E_{ARM}	$(E \times 10^{-6})_{100°F}$	29.9	29.9	29.9	29.9	29.9	29.9	29.9	29.9	29.9
E_{OPT}	$(E \times 10^{-6})_{T_F}$	29.9	27.72	28.46	27.90	29.32	27.72	27.55	27.72	29.9
E_B	$(E \times 10^{-6})_{T_B}$	29.9	27.72	29.05	27.78	28.79	27.72	27.55	27.72	29.9
P	Pressure (psi)	1.25	1.00	1.00	.185	0	1.25	0.185	1.00	1.565
P_O	Seal Leakage Load (#/in)	0	0	0	0	0	0	0	1.5	0
ET_T	Temp. Ref. $\times 10^3$	0	0	+438.25	+15.920	-233.04	0	0	0	0
D_V	$14.728 + 18.40\,E_{OPT}/E_B$	+33.128	+33.128	+32.755	+33.207	+33.467	+33.128	+33.128	+33.128	+33.128
N_V	$-77.710\,P + 8.3183\,P_O + ET_T$	-97.138	-77.710	+360.54	+1.544	-233.04	-97.138	-14.376	-65.232	-121.62
V	N_V/D_V (#/in)	-2.9322	-2.3457	+11.007	+0.0465	-6.9633	-2.9322	-0.43395	-1.9691	-3.6712
F_P	Applied (#/in)	+78.641	78.641	78.641	78.641	78.641	78.641	78.641	78.641	90.103
F	$F_P \frac{E_{OPT}}{E_{ARM}} + V$ (#/in)	75.709	70.567	85.860	73.426	70.152	64.975	72.026	70.938	86.431

COMBUSTION ENGINEERING, INC.
ENGINEERING DEPARTMENT, CHATTANOOGA, TENN.
CHARGE NO. 224" Flgd. NUMBER S-701 CALC 1139
DESCRIPTION Closure Region SHEET 62 OF 4-54
DATE 11-30-70 BY TP
CHECK DATE 11-30-70 BY JB

COMBUSTION ENGINEERING, INC.
ENGINEERING DEPARTMENT, CHATTANOOGA, TENN.
CHARGE NO. 224° BWR
DESCRIPTION Closure Region
NUMBER
SHEET 63 OF A 55
DATE 1-30-70 BY JB
CHECK DATE 1-30-70 BY JP

C.0 Detailed Analysis

C.6 Operating Loads (Pts & Peak)

Operating Loads are summarized below for the various operating conditions used in evaluation of the structure. Loads are given for both the primary plus secondary and the peak categories, where radial gradient effects are included only in the peak category.

Load / Condition	Design Operation	Design Bolt Tensioning	Design Bolt Preload	Design Pressure Test	Steady State Operation	Inner Seal Leakage	Vessel Over-Pressure	Startup Pts / Peak	Shutdn Flood Pts / Peak	End of Shutdn Pts / Peak	Rapid Heating	Rapid Cooling	Hydro Bolt Tensioning	Hydro Bolt Preload	Hydro Pressure Test
P	1.25	0	0	1.25	1.00	1.00	1.375	1.00	0.185	0	1.25	0.185	0	0	1.565
F	69.528	104.59	78.641	75.709	70.567	70.938	74.379	83.291 / 85.360	74.446 / 73.426	72.809 / 70.152	69.975	72.026	119.84	90.103	86431
P_o	0	0	0	0	0	1.50	0	0	0	0	0	0	0	0	0
B	2.00	109.48	82.32	8.47	17.24	16.13	0	30.56 / 33.25	67.45 / 66.39	76.21 / 73.44	2.47	64.32	125.45	94.32	1.85

C.0 Detailed Analysis

C.6 Operating Loads Peak

In addition to the operating loads on the preceeding pages, thermal skin stresses due to temperature differences must be calculated for the peak category. $\sigma_T = \frac{E\alpha_i}{1-\mu}\left(\bar{T} - T_{a,b}\right)$; where temperatures are from Part C.2.3.

Cond.	Vessel Overpressure		Startup		Shut down Flooding		Shutdown		Rapid Heating		Rapid Cooling	
Surface	a	b	a	b	a	b	a	b	a	b	a	b
$\bar{\sigma}_c$	27.7		27.8		28.2		29.7		27.7		27.6	
α_{ci}	8.06		8.01		7.77		6.26		8.06		8.20	
ΔT_c	-39.0	0	-8.4	+5.6	+6.1	-3.2	+8.6	-4.7	-27.0	0	+19.8.0	0
σ_c	-12.42	0	-2.68	+1.78	+1.91	-1.00	+2.28	-1.25	-8.60	0	+64.25	0
$\bar{\sigma}_1$	27.7		28.1		28.0		29.6		27.7		27.6	
α_{1i}	8.06		7.79		7.39		6.54		8.06		8.20	
ΔT_1	-39.0	0	-56.8	+62.9	+16.0	-15.4	+62.2	-74.4	-27.0	0	+182.0	0
σ_1	-12.42	0	-17.77	+21.56	+5.05	-4.86	+17.38	-20.62	-8.60	0	+64.25	0
$\bar{\sigma}_3$	27.7		28.1		28.0		29.6		27.7		27.6	
α_{3i}	8.06		7.82		7.70		6.49		8.06		8.20	
ΔT_3	-39.0	0	-49.5	+29.0	+17.4	-9.4	+52.5	-30.9	-27.0	0	+178.0	0
σ_3	-12.42	0	-15.56	+7.11	+5.49	-2.97	+14.40	-9.48	-8.60	0	+64.25	0
$\bar{\sigma}_v$	27.7		28.0		28.0		29.6		27.7		27.6	
α_{vi}	8.06		7.85		7.90		6.47		8.06		8.20	
ΔT_v	-39.0	0	-44.5	+24.8	+16.3	-8.5	+46.8	-26.3	-27.0	0	+198.0	0.
σ_v	-12.42	0	-13.99	+7.79	+5.15	-2.68	+12.84	-7.21	-8.60	0	+64.25	0

COMBUSTION ENGINEERING, INC.
ENGINEERING DEPARTMENT, CHATTANOOGA, TENN.
CHARGE NO. 224" BWR
DESCRIPTION Closure Region

NUMBER S101 | CENC 1139
SHEET 64 | OF A-56
DATE 1-30-70 BY JB
CHECK DATE 1-30-70 BY TP

COMBUSTION ENGINEERING, INC.
ENGINEERING DEPARTMENT, CHATTANOOGA, TENN.
CHARGE NO. 224 BWR
DESCRIPTION Closure Region
NUMBER
SHEET 65 OF A 57
DATE 1-30-70 BY TB
CHECK DATE 1-30-70 BY TP

C.0 Detailed Analysis

C.7 Continuity Loads P+S & Peak

Continuity Loads obtained by substituting the operating loads in Part C.6 into the continuity equations in Part C.5 are summarized below for Primary plus Secondary and Peak categories.

Condition	Design Operation	Design Bolt Tensioning	Design Bolt Preload	Design Pressure Test	Steady State Operation	Inner Seal Leakage	Vessel Over-Pressure	Startup P+S / Peak	Shutdown Flooding P+S / Peak	End of Shutdown P+S / Peak	Rapid Heating	Rapid Cooling	Hydro Bolt Tensioning	Hydro Bolt Preload	Hydro Pressure Test
H_c	2.8107	6.6979	4.3999	3.1565	3.0847	3.0930	2.9742	2.1221 / 2.6650	4.7193 / 4.4977	5.8896 / 5.3327	2.8857	3.8701	7.6745	5.0413	3.4844
M_c	-57.570	-46.584	-31.614	-60.055	-52.064	-52.163	-62.482	-59.293 / -66.187	-36.121 / -33.080	-26.530 / -19.31	-57.750	-33.338	-53.317	-36.221	-71.830
H_1	-2.4409	11.803	7.5432	-2.3480	-0.91921	-0.91330	-3.4366	-5.2257 / -5.2722	7.4132 / 2.480	15.088 / 13.136	-2.8980	5.4864	13.524	8.6427	-3.7413
M_1	-62.866	-127.17	-83.792	-69.452	-66.216	-66.384	-66.913	-51.420 / -62.507	-70.425 / -85.845	-108.21 / -76.632	-63.342	-75.084	-145.71	-96.005	-78.050
H_2	0.51652	0	4.5871	.87706	1.2849	1.2843	.44558	1.6478 / 1.4017	3.7707 / 3.8576	4.6987 / 4.9581	.54260	3.6774	0	5.2556	.61064
M_2	-21.258	0	47.037	-17.561	-8.0676	-8.7537	-24.641	-21.870 / -24.183	39.595 / 40.428	67.907 / 70.331	-20.991	33.779	0	53.892	-26.984
H_3	4.9768	17.857	10.372	5.7920	5.9524	5.8704	5.1973	5.5581 / 44377	9.8543 / 10.323	11.875 / 13.055	5.0858	8.8387	20.460	11.883	6.1495
M_3	-145.66	-494.70	-276.77	-167.41	-169.12	-166.65	-152.83	-223.04 / -260.75	-249.25 / -234.57	-245.71 / -306.60	-147.23	-238.83	-566.83	-312.11	-180.19
H_V	5.2129	18.476	10.640	6.0495	6.1930	6.1065	5.4497	6.3173 / 5.7224	10.000 / 10.258	11.620 / 12.234	5.2734	9.1274	21.170	12.195	6.4428
M_V	-135.12	-457.13	-255.05	-155.16	-156.56	-154.26	-141.81	-210.23 / -250.18	-228.73 / -213.32	-221.44 / -180.52	-136.57	-220.22	-523.78	-292.22	-167.16

C.0 Detailed Analysis

C.7 Continuity Loads

In addition to the loads shown on the preceeding page, "restrained" deformations are required for calculation of stresses in the structure.

Deformations of the closure shell are obtained from the spherical shell equations (Ref 3, pg 474).

$R_1 = 114.28$
$t_1 = 3.50$
$\varphi_c = 69.23°$
$\cos\varphi_c = .93507$
$\sin\varphi_c = .35446$

$$\lambda = \left[3(1-\mu^2)\left(\frac{R_1}{t_1}\right)^2\right]^{1/4} = 7.345$$

$$K_1 = 1 - \frac{(1-2\mu)\cos\varphi_c}{2\lambda \sin\varphi_c} = .98968$$

$$K_2 = 1 - \frac{(1+2\mu)\cos\varphi_c}{2\lambda \sin\varphi_c} = .95872$$

$$E\Delta_c = H_c\left(\frac{\lambda R_1 \sin^2\varphi_c}{t_1}\right)\left(\frac{1}{K_1} + K_2\right) + M_c\left(\frac{2\lambda^2 \sin\varphi_c}{t_1 K_1}\right) = \underline{412.91 H_c + 29.126 M_c}$$

At Cuts I & III, deflections are taken from Part C.4

$$E\Delta_{11} = 2.8480\ \bar{H}_1 R_{11} + .18559\ M_1 R_{11} = \underline{316.70 \bar{H}_1 + 20.638\ M_1}$$

$$E\Delta_{43} = 1.4862\ H_3 R_4 + .06552\ M_3 R_4 = \underline{173.51 H_3 + 7.6495 M_3}$$

At the vessel shell-hub junction (cut "V") deflections are determined from cylindrical shell equations (ref.3 page 393).

$R_4 = 116.75$
$t_4 = 7.00$

$$\frac{1}{\beta} = \left[\frac{R_4^2 t_4^2}{3(1-\mu^2)}\right]^{1/4} = 22.236$$

$$D = \frac{E t_4^3}{12(1-\mu^2)} = 907.76 \times 10^6$$

$$E\Delta_V = \frac{E H_V}{2\beta^3 D} + \frac{E M_V}{2\beta^2 D} = \underline{175.01\ H_V + 7.8706\ M_V}$$

ENGINEERING DEPARTMENT, CHATTANOOGA, TENN. SHEET 62 OF A 59

CHARGE NO. 284" BWR DATE 12-19-69 BY JB

DESCRIPTION Closure Region CHECK DATE 1-30-70 BY TP

C.0 Detailed Analysis

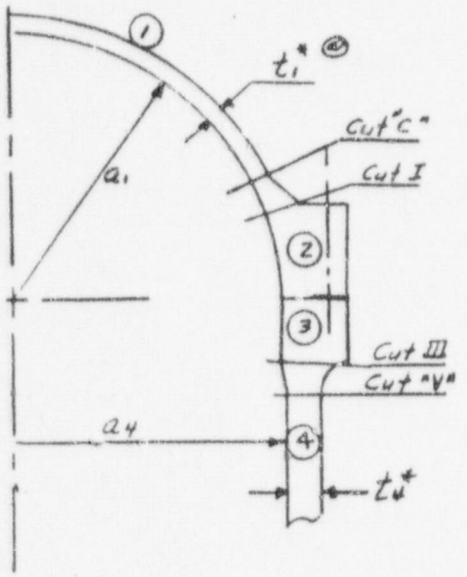
C.7 Continuity Loads P+S & Peak

"Restrained" deflections at cuts "c", I, III and "v" obtained by substituting the continuity Loads in Part C.7 into the equations on the preceeding page are summarized below for Primary plus Secondary and Peak categories.

Condition dcfl	Design Operation	Design Bolt Tensioning	Design Bolts Preloaded	Design Pressure Test	Steady State Operation	Inner Seal Leakage	Vessel Over-Pressure	Startup P+S / Peak	Shutdown Flooding P+S / Peak	4th Shutdown P+S / Peak	Rapid Heatup	Rapid Cooling	Hydro + Bolt Tensioning	Hydro Bolts Preloaded	Hydro Post Pressure
$E\Delta_c$	-516.22	1408.8	896.01	-445.80	-242.70	-242.18	-591.79	-850.74 / -827.4	896.57 / 893.68	1659.1 / 1635.4	-511.13	627.0	1614.2	1026.6	-653.3
$E\Delta_{II}$	-2228.3	1113.5	659.64	-2176.9	-1657.7	-1659.3	-2469.3	-2716.2 / -2959.7	481.74 / 598.02	1911.6 / 2166.0	-2225.1	187.98	1275.9	755.78	-2795.6
$E\Delta_{III}$	-250.68	-685.84	-317.59	-275.64	-260.89	-256.21	-267.26	-74.76 / -1224.6	-196.83 / -3.2376	184.37 / 684.89	-252.49	-286.42	-785.95	-383.88	-311.36
$E\Delta_v$	-151.17	-364.4	-144.57	-162.53	-148.41	-145.46	-162.42	-552.96 / -967.56	-50.083 / 116.38	240.57 / 720.30	-151.99	-135.86	-417.5	-165.64	-188.12

C.0 Detailed Analysis

C.8 Vessel Stresses



Categories of stress intensity included in the vessel stress calculations are:

General Primary Membrane Stress Intensity
Primary Local plus Bending Stress Intensity
Primary plus Secondary Stress Intensity Range
Peak Stress Intensity Range

Classification of loadings into the proper stress category, and evaluation of the stress intensities complys with rules of Article 9, Section III, ASME Code.

C.8.1 General Primary Membrane Stress Intensity

Comparison of geometries of each of the shell sections shows that maximum primary membrane stresses will be in either Element ① (Closure Shell) or Element ④ (Vessel Shell).

Component	Equation ⓐ	Load Condition	Stress ⓐ Intensity	Allowable Stress Intensity
Closure Shell Element ①	$S = \frac{P}{2}\left(\frac{a_1^2}{R_1 t_1^*} + 1\right)$	Design	21.9 ksi	S_m = 26.7 ksi @ 575 °F
		Hydro	27.4 ksi	0.90σ_y = 45.0 ksi @ 100 °F
Vessel Shell Element ④	$S = P\left(\frac{a_4^2}{R_4 t_4^*} + \frac{1}{2}\right)$	Design	21.8 ksi	S_m = 26.7 ksi @ 575 °F
		Hydro	27.3 ksi	0.90σ_y = 45.0 ksi @ 100 °F

C.8.2 Primary Local plus Bending Stress Intensity

Primary local plus bending stresses in the closure and vessel shells are equal to the primary membrane stresses. Primary local plus bending stresses at

Note ⓐ Minimum wall thickness t_1^* and t_4^* are used in the stress calculations to assure conservatism.

C.0 Detailed Analysis

C.8 Vessel Stresses

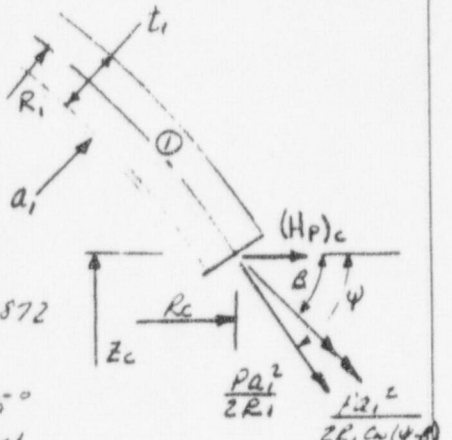
C.8.2 Primary Local plus Bending Stress Intensity

the closure shell-hub junction, and closure flange are calculated as follows. Adequacy of the vessel shell-flange region is shown by comparison to P+S stress intensity.

Element ① ~ Cut "C"

Change in direction of the line of force at the closure shell-hub junction generates a primary local stress when the structure is subjected to a pressure load. Since the angle of the load path changes along the length of the hub, it is assumed here that the angle of the load at the junction is equal to the average of the shell-hub and the hub-flange intersection angles, or where β is the angle of the load path and Ψ is the angle of the shell-hub intersection.

$$\beta = \frac{\Psi + \Phi}{2}$$



$R_1 = 114.28$ $\quad \Phi = 64.25°$ $\quad \lambda = \left[3(1-\mu^2)\left(\frac{R_1}{t_1}\right)^2\right]^{\frac{1}{4}}$

$a_1 = 112.44$ $\quad \cos\Phi = 0.4344$ $\quad = 7.3450$

$R_c = 106.86$ $\quad t_1 = 3.500"$

$Z_c = 40.5$ $\quad t_1^* = 3.250"$

$k_1 = 1 - \frac{1-2\mu}{2\lambda}\cot\Psi = 0.98968$ $\quad k_2 = 1 - \frac{1-2\mu}{2\lambda}\cot\Psi = 0.95872$

$\sin\Psi = \frac{R_c}{R_1} = 0.93507$ $\quad \cos\Psi = \frac{Z_c}{R_1} = 0.35439$

$\cot\Psi = \frac{Z_c}{R_c} = 0.37900$ $\quad \Psi = 69.249° \simeq 69.25°$

$\beta = \frac{1}{2}(\Psi + \Phi) = 66.75°$ $\quad \cos\beta = 0.39474$

$(\Psi - \beta) = 2.5°$ $\quad \cos(\Psi - \beta) = 0.99905$

$$(H_P)_c = \frac{Pa_1^2}{2R_1}\left(\frac{\cos\beta}{\cos(\beta-\Psi)} - \cos\Psi\right) = 2.2524P$$

$$(E\delta_P)_c = \frac{\lambda R_1 \sin^2\Psi}{t_1}\left(\frac{1}{k_1} + k_2\right)(H_P)_c = 930.06P$$

C.0 Detailed Analysis

C.8 Vessel Stresses

C.8.2 Primary Local plus Bending Stress Intensity

Element ① Cut "C" (Cont'd)

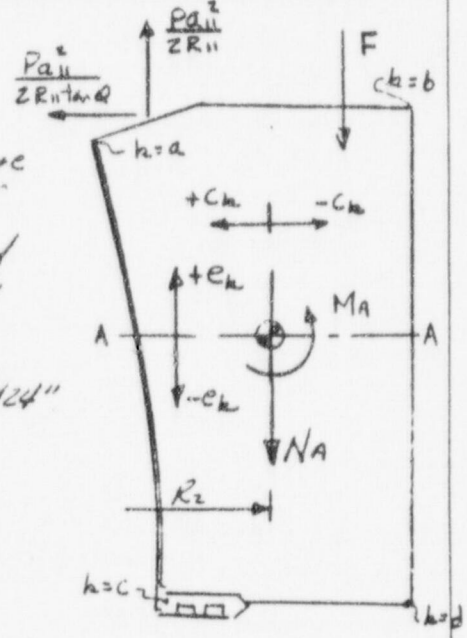
$$\sigma_x = \frac{Pa_i^2}{2R_i t_i^*} + \frac{(Hp)_c \cos\psi}{t_i^*} = P(17.020 + 0.2456) = 17.266P$$

$$\sigma_\theta = \frac{Pa_i^2}{2R_i t_i^*} + 4\frac{(Hp)_c \cos\psi}{t_i^*} + \frac{(ES_p)_c}{R_i \sin\psi} = P(17.020 + 0.07368 + 8.7035) = 25.977P$$

$$\sigma_r = -\frac{P}{2} \mp \frac{P}{2}$$

Condition	Pressure Psig	Surface	σ_x 17.266P	σ_θ 25.977P	σ_r -P/0	S_I $\sigma_{max} - \sigma_{min}$	Allowable Stress Intensity
Design	1.25	a	21.6	32.5	-1.3	33.8	$1.5 S_m = 40.0$
		b			0	32.5	@ 575°F
Code Hydro Test	1.565	a	27.0	40.7	-1.6	42.3	$1.35 \sigma_{yp} = 67.5$
		b			0	40.7	@ 100°F

Element ② - Closure Flange



Axial Load (N_A) and Moment (M_A) are assumed constant along length of flange. Bolt holes are compensated for by subtracting equivalent solid width, or

$$t_{h_c} = t_{actual} - \frac{N\pi d_w^2}{2\pi R_2} = t_{actual} - 2.424"$$

Stress at point "h_c" is

$$\sigma_x = \frac{N_A}{t_{h_c}} + \frac{12 M_A C_{h_c}}{t_{h_c}^3} \; ; \; \sigma_\theta = \mu\sigma_x + \frac{ES_{h_c}}{R_{h_c}}$$

$$\sigma_r = -\tfrac{1}{2}P \mp \tfrac{1}{2}P$$

where $N_A = \frac{Pa_{II}^2}{2R_2} - \frac{FR_F}{R_2} = 53.863P - 1.0236F$

$$M_A = \frac{(ES_2^*)_{P\&F} I_2}{R_2^2} = 1.2476(ES_2^*)_{P\&F}$$

C.0 Detailed Analysis

C.8 Vessel Stresses

C.8.2 Primary Local plus Bending Stress Intensity

Element ② - Closure Flange (Cont'd)

Including horizontal pressure component that was considered as part of the continuity load (H_1) in the deformation equations of Part C.2.2 gives

$$(H_P)_{II} = \frac{P a_{II}^2}{2 R_2 \tan\varphi} = \frac{(108.30)^2 P}{2(117.36)(2.0732)} = 24.102P$$

Using data from Part C.4,

$$ES_2 = P(956.32 - 358.17) - \frac{(H_P)_{II} R_2^2}{A_2} + 6.6213F$$
$$= 598.15P - 43.132(H_P)_{II} + 6.6213F = -441.42P + 6.6213F$$

$$ES_2^* = P(-214.46) + \frac{(H_P)_{II} R_2 e_{21}}{I_2} - 2.7159F$$
$$= -214.46P + 8.7706(H_P)_{II} - 2.7159F = +1.7494P - 2.7159F$$

$$\therefore M_A = 1.2476(ES_2^*) = 2.1826P - 3.4302F$$

Substituting pressure and temperature gives:

Condition	P	F	N_A	M_A	ES_2	ES_2^*
Design	1.25 ksi	69.528 #/in	-3.84	-235.77	-91.409	-186.64
Hydro	1.565 ksi	86.431 #/in	-4.175	-292.86	-118.54	-232.00

At $k = a$

$R_a = a_{II} + t_c = 108.52$ $\quad e_a = h_2 - e_{23} = 9.5415$

$C_a = R_2 - R_a = 8.54''$ $\quad t_a = 125.5 - R_a - 2.929 = 14.552$ $\quad (t_a^3 = 3084.1)$

At $k = b$

$R_b = 125.25$ $\quad e_b = e_{20} = 12.542$

$C_b = R_2 - R_b = -7.84$ $\quad t_b = t_a = 14.556$ $\quad (t_b^3 = 3087.1)$

C.0 Detailed Analysis

C.8 Vessel Stresses

C.8.2 Primary Local plus Bending Stress Intensity

Element ② ~ Closure Flange (Cont'd)

at $h = c$

$R_c = a_2 + t_c = 112.32"$ $\quad e_c = -e_{23} + 0.25 = -13.521"$

$c_c = R_2 - R_c = 5.04"$ $\quad t_c = 125.5 - R_c - 2.424 = 10.756"$ $(t_c' = 1244.4)$

at $h = d$

$R_d = 125.25$ $\quad e_d = -e_{23} + 0.25 = -13.521"$

$c_d = R_2 - R_c = -7.89$ $\quad t_d = t_c = 10.756"$ $(t_d' = 1244.4)$

Condition	Design Operation				Hydro Test			
Location (h)	a	b	c	d	a	b	c	d
Pressure (P)	1.25 ksi				1.565 ksi			
Bolt load (F)	69.528 kips/in				86.431 kips/in			
N_A	-3.84 kips/in				-4.175 kips/in			
M_A	-235.77 in-kips/in				-292.86 in-kips/in			
ES_2	-91.407 kips/in				-118.54 kips/in			
ES_2'	-186.24 kips/in				-232.00 kips/in			
t_h	14.556	14.556	10.756	10.756	14.556	14.556	10.756	10.756
c_h	2.64	-7.89	5.04	-7.89	8.84	-7.89	5.04	-7.89
e_h	9.8415	12.542	-13.521	-13.521	9.8415	12.542	-13.521	-13.521
$ES_h = ES_2 - ES_2' e_h$	+1745.4	2249.4	-2615.0	-2615.0	2164.7	2791.2	-3255.4	-3255.4
σ_x N_A/t_h	-0.3	-0.3	-0.4	-0.4	-0.3	-0.3	-0.4	-0.4
σ_x $12M_A c_h/t_h^3$	-8.1	+7.2	-11.5	+17.9	-10.1	+9.0	-14.2	+22.3
σ_x Σ	-8.4	+6.9	-11.9	+17.5	-10.4	+8.7	-14.6	+21.9
σ_θ M_A/R_h	-2.5	+2.0	-3.6	+5.3	-3.1	+2.6	-4.4	+6.6
σ_θ ES_h/R_h	+16.1	+18.0	-23.3	-20.9	+19.9	+22.3	-29.0	-26.0
σ_θ Σ	+13.6	+20.0	-26.9	-15.6	+16.8	+24.9	-33.4	-19.4
$\sigma_r = -P/2$	-0.6	-0.6	-0.6	-0.6	-0.8	-0.8	-0.8	-0.8
$S_I =$	-22.0	+20.6	-26.3	+33.1	-27.2	+24.1	-32.6	+41.3

$S_{MAX} = 33.1 < 1.5\ S_m = 40.0$ ⓐ Design Condition

$S_{MAX} = 41.3 < 1.35 \sigma_{yp} = 67.5$ ⓑ Hydro Test

C.0 Detailed Analysis

C.8 Vessel Stresses

C.8.2 Primary Local plus Bending Stress Intensity

Adequacy of the vessel shell-flange regions for primary local plus bending requirements is shown by primary plus secondary stress intensity calculations of Art C.8.3 where,

Element ④ Cut III

S_{max} = 20.5 ksi < 1.5Sm = 40.0 ksi @ Design Conditions
S_{max} = 25.5 ksi < 1.35σ_{yp} = 67.5 ksi @ Hydro Test

Element ④ Cut "V"

S_{max} = 29.8 ksi < 1.5Sm = 40.0 ksi @ Design Conditions
S_{max} = 37.0 ksi < 1.35σ_{yp} = 67.5 ksi @ Hydro Test

COMBUSTION ENGINEERING, INC.
ENGINEERING DEPARTMENT, CHATTANOOGA, TENN.
CHARGE NO. 224" PWR
DESCRIPTION Closure Region

NUMBER S-101 | CENC 1139
SHEET 70 | A-66
DATE 1-30-70 BY JB
CHECK DATE 1-30-70 BY TP

C.0 Detailed Analysis

C.8 Vessel Stresses

C.8.3 Primary plus Secondary Stress Intensity

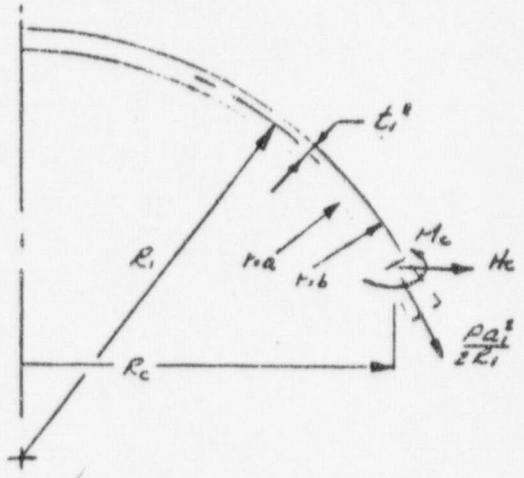
Element @ Cut "C"

$$\sigma_{xc} = \frac{Pa_i^2}{2R_i t_i^2} + \frac{H_c C_m P_c}{t_i^2} \pm \frac{6M_c}{(t_i^2)^2}$$

$$\sigma_{\theta c} = \frac{Pa_i^2}{2R_i t_i^2} + \frac{\mu H_c C_m P_c}{t_i^2} \pm \frac{6\mu M_c}{(t_i^2)^2} + \frac{E\bar{\Delta}_c}{R_c}$$

$$\sigma_{rc} = -\frac{P}{2} \mp \frac{P}{2}$$

$S_{x\theta} = \sigma_x - \sigma_\theta$ $S_{xr} = \sigma_x - \sigma_r$ $S_{\theta r} = \sigma_\theta - \sigma_r$



Condition	Design Operation		Design Bolt Tensioning		Design Bolts Preloaded		Design Pressure Test		Steady State Operation		Inner Seal Leakage	
Surface (+)	a	b	a	b	a	b	a	b	a	b	a	b
P	1.25		0		0		1.25		1.00		1.00	
F	69.528		104.59		78.64		75.709		70.567		70.938	
$E\bar{\Delta}_c$	-516.22		1408.8		896.01		-445.80		-242.70		-242.18	
H_c	2.8107		6.6979		4.3999		3.1565		3.0847		3.0930	
M_c	-57.670		-46.584		-31.614		-60.055		-52.064		-52.163	
$Pa_i^2/2R_i t_i^2$	21.27		0		0		21.27		17.02		17.02	
$+ H_c C_m P_c / t_i^2$	.31		.73		.48		.35		.34		.34	
$\pm 6M_c/(t_i^2)^2$	-32.70	32.70	-26.46	26.46	-17.96	17.96	-34.11	34.11	-29.57	29.57	-29.63	29.63
$\sigma_x = \Sigma$	-11.12	54.28	-25.73	27.19	-17.47	17.47	-12.49	55.73	-12.22	46.93	-12.27	46.99
$Pa_i^2/2R_i t_i^2$	21.27		0		0		21.27		17.02		17.02	
$+ \frac{\alpha H_c C_m P_c}{t_i^2}$	.09		.22		.14		.10		.10		.10	
$\pm 6\mu M_c/(t_i^2)^2$	-9.81	9.81	-7.94	7.94	-5.39	5.39	-10.23	10.23	-8.87	8.87	-8.89	8.89
$E\bar{\Delta}_c/R_c$	-4.83		13.18		8.38		-4.17		-2.27		-2.27	
$\sigma_\theta = \Sigma$	6.72	26.35	5.46	21.34	3.14	13.92	6.97	27.44	5.98	23.72	5.97	23.74
$\sigma_r = -\frac{P}{2} \mp \frac{P}{2}$	-1.25	0	0	0	0	0	-1.25	0	-1.00	0	-1.00	0
$S_{x\theta} = \sigma_x - \sigma_\theta$	-17.8	27.9	-31.2	5.85	-20.6	4.5	-19.5	28.3	-18.2	23.2	-18.2	23.2
$S_{xr} = \sigma_x - \sigma_r$	-9.9	54.3	-25.7	27.2	-17.5	18.4	-11.2	55.7	-11.2	46.9	-11.3	47.0
$S_{\theta r} = \sigma_\theta - \sigma_r$	8.0	26.3	5.5	21.3	3.1	13.9	8.2	27.4	7.0	23.7	7.0	23.7

C.0 Detailed Analysis

C.8 Vessel Stresses

C.8.3 Primary plus Secondary Stress Intensity

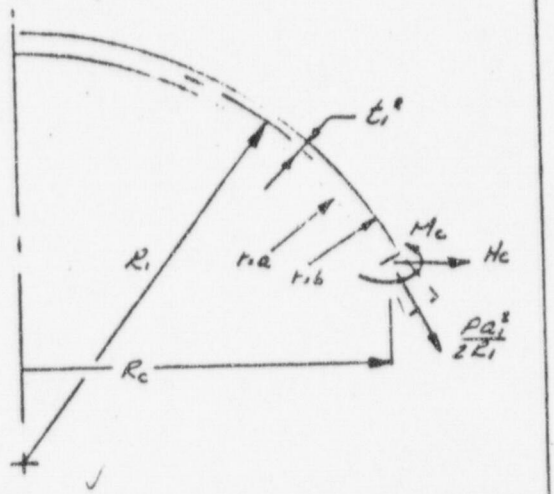
Element ① Cut "C"

$$\sigma_{xc} = \frac{pa_i^2}{2R_i t_i^2} + \frac{H_c \cos\theta_c}{t_i^2} \pm \frac{6M_c}{(t_i^2)^2}$$

$$\sigma_{\theta c} = \frac{pa_i^2}{2R_i t_i^2} + \frac{\mu H_c \cos\theta_c}{t_i^2} \pm \frac{6\mu M_c}{(t_i^2)^2} + \frac{E\bar{\Delta}_c}{R_c}$$

$$\sigma_{rc} = -\frac{p}{2} \mp \frac{p}{2}$$

$S_{x\theta} = \sigma_x - \sigma_\theta \qquad S_{xr} = \sigma_x - \sigma_r \qquad S_{\theta r} = \sigma_\theta - \sigma_r$



Condition	Vessel Over-Pressure		Startup		Shutdown Flooding		End of Shutdown		Rapid Heating		Rapid Cooling	
Surface (r)	a	b	a	b	a	b	a	b	a	b	a	b
p	1.375		1.00		.185		0		1.25		.185	
F	74.379		83.291		74.446		72.800		69.975		72.026	
$E\bar{\Delta}_c$	-591.79		-850.74		896.57		1659.1		-511.13		627.00	
H_c	2.9792		2.1221		4.7193		5.8896		2.8357		3.8701	
M_c	-62.482		-59.293		-36.121		-26.530		-57.750		-33.338	
$Pa_i^2/2R_i t_i^2$	23.40		17.02		3.15		0		21.27		3.15	
$+ H_c\cos\theta_c/t_i^2$	.32		.23		.52		.65		.31		.42	
$\pm 6M_c/(t_i^2)^2$	-35.49	35.49	-33.68	33.68	-20.52	20.52	-15.07	15.07	-32.80	32.80	-18.93	18.93
$\sigma_x = \Sigma$	-11.76	59.22	-16.43	50.93	-16.85	24.18	-14.42	15.72	-11.22	54.89	-15.36	22.51
$Pa_i^2/2R_i t_i^2$	23.40		17.02		3.15		0		21.27		3.15	
$+ \mu H_c\cos\theta_c/t_i^2$	.10		.07		.16		.19		.09		.13	
$\pm 6\mu M_c/(t_i^2)^2$	-10.65	10.65	-10.10	10.10	-6.16	6.16	-4.52	4.52	-9.84	9.84	-5.68	5.68
$E\bar{\Delta}_c/R_c$	-5.54		-7.96		8.39		+15.53		-4.78		5.87	
$\sigma_\theta = \Sigma$	7.31	28.61	-.98	19.23	5.54	17.85	11.20	20.24	6.74	26.43	3.46	14.82
$\sigma_r = -\frac{p}{2} \mp \frac{p}{2}$	-1.38	0	-1.00	0	-.18	0	0	0	-1.25	0	-.18	0
$S_{x\theta} = \sigma_x - \sigma_\theta$	-19.1	30.6	-15.4	31.7	-22.4	6.3	-25.6	-4.5	-18.0	28.0	-18.8	7.7
$S_{xr} = \sigma_x - \sigma_r$	-10.4	59.2	-15.4	50.9	-16.7	24.2	-14.4	15.7	-10.0	54.4	-15.2	22.5
$S_{\theta r} = \sigma_\theta - \sigma_r$	8.7	28.6	0	19.2	5.7	17.8	11.2	20.2	8.0	26.4	3.6	14.8

COMBUSTION ENGINEERING, INC.
ENGINEERING DEPARTMENT, CHATTANOOGA, TENN.
CHARGE NO. 224" BWR
DESCRIPTION Closure Repair

NUMBER S-101 | CENC 1139
SHEET 22 | A-67
DATE 12-30-70 BY JB
CHECK DATE 1-30-70 BY JP

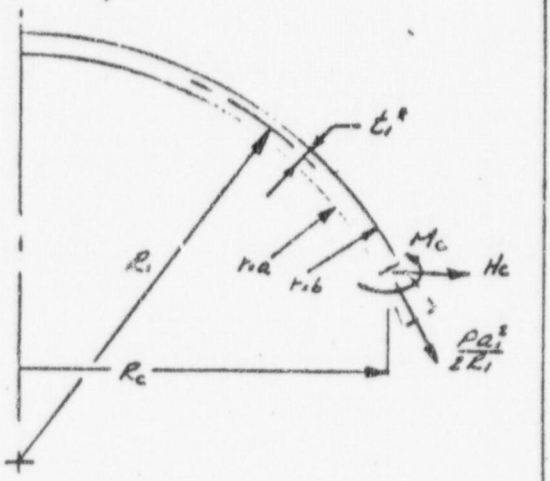
C.0 Detailed Analysis
C.B Vessel Stresses
C.B.3 Primary plus Secondary Stress Intensity
Element ① Cut "C"

$$\sigma_{xc} = \frac{Pa_i^2}{2R_i t_i^2} + \frac{H_c \cos\phi_c}{t_i^2} \pm \frac{6M_c}{(t_i^2)^2}$$

$$\sigma_{\theta c} = \frac{Pa_i^2}{2R_i t_i^2} + \frac{\mu H_c \cos\phi_c}{t_i^2} \pm \frac{6\mu M_c}{(t_i^2)^2} + \frac{E\bar{\delta}_c}{R_c}$$

$$\sigma_{rc} = -\frac{P}{2} \mp \frac{P}{2}$$

$S_{x\theta} = \sigma_x - \sigma_\theta$ $S_{xr} = \sigma_x - \sigma_r$ $S_{\theta r} = \sigma_\theta - \sigma_r$



Condition	Hydro Bolt Tensioning		Hydro Bolt Preload		Hydro Pressure Test							
Surface (r)	a	b	a	b	a	b	a	b	a	b	a	b
P	0		0		1,665							
F	119.84		90.103		86.481							
$E\bar{\Delta}_c$	1614.2		1026.6		-653.35							
H_c	7.6745		5.0413		3.4844							
M_c	-53.377		-36.221		-71.830							
$Pa_i^2/2R_i t_i^2$	0		0		26.64							
$+ H_c \cos\phi_c / t_i^2$	+.84		.55		.38							
$\pm 6M_c/(t_i^2)^2$	-30.32	+30.32	-20.57	20.57	-40.80	40.80						
$\sigma_x = \Sigma$	-29.48	31.16	-20.02	21.13	-13.78	67.82						
$Pa_i^2/2R_i t_i^2$	0		0		26.64							
$+ \frac{\mu H_c \cos\phi_c}{t_i^2}$	+.25		.17		.11							
$\pm 6\mu M_c/(t_i^2)^2$	-9.10	+9.10	-6.17	6.17	-12.24	12.24						
$E\bar{\Delta}_c/R_c$	15.11		9.61		-6.11							
$\sigma_\theta = \Sigma$	+6.26	24.46	3.60	15.94	8.40	32.88						
$\sigma_r = -\frac{P}{2} \mp \frac{P}{2}$	0	0	0	0	-1.56	0		0		0		0
$S_{x\theta} = \sigma_x - \sigma_\theta$	-35.7	6.7	-23.6	5.2	-22.2	34.9						
$S_{xr} = \sigma_x - \sigma_r$	-29.5	31.2	-20.0	21.1	-12.2	67.8						
$S_{\theta r} = \sigma_\theta - \sigma_r$	6.3	24.5	3.6	15.9	9.96	32.9						

COMBUSTION ENGINEERING, INC.
ENGINEERING DEPARTMENT, CHATTANOOGA, TENN.
CHARGE NO. 224" FINAL

DESCRIPTION Classic Design

NUMBER S-101 | CENC 1139
SHEET 73 | A-68
DATE 12-30-70 BY JB
CHECK DATE 1-30-70 BY TP

C.0 Detailed Analysis

C.6 Vessel Stresses

C.6.3 Primary plus Secondary Stress Intensity

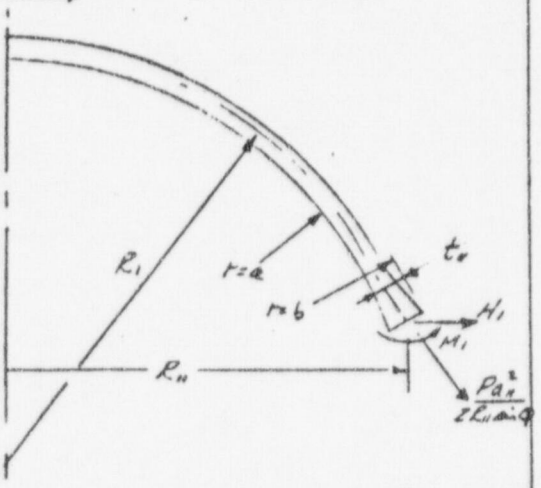
Element ① Cut I

$$\sigma_{x11} = \frac{Pa_{11}^2}{2R_{11}t_{11}\cos\phi} + \frac{H_1\cos\phi}{t_{11}} \pm \frac{6M_1}{t_{11}^2}$$

$$\sigma_{\theta 11} = \frac{Pa_{11}^2}{2R_{11}t_{11}\cos\phi} + \frac{\mu H_1\cos\phi}{t_{11}} \pm \frac{6\mu M_1}{t_{11}^2} + \frac{E\bar{\delta}_{11}}{R_{11}}$$

$$\sigma_{r11} = -\frac{P}{2} \mp \frac{P}{2}$$

$$S_{x\theta} = \sigma_x - \sigma_\theta \qquad S_{xr} = \sigma_x - \sigma_r \qquad S_{\theta r} = \sigma_\theta - \sigma_r$$



condition	Design Operation		Design Bolt Tensioning		Design Bolt Preload		Design Pressure Test		Steady State Operation		Inner Seal Leakage	
Surface (1)	a	b	a	b	a	b	a	b	a	b	a	b
P	1.25		0		0		1.25		1.00		1.00	
F	69.528		104.59		78.641		75.709		70.567		70.938	
$E\bar{\delta}_1$	-2228.8		+1113.5		+659.64		-2176.9		-1657.7		-1659.3	
H_1	-2.9409		11.803		7.5432		-2.3480		-0.91921		-0.91330	
M_1	-62.866		-127.17		-83.792		-69.452		-66.216		-66.384	
$\frac{Pa_{11}^2}{2R_{11}t_{11}\cos\phi}$	11.26		0		0		11.26		9.01		9.01	
$+\frac{H_1\cos\phi}{t_{11}}$	-.20		+.82		.52		-.16		-.06		-.06	
$\pm\frac{6M}{t_{11}^2}$	-9.66	9.66	-19.53	19.53	-12.87	12.87	-10.67	10.67	-10.17	10.17	-10.19	10.19
$\sigma_x = \Sigma$	1.40	20.7	-18.71	20.35	-12.39	13.39	.43	21.76	-1.227	19.11	-1.25	19.14
$\frac{Pa_{11}^2}{2R_{11}t_{11}\cos\phi}$	11.26		0		0		11.26		9.01		9.01	
$+\frac{\mu H_1\cos\phi}{t_{11}}$	-.06		+.25		.16		-.05		-.02		-.02	
$\pm\frac{6\mu M_1}{t_{11}^2}$	-2.89	2.89	-5.86	+5.86	-3.86	3.86	-3.20	3.20	-3.05	3.05	-3.06	3.06
$E\bar{\delta}_{11}/R_{11}$	-20.04		+10.01		5.93		-19.58		-14.91		-14.92	
$\sigma_\theta = \Sigma$	-11.74	-5.95	4.40	16.12	2.23	9.95	-11.57	-5.17	-8.97	-2.87	-8.99	-2.87
$\sigma_r = -\frac{P}{2} \mp \frac{P}{2}$	-1.25	0	0	0	0	0	-1.25	0	-1.00	0	-1.00	0
$S_{x\theta} = \sigma_x - \sigma_\theta$	13.1	26.7	-23.1	4.2	-14.6	3.4	12.0	26.9	7.7	22.0	7.7	22.0
$S_{xr} = \sigma_x - \sigma_r$	2.6	20.7	-18.7	20.4	-12.3	13.4	1.7	21.8	-.2	19.1	-.2	19.1
$S_{\theta r} = \sigma_\theta - \sigma_r$	-10.5	-5.9	4.4	16.1	2.2	10.0	-10.3	-5.2	-8.0	-2.9	-8.0	-2.9

COMBUSTION ENGINEERING, INC.
ENGINEERING DEPARTMENT, CHATTANOOGA, TENN.

CHARGE NO. 224" SINK

DESCRIPTION Closure Ring

NUMBER [illegible] | CENC 1137
SHEET 74 | 1-69
DATE 1-30-70 BY JB
CHECK DATE 1-30-70 BY TP

C.6 Detailed Analysis

C.6 Vessel Stresses

C.6.3 Primary plus Secondary Stress Intensity

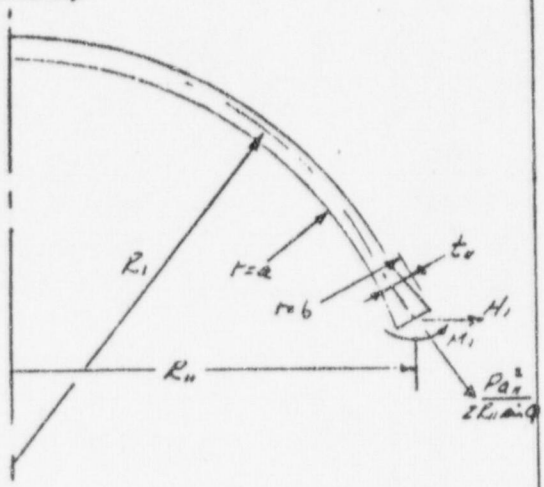
Element ① Cut I

$$\sigma_{x11} = \frac{Pa_H^2}{2R_{11}t_{11}\sin\phi} + \frac{H_1\cos\phi}{t_{11}} \pm \frac{6M_1}{t_{11}^2}$$

$$\sigma_{\theta 11} = \frac{Pa_H^2}{2R_{11}t_{11}\sin\phi} - \frac{\mu H_1\cos\phi}{t_{11}} \pm \frac{6\mu M_1}{t_{11}^2} + \frac{E\bar{\delta}_{11}}{R_{11}}$$

$$\sigma_{r11} = -\frac{P}{2} \pm \frac{P}{2}$$

$$S_{x\theta} = \sigma_x - \sigma_\theta \qquad S_{xr} = \sigma_x - \sigma_r \qquad S_{\theta r} = \sigma_\theta - \sigma_r$$



Condition	Vessel Over-Pressure		Startup		Shutdown Flooding		End of Shutdown		Rapid Heating		Rapid Cooling	
Surface (i)	a	b	a	b	a	b	a	b	a	b	a	b
P	1.375		1.00		.185		0		1.25		.185	
F	74.379		83.291		74.446		72.800		69.975		72.026	
$E\bar{\delta}_1$	-2469.3		-2716.2		481.74		1911.6		-2225.1		187.98	
H_1	-3.4366		-5.2257		7.4138		13.088		-2.8980		5.4864	
M_1	-66.913		-51.420		-90.425		-108.21		-63.342		-75.084	
$\frac{Pa_H^2}{2R_{11}t_{11}\sin\phi}$	12.39		9.01		1.67		0		11.26		1.67	
$+\frac{H_1\cos\phi}{t_{11}}$	-.24		-.36		.52		.91		-.20		.38	
$\pm 6M_1/t_{11}^2$	-10.28	10.28	-7.90	7.90	-13.89	13.89	-16.62	16.62	-9.73	9.73	-11.53	11.53
$\sigma_x = \Sigma$	1.87	22.42	.75	16.54	-11.71	16.07	-15.71	17.53	1.33	20.79	-9.48	13.58
$\frac{Pa_H^2}{2R_{11}t_{11}\sin\phi}$	12.39		9.01		1.67		0		11.26		1.67	
$+\frac{\mu H_1\cos\phi}{t_{11}}$	-.07		-.11		.15		.27		-.06		.11	
$\pm\frac{6\mu M_1}{t_{11}^2}$	-3.08	3.08	-2.37	2.37	4.17	4.17	-4.99	4.99	-2.92	+2.92	-3.46	3.46
$E\bar{\delta}_{11}/R_{11}$	-22.21		-24.45		4.33		17.19		-20.01		1.69	
$\sigma_\theta = \Sigma$	-12.98	-6.81	-17.90	-13.16	1.99	10.32	12.48	22.45	-11.73	-5.89	-.01	6.93
$\sigma_r = -\frac{P}{2} \pm \frac{P}{2}$	-1.38	0	-1.00	0	-.18	0	0	0	-1.25	0	-.18	0
$S_{x\theta} = \sigma_x - \sigma_\theta$	14.8	29.2	18.6	29.7	-13.7	5.8	-28.2	-4.9	13.1	26.7	-9.5	6.6
$S_{xr} = \sigma_x - \sigma_r$	3.2	22.4	1.7	16.5	-11.5	16.1	-15.7	17.5	2.6	20.8	-9.3	13.6
$S_{\theta r} = \sigma_\theta - \sigma_r$	-11.6	-6.8	-16.9	-13.2	2.2	10.3	12.5	22.4	-10.5	-5.9	.2	6.9

COMBUSTION ENGINEERING, INC.
ENGINEERING DEPARTMENT, CHATTANOOGA, TENN.
CHARGE NO. 224" ENC

DESCRIPTION Closure Region

NUMBER S-101 | CENC 1139
SHEET 75 | A-70
DATE 1-30-70 BY JB
CHECK DATE 1-30-70 BY TP

C.6 Detailed Analysis

C.6 Vessel Stresses

C.6.2 Primary plus Secondary Stress Intensity

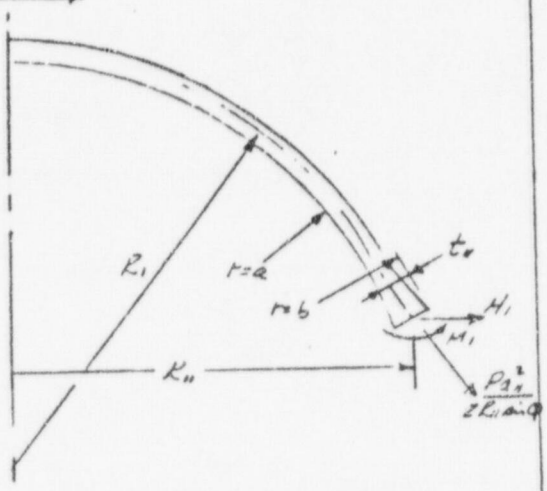
Element ① Cut I

$$\sigma_{x11} = \frac{P a_{11}^2}{2 R_{11} t_{11} \cos\phi} + \frac{H_1 \cos\phi}{t_{11}} \pm \frac{6 M_1}{t_{11}^2}$$

$$\sigma_{\theta 11} = \frac{P a_{11}^2}{2 R_1 t_{11} \cos\phi} + \frac{\nu H_1 \cos\phi}{t_{11}} \pm \frac{6 \nu M_1}{t_{11}^2} + \frac{E \bar{\Delta}_{11}}{R_{11}}$$

$$\sigma_{r11} = -\frac{P}{2} \mp \frac{P}{2}$$

$$S_{x\theta} = \sigma_x - \sigma_\theta \qquad S_{xr} = \sigma_x - \sigma_r \qquad S_{\theta r} = \sigma_\theta - \sigma_r$$



Condition	Hydro Bolt Tensioning		Hydro Bolt Preload		Hydro Pressure Test							
Surface (1)	a	b	a	b	a	b	a	b	a	b	a	b
P	0		0		1.565							
F	119.84		90.103		86.431							
$E\bar{\Delta}_1$	1275.9		755.78		-2795.6							
H_1	13.524		8.6427		-3.7413							
M_1	-145.71		-96.005		-78.050							
$\frac{P a_{11}^2}{2 R_1 t_{11} \cos\phi}$	0		0		14.10							
$+\frac{H_1 \cos\phi}{t_{11}}$	+.94		.60		-.26							
$\pm \frac{6M}{t_{11}^2}$	-22.38	22.38	-14.75	14.75	-11.99	11.99						
$\sigma_x = \Sigma$	-21.44	23.32	-14.14	15.35	1.85	25.82						
$\frac{P a_{11}^2}{2 R_1 t_{11} \cos\phi}$	0		0		14.10							
$+\frac{\nu H_1 \cos\phi}{t_{11}}$	+.28		.18		-.08							
$\pm \frac{6 \nu M_1}{t_{11}^2}$	-6.71	+6.71	-4.42	4.42	-3.60	3.60						
$E\bar{\Delta}_{11}/R_{11}$	11.47		6.80		-25.14							
$\sigma_\theta = \Sigma$	5.05	18.46	2.55	11.40	-14.72	-7.52						
$\sigma_r = -\frac{P}{2} \mp \frac{P}{2}$	0	0	0	0	-1.56	0						
$S_{\theta r} = \sigma_\theta - \sigma_r$	-26.5	4.9	-16.7	3.9	16.6	33.4						
$S_{xr} = \sigma_x - \sigma_r$	-21.4	23.3	-14.1	15.3	3.4	25.8						
$S_{x\theta} = \sigma_\theta - \sigma_x$	5.1	18.5	2.6	11.4	-13.2	-7.5						

COMBUSTION ENGINEERING, INC.
ENGINEERING DEPARTMENT, CHATTANOOGA, TENN.
CHARGE NO. 224 FINAL
DESCRIPTION Closure Design

NUMBER S-101 | CENC 1139
SHEET 76 | A. 71
DATE 1-30-70 BY JB
CHECK DATE 1-30-70 BY TP

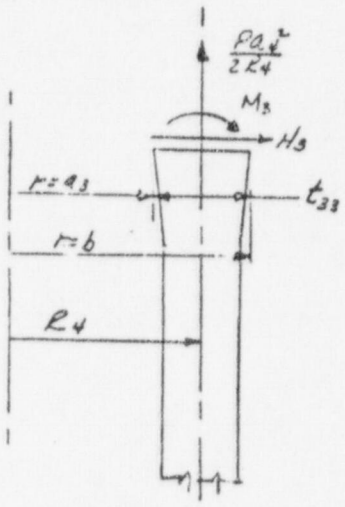
C.0 Detailed Analysis
C.6 Vessel Stresses
C.6.3 Primary plus Secondary Stress Intensity
Element ④ Cut III

$$\sigma_{x4} = \frac{Pa_3^2}{2R_4 t_{33}} \pm \frac{6M_3}{t_{33}^2}$$

$$\sigma_{\theta 4} = \frac{Pa_3^2}{R_4 t_{33}} \pm \frac{6\nu M_3}{t_{33}^2} + \frac{E\bar{\alpha}H_3}{R_4}$$

$$\sigma_{r4} = -\frac{P}{2} + \frac{P}{2}$$

$\sigma_{x\theta} = \sigma_x - \sigma_\theta$ $\sigma_{xr} = \sigma_x - \sigma_r$ $\sigma_{\theta r} = \sigma_\theta - \sigma_r$



Condition	Design Operation		Design Bolt Tensioning		Design Bolt PreLoad		Design Pressure Test		Steady State Operation		Inner Seal Leakage	
Surface (r)	a	b	a	b	a	b	a	b	a	b	a	b
P	1.25		0		0		1.25		1.00		1.00	
F	69.528		104.59		78.641		75.709		70.567		70.938	
$E\bar{\alpha}_{43}$	-250.68		-685.84		-317.59		-275.64		-260.89		-256.21	
H_3	4.9768		17.857		10.372		5.7920		5.9524		5.8704	
M_3	-145.66		-494.70		-276.77		-167.41		-169.12		-166.65	
Pa_3^2/R_4t_{33}	8.07		0		0		8.07		6.45		6.46	
$\pm 6M_3/t_{33}^2$	-12.46	12.46	-42.32	42.32	-23.68	23.68	-14.32	14.32	-14.47	14.47	-14.26	14.26
$\sigma_x = \Sigma$	-4.39	20.53	-42.32	42.32	-23.68	23.68	-6.25	22.39	-8.01	20.92	-7.80	20.71
Pa_3^2/R_4t_{33}	16.13		0		0		16.13		12.90		12.91	
$\pm 6\nu M_3/t_{33}^2$	-3.74	3.74	-12.69	12.69	-7.10	7.10	-4.30	4.30	-4.34	4.34	-4.28	4.28
$E\bar{\alpha}_{43}/R_4$	-2.15		-5.87		-2.72		-2.36		-2.23		-2.19	
$\sigma_\theta = \Sigma$	10.25	17.72	-18.56	6.82	-9.82	4.38	9.48	18.07	6.33	15.01	6.44	14.99
$\sigma_r = -\frac{P}{2} + \frac{P}{2}$	-1.25	0	0	0	0	0	-1.25	0	-1.00	0	-1.00	0
$\sigma_{x\theta} = \sigma_x - \sigma_\theta$	-14.6	2.8	-23.8	35.5	-13.8	19.3	-15.7	4.3	-14.3	5.9	-14.2	5.7
$\sigma_{xr} = \sigma_x - \sigma_r$	-3.1	20.5	-42.3	42.3	-23.7	23.7	-5.0	22.4	-7.0	20.9	-6.8	20.7
$\sigma_{\theta r} = \sigma_\theta - \sigma_r$	11.5	17.7	18.6	6.8	-9.8	4.4	10.7	18.1	7.3	15.0	7.4	15.0

COMBUSTION ENGINEERING, INC.
ENGINEERING DEPARTMENT, CHATTANOOGA, TENN.

CHARGE NO. 224" FNR

DESCRIPTION Elastic Analysis

NUMBER S-101 | CENC 1139
SHEET 77 | A-72
DATE 1-30-70 BY JB
CHECK DATE 1-30-70 BY TP

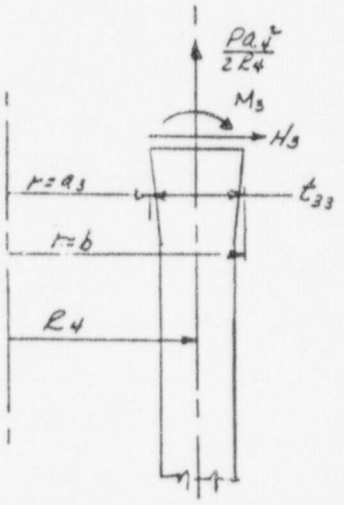
C.0 Elastic Analysis
C.E Vessel Stresses
C.E.3 Primary plus Secondary Stress Intensity
Element (F) Cut III

$$\sigma_{x4} = \frac{P a_3^2}{2 R_4 t_{33}} \pm \frac{6 M_3}{t_{33}^2}$$

$$\sigma_{\theta 4} = \frac{P a_3^2}{R_4 t_{33}} \pm \frac{6 \nu M_3}{t_{33}^2} + \frac{E \bar{\alpha} \Delta t_3}{R_4}$$

$$\sigma_{r4} = -\frac{P}{2} \mp \frac{P}{2}$$

$\sigma_{x\theta} = \sigma_x - \sigma_\theta$ $\sigma_{xr} = \sigma_x - \sigma_r$ $\sigma_{\theta r} = \sigma_\theta - \sigma_r$



Condition	Vessel Over-Pressure		Startup		Shutdown Flooding		End of Shutdown		Rapid Heating		Rapid Cooling	
Surface (r)	a	b	a	b	a	b	a	b	a	b	a	b
P	1.375		1.00		.185		0		1.25		.185	
F	74.379		83.291		74.446		72.800		69.975		72.026	
$E\bar{\alpha}\Delta t_3$	-267.26		-741.76		-196.83		184.37		-252.49		-286.42	
H_3	5.1973		5.5581		9.8542		11.895		5.0358		8.8787	
M_3	-152.83		-223.04		-249.25		-245.71		-147.23		-238.83	
$Pa_3^2/2R_4t_{33}$	8.87		6.45		1.19		0		8.07		1.19	
$\pm 6M_3/t_{33}^2$	-13.07	13.07	-19.08	19.08	-21.32	21.32	-21.02	21.02	-12.59	12.59	-20.43	20.43
$\sigma_x = \Sigma$	-4.20	21.95	-12.62	25.53	-20.13	22.51	-21.02	21.02	-4.53	20.66	-19.23	21.62
Pa_3^2/R_4t_{33}	17.75		+12.90		2.39		0		16.15		23.88	
$\pm 6\nu M_3/t_{33}^2$	-3.92	3.92	-5.72	5.72	-6.40	6.40	-6.31	6.31	-3.78	3.78	-6.13	6.13
$E\bar{\alpha}\Delta t_3/R_4$	-2.29		-6.35		-1.68		1.58		-2.16		-2.45	
$\sigma_\theta = \Sigma$	11.54	19.38	.83	12.28	-5.69	7.10	-4.73	7.28	10.19	17.75	-6.19	6.06
$\sigma_r = -\frac{P}{2} \mp \frac{P}{2}$	-1.38	0	-1.00	0	-.18	0	0	0	-1.25	0	-.18	0
$S_{x\theta} = \sigma_x - \sigma_\theta$	-15.7	2.6	-13.4	13.3	-14.4	15.4	-16.3	13.1	-14.7	2.9	-13.0	15.6
$S_{xr} = \sigma_x - \sigma_r$	-2.8	21.9	-11.6	25.5	-19.9	22.5	-21.0	21.0	-3.3	20.7	-19.1	21.6
$S_{\theta r} = \sigma_\theta - \sigma_r$	12.9	19.4	1.8	12.3	-5.5	7.1	-4.7	7.9	11.4	17.7	-6.0	6.1

C.0 Detailed Analysis

C.6 Vessel Stresses

C.6.3 Primary plus Secondary Stress Intensity

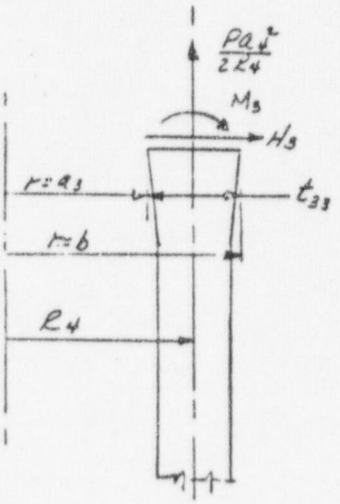
Element ⑦ Cut III

$$\sigma_{x4} = \frac{pa_3^2}{2R_4 t_{33}} \pm \frac{6M_3}{t_{33}^2}$$

$$\sigma_{\theta 4} = \frac{pa_3^2}{R_4 t_{33}} \pm \frac{6\nu M_3}{t_{33}^2} + \frac{E\bar{\delta}_{43}}{R_4}$$

$$\sigma_{r4} = -\frac{p}{2} \mp \frac{p}{2}$$

$\sigma_{x\theta} = \sigma_x - \sigma_\theta$ $\sigma_{xr} = \sigma_x - \sigma_r$ $\sigma_{\theta r} = \sigma_\theta - \sigma_r$



Condition	Hydro Bolt Tensioning		Hydro Bolt Preload		Hydro Pressure Test							
Surface (r)	a	b	a	b	a	b	a	b	a	b	a	b
p	0		0		1.565							
F	119.84		90.103		86.431							
$E\bar{\delta}_{43}$	-785.95		-363.88		-311.36							
H_3	20.460		11.883		6.1495							
M_3	-566.83		-317.11		-180.19							
$pa_3^2/2R_4t_{33}$	0		0		10.10							
$\mp 6\nu M_3/t_{33}^2$	-48.49	+48.49	-27.12	27.12	-15.41	15.41						
$\sigma_x = \Sigma$	-48.49	48.49	-27.12	27.12	-5.31	25.51						
Fa_3^2/R_4t_{33}	0		0		20.20							
$\mp 6\nu M_3/t_{33}^2$	-14.54	+14.54	-8.14	8.14	-4.62	4.62						
$E\bar{\delta}_{43}/R_4$	-6.73		-3.12		-2.67							
$\sigma_\theta = \Sigma$	-21.27	7.81	-11.25	5.02	12.91	22.16						
$\sigma_r = -\frac{p}{2} \mp \frac{p}{2}$	0	0	0	0	-1.56	0		0		0		0
$S_{x\theta} = \sigma_x - \sigma_\theta$	-27.2	40.7	-15.9	22.1	-18.2	3.4						
$S_{xr} = \sigma_x - \sigma_r$	-48.5	48.5	-27.1	27.1	-3.7	25.5						
$S_{\theta r} = \sigma_\theta - \sigma_r$	-21.3	7.8	-11.2	5.0	14.5	22.2						

COMBUSTION ENGINEERING, INC.
ENGINEERING DEPARTMENT, CHATTANOOGA, TENN.

CHARGE NO. 224" FWE
DESCRIPTION Closure Region

NUMBER S-121 | CENC 1139
SHEET 79 | A-74
DATE 1-30-70 BY JB
CHECK DATE 1-30-70 BY TP

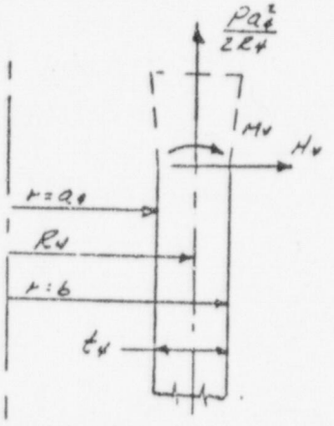
C.0 Detailed Analysis
C.6 Vessel Stresses
C.6.3 Primary plus Secondary Stress Intensity
Element (9) Cut "V"

$$\sigma_{xv} = \frac{pa_s^2}{2R_4 t_4^2} \pm \frac{6M_v}{(t_4)^2}$$

$$\sigma_{\theta v} = \frac{pa_s^2}{R_4 t_4^2} \pm \frac{6\mu M_v}{(t_4)^2} + \frac{E\bar{\alpha}T}{R_4}$$

$$\sigma_{rv} = -\frac{p}{2} \text{ or } \frac{p}{2}$$

$$S_{xe} = \sigma_x - \sigma_\theta \qquad S_{xr} = \sigma_x - \sigma_r \qquad S_{\theta r} = \sigma_\theta - \sigma_r$$



Condition	Design Operation		Design Bolt Tensioning		Design Bolt PreLoad		Design Pressure Test		Steady State Operation		Inner Seal Leakage	
Surface (r)	a	b	a	b	a	b	a	b	a	b	a	b
p	1.25		0		0		1.25		1.00		1.375	
F	69.528		104.59		78.641		75.709		70.567		70.938	
$E\bar{\alpha}T$	-151.17		-364.4		-144.57		-162.53		-148.41		-145.46	
H_v	5.2129		18.476		10.64		6.0495		6.1930 5.9524		6.1065	
M_v	-135.12		-457.13		-255.05		-155.16		-156.56 -169.12		-154.26	
$pa_s^2/2R_4t_4^2$	10.57		0		0		10.57		8.45		8.45	
$\pm 6M_v/(t_4^2)$	-19.19	+19.19	-64.92	64.92	-36.22	36.22	-22.04	22.04	-22.23	22.23	-21.91	21.91
$\sigma_x = \Sigma$	-8.62	29.76	-64.92	64.92	-36.22	36.22	-11.47	32.60	-13.78	30.69	-13.45	30.36
$pa_s^2/R_4t_4^2$	21.14		0		0		21.14		+16.91		16.91	
$\pm 6\mu M_v/(t_4^2)$	-5.76	5.76	-19.48	19.48	-10.86	10.86	-6.61	6.61	-6.67	6.67	-6.57	6.57
$E\bar{\alpha}T/R_4$	-1.29		-3.12		-1.24		-1.39		-1.27		-1.24	
$\sigma_\theta = \Sigma$	14.08	25.60	-22.60	16.56	-12.10	9.63	13.13	26.36	8.97	22.31	9.09	22.24
$\sigma_r = -\frac{p}{2}$ or $\frac{p}{2}$	-1.25	0	0	0	0	0	-1.25	0	-1.00	0	-1.00	0
$S_{x\theta} = \sigma_x - \sigma_\theta$	-22.7	4.2	-42.3	48.7	-24.1	26.6	-24.6	6.2	-22.7	8.4	-22.5	8.1
$S_{xr} = \sigma_x - \sigma_r$	-7.4	29.8	-64.9	64.9	-36.2	36.2	-10.2	32.6	-12.8	30.7	-12.4	30.4
$S_{\theta r} = \sigma_\theta - \sigma_r$	15.3	25.6	-22.6	16.6	-12.1	9.6	14.4	26.4	10.0	22.3	10.1	22.2

C.0 Detailed Analysis

C.B Vessel Stresses

C.B.3 Primary plus Secondary Stress Intensity

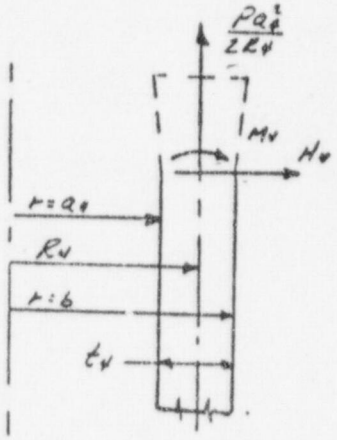
Element ④ Cut "V"

$$\sigma_{xv} = \frac{PQ_v^2}{2R_v t_v^2} \pm \frac{6M_v}{(t_v)^2}$$

$$\sigma_{ov} = \frac{PQ_v^2}{R_v t_v} \pm \frac{6\nu M_v}{(t_v)^2} + \frac{E\bar{\Delta}_v}{R_v}$$

$$\sigma_{rv} = -\frac{P}{2} \neq \frac{P}{2}$$

$$S_{xo} = \sigma_x - \sigma_o \qquad S_{xr} = \sigma_x - \sigma_r \qquad S_{or} = \sigma_o - \sigma_r$$



Condition	Vessel Over-Pressure		Startup		Shutdown Flooding		End of Shutdown		Rapid Heating		Rapid Cooling	
Surface (+)	a	b	a	b	a	b	a	b	a	b	a	b
P	1.375		1.00		.185		0		1.25		.185	
F	74.379		83.291		74.446		72.800		69.975		72.026	
$E\bar{\Delta}_v$	-162.42		-552.96		-50.083		290.57		-151.99		-135.86	
H_v	5.4497		6.3173		10.000		11.62		5.2734		9.1274	
M_v	-141.81		-210.73		-228.73		-221.44		-136.57		-220.22	
$PQ_v^2/2R_v t_v^2$	11.62		8.45		1.56		0		10.57		1.56	
$\pm 6M_v/(t_v)^2$	-20.14	28.14	-29.93	29.93	-32.48	32.2	-31.45	31.45	-19.39	19.39	-31.27	31.27
$\sigma_x = \Sigma$	8.51	31.76	-21.47	38.38	-30.92	34.05	-31.45	31.45	-8.83	29.96	-29.71	32.84
$P\alpha_v^2/R_v t_v^2$	23.25		16.91		3.13		0		21.14		3.13	
$\pm 6\nu M_v/(t_v)^2$	-6.04	6.04	-8.98	8.98	-9.74	9.74	-9.43	9.43	-5.82	5.82	-9.38	9.38
$E\bar{\Delta}_v/R_v$	-1.39		-4.74		-.43		2.49		-1.30		-1.16	
$\sigma_o = \Sigma$	15.82	27.90	3.20	21.15	-7.04	12.44	-6.94	11.92	14.02	25.65	-7.42	11.35
$\sigma_r = -\frac{P}{2} \neq \frac{P}{2}$	-1.38	0	-1.00	0	-.18	0	0	0	-1.25	0	-.18	0
$S_{xo} = \sigma_x - \sigma_o$	-24.3	3.9	-24.7	17.2	-23.9	21.6	-24.5	19.5	-22.8	4.3	-22.3	21.5
$S_{xr} = \sigma_x - \sigma_r$	-7.1	31.8	-20.5	38.4	-30.7	34.0	-31.4	31.4	-7.6	30.0	-29.5	32.8
$S_{or} = \sigma_o - \sigma_r$	17.2	27.9	4.2	21.2	-6.9	12.4	-6.9	11.9	15.2	25.6	-7.2	11.3

COMBUSTION ENGINEERING, INC.
ENGINEERING DEPARTMENT, CHATTANOOGA, TENN.

CHARGE NO. 224" FNL

DESCRIPTION Closure Region

NUMBER 5121 | CENC 1139
SHEET 81 | A-76
DATE 1-30-70 BY JB
CHECK DATE 1-30-70 BY TP

C.0 General Analysis

C.6 Vessel Stresses

C.6.3 Primary plus Secondary Stress Intensity

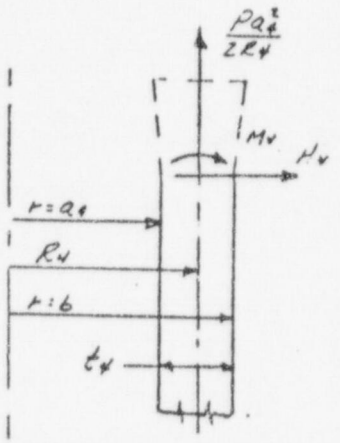
Element (4) Cut "V"

$$\sigma_{xv} = \frac{Pa_i^2}{2R_4 t_i^2} \pm \frac{6M_v}{(t_4)^2}$$

$$\sigma_{\theta v} = \frac{Pa_i^2}{R_4 t_4^2} \pm \frac{6\nu M_v}{(t_4)^2} + \frac{E\bar{\alpha}T}{R_4}$$

$$\sigma_{rv} = -\frac{P}{2} \text{ or } \frac{P}{2}$$

$$S_{x\theta} = \sigma_x - \sigma_\theta \qquad S_{xr} = \sigma_x - \sigma_r \qquad S_{\theta r} = \sigma_\theta - \sigma_r$$



Condition	Hydro Bolt Tensioning		Hydro Bolt Preload		Hydro Pressure Test							
Surface (r)	a	b	a	b	a	b	a	b	a	b	a	b
P	0		0		1.565							
F	119.84		90.103		86.431							
$E\bar{\alpha}T$	-417.5		-165.64		-188.12							
M_v	21.17		12.195		6.4428							
νM_v	-523.78		-292.22		-167.16							
$Pa_i^2/(2R_4t_4^2)$	0		0		13.23							
$\pm 6\nu M_v/(t_4)^2$	-74.38	74.38	-41.50	41.50	-23.74	23.74						
$\sigma_x = \Sigma$	-74.4	74.4	-41.50	41.50	-10.51	36.97						
$Pa_i^2/R_4t_4^2$	0		0		26.46							
$\pm 6M_v/(t_4)^2$	-22.31	+22.31	-12.45	12.45	-7.12	7.12						
$E\bar{\alpha}T/R_4$	-3.58		-1.42		-1.61							
$\sigma_\theta = \Sigma$	-22.3	22.3	-13.87	11.03	17.73	31.97						
$\sigma_r = -\frac{P}{2}$ or $\frac{P}{2}$	0	0	0	0	-1.56	0	0		0		0	
$S_{x\theta} = \sigma_x - \sigma_\theta$	-48.5	55.6	-27.6	30.5	-28.2	4.9						
$S_{xr} = \sigma_x - \sigma_r$	-74.4	74.4	-41.5	41.5	-8.9	37.0						
$S_{\theta r} = \sigma_\theta - \sigma_r$	-25.9	18.7	-13.9	11.0	19.3	32.0						

C.0 Detailed Analysis
C.8 Vessel Stresses
C.8.3 P+S Stress Intensities

P+S Stress Intensities are summarized below for convienence.

Location	Stress Index	Surface	Design Operation	Design Bolt Tensioning	Design Bolts Preloaded	Design Pressure Test	Steady State Operation	Inner Seal Leakage	Vessel Over Pressure	Startup	Shutdown Flooding	End of shutdown	Rapid Heating	Rapid Cooling	Hydro Test Bolt Tensioning	Hydro Bolts Preloaded	Hydro Pressure Test
Element ① cut "C"	$S_{x\theta}$	a	-17.8	-31.2	-20.6	-19.5	-18.2	-18.2	-19.1	-15.4	-22.4	-25.6	-18.0	-18.8	-36.7	-23.6	-22.2
		b	27.9	5.8	4.5	28.3	23.2	23.2	30.6	31.7	6.3	-4.5	28.0	7.7	6.7	5.2	34.9
	S_{xr}	a	-9.9	-25.7	-17.5	-11.2	-11.2	-11.3	-10.4	-15.4	-16.7	-14.4	-10.0	-15.2	-29.5	-20.0	-12.2
		b	51.3	27.2	18.4	55.7	46.9	47.0	59.2	50.9	24.2	15.7	54.4	22.5	31.2	21.1	67.8
	$S_{\theta r}$	a	8.0	5.5	3.1	8.2	7.0	7.0	8.7	0	5.7	11.2	8.0	3.6	6.3	3.6	10.0
		b	26.3	21.3	13.9	27.4	23.7	23.7	28.6	19.2	17.8	20.2	26.4	14.8	24.5	15.9	32.9
Element ① cut "I"	$S_{x\theta}$	a	13.1	-23.1	-14.6	12.0	7.7	7.7	14.8	18.6	-13.7	-28.2	13.1	-9.5	-26.5	-16.7	16.6
		b	26.7	4.2	3.4	26.9	22.0	22.0	29.2	29.7	5.8	-4.9	26.7	6.6	4.9	3.9	33.4
	S_{xr}	a	2.6	-18.7	-12.3	1.7	-.2	-.2	3.2	1.7	-11.5	-15.7	2.6	-9.3	-21.4	-14.1	3.4
		b	20.7	20.4	13.4	21.8	19.1	19.1	22.4	16.5	16.1	17.5	20.8	13.6	23.3	15.3	25.8
	$S_{\theta r}$	a	-10.5	4.4	2.2	-10.3	-8.0	-8.0	-11.6	-16.9	2.2	12.5	-10.5	.2	5.1	2.6	-13.2
		b	-5.9	16.1	10.0	-5.2	-2.9	-2.9	-6.8	-13.2	10.3	22.4	-5.9	6.9	18.5	11.4	-7.5
Element ① cut "III"	$S_{x\theta}$	a	-14.6	-23.8	-13.8	-15.7	-14.3	-14.2	-15.7	-13.4	-14.4	-16.3	-14.7	-13.0	-27.2	-15.9	-18.2
		b	2.8	35.5	19.3	4.3	6.9	5.7	2.6	13.3	15.4	13.1	2.9	15.6	40.7	22.1	3.4
	S_{xr}	a	-7.1	-42.3	-23.7	-5.0	-7.0	-6.8	-2.8	-11.6	-19.9	-21.0	-3.3	-19.1	-48.5	-27.1	-3.7
		b	20.5	42.3	23.7	22.4	20.9	20.7	21.9	25.5	22.5	21.0	20.7	21.6	48.5	27.1	25.5
	$S_{\theta r}$	a	11.5	18.6	-9.8	10.7	7.3	7.4	12.9	1.8	-5.5	-4.7	11.4	-6.0	-21.3	-11.2	14.5
		b	17.7	6.8	4.4	18.1	15.1	15.0	19.4	12.3	7.1	7.9	17.7	6.1	7.8	5.0	22.2
Element ① cut "II"	$S_{x\theta}$	a	-22.7	-42.3	-24.1	-24.6	-22.7	-22.5	-24.3	-24.7	-23.9	-24.5	-22.8	-22.3	-48.5	-27.6	-28.2
		b	4.2	48.7	26.6	6.2	8.7	18.1	3.9	17.2	21.6	19.5	4.3	21.5	55.6	30.5	4.9
	S_{xr}	a	-7.4	-64.9	-36.2	-10.2	-12.8	-12.4	-7.1	-20.5	-30.7	-31.4	-7.6	-29.5	-74.4	-41.5	-8.9
		b	29.8	64.9	36.2	32.6	30.7	30.4	31.8	28.4	34.0	31.4	30.0	32.8	74.4	41.5	37.0
	$S_{\theta r}$	a	15.3	-22.6	-12.1	14.4	10.0	10.1	17.2	4.2	-6.9	-6.9	15.7	-7.2	-25.9	-13.9	19.3
		b	25.6	16.6	9.6	26.4	22.3	22.2	27.9	21.2	12.4	11.9	25.6	11.3	18.7	11.0	32.0

C.0 Detailed Analysis

C.8 Vessel Stresses

C.8.3 Primary + Secondary Stress Intensities

The maximum P+S Stress Intensity Range at each cut is summarized below.

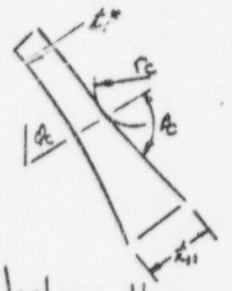
Element	Cut	Surface	Stress Intensity Index	Max Stress Intensity: Load Condition	Max Stress Intensity: Stress Intensity	Min Stress Intensity: Load Condition	Min Stress Intensity: Stress Intensity	Range: Smax - Smin
①	"C"	a	$S_{x\theta}$	Zero Load	0	Hydro Tensioning	-35.7	35.7
		b	S_{xr}	Hydro Test	67.8	Zero Load	0	67.8
①	"I"	a	$S_{x\theta}$	Hydro Test	16.6	End of Shutdown	-28.2	44.8
		b	$S_{x\theta}$	Hydro Test	33.4	End of Shutdown	-4.9	38.3
④	"III"	a	S_{xr}	Zero Load	0	Hydro Tensioning	-48.5	48.5
		b	S_{xr}	Hydro Tensioning	48.5	Zero Load	0	48.5
④	"V"	a	S_{xr}	Zero Load	0	Hydro Tensioning	-74.4	74.4
		b	S_{xr}	Hydro Tensioning	74.4	Zero Load	0	74.4

Thus, the maximum P+S Stress Intensity Range in the Vessel Closure Region is at Element ④ cut "V" for the Hydro Test Bolt Tensioning Load condition where at the a & b surfaces: (S_{xr}) = 74.4 ksi < $3S_m$ = 80.1 ksi

COMBUSTION ENGINEERING, INC.
ENGINEERING DEPARTMENT, CHATTANOOGA, TENN.
CHARGE NO. 224" BWR
DESCRIPTION Closure Region

NUMBER
SHEET 84 OF A-79
DATE 1-30-70 BY JB
CHECK DATE 1-30-70 BY TP

C.0 Detailed Analysis
C.8 Vessel Stresses
C.8.4 Peak Stress Intensities



$r_c = 5.0$
$t_1^* = 3.25$
$t_{11} = 6.25$

Element ① Cut "C"

$$\sigma_{x_c} = \frac{Pa_i^2}{2R_i t_i^*} K_{T_c} + \frac{H_c \cos\theta_c}{t_i^*} K_{T_c} \pm \frac{6M_c}{(t_i^*)^2} K_{B_c} + \sigma_{T_c}$$

$$\sigma_{\theta_c} = \frac{Pa_i^2}{2R_i t_i^*} + \frac{\mu H_c \cos\theta_c}{t_i^*} K_{T_c} \pm \frac{\mu 6 M_c}{t_i^*} K_{B_c} + \frac{E\Delta_c}{R_c} - \sigma_{T_c}$$

$$\sigma_{r_c} = -\frac{P}{2} \mp \frac{P}{2}$$

Conservatively neglecting the taper effect, the stress concentration factor from Ref 11, Fig A.7.1 for $\frac{r_c}{t_{11}} = .80$ is: $K_{T_c} = 1.60$, $K_{B_c} = 1.35$

Condition	Design Operation		Design Bolt Tensioning		Design Bolt Preload		Design Pressure Test		Steady State Operation		Inner Seal Leakage	
Surface	a	b	a	b	a	b	a	b	a	b	a	b
P	1.25		0		0		1.25		1.00		1.00	
F	69.528		104.59		78.641		75.709		70.567		70.938	
$E\Delta_c$	-516.22		1408.8		896.01		-445.79		-242.70		-242.18	
H_c	2.8107		6.6979		4.3999		3.1565		3.0847		3.0930	
M_c	-57.570		-46.584		-31.613		-60.055		-52.064		-52.163	
$\frac{Pa_i^2}{2R_i t_i^*} K_{T_c}$	21.27	34.04	0	0	0	0	21.27	34.04	17.02	27.23	17.02	27.23
$+\frac{H_c K_{T_c} \cos\theta_c}{t_i^*}$	+.31	+.49	+.73	+1.2	+.48	+.77	+.34	+.55	+.34	+.54	+.34	+.54
$\pm \frac{6 M_c K_{B_c}}{(t_i^*)^2}$	-32.70	+44.15	-26.46	+35.72	-17.96	24.24	-34.11	46.05	-29.57	39.92	-29.63	40.00
σ_{T_c}	0	0	0	0	0	0	0	0	0	0	0	0
$\sigma_x = \Sigma$	-11.12	78.68	-25.73	36.92	-17.48	25.01	-12.49	80.65	-12.22	67.70	-12.27	67.78
$\frac{Pa_i^2}{2R_i t_i^*}$	21.27		0		0		21.27		17.02		17.02	
$+\frac{\mu H_c \cos\theta_c}{t_i^*} K_{T_c}$	+.09	+.15	+.22	+.36	+.14	+.23	+10	+.17	+.10	+.16	.10	.16
$\pm \frac{\mu 6 M_c}{(t_i^*)^2} K_{B_c}$	-9.81	+13.24	-7.94	10.72	-5.39	+7.27	-10.23	13.82	-8.87	+11.98	-8.89	12.00
$E\Delta_c/R_c$	-4.83		13.18		8.38		-4.17		-2.27		-2.27	
σ_{T_c}	0	0	0	0	0	0	0	0	0	0	0	0
$\sigma_\theta = \Sigma$	6.72	29.8	5.46	24.26	3.14	15.89	6.97	31.08	5.98	26.89	5.97	26.92
$\sigma_r = -\frac{P}{2} \mp \frac{P}{2}$	-1.25	0	0	0	0	0	-1.25	0	-1.00	0	-1.00	0
$S_{AD} = \sigma_x - \sigma_\theta$	-17.8	48.8	-31.2	12.7	-20.6	9.1	-19.5	49.6	-18.2	40.8	-18.2	40.9
$S_{xr} = \sigma_x - \sigma_r$	-9.9	78.7	-25.7	36.9	-17.5	25.0	-11.2	80.6	-11.2	67.7	-11.3	67.8
$S_{\theta r} = \sigma_\theta - \sigma_r$	8.0	29.8	5.5	24.3	3.1	15.9	8.2	31.1	7.0	26.9	7.00	26.9

C.0 Detailed Analysis

C.8 Vessel Stresses

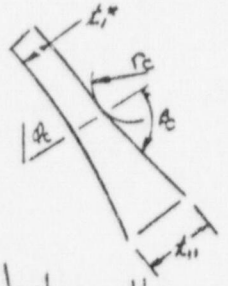
C8.4 Peak Stress Intensities

Element ① Cut "C"

$$\sigma_{x_c} = \frac{Pa_1^2}{2R_1 t_1^*} K_{T_c} + \frac{H_c \cos\phi_c}{t_1^*} K_{T_c} \pm \frac{6M_c}{(t_1^*)^2} K_{B_c} + \sigma_{T_c}$$

$$\sigma_{\theta_c} = \frac{Pa_1^2}{2R_1 t_1^*} + \frac{\mu H_c \cos\phi_c}{t_1^*} K_{T_c} \pm \frac{\mu 6M_c}{t_1^*} K_{B_c} + \frac{E\Delta_c}{R_c} + \sigma_{T_c}$$

$$\sigma_{T_c} = -\frac{P}{2} + \frac{P}{2}$$



$r_c = 5.0$
$t_1^* = 3.25$
$t_{11} = 6.25$

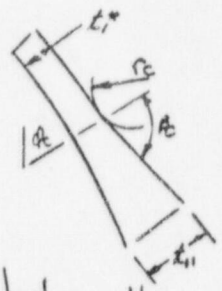
Conservatively neglecting the taper effect, the stress concentration factor from Ref 11, Fig A.7.1 for $\frac{r_c}{t_{11}} = .80$ is: $K_{T_c} = 1.60$, $K_{B_c} = 1.35$

Condition	Vessel Over-Pressure		Startup		Shutdown Flooding		End of Shutdown		Rapid Heating		Rapid Cooling	
Surface	a	b	a	b	a	b	a	b	a	b	a	b
P	1.375		1.00		.185		0		1.25		.185	
F	74.379		85.860		73.426		70.152		69.975		72.026	
$E\Delta_c$	-591.79		-827.42		893.68		+1635.4		-511.13		627.00	
H_c	2.9742		2.6650		4.4977		5.3327		2.8375		3.8701	
M_c	-62.482		-66.189		-33.080		-19.31		-57.749		-33.34	
$\frac{Pa_1^2}{2R_1 t_1^*} K_{T_c}$	23.40	37.44	+17.02	27.23	3.15	5.04	0	0	21.27	34.04	3.15	5.04
$+\frac{H_c K_{T_c} \cos\phi_c}{t_1^*}$	.33	.52	.29	.47	.49	.79	.58	.93	.31	.50	.42	.68
$\pm \frac{6M_c}{(t_1^*)^2} K_{B_c}$	-35.49	47.91	-37.60	50.76	-18.79	25.37	-10.97	14.81	-32.80	44.28	-18.94	25.57
σ_{T_c}	-12.42	0	-2.68	1.78	1.91	-1.00	2.28	-1.25	-8.60	0	64.25	0
$\sigma_x = \Sigma$	-24.18	85.88	-22.97	80.24	-13.24	30.19	-8.10	14.49	-19.82	78.82	48.88	31.28
$\frac{Pa_1^2}{2R_1 t_1^*}$	23.40		17.02		3.15		0		21.27		3.15	
$+\frac{\mu H_c \cos\phi_c}{t_1^*} K_{T_c}$	+.10	.16	.09	.14	.15	.24	.18	.28	.09	.15	.13	.20
$\pm \frac{\mu 6M_c}{(t_1^*)^2} K_{B_c}$	-10.65	14.37	-11.28	15.23	-5.64	7.61	-3.29	4.44	-9.84	13.28	-5.68	7.67
$E\Delta_c/R_c$	-5.54		-7.74		8.36		15.30		-4.78		5.87	
σ_{T_c}	-12.42	0	-2.68	1.78	1.91	-1.00	2.28	-1.25	-8.60	0	64.25	0
$\sigma_\theta = \Sigma$	-5.11	32.40	-4.59	26.42	7.93	18.36	14.47	18.78	-1.86	29.93	67.71	16.89
$\sigma_r = -\frac{P}{2} + \frac{P}{2}$	-1.38	0	-1.00	0	-.18	0	0	0	-1.25	0	-.18	0
$S_{A\theta} = \sigma_x - \sigma_\theta$	-19.1	53.5	-18.4	53.8	-21.2	11.8	-22.6	-4.3	-18.0	48.9	-18.8	14.4
$S_{xr} = \sigma_x - \sigma_r$	-22.8	85.9	-22.0	80.2	-13.1	30.2	-8.1	14.5	-18.6	78.8	49.1	31.3
$S_{\theta r} = \sigma_\theta - \sigma_r$	-3.7	32.4	-3.6	26.4	8.1	18.4	14.5	18.8	-.6	29.9	67.9	16.9

COMBUSTION ENGINEERING, INC.
ENGINEERING DEPARTMENT, CHATTANOOGA, TENN.
CHARGE NO. 224" BWR
DESCRIPTION Closure Region

NUMBER [illegible]
SHEET 86 OF A-81
DATE 1-30-70 BY JB
CHECK DATE 1-30-70 BY TP

C.0 Detailed Analysis
C.8 Vessel Stresses
C.8.4 Peak Stress Intensities



$r_c = 5.0$
$t_1^* = 3.25$
$t_{11} = 6.25$

Conservatively neglecting the taper effect, the stress concentration factor from Ref 11, Fig A.7.1 for $\frac{r_c}{t_{11}} = .80$ is: $K_{T_c} = 1.60$, $K_{B_c} = 1.55$

Element ① Cut "C"

$$\sigma_{x_c} = \frac{Pa_1^2}{2R_1 t_1^*} K_{T_c} + \frac{H_c \cos\theta_c}{t_1^*} K_{T_c} \pm \frac{6M_c}{(t_1^*)^2} K_{B_c} + \sigma_{T_c}$$

$$\sigma_{\theta_c} = \frac{Pa_1^2}{2R_1 t_1^*} + \frac{\mu H_c \cos\theta_c}{t_1^*} K_{T_c} \pm \frac{\mu 6M_c}{t_1^*} K_{B_c} + \frac{E\Delta_c}{R_c} + \sigma_{T_c}$$

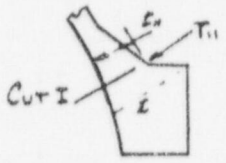
$$\sigma_{r_c} = -\frac{P}{2} \mp \frac{P}{2}$$

Condition	Hydro Bolt Tensioning		Hydro Bolt Preload		Hydro Pressure Test							
Surface	a	b	a	b	a	b	a	b	a	b	a	b
P	0		0		1.565							
F	119.84		90.103		86.431							
$E\Delta_c$	1614.2		1026.6		-653.35							
H_c	7.6745		5.0413		3.4844							
M_c	-53.377		-36.221		-71.830							
$\frac{Pa_1^2}{2R_1 t_1^*} K_{T_c}$	0	0	0	0	26.64	42.62						
$+\frac{H_c K_{T_c} \cos\theta_c}{t_1^*}$	+.84	+1.39	.55	.88	.38	.61						
$\pm \frac{6M_c K_{B_c}}{(t_1^*)^2}$	-30.32	+40.93	-20.58	27.78	-40.80	55.08						
σ_{T_c}	0	0	0	0	0	0	0	0	0	0	0	0
$\sigma_x = \Sigma$	-29.48	42.32	-20.02	28.66	-13.78	98.31						
$\frac{Pa_1^2}{2R_1 t_1^*}$	0		0		26.64							
$+\frac{\mu H_c \cos\theta_c}{t_1^*} K_{T_c}$	+.25	+.41	.17	.26	.11	.18						
$\pm \frac{\mu 6M_c}{(t_1^*)^2} K_{B_c}$	-9.10	+12.28	-6.17	8.33	-12.24	+16.52						
$E\Delta_c / R_c$	15.11		9.61		-6.11							
σ_{T_c}	0	0	0	0	0	0	0	0	0	0	0	0
$\sigma_\theta = \Sigma$	+6.26	27.8	3.60	18.20	8.40	37.2						
$\sigma_r = -\frac{P}{2} \mp \frac{P}{2}$	0	0	0	0	-1.56	0		0		0		0
$S_{\theta\theta} = \sigma_\theta - \sigma_\theta$	-35.7	14.5	-23.6	10.4	-22.2	61.1						
$S_{xx} = \sigma_x - \sigma_r$	-29.5	42.3	-20.0	28.7	-12.2	98.3						
$S_{\theta r} = \sigma_\theta - \sigma_r$	6.3	27.8	3.6	18.2	10.0	37.2						

COMBUSTION ENGINEERING, INC.
ENGINEERING DEPARTMENT, CHATTANOOGA, TENN.
CHARGE NO. 224" BWR
DESCRIPTION Closure Region

NUMBER S101 CENC 1139
SHEET 87 OF A 82
DATE 1-30-70 BY JB
CHECK DATE 1-30-70 BY TP

C.0 Detailed Analysis
C.8 Vessel Stresses
C.8.4 Peak Stress Intensities



$t_{11} = 6.25$
$t = 17.5$
$r_{11} = 3.0$

Conservatively neglecting the taper effect, the stress concentration factor from Ref 11, Fig A.7.1,

for $\frac{r_{11}}{t} = \frac{3.0}{17.5}$; $K_{T_1} = 2.65$
$K_{B_1} = 2.20$

Element ① Cut I

$$\sigma_x = \frac{Pa_{11}^2}{2R_{11}t_{11}\sin\phi_1} K_{T_1} + \frac{\bar{H}_1 \cos\phi_1}{t_{11}} K_{T_1} \pm \frac{6M_1}{(t_{11})^2} K_{B_1} + \sigma_{T_1}$$

$$\sigma_\theta = \frac{Pa_{11}^2}{2R_{11}r_{11}\sin\phi_1} + \mu \frac{\bar{H}_1 \cos\phi_1 K_{T_1}}{t_{11}} \pm \mu \frac{6M_1}{(t_{11})^2} K_{B_1} + \frac{E\Delta_{11}}{R_{11}} + \sigma_{T_1}$$

$$\sigma_r = -\frac{P}{2} \mp \frac{P}{2}$$

Condition	Design Operation		Design Bolt Tensioning		Design Bolt Preload		Design Pressure Test		Steady State Operation		Inner Seal Leakage	
Surface	a	b	a	b	a	b	a	b	a	b	a	b
P	1.25		0		0		1.25		1.00		1.0	
F	69.528		104.59		78.641		75.709		70.567		70.938	
$E\Delta_{11}$	-2228.8		1113.5		659.64		-2176.9		-1657.7		-1659.3	
$\bar{H}_1$	-2.9408		11.805		7.5432		-2.3480		-.91922		-.91330	
M_1	62.866		-127.17		-83.792		-69.452		-66.216		-66.384	
$\frac{Pa_{11}^2}{2R_{11}t_{11}\sin\phi_1} K_{T_1}$	11.26	29.83	0	0	0	0	11.26	29.84	9.01	23.87	9.01	23.87
$+\frac{\bar{H}_1\cos\phi_1}{t_{11}} K_{T_1}$	-.20	-.54	.82	2.17	.52	1.39	-.16	-.43	-.06	-.17	-.06	-.17
$\pm\frac{6M_1}{t_{11}^2} K_{B_1}$	-9.66	21.24	-19.53	42.97	-12.87	28.32	-10.67	23.47	-10.17	22.38	-10.20	+22.43
σ_{T_1}	0	0	0	0	0	0	0	0	0	0	0	0
$\sigma_x = \Sigma$	1.40	50.54	-18.71	45.14	-12.35	29.70	.43	52.88	-1.23	46.08	-1.25	46.13
$\frac{Pa_{11}^2}{2R_{11}r_{11}\sin\phi_1}$	11.26		0		0		11.26		9.01		9.01	
$+\frac{\mu\bar{H}_1\cos\phi_1 K_{T_1}}{t_{11}}$	-.06	-.16	.25	.66	.16	.41	-.05	-.13	-.02	-.05	-.02	-.05
$\pm\frac{\mu 6M_1 K_{B_1}}{t_{11}^2}$	-2.89	6.37	-5.86	12.89	-3.86	8.49	-3.20	7.04	-3.05	6.71	-3.06	6.73
$+E\Delta_{11}/R_{11}$	-20.04		10.01		5.93		-19.58		-14.91		-14.92	
σ_{T_1}	0	0	0	0	0	0	0	0	0	0	0	0
$\sigma_\theta = \Sigma$	-11.74	-2.57	4.40	23.56	2.23	14.84	-11.57	-1.41	-8.97	.76	-8.99	.77
$\sigma_r = -\frac{P}{2} \mp \frac{P}{2}$	-1.25	0	0	0	0	0	-1.25	0	-1.00	0	-1.00	0
$S_{x\theta} = \sigma_x - \sigma_\theta$	13.1	53.1	-23.1	21.7	-14.6	14.9	12.0	54.3	7.7	45.3	7.7	45.4
$S_{x1} = \sigma_x - \sigma_r$	2.6	50.5	-18.7	45.1	-12.3	29.7	1.7	52.9	.8	46.1	.2	46.1
$S_{\theta 1} = \sigma_\theta - \sigma_r$	-10.5	-2.6	4.4	23.6	2.2	14.8	-10.3	-1.4	-8.0	.8	-8.0	.8

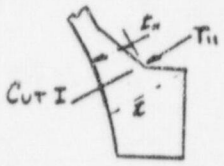
C.0 Detailed Analysis
C.8 Vessel Stresses
C.8.4 Peak Stress Intensities

Element ① Cut I

$$\sigma_x = \frac{Pa_{11}^2}{2R_{11}t_{11}\sin\varphi_1}K_{T_1} + \frac{\bar{H}_1\cos\varphi_1}{t_{11}}K_{T_1} \pm \frac{6M_1}{(t_{11})^2}K_{B_1} + \sigma_{T_1}$$

$$\sigma_\theta = \frac{Pa_{11}^2}{2R_{11}t_{11}\sin\varphi_1} + \mu\frac{\bar{H}_1\cos\varphi_1 K_{T_1}}{t_{11}} \pm \mu\frac{6M_1}{(t_{11})^2}K_{B_1} + \frac{E\Delta_{11}}{R_{11}} + \sigma_{T_1}$$

$$\sigma_r = -\frac{P}{2} \mp \frac{P}{2}$$



$t_{11} = 6.25$
$t = 17.5$
$r_{11} = 3.0$

Conservatively neglecting the taper effect, the stress concentration factor from Ref 11, Fig A.7.1,

for $\frac{r_{11}}{t} = \frac{3.0}{17.5}$; $K_{T_1} = 2.65$
$K_{B_1} = 2.20$

Condition	Vessel Over-Pressure		Startup		Shutdown Flooding		End of Shutdown		Rapid Heating		Rapid Cooling	
Surface	a	b	a	b	a	b	a	b	a	b	a	b
P	1.375		1.00		.185		0		1.25		.185	
F	74.379		85.860		73.426		70.152		69.975		72.026	
$E\Delta_{11}$	-2469.3		-2959.7		598.02		2166.0		-2225.0		187.98	
$\bar{H}_1$	-3.4366		-5.2722		7.48		13.136		-2.8980		5.4864	
M_1	-66.913		-62.507		-85.845		-96.632		-63.342		-75.084	
$\frac{Pa_{11}^2}{2R_{11}t_{11}\sin\varphi_1}K_{T_1}$	12.39	32.82	9.01	23.87	1.67	4.42	0	0	11.26	29.84	1.67	4.42
$+\frac{\bar{H}_1\cos\varphi_1}{t_{11}}K_{T_1}$	-.24	-.63	-.37	-.97	.52	1.38	.91	2.42	-.20	-.53	.38	1.01
$\pm\frac{6M_1}{t_{11}^2}K_{B_1}$	-10.28	22.61	-9.60	21.12	-13.18	+29.01	-14.84	32.65	-9.73	21.40	-11.53	25.37
σ_{T_1}	-12.42	0	-17.77	21.56	5.05	-4.86	17.38	-20.62	-8.60	0	64.25	0
$\sigma_x = \Sigma$	-10.35	54.80	-18.73	65.68	-5.95	29.94	3.45	14.46	-7.27	50.71	54.76	30.80
$\frac{Pa_{11}^2}{2R_{11}t_{11}\sin\varphi_1}$	12.39		9.01		1.67		0		11.26		1.67	
$+\frac{\mu\bar{H}_1\cos\varphi_1}{t_{11}}K_{T_1}$	-.07	-.19	-.11	-.29	.16	.41	.27	.72	-.06	-.16	.11	.30
$\pm\frac{\mu 6M_1}{t_{11}^2}K_{B_1}$	-3.08	6.78	-2.88	+6.34	-3.96	8.70	-4.45	9.80	-2.92	6.42	-3.46	7.61
$+E\Delta_{11}/R_{11}$	-22.21		-26.62		5.38		19.48		-20.01		1.69	
σ_{T_1}	-12.42	0	-17.77	21.56	5.05	-4.86	17.38	-20.62	-8.60	0	64.25	0
$\sigma_\theta = \Sigma$	-25.40	-3.23	-38.37	10.00	8.29	11.30	32.68	9.38	-20.33	-2.49	64.26	11.27
$\sigma_r = -\frac{P}{2} \mp \frac{P}{2}$	-1.38	0	-1.00	0	-.18	0	0	0	-1.25	0	-.18	0
$S_{x\theta} = \sigma_x - \sigma_\theta$	14.8	58.0	19.6	55.6	-14.2	18.6	-29.2	5.1	13.1	53.2	-9.5	19.5
$S_{xr} = \sigma_x - \sigma_r$	-9.2	54.8	-17.7	65.6	-5.8	29.9	3.4	14.4	-6.0	50.7	54.9	30.8
$S_{\theta r} = \sigma_\theta - \sigma_r$	-24.0	-3.2	-37.4	10.0	8.5	11.3	32.7	9.4	-19.1	-2.5	64.4	11.3

COMBUSTION ENGINEERING, INC.
ENGINEERING DEPARTMENT, CHATTANOOGA, TENN.
CHARGE NO. 224" BWR
DESCRIPTION Closure Region

NUMBER S101 CENC 1139
SHEET 89 OF A 84
DATE 1-30-70 BY JB
CHECK DATE 1-30-70 BY TP

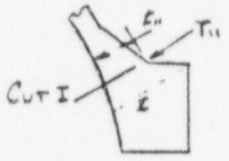
C.0 Detailed Analysis
C.8 Vessel Stresses
C.8.4 Peak Stress Intensities

Element ① Cut I

$$\sigma_x = \frac{Pa_{11}^2}{2R_{11}t_{11}\sin\varphi_1}K_{T_1} + \frac{\bar{H}_1\cos\varphi_1}{t_{11}}K_{T_1} \pm \frac{6M_1}{(t_{11})^2}K_{B_1} + \sigma_{T_1}$$

$$\sigma_\theta = \frac{Pa_{11}^2}{2R_{11}t_{11}\sin\varphi_1} + \mu\frac{\bar{H}_1\cos\varphi_1 K_{T_1}}{t_{11}} \pm \mu\frac{6M_1}{(t_{11})^2}K_{B_1} + \frac{E\Delta_{11}}{R_{11}} + \sigma_{T_1}$$

$$\sigma_r = -\frac{P}{2} \mp \frac{P}{2}$$



$t_{11} = 6.25$
$t = 17.5$
$r_{11} = 3.0$

Conservatively neglecting the taper effect, the stress concentration factor from Ref 11, Fig A.7.1,

for $\frac{r_{11}}{t} = \frac{3.0}{17.5}$; $K_{T_1} = 2.65$
$K_{B_1} = 2.20$

Condition	Hydro Bolt Tensioning		Hydro Bolt Preload		Hydro Pressure Test							
Surface	a	b	a	b	a	b	a	b	a	b	a	b
P	0		0		1.565							
F	119.84		90.103		86.431							
$E\Delta_{11}$	1275.9		755.78		-2795.6							
$\bar{H}_1$	13.524		8.6427		-3.7413							
M_1	-145.71		-96.005		-78.050							
$\frac{Pa_{11}^2}{2R_{11}t_{11}\sin\varphi_1}K_{T_1}$	0	0	0	0	14.10	37.36						
$+\frac{\bar{H}_1\cos\varphi_1}{t_{11}}K_{T_1}$	+.94	+2.49	.60	1.59	-.26	-.69						
$\pm\frac{6M_1}{t_{11}^2}K_{B_1}$	-22.38	+49.24	-14.75	32.44	-11.99	26.37						
σ_{T_1}	0	0	0	0	0	0						
$\sigma_x = \Sigma$	-21.44	51.73	-14.14	34.03	1.85	63.04						
$\frac{Pa_{11}^2}{2R_{11}t_{11}\sin\varphi_1}$	0		0		14.10							
$+\frac{\mu\bar{H}_1\cos\varphi_1 K_{T_1}}{t_{11}}$	+.28	+.74	.18	.48	-.08	-.21						
$\pm\frac{\mu 6M_1 K_{B_1}}{t_{11}^2}$	-6.71	+14.76	-4.42	9.73	-3.60	7.91						
$+E\Delta_{11}/R_{11}$	11.47		6.80		-25.14							
σ_{T_1}	0	0	0	0	0	0						
$\sigma_A = \Sigma$	5.04	26.97	2.55	17.01	-14.72	-3.34						
$\sigma_r = -\frac{P}{2} \mp \frac{P}{2}$	0	0	0	0	-1.56	0						
$S_{x\theta} = \sigma_x - \sigma_\theta$	-26.5	24.8	-16.7	17.0	16.6	66.4						
$S_{xr} = \sigma_x - \sigma_r$	-21.4	51.7	-14.1	34.0	3.4	63.0						
$S_{\theta r} = \sigma_\theta - \sigma_r$	5.0	27.0	2.6	17.0	-13.2	-3.3						

C.0 Detailed Analysis
C.8 Vessel Stresses
C.8.4 Peak Stress Intensities

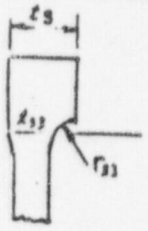
Element ④ CUT III

$$\sigma_x = \frac{Pa_3^2}{2R_4 t_{33}} K_{T_3} \pm \frac{6M_3}{t_{33}^2} K_{B_3} + \sigma_{T_3}$$

$$\sigma_\theta = \frac{Pa_3^2}{R_4 t_{33}} \pm \mu \frac{6M_3 K_{B_3}}{t_{33}^2} + \frac{E\Delta_{43}}{R_4} + \sigma_{T_3}$$

$$\sigma_r = -\frac{P}{2} \mp \frac{P}{2}$$

$t_3 = 12.81$
$t_{33} = 8.38$
$r_{33} = 5.0$



From Ref. 11, fig A.7.1

for $\frac{r_{33}}{t_3} = \frac{5}{12.81}$; $K_{T_3} = 1.95$
$K_{B_3} = 1.62$

Condition	Design Operation		Design Bolt Tensioning		Design Bolt Preload		Design Pressure Test		Steady State Operation		Inner Seal Leakage	
Surface	a	b	a	b	a	b	a	b	a	b	a	b
P	1.25		0		0		1.25		1.00		1.00	
F	69.528		104.59		78.641		75.709		70.567		70.938	
$E\Delta_{43}$	-250.68		-685.84		-317.59		-275.64		-260.90		-256.21	
H_3	+4.9768		17.857		10.372		5.7920		5.9524		5.8704	
M_3	-145.66		-494.70		-276.77		-167.41		-169.12		-166.65	
$\frac{Pa_3^2}{2R_4 t_{33}} K_{T_3}$	8.07	15.73	0	0	0	0	8.07	15.73	6.45	12.58	6.45	12.58
$\pm \frac{6M_3}{t_{33}^2} K_{B_3}$	-12.46	+20.18	-42.32	+68.56	-23.67	38.35	-14.32	23.20	-14.47	23.44	-14.25	23.09
σ_{T_3}	0	0	0	0	0	0	0	0	0	0	0	0
$\sigma_x = \Sigma$	-4.39	35.91	-42.32	68.56	-23.67	38.35	-6.25	38.93	-8.01	36.02	-7.80	35.68
$\frac{Pa_3^2}{R_4 t_{33}}$	16.13		0		0		16.13		12.91		12.91	
$-\frac{\mu 6M_3 K_{B_3}}{t_{33}^2}$	-3.74	+6.06	-12.69	20.56	-7.10	11.51	-4.30	6.96	-4.34	7.03	-4.28	6.93
$E\Delta_{43}/R_4$	-2.15		-5.87		-2.72		-2.36		-2.23		-2.19	
σ_{T_3}	0	0	0	0	0	0	0	0	0	0	0	0
$\sigma_\theta = \Sigma$	10.25	20.04	-18.56	1469	-9.82	8.79	9.48	20.73	6.33	17.70	6.44	17.64
$\sigma_r = -\frac{P}{2} \mp \frac{P}{2}$	-1.25	0	0	0	0	0	-1.25	0	-1.00	0	-1.00	0
$S_{x\theta} = \sigma_x - \sigma_\theta$	-14.6	15.9	-23.8	53.9	-13.8	29.6	-15.7	18.2	-14.3	18.3	-14.2	18.0
$S_{xr} = \sigma_x - \sigma_r$	-3.1	35.9	-42.3	68.6	-23.7	38.4	-5.0	38.9	-7.0	36.0	-6.8	35.7
$S_{\theta r} = \sigma_\theta - \sigma_r$	11.5	20.0	-18.6	14.7	-9.8	8.8	10.7	20.7	7.3	17.7	7.4	17.6

COMBUSTION ENGINEERING, INC.
ENGINEERING DEPARTMENT, CHATTANOOGA, TENN.
CHARGE NO. 224" BWR
DESCRIPTION Closure Region

NUMBER S101 CENC 1139
SHEET 91 OF A 86
DATE 1-30-70 BY JB
CHECK DATE 1-30-70 BY TP

C.0 Detailed Analysis
C.8 Vessel Stresses
C.8.4 Pe ½ Stress Intensities

Element ④ CUT III

$$\sigma_x = \frac{Pa_3^2}{2R_4 t_{33}} K_{T_3} \pm \frac{6M_3}{t_{33}^2} K_{B_3} + \sigma_{T_3}$$

$$\sigma_\theta = \frac{Pa_3^2}{R_4 t_{33}} \pm \mu \frac{6M_3 K_{B_3}}{t_{33}^2} + \frac{E\Delta_{43}}{R_4} + \sigma_{T_3}$$

$$\sigma_r = -\frac{P}{2} \mp \frac{P}{2}$$

$t_3 = 12.81$
$t_{33} = 8.38$
$r_{33} = 5.0$



From Ref. 11, fig A.7.1

for $\frac{r_{33}}{t_3} = \frac{5}{12.81}$; $K_{T_3} = 1.95$
$K_{B_3} = 1.62$

Condition	Vessel Over-Pressure		Startup		Shutdown Flooding		End of Shutdown		Rapid Heating		Rapid Cooling	
Surface	a	b	a	b	a	b	a	b	a	b	a	b
P	1.375		1.00		.185		0		1.25		.185	
F	74.379		85.860		73.426		70.152		69.975		72.026	
$E\Delta_{43}$	-267.26		-1224.6		-3.2376		684.89		-252.49		-286.42	
H_3	5.1973		4.4377		10.3230		13.055		5.0358		8.8787	
M_3	-152.83		-260.75		-234.57		-206.60		-147.23		-238.83	
$\frac{Pa_3^2}{2R_4 t_{33}} K_{T_3}$	8.87	17.30	6.45	12.58	1.19	2.33	0	0	807	15.73	1.19	2.33
$\pm \frac{6M_3}{t_{33}^2} K_{B_3}$	-13.07	21.18	-22.30	36.13	-20.06	32.51	-17.67	28.63	-12.59	20.40	-20.43	33.10
σ_{T_3}	-12.42	0	-15.56	9.11	5.49	-2.97	14.40	-8.48	-8.60	0	6.425	0
$\sigma_x = \Sigma$	-16.62	38.48	-31.41	57.83	-13.38	31.86	-3.27	20.15	-13.13	36.13	45.01	35.42
$\frac{Pa_3^2}{R_4 t_{33}}$	17.74		12.91		2.39		0		16.13		2.39	
$-\frac{\mu 6M_3 K_{B_3}}{t_{33}^2}$	-3.92	6.35	-6.69	10.84	-6.02	9.75	-5.30	8.59	-3.78	6.12	-6.13	9.93
$E\Delta_{43}/R_4$	-2.29		-10.49		-.03		5.87		-2.16		-2.45	
σ_{T_3}	-12.42	0	-15.56	9.11	5.49	-2.97	14.40	-8.48	-8.60	0	6.425	0
$\sigma_\theta = \Sigma$	-.88	21.81	-19.83	22.37	1.83	9.14	14.96	5.98	1.59	20.09	58.06	9.86
$\sigma_r = -\frac{P}{2} \mp \frac{P}{2}$	-1.38	0	-1.00	0	-.18	0	0	0	-1.25	0	-.18	0
$S_{x\theta} = \sigma_x - \sigma_\theta$	-15.7	16.7	-11.6	35.5	-15.2	22.7	-18.2	14.2	-14.7	16.0	-13.0	25.6
$S_{xr} = \sigma_x - \sigma_r$	-15.2	38.5	-30.4	57.8	-13.2	31.9	-3.3	20.1	-11.9	36.1	45.2	35.4
$S_{\theta r} = \sigma_\theta - \sigma_r$	.5	21.8	-18.8	22.4	2.0	9.1	15.0	6.0	2.8	20.1	58.2	9.9

C.0 Detailed Analysis
C.8 Vessel Stresses
C.8.4 Peak Stress Intensities

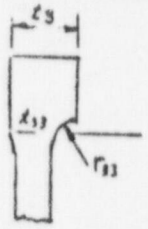
Element ④ CUT III

$$\sigma_x = \frac{Pa_3^2}{2R_4 t_{33}} K_{T_3} \pm \frac{6M_3}{t_{33}^2} K_{B_3} + \sigma_{T_3}$$

$$\sigma_\theta = \frac{Pa_3^2}{R_4 t_{33}} \pm \mu \frac{6M_3 K_{B_3}}{t_{33}^2} + \frac{E\Delta_{43}}{R_4} + \sigma_{T_3}$$

$$\sigma_r = -\frac{P}{2} \mp \frac{P}{2}$$

$a_3 = 12.81$
$t_{33} = 8.38$
$r_{33} = 5.0$



From Ref. 11, fig A.7.1

for $\frac{r_{33}}{t_3} = \frac{5}{12.81}$; $K_{T_3} = 1.95$
$K_{B_3} = 1.62$

Condition	Hydro Bolt Tensioning		Hydro Bolt Preload		Hydro Pressure Test							
Surface	a	b	a	b	a	b	a	b	a	b	a	b
P	0		0		1.565							
F	119.84		90.103		86.431							
$E\Delta_{43}$	-785.95		-363.88		-311.36							
H_3	20.460		11.883		6.1495							
M_3	-566.83		-317.11		-180.19							
$\frac{Pa_3^2}{2R_4 t_{33}} K_{T_3}$	0	0	0	0	10.10	19.69						
$\pm \frac{6M_3}{t_{33}^2} K_{B_3}$	-48.49	+78.55	-27.12	+43.94	-15.41	24.97						
σ_{T_3}	0	0	0	0	0	0						
$\sigma_x = \Sigma$	-48.49	78.55	-27.12	43.94	-5.31	44.66						
$\frac{Pa_3^2}{R_4 t_{33}}$	0		0		20.20							
$-\frac{\mu 6M_3 K_{B_3}}{t_{33}^2}$	-14.54	+23.55	-8.14	+13.18	-4.62	+7.49						
$E\Delta_{43}/R_4$	-6.73		-3.12		-2.67							
σ_{T_3}	0	0	0	0	0	0						
$\sigma_\theta = \Sigma$	-21.27	16.82	-11.25	10.07	12.91	25.02						
$\sigma_r = -\frac{P}{2} \mp \frac{P}{2}$	0	0	0	0	-1.56	0						
$S_{x\theta} = \sigma_x - \sigma_\theta$	-27.2	61.7	-15.9	33.9	-18.2	19.6						
$S_{xr} = \sigma_x - \sigma_r$	-48.5	78.6	-27.1	43.9	-3.7	44.7						
$S_{\theta r} = \sigma_\theta - \sigma_r$	-21.3	16.8	-11.2	10.1	14.5	25.0						

C.0 Detailed Analysis
C.8 Vessel Stresses
C.8.4 Peak Stress Intensities

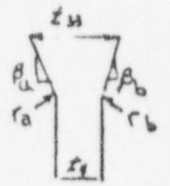
Element ④ CUT "V"

$$\sigma_x = \frac{Pa_4^2 K_{TV}}{2R_4 t_4^*} \pm \frac{6M_V K_{BV}}{(t_4^*)^2} + \sigma_{TV}$$

$$\sigma_\theta = \frac{Pa_4^2}{R_4 t_4^*} \pm \frac{\mu 6M_V K_{BV}}{(t_4^*)^2} - \frac{E\Delta_V}{R_4} + \sigma_{TV}$$

$$\sigma_r = -\frac{P}{2} \mp \frac{P}{2}$$

$r_a = .06$
$r_b = .06$
$t_{33} = 8.375$
$t_4^* = 6.50$
$\beta_a = 4:1$
$\beta_b = 3\frac{1}{2}:1$



From Ref. 11, fig A.7.2;
for $\beta_a = 4:1$, $\frac{r_s}{t_{33}} - t_H = .09$ $\therefore \frac{K'-1}{K_o-1} = .25$

for $\beta_b = 3.5:1$, $\frac{r_s}{t_{33}} - t_4 = .05$ $\therefore \frac{K'-1}{K_o-1} = .25$

From Ref 11, Fig A.7.1:
for $\frac{r_s}{t_{33}} = .01$ $K_o = 5.0$

$\therefore K_{TV_a} = 2.0$ $K_{BV_a} = 2.0$ (inside)
$K_{TV_b} = 2.0$ $K_{BV_b} = 2.0$ (outside)

Condition	Design Operation		Design Bolt Tensioning		Design Bolt Preload		Design Pressure Test		Steady State Operation		Inner Seal Leakage	
Surface	a	b	a	b	a	b	a	b	a	b	a	b
P	1.25		0		0		1.25		1.00		1.00	
F	69.528		104.59		78.641		75.709		70.567		70.938	
$E\Delta_V$	-151.17		-364.4		-144.57		-162.53		-148.41		-145.46	
H_V	5.2129		18.476		10.6441		6.0495		6.1930		6.1065	
M_V	-135.12		-457.13		-255.05		-155.16		-156.56		-154.26	
$\frac{Pa_4^2}{2R_4 t_4^*} K_{TV}$	21.14		0		0		21.14		16.91		16.91	
$\pm \frac{6M_V}{(t_4^*)^2} K_{BV}$	-38.37	38.37	-129.8	129.8	-72.44	72.44	-44.07	44.07	44.47	44.47	-43.81	43.81
σ_{TV}	0	0	0	0	0	0	0	0	0	0	0	0
$\sigma_x = \Sigma$	-17.24	59.51	-129.8	129.8	-72.44	72.44	-22.93	65.21	-27.56	61.38	-26.90	60.72
$\frac{Pa_4^2}{R_4 t_4^*}$	21.14		0		0		21.14		16.91		16.91	
$\pm \frac{\mu 6M_V}{(t_4^*)^2} K_{BV}$	-11.51	11.51	-39.0	39.0	-21.73	21.73	-13.22	13.22	-13.34	13.34	-13.14	13.14
$E\Delta_V / R_4$	-1.29		-3.12		-1.24		-1.39		-1.27		-1.25	
σ_{TV}	0	0	0	0	0	0	0	0	0	0	0	0
$\sigma_\theta = \Sigma$	8.33	31.36	-42.12	35.88	-22.97	20.49	6.52	32.97	2.30	28.98	2.52	28.81
$\sigma_r = -\frac{P}{2} + \frac{P}{2}$	-1.25	0	0	0	0	0	-1.25	0	-1.00	0	-1.00	0
$S_{1\theta} = \sigma_1 - \sigma_\theta$	-25.6	28.2	-87.7	93.9	-49.5	51.9	-29.4	32.2	-29.9	32.4	-29.4	31.9
$S_{xr} = \sigma_x - \sigma_r$	-16.0	59.5	-129.8	129.8	-72.4	72.4	-21.7	65.2	-26.6	61.4	-25.9	60.7
$S_{\theta r} = \sigma_\theta - \sigma_r$	9.6	31.4	-42.1	35.9	-23.0	20.5	7.8	33.0	3.3	29.0	3.5	28.8

C.0 Detailed Analysis
C.8 Vessel Stresses
C.8.4 Peak Stress Intensities

Element ④ cut "V"

$$\sigma_x = \frac{Pa_4^2 K_{TV}}{2R_4 t_4^*} \pm \frac{6M_V K_{BV}}{(t_4^*)^2} + \sigma_{TV}$$

$$\sigma_\theta = \frac{Pa_4^2}{R_4 t_4^*} \pm \frac{\mu 6M_V K_{BV}}{(t_4^*)^2} + \frac{E\Delta v}{R_4} + \sigma_{TV}$$

$$\sigma_r = -\frac{P}{2} \mp \frac{P}{2}$$

$r_a = .06$
$r_b = .06$
$t_{33} = 8.375$
$t_4^* = 6.50$
$\beta_a = 4{:}1$
$\beta_b = 3.5{:}1$



From Ref. 11, fig A.7.2;
for $\beta_a = 4{:}1$, $\frac{r_s}{t_{33}} - t_4 = .09$ $\therefore \frac{K'-1}{K_0-1} = .25$

for $\beta_b = 3.5{:}1$, $\frac{r_s}{t_{33}} - t_4 = .06$ $\therefore \frac{K'-1}{K_0-1} = .25$

From Ref 11, Fig A.7.1:
for $\frac{r_4}{t_{33}} = .01$ $K_0 = 5.0$

$\therefore K_{TVa} = 2.0$ $K_{BVa} = 2.0$ (inside)
$K_{TVb} = 2.0$ $K_{BVb} = 2.0$ (outside)

Condition	Vessel Over-Pressure		Startup		Shutdown Flooding		End of Shutdown		Rapid Heating		Rapid Cooling	
Surface	a	b	a	b	a	b	a	b	a	b	a	b
P	1.375		1.00		.185		0		1.25		.185	
F	74.379		85.860		73.426		70.152		69.975		72.026	
$E\Delta v$	-162.42		-967.56		116.35		720.30		-151.99		-135.86	
H_V	5.4497		5.7224		10.258		12.234		5.2734		9.1274	
M_V	-141.81		-250.18		-213.32		-180.52		-136.57		-220.22	
$\frac{Pa_4^2}{2R_4 t_4^*} K_{TV}$	23.25		16.91		3.128		0		21.14		3.13	
$\pm \frac{6M_V}{(t_4^*)^2} K_{BV}$	-40.28	40.28	-71.06	71.06	-60.59	60.59	-51.27	51.27	-38.79	38.79	-62.55	62.55
σ_{TV}	-12.42	0	-13.99	7.79	5.15	-2.68	12.84	-7.21	-8.60	0	64.25	0
$\sigma_x = \Sigma$	-29.45	63.53	-68.14	95.75	-52.31	61.04	-38.43	44.06	-26.25	59.92	4.83	65.67
$\frac{Pa_4^2}{R_4 t_4^*}$	23.25		16.91		3.13		0		21.14		3.13	
$\pm \frac{\mu 6M_V}{(t_4^*)^2} K_{BV}$	-12.08	12.08	-21.32	21.32	-18.18	18.18	-15.38	15.38	-11.64	11.64	-18.76	18.76
$E\Delta v/R_4$	-1.39		-8.29		1.00		6.17		-1.30		-1.16	
σ_{TV}	-12.42	0	-13.99	7.79	5.15	-2.68	12.84	-7.21	-8.60	0	64.25	0
$\sigma_\theta = \Sigma$	-2.64	33.94	-26.68	37.73	-8.90	19.62	3.63	14.3	-.40	31.47	47.45	20.73
$\sigma_r = -\frac{P}{2} \mp \frac{P}{2}$	-1.38	0	-1.00	0	-.18	0	0	0	-1.25	0	-.18	0
$S_{x\theta} = \sigma_x - \sigma_\theta$	-26.8	29.6	-41.4	58.0	-43.4	41.4	-42.1	29.7	-25.8	28.4	-42.6	44.9
$S_{xr} = \sigma_x - \sigma_r$	-28.1	63.5	-67.1	95.8	-52.1	61.0	-38.4	44.1	-25.0	59.9	+5.0	65.7
$S_{\theta r} = \sigma_\theta - \sigma_r$	-1.3	33.9	-25.7	37.7	-8.7	19.6	3.6	14.3	.8	31.5	47.6	20.7

COMBUSTION ENGINEERING, INC.
ENGINEERING DEPARTMENT, CHATTANOOGA, TENN.
CHARGE NO. 224" BWR
DESCRIPTION Closure Region

NUMBER C101 CENC 1139
SHEET 95 OF A-90
DATE 1-30-70 BY JB
CHECK DATE 1-30-70 BY TP

C.0 Detailed Analysis
C.8 Vessel Stresses
C.8.4 Peak Stress Intensities

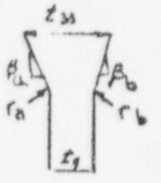
Element ④ cut "V"

$$\sigma_x = \frac{Pa_4^2 K_{TV}}{2 t_4^* t_4^*} \pm \frac{6 M_V K_{BV}}{(t_4^*)^2} + \sigma_{TV}$$

$$\sigma_\theta = \frac{Pa_4^2}{R_4 t_4^*} \pm \frac{\mu\, 6 M_V K_{BV}}{(t_4^*)^2} + \frac{E\Delta_V}{R_4} + \sigma_{TV}$$

$$\sigma_r = -\frac{P}{2} \mp \frac{P}{2}$$

$r_a = .06$
$r_b = .06$
$t_{33} = 8.375$
$t_4^* = 6.50$
$\beta_a = 4{:}1$
$\beta_b = 3.5{:}1$



From Ref. 11, fig A.7.2;
for $\beta_a = 4{:}1$, $\frac{r_c}{t_{33}} - t_4 = .09$ $\therefore \frac{K'-1}{K_0-1} = .25$

for $\beta_b = 3.5{:}1$, $\frac{r_c}{t_{33}} - t_4 = .06$ $\therefore \frac{K'-1}{K_0-1} = .25$

From Ref 11, Fig A.7.1:
for $\frac{r_c}{t_{33}} = .01$ $K_0 = 5.0$

$\therefore K_{TV_a} = 2.0$ $K_{BV_a} = 2.0$ (INSIDE)
$K_{TV_b} = 2.0$ $K_{BV_b} = 2.0$ (outside)

Condition	Hydro Bolt Tensioning		Hydro Bolt Preload		Hydro Pressure Test							
Surface	a	b	a	b	a	b	a	b	a	b	a	b
P	0		0		1.565							
F	119.84		90.103		86.431							
$E\Delta_V$	-417.5		-165.64		-188.12							
H_V	21.17		+12.195		6.4428							
M_V	-523.78		-292.22		-167.16							
$\frac{Pa_4^2}{2R_4 t_4^*} K_{TV}$	0		0		26.46							
$\pm \frac{6M_V}{(t_4^*)^2} K_{BV}$	-48.8	+148.8	-83.0	83.0	-47.48	47.48						
σ_{TV}	0	0	0	0	0	0						
$\sigma_x = \Sigma$	-148.8	+148.8	-83.0	83.0	-21.01	73.94						
$\frac{Pa_4^2}{R_4 t_4^*}$	0		0		26.46							
$\pm \frac{\mu 6 M_V}{(t_4^*)^2} K_{BV}$	-44.62	+44.62	-24.90	24.90	-14.24	14.24						
$E\Delta_V/R_4$	-3.58		-1.42		-1.61							
σ_{TV}	0	0	0	0	0	0						
$\sigma_\theta = \Sigma$	-48.2	41.04	-26.32	23.48	10.61	39.10						
$\sigma_r = -\frac{P}{2} \mp \frac{P}{2}$	0	0	0	0	-1.56	0						
$S_{x\theta} = \sigma_x - \sigma_\theta$	-100.6	-107.8	-56.7	59.5	-31.6	34.8						
$S_{xr} = \sigma_x - \sigma_r$	-148.8	148.8	-83.0	83.0	-19.4	73.9						
$S_{\theta r} = \sigma_\theta - \sigma_r$	-48.2	+41.0	-26.3	23.5	12.2	39.1						

C.0 Detailed Analysis

C.8 Vessel Stresses

C.8.4 Peak Stress Intensities

Peak Stress Intensities are summarized below for convienence.

Location	Stress Index	Surface	Design Operation	Design Bolt Positioning	Design Bolts Preloaded	Design Pressure Test	Steady State Operation	Inner Seal Leakage	Vessel Over Pressure	Startup	Shutdown Flooding	End of Shutdown	Rapid Heating	Rapid Cooling	Hydro Test Bolt Tensioning	Hydro Bolts Unloaded	Hydro Pressure Test
Element ① cut "C"	$S_{x\theta}$	a	-17.8	-31.2	-20.6	-19.5	-18.2	-18.2	-19.1	-18.4	-21.2	-22.6	-18.0	-18.8	-35.7	-23.6	-22.2
		b	48.8	12.7	9.1	49.6	40.8	40.9	53.5	53.8	11.8	-4.3	48.9	14.4	14.5	10.4	61.1
	S_{xr}	a	-9.9	-25.7	-17.5	-11.2	-11.2	-11.3	-22.8	-22.0	-13.1	-8.1	-18.6	49.1	-29.5	-20.0	-12.2
		b	78.7	36.9	25.0	80.6	67.7	67.8	85.9	80.2	30.2	14.5	78.8	31.3	42.3	28.7	98.3
	$S_{\theta r}$	a	8.0	5.5	8.1	8.2	7.0	7.0	-3.7	-3.6	8.1	14.5	-.6	67.9	6.3	3.6	10.0
		b	29.8	24.3	15.9	31.1	26.9	26.9	32.4	26.4	18.4	18.8	29.9	16.9	27.8	18.2	37.2
Element ① cut "I"	$S_{x\theta}$	a	13.1	-23.1	-14.6	12.0	7.7	7.7	14.8	19.6	-14.2	-29.2	13.1	-9.5	-26.5	-16.7	16.6
		b	53.1	21.7	14.9	54.3	45.3	45.5	58.0	55.6	18.6	5.1	53.2	19.5	24.8	17.0	66.4
	S_{xr}	a	2.6	-18.7	-12.3	1.7	-.2	-.2	-9.2	-17.7	-5.8	3.4	-6.0	54.9	-21.4	-14.1	3.4
		b	50.5	45.1	29.7	52.9	46.1	46.1	54.8	65.6	29.9	14.4	50.7	30.8	51.7	34.0	63.0
	$S_{\theta r}$	a	-10.5	4.4	2.2	-10.3	-8.0	-8.0	-24.0	-37.4	8.5	32.7	-19.1	64.4	5.0	2.6	-13.2
		b	-2.6	23.6	14.8	-1.4	.8	.8	-3.2	10.0	11.3	9.4	-2.5	11.3	27.0	17.0	-3.3
Element ② cut III	$S_{x\theta}$	a	-14.6	-23.8	-13.8	-15.7	-14.3	-14.2	-15.7	-11.6	-15.2	-18.2	-14.7	-13.0	-27.2	-15.9	-18.2
		b	15.9	53.9	29.6	19.2	18.3	18.0	16.7	35.5	22.7	14.2	16.0	25.6	61.7	33.9	19.6
	S_{xr}	a	-3.1	-42.3	-23.7	-5.0	-7.0	-6.8	-15.2	-30.4	-13.2	-3.3	-11.9	45.2	-48.5	-27.1	-3.7
		b	35.9	68.6	38.4	38.9	36.0	35.7	38.5	57.8	31.9	20.1	36.1	35.4	78.6	43.9	44.7
	$S_{\theta r}$	a	11.5	-18.6	-9.8	10.7	7.3	7.4	.5	-18.8	2.0	15.0	2.8	58.2	-21.3	-11.2	14.5
		b	20.0	14.7	8.8	20.7	17.7	17.6	21.8	22.4	9.1	6.0	20.1	9.9	16.8	10.1	25.0
Element ④ cut "I"	$S_{x\theta}$	a	-25.6	-87.7	-49.5	-27.4	-29.9	-29.4	-26.8	-41.4	-43.4	-42.1	-25.8	-42.6	-100.6	-56.7	-31.6
		b	23.2	93.9	51.9	32.2	32.4	31.9	29.6	58.0	41.4	29.7	28.4	44.9	107.8	59.5	34.8
	S_{xr}	a	-16.0	-129.8	-72.4	-21.7	-26.6	-25.9	-28.1	-67.1	-52.1	-38.4	-25.0	5.0	-148.8	-83.0	-19.4
		b	59.5	129.8	72.4	65.2	61.4	60.7	63.5	95.8	61.0	44.1	59.9	65.7	148.8	83.0	73.9
	$S_{\theta r}$	a	9.6	-42.1	-13.0	7.8	3.3	3.5	-1.3	-25.7	-8.7	3.6	.8	47.6	-48.2	-26.3	12.2
		b	31.4	35.9	20.5	33.0	29.0	28.8	33.9	37.7	19.6	14.3	31.5	20.7	44.0	23.5	39.1

C.0 Detailed Analysis
C.8 Vessel Stresses
C.8.4 Peak Stress Intensities

The maximum alternating stress intensity at each cut is tabulated below:

Element	cut	Surface	Stress Index	Max Stress Intensity: Load Condition	Max Stress Intensity: Stress Intensity	Min Stress Intensity: Load Condition	Min Stress Intensity: Stress Intensity	Peak Stress Range	ALT. Stress Intensity	Allowable Cycles $N \times 10^{-3}$
1	C'	a	Sxr	Rapid Cooling	49.1	Hydro Tensioning	-29.5	78.6	39.3	9.0
		b	Sxr	Rapid Heating	85.9	Zero Load	0	85.9	42.9	8.5
2	I'	a	Sor	Rapid Cooling	64.4	Startup	-37.4	101.8	50.9	4.1
		b	Sxo	Hydro Test	66.4	Zero Load	0	66.4	33.2	16.0
3	H'	a	Sxr	Rapid Cooling	45.2	Hydro Tensioning	-48.5	93.7	46.8	6.0
		b	Sxr	Hydro Tensioning	78.6	Zero Load	0	78.6	39.3	9.0
4	V'	a	Sxr	Rapid Cooling	5.0	Hydro Tensioning	-148.8	153.8	76.9	1.1
		b	Sxr	Hydro Tensioning	148.8	Zero Load	0	148.8	74.4	1.2

Conservatively assuming that the maximum alternating stress intensity is applicable for all the cyclic loading conditions gives the following fatigue evaluation:

Total number of composite cycles (from next page) = 843

Minimum number of cycles allowed for the maximum alternating stress of 76.9 ksi $= 1.1 \times 10^3$

Thus the conservative useage factor $U = \frac{843}{1100} = .77 < 1.0$

COMBUSTION ENGINEERING, INC.
ENGINEERING DEPARTMENT, CHATTANOOGA, TENN.

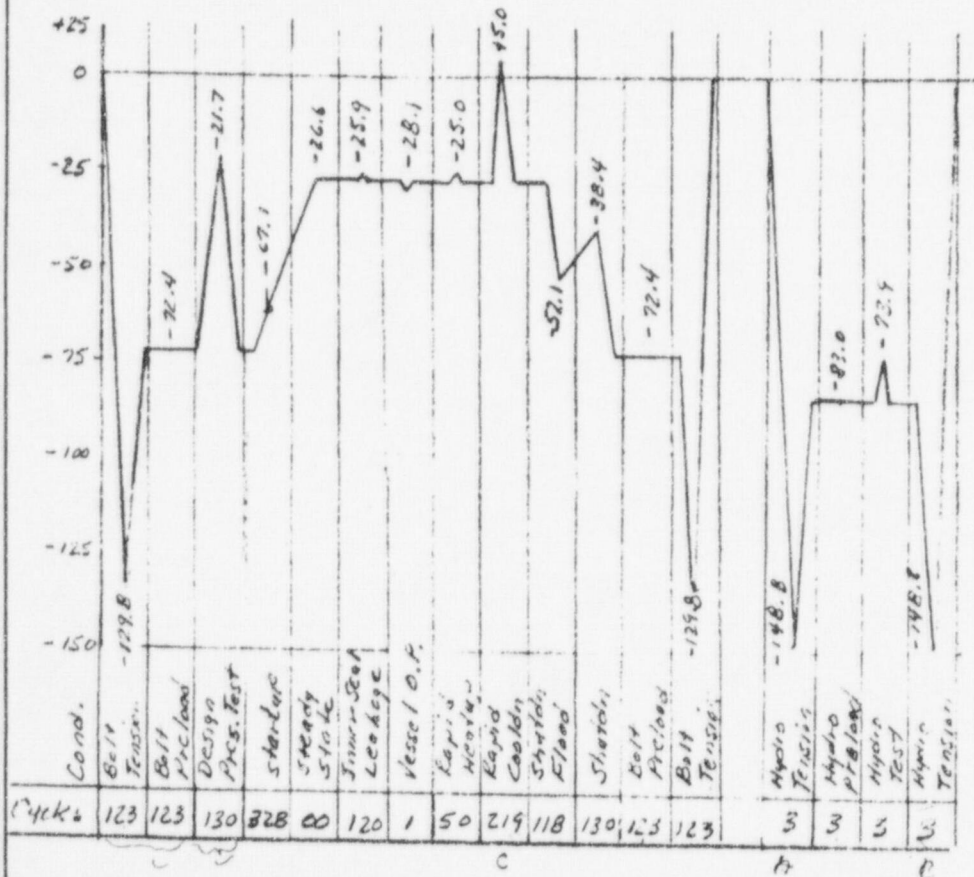
CHARGE NO. 224" BWR

DESCRIPTION Closure Region

NUMBER S-101 CENC 1139
SHEET 97a OF A-92a
DATE 1-30-70 BY TP
CHECK DATE 1-30-70 BY JB

C.0 Detailed Analysis
C.8 Vessel Stresses
C.8.4 Peak Stress Intensities

Required cycles are determined by assuming maximum stress range applies to total fluctuations, neglecting conditions where stress range is less than twice the endurance limit. Thus, at Element (4), Cut "4", Surface "a":



Smax	Smin	Cycles
+5.0	-148.8	6
+5.0	-129.8	214
0	-129.8	33
0	-83	6
0	-73.9	3
0	-72.4	84
-21.7	-72.4	130

A + B C + D

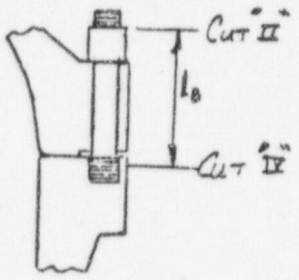
Smax	Smin	Cycles
-25.0	-72.4	39
-25.0	-67.1	11
-25.9	-67.1	120
-26.6	-67.1	197
-26.6	-32.1	—
-26.6	-38.4	—
-26.6	-28.1	—

54
130
39
253
123
120
253

The sum of cycles in the tables at the left is n = 843

C.0 Detailed Analysis

C.9 Bolt Stresses



Stresses in the bolts are limited per Par. N-416, Section III ASME Code (Ref 2).
Categories of loads included in this analysis are: Primary + Secondary
Peak

C.9.1 Maximum Service Stresses

Par. N-416.1 limits service stresses according ~~to~~ two categories: Maximum Average Bolt Service Stress
Maximum Bolt Service Stress

The Maximum Average Service Stress is limited to twice the allowable design stress. From the load summary of Part C.6, the maximum bolt load occurs during hydro preload where $F = 119.84$ kips/in.

Thus; $\sigma_B = \frac{2\pi R_F F}{N A_B} = 59.2$ ksi $< 2S_m = 86.6$ ksi

From C.6, The maximum bolt load during operation occurs at the end of startup and is 83.291 kips/in

Thus; $\sigma_B = \frac{2\pi R_F F}{N A_B} = 41.2$ ksi $< 2S_m = 73.6$ ksi

The Maximum Service Stress across the bolt section is limited to three times the allowable design stress

At Cut "II"; $\sigma_{B_2} = \frac{2\pi R_F F}{N A_B} + \frac{\pi R_F M_2 d}{N I_B}$

At Cut "IV"; $\sigma_{B_4} = \frac{2\pi R_F F}{N A_B} + \frac{\pi R_F M_2 d}{N I_B} + \frac{\pi R_F d H_2 l_B}{N I_B}$

C.0 Detailed Analysis

C.9 Bolt Stresses

C.9.1 Maximum Service Stresses

The Maximum Service Stress Intensities obtained by substituting the primary + secondary load conditions from Parts C.6 and C.7 are summarized below

Condition		Design Operation		Design Bolt Tensioning		Design Bolt Preload		Design Pressure Test		Steady State Operation		Inner Seal Leakage		Vessel Over-Pressure		Startup		Shutdown Flooding		End of Shutdown		Rapid Heating		Rapid Cooling		Hydro Bolt Tensioning		Hydro Bolt Preload		Hydro Pressure Test	
Surface		a	b	a	b	a	b	a	b	a	b	a	b	a	b	a	b	a	b	a	b	a	b	a	b	a	b	a	b	a	b
Loads	F	69.528		104.59		78.641		75.709		70.567		70.938		74.379		83.291		74.446		72.880		69.975		72.026		119.84		90.103		86.431	
	H_2	.5165'2		0		4.5871		.87706		1.2949		1.2363		.44558		1.6478		3.7707		4.6989		.54760		3.6774		0		5.2556		.61044	
	M_2	-21.258		0		47.037		-17.561		-8.0676		-8.7537		-24.641		-21.870		39.593		67.907		-20.791		33.779		0		53.892		-26.984	
$\frac{2\pi R_2 F}{NA_B}$		34.4		51.7		38.8		37.4		34.9		35.1		36.7		41.2		36.8		36.0		34.6		35.6		59.2		44.5		42.7	
$\pm\frac{R_2 M_2 C_B}{NI_B}$		13.5	-13.5	0	0	-29.9	29.9	11.2	-11.2	5.1	-5.1	5.6	-5.6	15.7	-15.7	13.9	-13.9	25.2	-25.2	43.2	-43.2	13.4	-13.4	21.5	-21.5	0	0	34.3	-34.3	17.2	-17.2
$\pm\frac{R_2 H_2 C_B}{NI_B}$		11.0	-11.0	0	0	-97.4	97.4	18.6	-18.6	27.3	-27.3	26.2	-26.2	9.5	-9.5	35.0	-35.0	80.1	-80.1	99.8	-99.8	11.5	-11.5	78.1	-78.1	0	0	111.6	-111.6	13.0	-13.0
σ_{B2}		47.9	20.8	51.7	51.7	84	68.8	48.6	26.2	40.0	29.7	40.6	29.5	52.4	21.1	55.1	27.2	11.6	62.0	7.2	79.2	47.7	21.2	14.1	57.1	59.2	59.2	10.2	78.8	57.9	15.5
σ_{B4}		58.8	9.9	51.7	51.7	106.3	-28.6	67.2	7.6	67.3	2.4	66.8	3.3	61.9	11.6	90.1	-7.8	91.7	-18.1	92.6	-20.6	59.4	9.7	92.2	-21.0	59.2	59.2	121.8	-32.8	72.8	12.6

Thus, the Maximum Service Stress across the bolt cross section occurs at the lower end of the bolt at the inner periphery during the Hydro Bolts Preload load condition.

$(\bar{\sigma}_{XB})_4 = 121.8$ ksi $< 3S_m = 129.9$ ksi

C.0 Detailed Analysis
C.9 Bolt Stresses
C.9.2 Fatigue Analysis of Bolts

Suitability of the bolts for cyclic operation is evaluated in accordance with Par N-416.2 through N-416.4 of Section III ASME Code (Ref 2).

The peak stress equations are: $\sigma_{B2} = \frac{2\pi R_F F}{NA_B} K_T \pm \frac{\pi R_F d M_2}{NI_B} K_B$

$$\sigma_{B4} = \frac{2\pi R_F F}{NA_B} K_T \pm \frac{\pi R_F d M_2}{NI_B} K_B \pm \frac{\pi R_F d H_2 l_B}{NI_B}$$

The peak stresses obtained by substituting Peak loads from Parts C.6 AND C.7 and using a stress concentration factor $K_T = K_B = 4.0$ (from Par N-416.4) are summarized below:

Condition	Design Operation		Design Bolt Tensioning		Design Bolt Preload		Design Pressure Test		Steady State Operation		Inner Seal Leakage		Vessel Over-Pressure		Startup		Shutdown Flooding		End of Shutdown		Rapid Heating		Rapid Cooling		Hydro Bolt Tensioning		Hydro Bolt Preload		Hydro Pressure Test	
Surface	a	b	a	b	a	b	a	b	a	b	a	b	a	b	a	b	a	b	a	b	a	b	a	b	a	b	a	b	a	b
Loads F	69.528		104.59		78.641		75.709		70.567		70.938		74.379		85.860		73.426		70.152		69.975		72.028		119.84		90.103		86.431	
Loads H_2	.51652		0		4.5871		.87706		1.2849		1.2343		.44558		1.4017		3.8576		4.9581		.54260		5.6774		0		5.2556		.61064	
Loads M_2	-21.258		0		47.037		-17.561		-8.0676		-8.7538		-24.641		-24.183		40.428		70.331		-20.991		33.779		0		53.892		-26.984	
$\frac{2\pi R_F F K_T}{NA_B}$	137.4		206.7		155.4		149.6		139.4		140.2		147.0		169.7		145.1		138.6		138.3		142.3		236.8		178.1		170.8	
$\pm \frac{\pi R_F d M_2 K_B}{NI_B}$	-54.1	-54.1	0	0	419.7	419.7	44.7	-44.7	20.5	-20.5	22.3	-22.3	+62.7	-62.7	61.6	-61.6	-102.9	102.9	-179.	179.0	53.4	-53.4	-86.	86.0	0	0	-137.2	137.2	+68.7	-68.7
$\pm \frac{\pi R_F d H_2 l_B}{NI_B}$	43.9	-43.9	0	0	389.7	-389.7	74.5	-74.5	109.2	-109.2	104.8	-104.8	37.8	-37.8	119.1	-119.1	327.7	-327.7	421.2	-421.2	46.1	-46.1	312.9	-312.9	0	0	446.5	-446.5	51.9	-51.9
σ_{B2}	191.5	83.3	206.7	206.7	35.7	275.4	194.3	104.9	160.0	118.9	162.5	117.9	209.7	84.3	231.2	108.1	42.2	248.0	-40.4	317.7	191.7	84.8	56.4	228.3	236.8	236.8	40.9	315.2	239.5	102.1
σ_{B4}	235.4	39.4	206.7	206.7	425.4	-114.5	268.8	30.4	269.2	9.8	267.3	13.1	247.6	46.4	350.3	-11.0	369.9	-79.7	380.8	-103.5	237.8	33.8	368.8	-84.1	236.8	236.8	487.4	-131.2	291.4	50.2

C.0 Detailed Analysis
C.9 Bolt Stresses
C.9.2 Fatigue Evaluation

The investigation of the cyclic life of the bolts is carried out as follows:

The peak stresses calculated on the preceeding page are plotted as stress cycles for each transient at each of the 4 locations being investigated. The alternating stress intensity is then as :

$$S_{ALT} = \frac{S_{max} - S_{min}}{2}$$

The corresponding cyclic life, N^*, is conviently taken from Ref 2, Figure N416, Summer 1963 Adenda. The lower curve for $S_{max} \geq 3.0\ S_m$ is conservatively used.
nominal

The actual number of occurances that will be encountered during the bolt life, n, is taken from Part C.2.2.

The usage factors for each cycle, $u_i = \frac{n_i}{N_i^*}$, are calculated and summed to give the accumulative usage factor U_o, which is compared to the allowable $U_o = 1.0$.

Investigation of each location in the manner above gives the following usage factors:

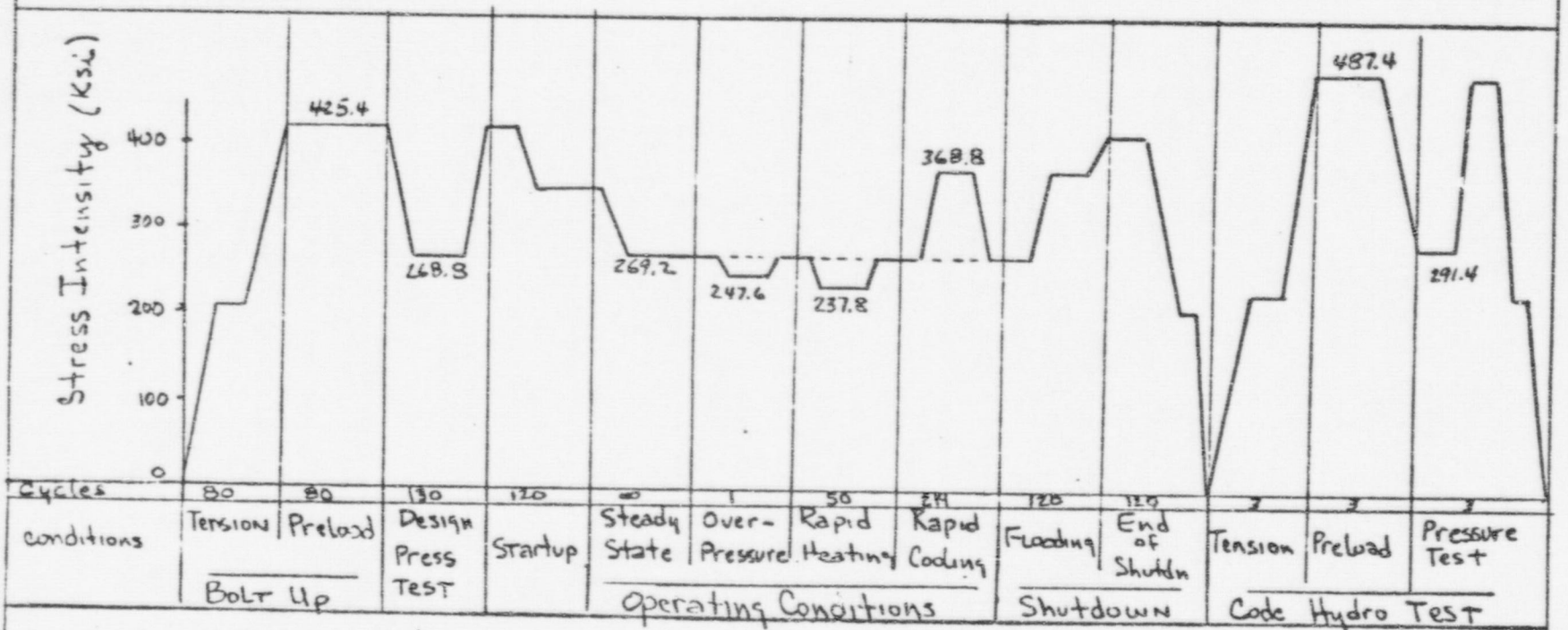
CUT	SURFACE	U_o
II	inner	.749
	outer	.675
IV	inner	.786
	outer	.417

Thus, the maximum usage factor occurs at IV a. The stress cycle plot and usage factor derivation for this cut are presented on the following page.

COMBUSTION ENGINEERING, INC.
ENGINEERING DEPARTMENT, CHATTANOOGA, TENN.
CHARGE NO. 224* BWR
DESCRIPTION Closure Region

NUMBER SIDI CENC 1134
SHEET 102 OF A-97
DATE 1-30-70 BY JB
CHECK DATE 1-30-70 BY TP

C.0 Detailed Analysis
C.9 Bolt Stresses
C.9.2 Fatigue Evaluation



S_{max}	S_{min}	n	S_{alt}	N^*	U_i
425.4	0	80	212.7	180	.444
425.4	268.8	130	78.4	1100	.118
425.4	269.2	120	78.1	1100	.109
368.8	269.2	219	49.8	2400	.091
269.2	237.8	50	15.7	20,000	0
487.4	0	3	243.7	150	.020
487.4	291.4	3	98	720	.004

$\therefore U_o = .786 \leq 1.0$

N^* values are from Ref 3 Summer 68 Addenda.

C.0 Detailed Analysis

C.10 Bearing Stresses

Adequacy of the bearing areas under the washer and on the mating surface are verified by calculation of the stresses during the maximum loading condition, which occurs when the bolts are preloaded.

The stress under the washer, $\sigma_{BW} = \frac{2\pi R_2 F}{A_W} = .5542F$

The stress on the mating surface, $\sigma_{Bm} = \frac{2\pi R_F B}{A_m} = .5664B$

Thus for design preload,

$\sigma_{BW} = (.5542)(78.641) = 43.6$ ksi $< S_{yp} = 50$ ksi
$\sigma_{Bm} = (.5664)(32.32) = 46.6$ ksi $< S_{yp} = 50$ ksi

And for hydro preload,

$\sigma_{BW} = (.5542)(90.103) = 49.9$ ksi $< 1.35 S_{yp} = 67.5$ ksi
$\sigma_{Bm} = (.5664)(94.320) = 53.4$ ksi $< 1.35 S_{yp} = 67.5$ ksi

For Design Operation

$\sigma_{BW} = (0.5542)(69.526) = 38.5 < \sigma_{yp} = 42.3$ @ 575°F
$\sigma_{Bm} = (0.5664)(2.0) = 1.1 < \sigma_{yp} = 42.3$ @ 575°F

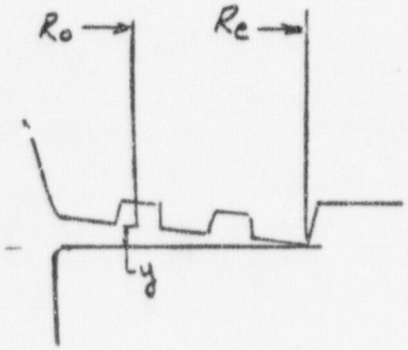
For Steady State Operation

$\sigma_{BW} = (0.5542)(70.567) = 39.1 < \sigma_{yp} = 42.6$ @ 550°F
$\sigma_{Bm} = (0.5664)(17.24) = 9.8 < \sigma_{yp} = 42.6$ @ 550°F

C.0 Detailed Analysis

C.11 O-Ring Sealing Capability

Paragraph 6.4, G.E.-APED Specification 21A1110 (Ref. 1) requires that sealing of the O-Rings be verified by limiting mating surface separation at the o-rings to the springback capability. Test data obtained by C.E. shows that the o-rings have a .010" springback under the 1 K/in compressive load required to seal steam.



Calculation of the mating surface separation at the inner o-ring is carried out by conservatively assuming rigid body rotation about the outer edge of the flange. Thus, the separation equation becomes:

$$y = (R_e - R_o)\left[(\theta_3 - \theta_2) - \theta_T\right]$$

where θ_T is the taper machined on the closure flange.

	Design Operation	Design Pressure Test	Steady State	Startup	Shutdown Flooding	End of Shutdown	Rapid Heating	Rapid Cooling
P	1.25	1.25	1.00	1.00	.185	0	1.25	.185
F	69.528	75.709	70.567	83.291	74.446	72.800	69.975	72.026
$E(\theta_3-\theta_2)^{Axial}$	207.49	222.56	201.80	232.02	183.14	172.90	208.94	1:7.39
$E(\theta_1-\theta_2)^{Axial}_{Th}$	0	0	0	102.49	34.38	114.61	0	0
$E \times 10^{-6}$	27.55	29.9	27.72	29.46	27.90	29.32	27.72	27.55
$\theta_3 - \theta_2$	.00753	.00744	.00728	.01175	.00779	.00639	.00754	.00645

Thus, where the angle of taper $\theta_T = \frac{.036}{2.966} = .01213$,
the inner o-ring will be sealed for all conditions.

APPENDIX B

THERMAL ANALYSIS

APPENDIX B

THERMAL ANALYSIS

Report	Title	Page
T-100-F	General Description for Thermal Analysis	B-3
	Physical Properties	B-16
	Nomenclature	B-19
	References	B-21
T-101-F	Closure Region	B-23
T-102-F	Vessel Shell	B-40
T-103-F	Support Skirt	B-43
T-212-F	Feedwater Nozzle	B-57
T-213-F	Core Spray Nozzle	B-68
T-214-F	Control Rod Drive Hydraulic System Return Nozzle	B-81
T-221-F	Recirculation Outlet Nozzle	B-89
T-222-F	Recirculation Inlet Nozzle	B-98
T-234-F	Control Rod Drive Nozzle	B-125
T-407-F	Shroud Support	B-134

ABSTRACT

This portion of the thermal report contains the information which is common to all of the various analyses performed for determining temperature condition to be considered in the stress analyses. Phases considered are Methods of Analysis, Correlations for Film Coefficients, Fluid Flow, General Assumptions, and Physical Properties. A table of Nomenclature and a list of References are included.

The thermal analysis for each specific area defines the transients and boundary conditions, and presents the nodal pattern assumed and the temperature conditions at the critical times in the transients.

METHODS OF ANALYSIS

Digital Computer Solutions - Transient and steady state temperature distributions are determined by use of the finite difference relaxation method as programmed for a digital computer. The general equations used are those developed by Hellman, et al, (1), which permit the calculation of film coefficients, flows, variable properties, and internal heat generation. One program applies to bodies of irregular shape or having boundary conditions that involve two- or three-dimensional heat flow while a simpler program is used for one-dimensional analyses.

The body being analyzed is divided into a system of blocks or nodes. The general finite difference equation for the change in temperature of any node "j" in a time interval is:

$$\Delta T_j = \frac{\Delta\tau}{C_j} \sum_{n=1}^{n=N} \frac{T_n - T_j}{{}_jR_n} \qquad 1.$$

The term ${}_jR_n$ represents the thermal resistance between node j and node n. The basic equation for thermal resistance is:

$$R = \frac{L}{kA} \qquad 2.$$

where L is the length of the heat flow path, k is the thermal conductivity of the material, and A is the area normal to the heat flow path.

In the case where the resistance between two nodes is composed of two different materials or there is a film coefficient to consider, the resistances are simply added in series:

$${}_jR_n = R_n + R_f + R_j \qquad 3.$$

The thermal resistance of a film is

$$R_f = \frac{1}{hA} \qquad 4.$$

where h is the film coefficient and A is again the area normal to heat flow.

Occasionally, block geometry or material make up necessitate calculating ${}_jR_n$ as several resistances in parallel. In that case, the following form is applicable:

$$\frac{1}{{}_jR_n} = \frac{1}{R_1} + \frac{1}{R_2} + \ldots + \frac{1}{R_1} \qquad 5.$$

The temperature of node "j" is calculated at successive time intervals $\Delta\tau$ using ΔT_j from equation 1 as follows:

$$T_j(\tau+\Delta\tau) = T_{j(\tau)} + \Delta T_j \qquad 6.$$

The stability criteria for the temperature equation is:

$$\Delta\tau < \frac{C_j}{\sum_{n=1}^{n=N} \frac{1}{R_n}} \qquad 7.$$

where the thermal capacitance (C_j) is the product of density, specific heat and volume of node "j".

Output at specified iterations or times consists of the nodal temperatures and any film coefficients, flows, or other special values computed.

Steady State Temperature Distributions as determined by the finite difference relaxation method utilize the following equation:

$$T_j = \frac{\sum_{n=1}^{n=N} \frac{T_n}{{}_jR_n} + q'''}{\sum_{n=1}^{n=N} \frac{1}{{}_jR_n}} \qquad 8.$$

where q''' represents internal heat generation.

The expression is equivalent to performing a heat balance about node "j".

The computation proceeds from an initially specified temperature distribution through as many iterations as necessary to reach the point where the maximum change in temperature for any node from one iteration to the next is less than a specified convergence accuracy.

Mathematical Solutions - The basic differential equation (2) in Cartesian coordinates is

$$\frac{\partial^2 T}{\partial x^2} + \frac{\partial^2 T}{\partial y^2} + \frac{\partial^2 T}{\partial z^2} + \frac{q'''}{k} = \frac{\rho\, C_p}{k}\frac{\partial T}{\partial \tau} \qquad 9.$$

Many specific solutions of this equation for various boundary conditions have been published (3, 4, 5, 6, 7). In general, these solutions may be applied to cylinders and plates subject to a temperature transient in the fluid, and to steady state conditions in fins and tube walls, generally without internal heat generation.

For gamma heating, the internal heat generation term q''' varies exponentially with the distance from the surface. The steady state temperature equation for a flat plate in a gamma flux and cooled on the incident face is

$$T_x - T_{ff} = \frac{q_o'''}{\mu^2 k}\left[1 - \exp(-\mu x) - \mu x \exp(-\mu t)\right] \qquad 10.$$

When cooled on the shielded face, the equation is:

$$T_x - T_{ff} = \frac{q_o'''}{\mu^2 k}\left[\mu x - \exp[-\mu(t-x)] + \exp(-\mu t)\right] \qquad 11.$$

The maximum thermal mismatch and consequently the maximum thermal stress that a temperature transient could cause is to assume that the surface of a body or a thin member attached to a heavy body instantly assumes the fluid temperature, while the average temperature of the body has not changed. This conservative assumption frequently shows such low stresses relative to the number of occurrences that a more exact analysis is not required. Mathematically, this is the condition of step change in fluid temperature with an infinite film coefficient. The average temperature as a function of time and slab thickness is given by:

$$\bar{T} = T_o + (T_f - T_o)\left[1 - 2\sum_{n=0}^{\infty} \frac{\exp[-(n+1/2)^2\, \pi^2\, F_o]}{(n+1/2)^2\, \pi^2}\right] \qquad 12.$$

The temperature equation for this condition is:

$$T_x = T_o + (T_f - T_o)\left[1 - 2\sum_{n=o}^{\infty} \frac{\exp[-(n+1/2)^2 \pi^2 F_o] \operatorname{Sin}(n+1/2)\pi x/t}{(n+1/2)\pi}\right] \qquad 13.$$

Fig. 1 will give the average temperatures of two slabs for maximum temperature difference as a function of relative slab thickness.

For a linear gradient terminated by a zero or reversed gradient, the maximum difference between surface and average temperature and between average temperatures of different thicknesses occurs at the end of the transient. The limiting value is given by:

$$\bar{T} - T_s = -(\Delta T/\Delta\tau)\,\rho\, C_p t^2/3k \qquad 14.$$

This expression applies to flat slabs. For a cylinder cooled on the inside, this equation is:

$$\bar{T} - T_s = -\frac{(\Delta T/\Delta\tau)\,\rho\, C_p}{2k}\left[\frac{R_o^4 \ln R_o/R_i}{R_o^2 - R_i^2} - \frac{3R_o^2 - R_i^2}{4}\right] \qquad 15.$$

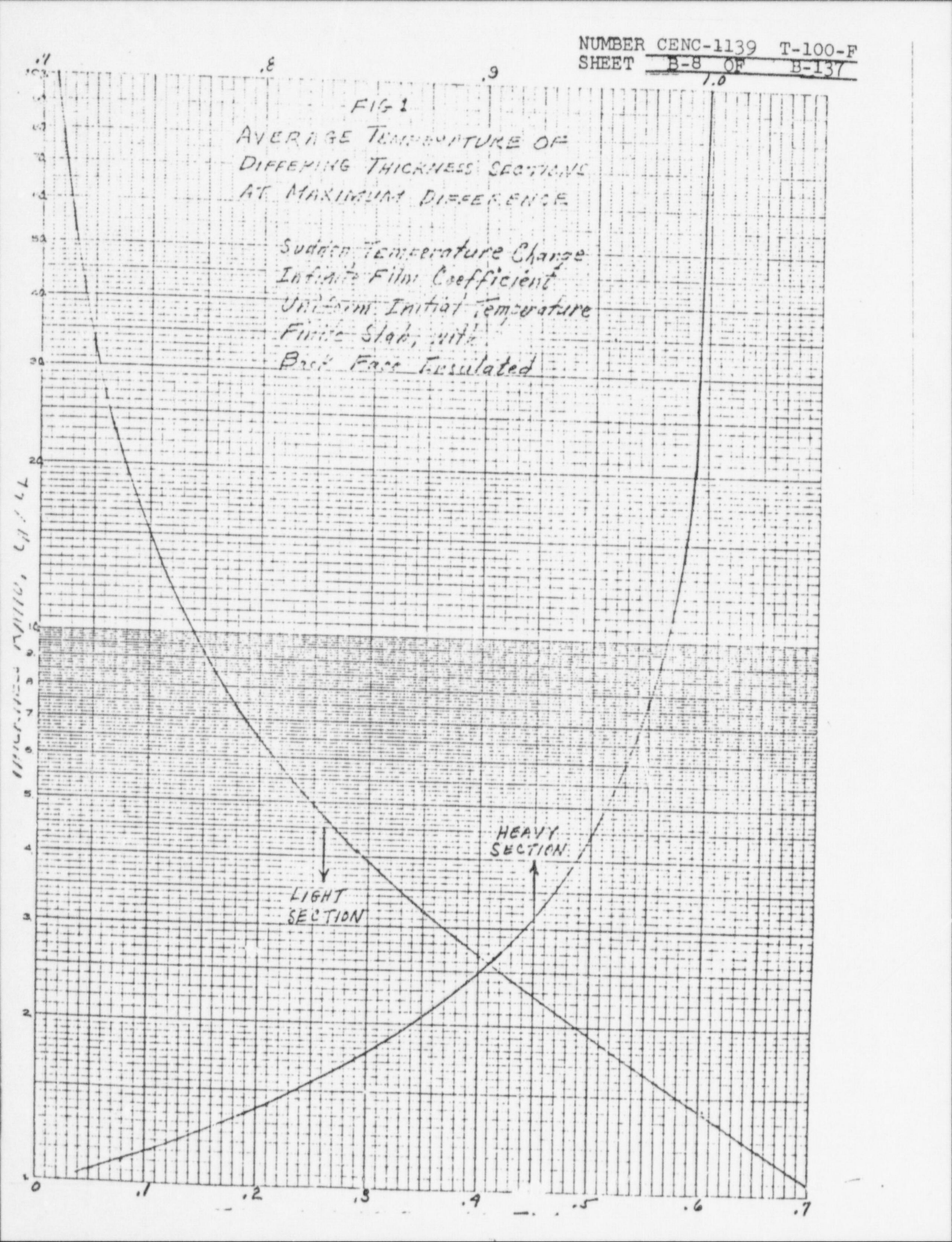
When applied to adjacent sections of differing thickness, the temperature difference is over-estimated, as axial heat flow tends to reduce the difference.

For a sudden temperature change with a finite film coefficient, the maximum difference between the surface and the bulk mean temperature of a slab occurs at the time given by:

$$\sum_{n=o}^{\infty} \frac{[\exp(-\eta_n^2 Fo)]\, Nu(\eta_n^2 - Nu)}{\eta_n^2 (Nu^2 + Nu + \eta_n^2)} = 0 \qquad 16.$$

where η_n are the positive roots of $\eta \tan \eta = Nu$. A curve for the maximum temperature difference as a function of Nusselt modulus and temperature ratio is shown in Fig. 2.

Thermal gradients of thin-walled cylinder and cylinder subjected to a step change on the inside are approximated by flat slab equations. For linear temperature changes, Fig. 3 plots the ratio of $T_s - \bar{T}$ for a cylinder vs a slab as a function of radius to thickness ratio.


FIG 1
AVERAGE TEMPERATURE OF
DIFFERING THICKNESS SECTIONS
AT MAXIMUM DIFFERENCE
Sudden Temperature Change
Infinite Film Coefficient
Uniform Initial Temperature
Finite Slab, with
Both Faces Insulated
HEAVY SECTION
LIGHT SECTION
.7
.8
.9
1.0
.1
.2
.3
.4
.5
.6
0
1
2
3
4
5
6
7
8
9
10
20
30
40
50
60
70
80
90
100

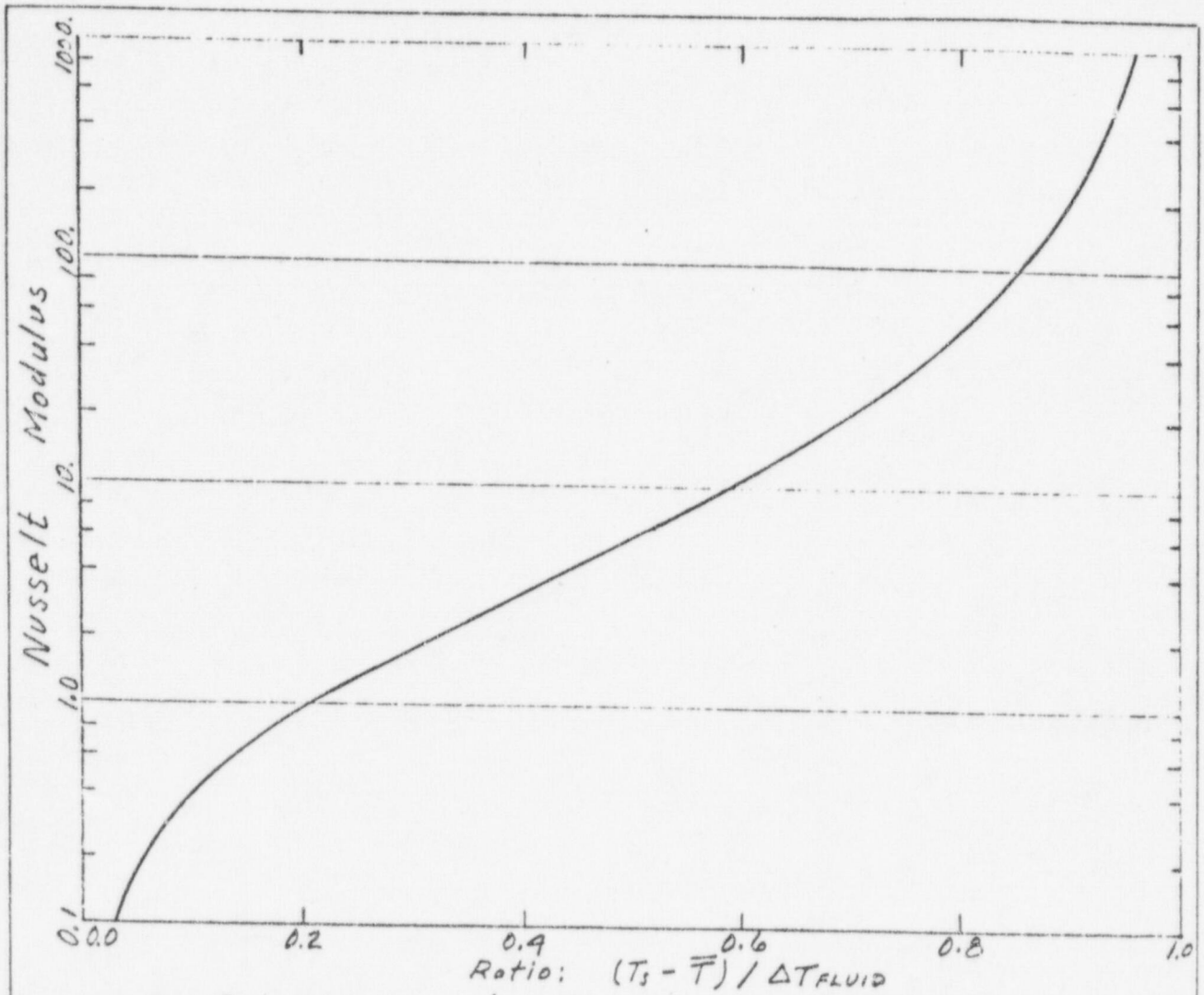


FIG. 2. Maximum $(T_s - \bar{T})$ vs Nusselt Modulus for sudden temperature change with finite film coefficient

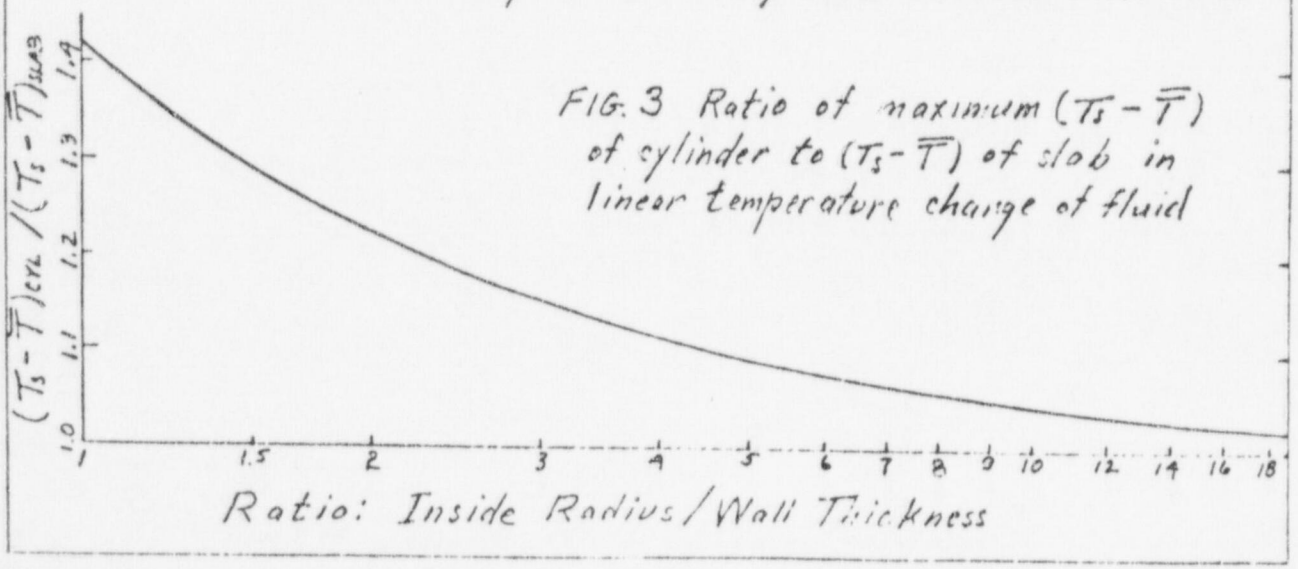


FIG. 3 Ratio of maximum $(T_s - \bar{T})$ of cylinder to $(T_s - \bar{T})$ of slab in linear temperature change of fluid

CORRELATIONS FOR FILM COEFFICIENTS

Various correlations are used to evaluate the film coefficient for transfer of heat across a metal-fluid interface. The value of the coefficient in general varies with temperature, temperature difference, and flow. For most analyses, film coefficients are taken as constant at an average value that over-estimates the stresses. When more exact temperature distributions are needed, the effect of temperature, temperature difference, and flow are included in the computation of the film coefficient for each iteration in the computer solution of the temperature distribution.

Turbulent Flow in Pipes and Annuli - The Dittus-Boelter correlation (8) is the basic expression used for this condition:

$$Nu = .023\ Re^{.8}\ Pr^{.4} \qquad 17.$$

This equation evaluates fluid properties at the bulk temperature. Colburn and Seider-Tate correlations (8), which are modifications that include evaluation of fluid properties at film or wall temperatures, are used if the value is more conservative.

Laminar Flow in Pipes and Annuli - The correlation for pipes (8) is:

$$Nu = 1.86\left(Re\ Pr\ \frac{D_H}{L}\right)^{\frac{1}{3}} \left(\frac{\mu_b}{\mu_w}\right)^{.14} \qquad 18.$$

For annuli, the constant is increased by 33% (8).

Free Convection - Heat transfer between a body and a bulk fluid without change of phase is correlated (9) by equations of the form

$$Nu = C\ Ra^n \qquad 19.$$

The values of the constants C and n vary with the physical arrangement, the fluid, and the value of the Rayleigh modulus, which is the product of the Grashof and Prandtl moduli.

These equations are based on steady state conditions, after natural convection flow has been established. In the analyses, however, the calculated coefficients are assumed to apply from the start of the conditions that induce free convection. Normally this is the conservative assumption.

TABLE 1

VALUES OF CONSTANTS FOR FREE CONVECTION

Arrangement	Fluid	Characteristic Dimension	Rayleigh Modulus	C	n
Vertical Plates or Cylinders	Gas/Liquid	Height	$< 10^8$	.56	.25
	Gas	"	$> 10^8$	.12	.33
	Liquid	"	$> 10^8$	.17	.33
Horizontal Plate, Hot, Facing Up, or Cold, Facing Down	Gas/Liquid	Long Side	$< 10^8$	.54	.25
	" "	" "	$> 10^8$	.14	.33
Reverse of Above	" "	" "	All	.25	.25

Boiling and Condensing Vapors - During an increasing temperature transient, the saturated steam will condense on the head and vessel wall above the water level. The correlation for film condensation on a vertical surface (10) is taken to be

$$h = .943 \left[\frac{g\rho(\rho-\rho_v)k^3 h_{fg} (1 + .68 C_p \Delta T/h_{fg})}{L\mu \Delta T} \right]^{\frac{1}{4}} \qquad 20.$$

This equation is valid for $Pr > .5$ and $C_p \Delta T/h_{fg} \leq 1$. The viscosity is evaluated at an average temperature taken as $Tw + 1/4 \Delta Tsat$ where $\Delta Tsat$ is the difference between the saturation and the wall surface temperatures.

When the pressure is reducing, as during a cooldown transient or due to loss of pressure, the water will keep at the saturation temperature by a portion of it flashing to steam. The hotter walls will produce boiling at the surface. A correlation for boiling of saturated water (10) is given as:

$$\frac{C_p \Delta T_{sat}}{h_{fg}} = .006 \left[\frac{q/A}{\mu h_{fg}} \sqrt{\frac{g_o \sigma}{g(\rho_l-\rho_v)}} \right]^{\frac{1}{3}} Pr^{1.7} \qquad 21.$$

This gives the film coefficient at atmospheric pressure as $272 (\Delta T_{sat})^2$. In addition to the heat transferred by the boiling, the turbulence due to the flashing to steam will transfer an additional amount of heat (10). Thus, the boiling film coefficient is high at all times, and generally may be considered as infinite.

Normal correlations for convective heat transfer apply for the steam when the wall is hotter, and for the water when the wall is cooler.

Enclosed Gaps - A correlation for heat transfer across an enclosed gap at various angles with respect to the horizontal (11) is given by:

$$Nu = C\ Ra^{\frac{1}{3}}\ Pr^{.074}$$

22.

The values of C for various angles and the ranges of Rayleigh moduli for which the correlations apply are given in Table 2.

TABLE 2

Angle, Degrees	C	
0 (Horizontal)	.069	$1.5 \times 10^5 < Ra < 7.5 \times 10^8$
30	.065	$1.5 \times 10^5 < Ra < 2.5 \times 10^8$
45	.059	$1.5 \times 10^5 < Ra < 2.5 \times 10^8$
60	.057	$1.5 \times 10^5 < Ra < 2.5 \times 10^8$
90 (Vertical)	.049	$5 \times 10^4 < Ra < 2.5 \times 10^8$

For Rayleigh moduli below the minimum, as occurs between the sleeves in the control rod drive nozzles, convection is suppressed and heat transfer is by straight conduction.

Water behind a nozzle liner, if flow is low, may be considered as being in an enclosed gap. Heat transfer is a maximum at the top or bottom, and a minimum at the other position. The correlation for the maximum heat transfer coefficient as given in Table 2 is used, and the resulting temperature distribution assumed to be symmetrical about the axis.

For rapid transients, the thermal inertia of the liner and the water has significant effect in reducing thermal stresses, while for longer transients and steady state conditions only the thermal resistance is a factor.

For the condition that has appreciable flow behind the nozzle liner, the fluid is taken as being at the ambient temperature of the nozzle fluid. This is conservative, but nearly correct, as the water changes temperature very slightly in flowing through the annulus. The flow in the annulus determines the film coefficient, which generally is much lower than in the nozzle.

Radiation - Radiant heat interchange is a factor at the support skirt-vessel junction and between the studs and the head flange. The expression for radiant heat transfer (12) is:

$$q/A = .173\,\bar{\epsilon}\left[\frac{(T_{A_1})^4}{(100)} - \frac{(T_{A_2})^4}{(100)}\right] \qquad 23.$$

Where the view factor is about 1, and $A_1 = A_2$,

$$\bar{\epsilon} \cong \frac{1}{1/\epsilon_1 + 1/\epsilon_2 - 1} \qquad 24.$$

When equation (23) is rearranged to solve for an equivalent film coefficient for radiation and simplified by eliminating second order effects, the expression becomes:

$$h_{rad} = \frac{q/A}{T_1 - T_2} \cong .000865\,\bar{\epsilon}\left\{\frac{T_{A_1} + T_{A_2}}{100}\right\}^3 \qquad 25.$$

This simplified form, which is a convenient form for use in the computer program, gives an error of less than 2% for a temperature difference of 100 degrees at an average temperature of 300°F.

Metallic Joints - Thermal resistance at metal joints is considered for those surfaces in contact in air or steam, but not when water can wet the joint. Correlation of the conductance is by the dimensionless group, $h\,P/k\rho$, corresponding to the Nusselt modulus, being plotted against the "dimensionless" ratio P/B, pressure in pounds per square inch divided by the Brinell number, which is kilograms per square millimeter. Curves for various materials and surface roughness conditions are given in Reference 13.

In general, the thermal resistance at the contact surfaces of the studs, nuts, and washers is very low, as the surfaces are relatively smooth and the pressures high. This gives a short heat path through the air filling the hollows, as well as a relatively large proportion of the surface in contact. When these hollows are filled with water, as at vessel flanges and rolled-in nozzle liners, contact resistance essentially disappears.

FLUID FLOW

Pressure drops associated with coolant flow are determined by use of Bernoulli's theorem, which in the general methematical expression is:

$$z_1 + \frac{144P_1}{\rho_1} + \frac{v_1^2}{2g} = z_2 + \frac{144P_2}{\rho_2} + \frac{v_2^2}{2g} + H_L \qquad 26.$$

The head loss, H_L, is due to energy dissipation between points 1 and 2 due to expansions, contractions, turns and friction.

"Friction Factors for Pipe Flow" by L. F. Moody (14) is used in determining the pressure drop due to friction with turbulent flow, giving the factor "f" used in the equation

$$\Delta P = f \frac{L}{D_H} \frac{v^2\rho}{2g \times 144} \qquad 27.$$

For laminar flow in a circular duct (15) the friction factor is given by

$$f = 64/Re \qquad 28.$$

and is an annulus, by

$$f = 96/Re \qquad 29.$$

Factors for coefficients for losses due to expansion, contractions, and turns are given in standard handbooks and text books (15, 16, 17).

GENERAL ASSUMPTIONS

There are several general assumptions that apply to the analyses. These are:

1. Physical properties are considered to be constant over the range of temperatures considered.

2. Insulated surfaces are adiabatic.

3. No axial heat flow in the vessel wall or a pipe wall beyond about 4 x wall thickness from the change in thickness.

4. The attenuation factor, and consequently the gamma ray energy, is constant through the vessel wall thickness.

The physical properties considered in the thermal analyses include density, specific heat, thermal conductivity and thermal expansion for all materials, with viscosity and heat of vaporization being additional factors for the water. The modulus of elasticity and emissivity are factors in structural materials. These properties are all variable with temperature, so that the value selected is average or one that gives a conservative result. Where the variable film coefficient option is used in computer calculations, the variation of the properties with temperature is included in the equations.

Considering insulated surfaces as adiabatic is a reasonable simplification, as the heat flow through the insulation is a small part of the total heat flow involved in the transients. Another factor is that when the stress range is being determined the radial heat flow through the insulation produces thermal stresses that tend to cancel out, producing little net effect.

Axial heat flow in a pipe or vessel wall with heat transfer from the surface is approximated (9) by the relation

$$\frac{T_z - T_C}{T_H - T_C} = \exp(-z\sqrt{h/kt}) \qquad 30.$$

The slope of the axial temperature gradient is a function of the thickness, conductivity, and film coefficient. The slope is 5% as great at $3\sqrt{kt/h}$ wall thicknesses away from a heavier section, and less than 2% as great at $4\sqrt{kt/h}$ wall thicknesses away, as at the junction. For a clad vessel wall six inches thick, the 2% of the slope condition is reached in about 14.4 inches when the film coefficient is 200 BTU/hr-ft^2-^{o}F.

The gamma flux at the vessel wall comprises a spectrum of energies incident at various angles. As the attenuation factor is higher for low energy gamma radiation, the radiation reaching the outer surface contains a higher fraction of the more energetic gamma's, and the energy deposition rate is lower. Thus assuming the gamma flux to be a beam of mono-energetic radiation normal to the surface over-estimates the temperature difference due to the gamma heating.

PHYSICAL PROPERTIES

The materials for which physical property values are needed include carbon and low alloy steel, type 304 stainless steel, Inconel Type 600, air, liquid water, and steam. In Table 3 are shown values of the various properties at several temperatures which cover the range required for the different analyses. For air and steam, the volumetric coefficient of thermal expansion is taken as the reciprocal of the absolute temperature. This is used in the Rayleigh modulus in the correlation for natural convection heat transfer. The values of the combined physical properties and gravity constant, $\frac{g\beta\rho^2 c_p}{\mu k}$, for the fluids are tabulated as the Rayleigh factor. For steam, the Rayleigh factor is taken at the steam film temperature, which is midway between the saturation temperature for the pressure during a cooldown and the wall temperature.

To establish the thermal capacitance of the metal nodes, the density and dimensions at 70F are used to determine the mass, and the specific heat selected for the temperature range. The density and specific heat vary more for liquid water than for the structural materials, but the product is quire constant over the temperature range of interest, so that the thermal capacitance of water nodes can be considered constant.

The linear coefficient of thermal expansion and the modulus of elasticity of the metals are of interest in determining effective gaps at operating conditions. Differential expansions due to temperatures and pressures can produce large percentage changes in gap widths at thermal sleeves and in control rod drive nozzles, with correspondingly large changes in thermal resistances.

TABLE 3

Material Symbol	Property	Temperatures 70	200	400	600
Carbon and Low Alloy Steel (Refs. 18, 19)					
α	Avg. linear coeff. of thermal exp. from 70 to temp, $x10^{6}$, per ^{o}F	6.07	6.38	6.82	7.23
E	Modulus of elasticity $x10^{-6}$, lb/in^2	27.9	27.7	27.0	25.7
k	Thermal conductivity, BTU/hr-ft-^{o}F	26.5	25.7	24.5	23.3
c_p	Specific heat, BTU/lb	.114	.118	.125	.135
ρ	Density, lb/ft^3	483.			
Type 304 Stainless Steel (Refs. 19, 23)					
α	Avg. linear coeff. of thermal exp. from 70 to temp, $x10^{6}$, per ^{o}F	9.11	9.34	9.59	9.82
E	Modulus of elasticity $x10^{-6}$, lb/in^2	27.4	27.1	26.4	25.4
k	Thermal conductivity, BTU/hr-ft-^{o}F	8.5	9.0	9.8	10.6
c_p	Specified heat, BTU/lb	.108	.116	.124	.131
ρ	Density, lb/ft^3	495.			
Inconel Alloy 600 (Refs. 19, 20)					
α	Avg. linear Coeff. of thermal exp. from 70 to temp, $x10^{6}$, per ^{o}F	7.13	7.40	7.70	7.90
E	Modulus of elasticity $x10^{-6}$, lb/in^2	31.7	30.9	30.0	29.2
k	Thermal conductivity, BTU/hr-ft-^{o}F	8.3	9.0	10.0	11.1
c_p	Specified heat, BTU/lb	.102	.109	.117	.123
ρ	Density, lb/ft^3	528.6			

TABLE 3 (Cont'd)

Material	Symbol	Property	Temperatures			
Water (Refs. 2, 10, 21, 22)			70	200	400	600
	ρ	Density at saturation, lb/ft^3	62.2	60.1	53.6	42.3
	ρ	Density at 1000 psia, lb/ft^3	62.4	60.3	53.9	-
	μ	Viscosity, lb/ft-hr	2.3	.75	.325	.210
	k	Thermal conductivity, BTU/hr-ft-F	.348	.396	.383	.291
	c_p	Specific heat, BTU/lb-F	.998	1.005	1.08	1.52
	σ	Surface tension, lb/ft	-	.0041	.0024	.0006
	Pr	Prandtl modulus, dimensionless	6.8	1.9	.925	1.09
	β	Vol. coeff. of thermal expansion x10^6, 1/^{o}F	130.	400.	730.	960.
	$Ra/L^3\Delta T$	Raleigh factor x10^{-6}, 1/ft^3-F	238.	2270.	8320.	14100 (at 500F)
Air (Ref. 2)						
	c_p	Specific heat, BTU/lb-F	.240	.241	.245	.250
	μ	Viscosity, lb/ft-hr	.044	.0519	.0626	.0721
	k	Thermal conductivity, BTU/hr-ft-F	.0149	.0181	.0225	.0265
	Pr	Prandtl modulus, dimensionless	.709	.693	.682	.680
	$Ra/L^3\Delta T$	Rayleigh factor x10^{-6}, 1/ft^3-F		.59	.18	.072
	ρ	Density, lb/ft^3	.074 at one atmosphere			
Steam (Ref. 21)						
	h_{fg}	Heat of vaporization, BTU/lb		978.	826.	549.
	ρ	Density, lb/ft^3		.0297	.537	3.74
		For Rayleigh factor:				
		Pressure, PSIA	184.	325.	540.	850.
		Film temperature, F	460.	485.	510.	535.
	$Ra/L^3\Delta T$	Rayleigh factor x10^{-6}, 1/ft^3-F	35.2	105.	340.	890.

NOMENCLATURE

A	Area, ft^2
B	Brinell hardness number, kg/mm^2
C	Constant, dimensionless
C_j	Thermal capacitance of node j, BTU/F
c_p	Specific heat, BTU/lb-F
D_H	Hydraulic diameter, ft
E	Modulus of elasticity, lb/in^2
F	Temperature, degress Fahrenheit
f	Friction factor, dimensionless
g	Acceleration due to gravity, 32.17 ft/sec^2 or 4.17×10^8 ft/hr^2
H_L	Head loss, ft
h	Film coefficient, $BTU/hr\text{-}ft^2\text{-}F$
k	Thermal conductivity, BTU/hr-ft-F
L	Length or geometrical factor, ft
N,n	Indexing numbers, dimensionless
n	Exponent, dimensionless
P	Pressure, lbs/ft^2 or lbs/in^2
q	Heat, BTU/hr
q'''	Heat generation, $BTU/hr\text{-}ft^3$
R	Thermal resistance hr-F/BTU; radius, ft.
T	Temperature, degrees Fahrenheit
T_A	Temperature, degrees Rankine
ΔT	Temperature difference or increment, degrees Fahrenheit
t	Thickness, ft
v	Velocity, ft/sec
x,y,z	Length on coordinate axes, ft

Greek

α	Linear coefficient of thermal expansion, 1/F; diffusivity, $ft^2/hr.$
β	Volumetric coefficient of thermal expansion, 1/F
ϵ	Emissivity factor, dimensionless
μ	Viscosity, lb/ft-hr
μ	Gamma attenuation factor, 1/ft
ρ	Density, lb/ft^3
σ	Surface tension, lb/ft
$\tau, \Delta\tau$	Time, time increment, hr

NOMENCLATURE (Cont'd)

Dimensionless Moduli

Fo	Fourier modulus, $\sigma \tau / t^2$
Gr	Grashof modulus, $L^3 \beta g \Delta T \rho^2 / \mu^2$
Nu	Nusselt modulus, $h L / k$
Pr	Prandtl modulus, $C_p \mu / k$
Ra	Rayleigh modulus, Gr x Pr
Re	Reynolds modulus, $D_H \nu \rho / \mu$

Subscripts

b	Bulk
C	Cold
f	Film; fluid
ff	Front face
fg	Evaporation
H	Hot
i	Index number; inside
j	Index number
l	Liquid
n	Index number
o	Zero; original; outside
rad	Radiation
sat	Saturation
v	Vapor
w	Wall
x,z	Position on x, z axis
τ	At time τ

REFERENCES

1. "Use of Numerical Analysis in Transient Solution of Two-Dimensional Heat Transfer Problem with Natural and Forced Convection", by S. K. Hellman, et al. ASME Paper No. 54-SA-53, 1954.

2. "Heat Transfer", by Benjamin Gebhart, McGraw-Hil Book Co., Inc., New York, 1961.

3. "Conduction of Heat in Solids", by H. S. Carslaw and J. C. Jaeger, Oxford University Press, 1948.

4. "Temperature Distributions in Slabs with a Linear Temperature Rise at One Surface", by Anthony, M. L. Proceedings of the General Discussion on Heat Transfer, pp. 236-262, Institution of Mechanical Engineers, London, and American Society of Mechanical Engineers, New York, 1951.

5. "Transient Thermal Stresses in Slabs and Circular Pressure Vessels", by M. P. Heisler, J. of Applied Mechanics, June 1953.

6. "Thermal Stresses in Spheres and Cylinders Produced by Temperatures Varying with Time", by Kent, C. H., Trans. Am. Soc. Mech. Eng., Vol. 54, No. 118, p. 185; 1932.

7. "Tentative Structural Design Basis for Reactor Pressure Vessels and Directly Associated Components (Pressurized, Water Cooled Systems)" PB 151987 U.S. Dept. of Commerce, Office of Technical Services.

8. "Heat Transmission" by W. H. McAdams, McGraw-Hill Book Co., New York, 3rd Ed., 1954.

9. "Heat Transfer Engineering", by Hilbert Schenk, Jr., Prentice-Hall, Inc., Englewood Cliffs, N.J., 1st Ed., 1959.

10. "Heat, Mass, and Momentum Transfer" by Warren M. Rohsenow and Harry Y. Choi, Prentice-Hall, Inc., Englewood Cliffs, N.J., 1961.

REFERENCES

11. "Heat Transfer by Natural Convection in Liquids Confined by Two Parallel Plates Which are Inclined at Various Angles with Respect to the Horizontal", D. Dropkin and E. Somerscales Paper #64 HT-22 AIChE and ASME Heat Transfer Conference, August 1964. Trans. of ASME, Series C, Feb. 1965.

12. "Chemical Engineers Handbook" Edited by J. H. Perry, 2nd Ed., McGraw-Hill Book Co., 1941.

13. "Thermal Conductance Across Metal Joints", by W. J. Graff, Machine Design, Sept. 15, 1960, pp. 166-172.

14. "Friction Factors for Pipe Flow" by L. F. Moody, Trans. ASME Vol. 66, p. 671, 1944.

15. "Fluid Mechanics" by Victor L. Streeter, McGraw-Hill Book Co., Inc., New York, 2nd Ed., 1958.

16. "Marks' Mechanical Engineers Handbook", Edited by Theodore Baumeister, 6th Ed., McGraw-Hill Book Co., 1958.

17. "Flow of Fluids", Technical Paper No. 410, Crane Co., Chicago, Ill., 1957.

18. "Physical Constants of Some Commercial Steels at Elevated Temperatures", British Iron and Steel Research Association, 1953.

19. "ASME Boiler and Pressure Vessel Code Section III - Nuclear Vessels", 1965 Edition - Revised. ASME, New York, N.Y.

20. AF TR 6145 Parts I, II, III International Nickel Co.

21. "Thermodynamic Properties of Steam", by J. H. Keenan and Frederick G. Keyes, John Wiley & Sons, Inc., New York, First Edition, 24th Printing.

22. "A Survey of the Thermodynamic and Physical Properties of Water", by E. J. Wellman. M.S. Thesis, Purdue University, 1950.

23. "Metals Handbook", Vol. 1, 8th Ed.; American Society for Metals, Metals Park, Ohio, 1961.

SUMMARY

The thermal analysis of the closure region considers the end of heatup, shutdown flooding and the end of shutdown. The results are used in Calculation CE-S-101.

TRANSIENTS

The heatup transient is from 100F to 546F at 100F per hour, with the critical time at the end of heating. Cooldown is at -100F per hour from 546F to 375F, when flooding starts. The temperatures of the water and steam drop to 330F in 10 minutes. The shutdown transient then continues at -100F to 100F. The critical time is at the end of shutdown. The flanges are flooded at 1.81 hours, when the temperature has dropped to 348F. Maximum skin stresses occur at the moment of flooding of the flanges.

Other transients are not as severe, as the film coefficient is very low during the cooling portion of a transient, when the metal is hotter than the steam. In the return to temperature, there is condensation and a high film coefficient after the steam temperature rises above that of the wall. This is treated as a skin stress, using the temperature range.

THERMAL MODEL

Three-dimensional nodal pattern is used to cover a section included between the adiabatic planes of the bolt centerline and mid-way between bolts. Two layers are employed in the circumferential direction.

Included in this model are head and vessel flanges, the adjacent head and wall sections, the bolt with the washer and nut, and refueling basin seal skirt.

Figures 1 and 2 show the nodal pattern for the upper and lower flange sections.

BOUNDARY CONDITIONS

The film coefficient for the steam condensing on the inner surfaces of the flanges during heatup is considered as infinite. During cooldown prior to flooding, the correlation

for natural convection is used, the value being calculated in the program according to the instantaneous conditions. After flooding, the film coefficient is again considered as infinite due to local boiling.

Heat transfer across the gap between the bolt and the head is mainly by radiation, while that across the gap between the vessel and the refueling basin seal skirt is by radiation and convection. Both are taken as temperature dependent in the program.

Conduction across the threads and between the nut, washer and the head is considered as having the same values as solid metal. The thermal resistance between the flange surfaces in contact is reduced to a negligible amount by the contact pressure. The thermal resistance across the gap outside the seal region is taken as constant regardless of the slight variation in the air properties due to changes in temperature.

CALCULATIONS

The film coefficient in the shutdown transient prior to flooding is evaluated by Equation 19 of T-100. Due to the temperature and pressure dependence of the steam properties, the equation for the temperature range between 546F and 348F is:

$$h = 1.469 \times 10^{-5} (T_{sat} - 100)^{2.278} \quad \text{Btu/hr-ft}^2\text{-F}$$

These values are used to calculate film resistances which are then combined with the resistance through the cladding to compute the overall conductances between the steam and the interface.

The equivalent film coefficient for radiation is evaluated by Equation 23 of T-100. Using $\epsilon_1 = \epsilon_2 = 0.8$ for the studs and head flange, the equivalent film coefficient is:

$$h_{rad} = 0.001154 \left[\left(\frac{T_1 + 460}{100} \right)^2 + \left(\frac{T_j + 460}{100} \right)^2 \right] \times \left[\left(\frac{T_j + 460}{100} \right) + \left(\frac{T_j + 460}{100} \right) \right] \quad \text{Btu/hr-ft}^2\text{-F}$$

A higher emissivity value of 0.9 is taken for the painted surfaces of the basin seal skirt and the vessel, giving a constant of 0.001415 for the above equation. For simplicity, each node is only connected to the opposite node across the gap, using the smaller area and a view factor of 1.

Convection is suppressed in the gap between the studs and the head flange, and the relatively small conduction by the air is neglected. The convective film coefficient for the gap between the vessel and the basin seal skirt is calculated in the computer using

$$h = 0.0626\ \Delta T^{1/3}\ \text{Btu/hr-ft}^2\text{-F}$$

This is derived from Equation 19, T-100. The ΔT is specified as the temperature between Nodes 139 and 353.

RESULTS

The thermal data for stress calculation are listed in Table 1. The time at which shutdown flooding occurs is 1.81 hours when the water is 348F.

The cut locations are shown in the nodal layouts, and the Index identification is given in the stress report CE-S-101. The print pattern to identify the nodal temperatures is shown in Figures 3 and 4. The computer output from which these data are taken are presented following Figure 4.

TABLE 1

AVERAGE TEMPERATURE, F, AND SLOPE OF AXIAL TEMPERATURE GRADIENTS, F/IN

Index	End of Heatup	Shutdown Flooding	End of Shutdown
T_{21}	450.0	511.9	204.2
T_{22}	354.0	530.4	309.8
T_{23}	483.0	506.0	168.6
$\bar{T}_2$	422.9	517.4	235.0
T_{3B}	487.4	505.2	162.2
T_{32B}	476.9	508.1	173.5
T_{32F}	420.0	523.1	235.0
T_{33B}	496.9	502.6	151.7
T_{33F}	441.7	518.9	211.3
$\bar{T}_3$	453.9	513.7	198.4
T_B	290.5	536.0	353.0
m_2	1.271	-0.0879	-1.32
m_3	1.83	-0.347	-1.986

Radial Temperature Distributions at Indicated Sections of Vessel Head and Vessel Wall

End of Heatup for Vessel Head

Cut No.	$\bar{T}$	Temperature, F T_1	$T_{1/4}$	$T_{1/2}$	$T_{3/4}$	T_o
19	536.1	542.5	539.0	534.5	533.5	532.0
20	533.4	541.8	536.6	531.4	530.1	528.8
23	520.1	539.3	527.8	516.2	512.5	508.8
25	478.5	535.3	503.6	480.7	457.3	409.6

TABLE 1 (Continued)

End of Heatup for Vessel Wall

Cut No.	$\bar{T}$	T_i	Temperature, F $T_{1/4}$	$T_{1/2}$	$T_{3/4}$	T_o
0	487.3	536.8	505.2	481.3	465.1	458.3
3	492.6	537.1	508.3	486.9	472.9	467.8
4	499.4	537.6	512.9	494.4	482.3	478.3
6	498.3	537.7	513.6	494.5	480.1	472.0
8	507.8	538.7	518.1	503.3	494.4	492.4

Shutdown Flooding for Vessel Head

Cut No.	$\bar{T}$	T_i	Temperature, F $T_{1/4}$	$T_{1/2}$	$T_{3/4}$	T_o
19	466.3	461.0	463.9	467.7	468.5	469.3
20	472.3	466.2	470.0	473.7	474.6	475.5
23	484.6	476.1	481.3	486.5	488.0	489.4
25	501.6	485.6	495.3	501.8	507.8	517.0

Shutdown Flooding for Vessel Wall

Cut No.	$\bar{T}$	T_i	Temperature, F $T_{1/4}$	$T_{1/2}$	$T_{3/4}$	T_o
0	505.7	488.3	500.0	508.1	513.1	515.1
3	504.1	487.8	498.9	506.4	511.0	512.6
4	501.8	487.0	497.0	503.9	508.1	509.4
6	500.9	485.9	495.8	502.8	507.4	509.4
8	498.6	484.5	494.2	500.7	504.5	505.4

TABLE 1 (Continued)

End of Shutdown for Vessel Head

Cut No.	$\bar{T}$	Temperature, F T_1	$T_{1/4}$	$T_{1/2}$	$T_{3/4}$	T_o
19	109.4	103.1	106.6	111.1	112.1	113.1
20	112.4	103.8	109.1	114.4	115.7	117.1
23	126.6	106.5	118.7	130.8	134.7	138.6
25	172.1	111.0	145.0	169.7	195.2	246.6

End of Shutdown for Vessel Wall

Cut No.	$\bar{T}$	Temperature, F T_1	$T_{1/4}$	$T_{1/2}$	$T_{3/4}$	T_o
0	151.7	109.3	142.6	168.0	185.4	192.7
3	155.7	108.9	139.1	161.7	176.6	182.0
4	148.0	108.3	133.9	153.3	165.8	170.0
6	149.1	108.1	133.1	152.9	168.0	176.4
8	138.7	107.0	128.1	143.3	152.5	154.5

TABLE 1 (Continued)

Axial Temperature Distributions of Refueling Basin Skirt

X(In)*	Temperature, F		
	End of Heatup	Shutdown Flooding	End of Shutdown
0.9	402.9	527.7	253.7
2.45	403.3	527.9	252.8
4.30	408.0	527.0	246.9
6.75	414.1	525.6	239.5
9.00	423.8	523.3	227.7
11.55	443.0	518.5	204.9
14.70	449.8	516.7	196.4
18.90	447.3	514.7	193.6
22.90	410.7	518.3	225.3
25.70	318.4	530.1	313.2
27.25	291.2	533.4	339.5

*The origin and direction of "X" is indicated in Figure 2.

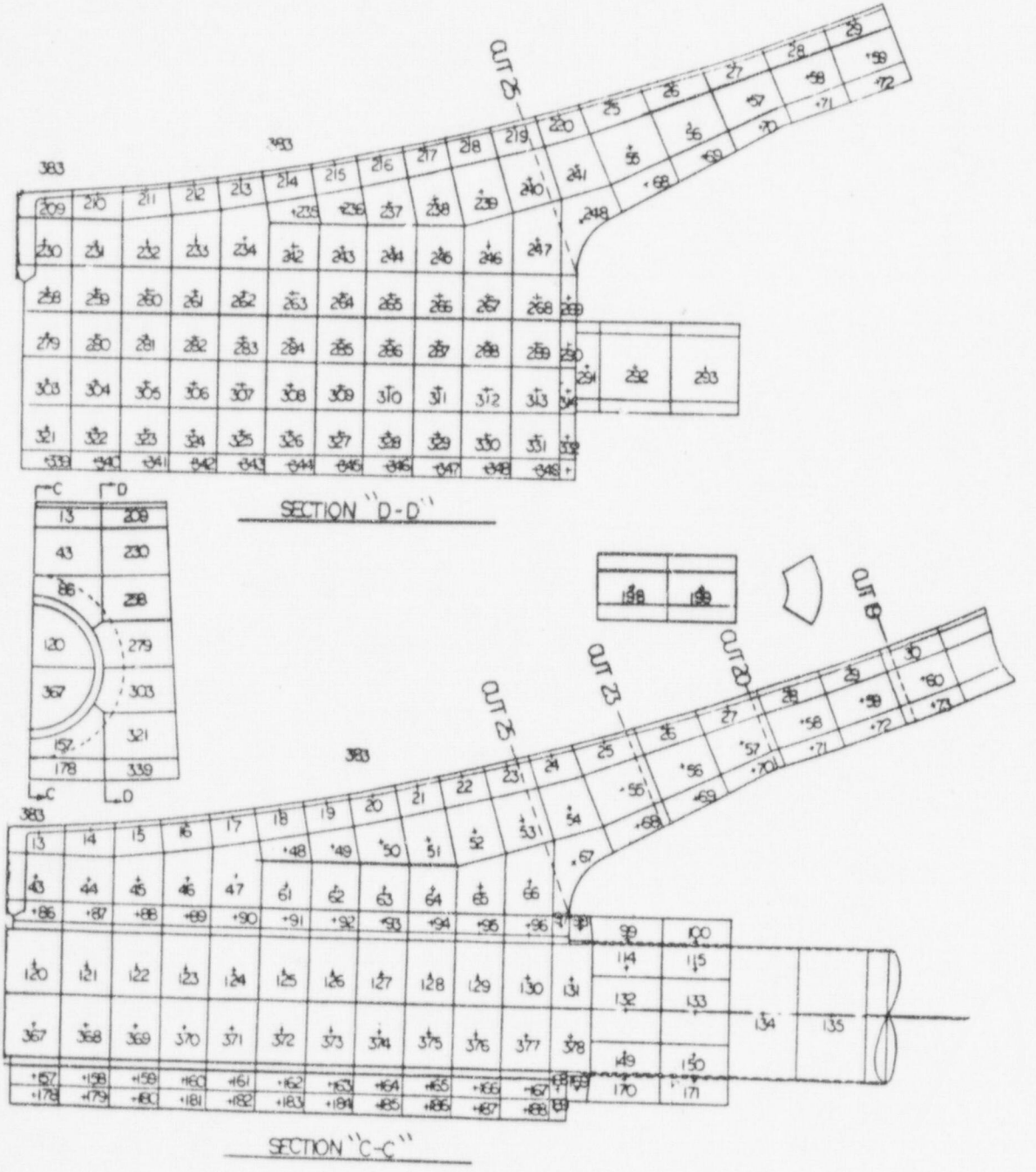


FIGURE 1. NODAL LAYOUT OF UPPER FLANGE SECTION

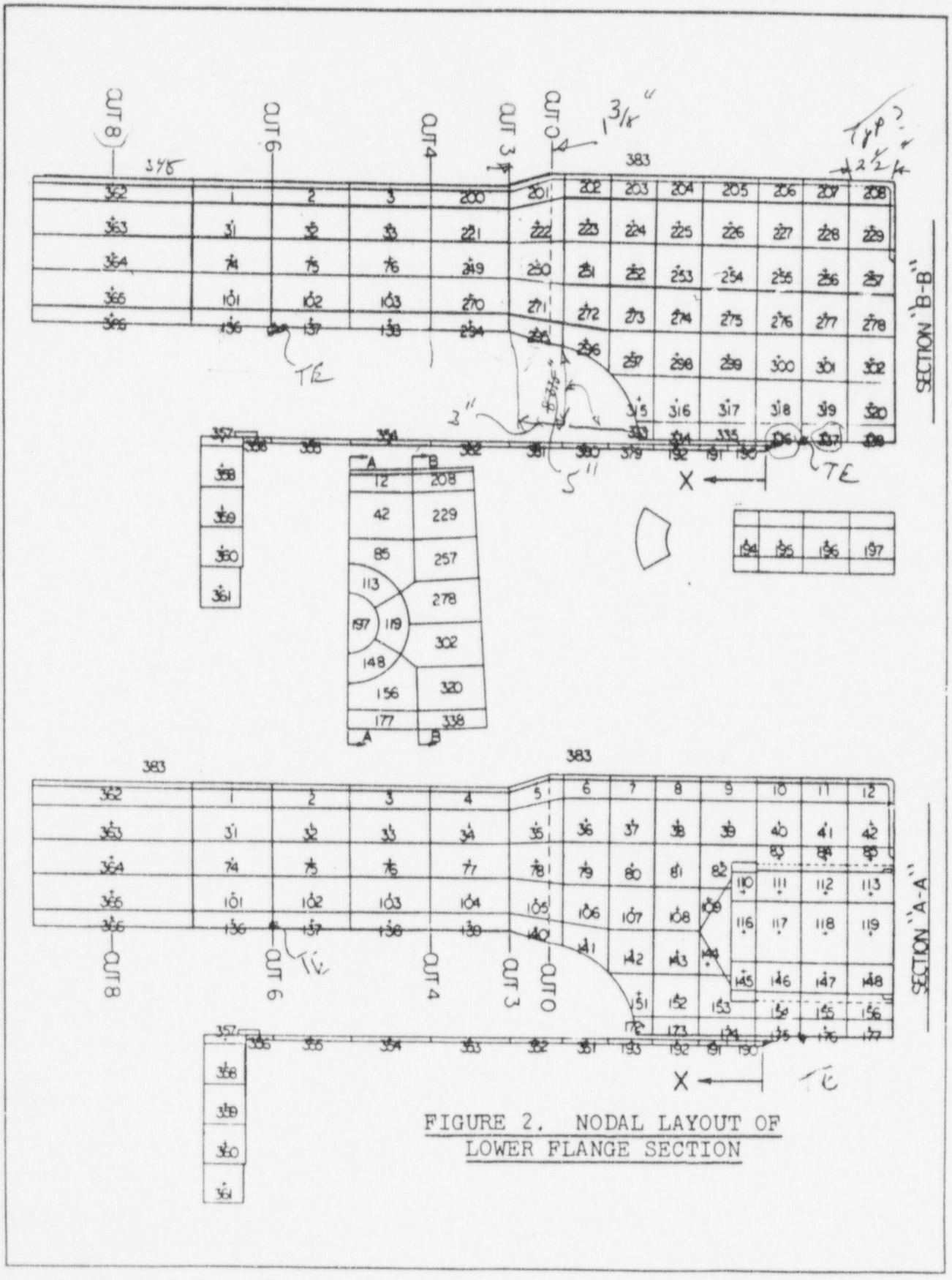


FIGURE 2. NODAL LAYOUT OF LOWER FLANGE SECTION

COMBUSTION ENGINEERING, INC.
ENGINEERING DEPARTMENT, CHATTANOOGA, TENN.

CHARGE NO. 21466

DESCRIPTION THERMAL ANALYSIS OF PILGRIM STATION CLOSURE REGION

NUMBER CENC-1139 T-101-F
SHEET B-32 OF B-137
DATE 11/3/69 BY Chen
CHECK DATE 11/5/69 BY Kinyon

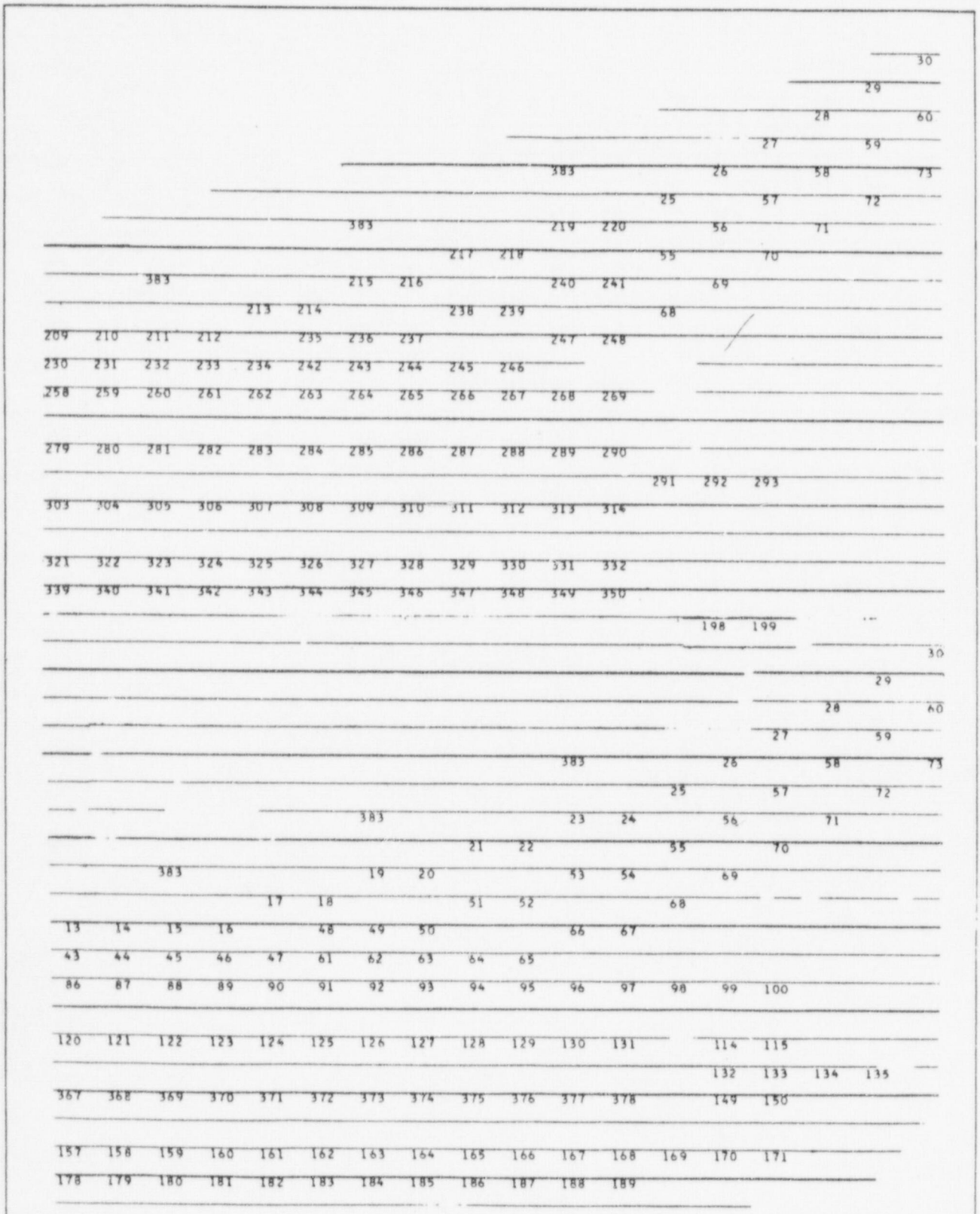


FIGURE 3. PRINT PATTERN OF UPPER FLANGE

383					201	202	203	204	205		206	207	208
362	1	2	3	200	222	223	224	225	226		227	228	229
363	31	32	33	221	250	251	252	253	254		255	256	257
364	74	75	76	249									
365	101	102	103	270	271	272	273	274	275		276	277	278
366	136	137	138	294									
					295	296	297	298	299		300	301	302
							315	316	317		318	319	320
							333	334	335		336	337	338
357	356	355	354	382	381	380	379	192	191	190			
358													
359													
360													
361										194	195	196	197
383					5	6	7	8	9		10	11	12
362	1	2	3	4	35	36	37	38	39		40	41	42
363	31	32	33	34	78	79	80	81	82		83	84	85
364	74	75	76	77						110	111	112	113
365	101	102	103	104	105	106	107	108	109				
366	136	137	138	139						116	117	118	119
					140	141	142	143	144				
										145	146	147	148
							151	152	153		154	155	156
							172	173	174		175	176	177
357	356	355	354	353	352	351	193	192	191	190			
358													
359													
360													
361													

FIGURE 4. PRINT PATTERN OF LOWER FLANGE

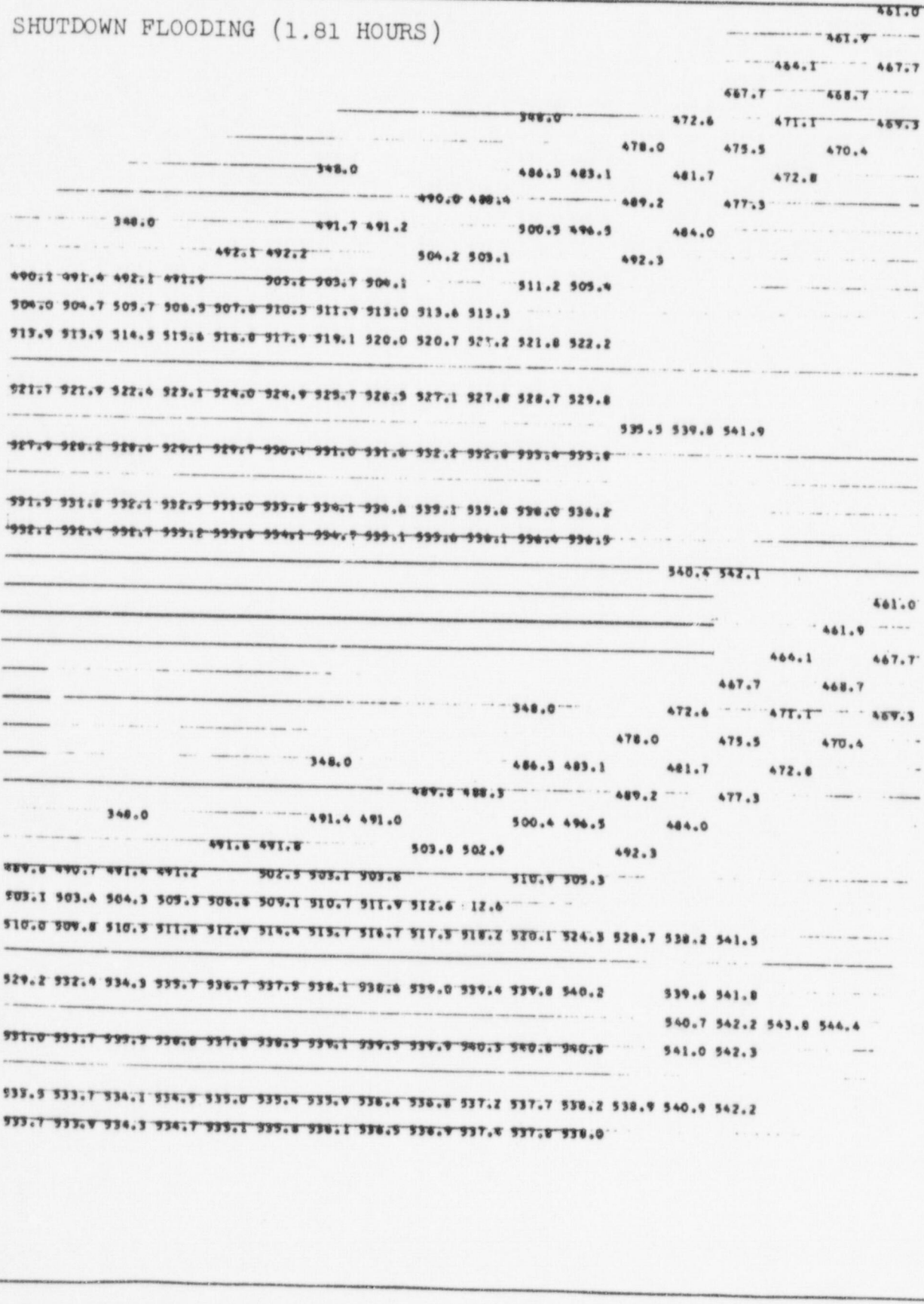
END OF HEAT-UP (4.46 HOURS)

542.5
542.4
542.2 534.3
541.6 534.3
545.7 540.5 533.2 532.5
538.7 530.2 532.1
545.7 535.0 536.3 523.8 530.9
533.9 534.4 512.1 527.3
545.7 533.6 533.4 487.7 496.1 519.1
533.6 533.3 482.9 483.1 503.3
535.3 534.1 533.5 534.0 492.9 489.8 488.3 485.4 485.6
489.8 487.7 484.6 481.6 478.9 465.2 457.1 449.9 443.8 441.0
451.2 451.1 448.4 443.6 437.6 431.5 424.6 417.6 410.6 403.0 394.5 390.3
416.5 415.3 412.5 408.2 403.0 397.3 390.9 384.2 376.9 368.6 357.8 348.2
298.6 253.3 230.3
386.9 385.0 382.1 378.1 373.3 368.0 362.0 355.5 348.5 340.6 331.7 326.0
368.8 366.7 363.7 359.9 355.4 350.2 344.5 338.2 331.4 324.2 317.3 314.9
369.6 363.5 360.5 356.7 352.2 347.1 341.3 339.1 328.4 321.6 315.1 313.8
246.4 227.7
542.5
542.4
542.2 534.3
541.6 534.3
545.7 540.5 533.2 532.5
538.7 530.2 532.1
545.7 535.0 536.3 523.8 530.9
534.1 534.6 512.1 527.3
545.7 534.1 533.8 488.1 496.2 519.1
534.2 533.9 484.6 484.1 503.3
535.9 534.9 534.4 534.7 495.8 492.3 488.5 446.3 465.3
493.6 493.1 490.3 486.8 481.7 470.9 462.9 455.6 449.0 444.3
468.1 468.9 466.4 461.7 455.5 448.8 441.5 434.3 427.0 418.1 399.8 368.3 337.4 262.4 233.3
366.9 337.0 315.0 297.0 281.9 268.9 258.9 251.3 245.8 242.4 240.9 241.5 251.4 230.1
243.1 226.4 204.8 195.2
360.1 332.3 311.1 293.3 278.4 265.8 255.9 248.3 243.0 239.6 238.3 239.2 243.0 226.9
358.2 355.7 352.4 348.4 343.8 338.8 333.1 326.8 319.8 312.0 302.2 291.7 280.3 246.9 228.6
357.1 354.7 351.4 347.5 343.0 337.9 332.2 325.9 319.0 311.2 302.5 299.2

END OF HEAT-UP (4.46 HOURS)

13	12	11	10	9	8	7	6	5	4	3	2	1
545.7					537.0	536.1	535.3	534.7	540.7	533.7	533.5	533.5
538.7	537.7	537.8	537.8	537.3	506.0	502.6	498.9	493.8	480.2	488.9	489.9	489.8
518.1	513.3	513.9	514.1	511.7	483.2	475.3	469.0	463.0	456.0	454.3	452.4	451.5
503.3	493.5	495.5	496.2	492.5								
494.4	477.5	482.7	484.6	480.1	468.1	455.8	446.8	439.9	433.7	427.7	423.8	420.8
492.4	466.7	477.3	480.6	476.1								
					462.3	446.0	431.1	423.1	416.3	411.1	406.2	402.0
							416.8	412.0	406.6	403.2	396.6	392.0
							412.3	409.6	404.7	406.5	395.5	390.3
291.2	318.4	410.7	447.3	449.9	443.0	423.8	414.1	408.0	403.3	402.9		
276.4												
258.7												
247.2												
241.3										414.8	414.9	409.4	396.7
545.7					537.0	536.1	535.5	534.9	534.4	533.6	533.4	533.4
538.7	537.7	537.8	537.8	537.3	506.1	502.8	499.7	496.7	493.3	490.6	489.4	489.1
518.1	513.3	513.9	514.1	511.7	483.3	475.6	469.8	465.6	463.5	455.6	452.6	450.4
503.3	493.5	495.5	496.2	492.5						428.9	433.1	428.8	415.0
494.4	477.5	482.7	484.6	480.1	468.2	456.1	447.6	442.4	443.2			
492.4	466.7	477.3	480.6	476.1						415.0	414.0	407.9	394.1
					462.3	446.2	431.4	423.5	418.2			
										407.2	403.6	397.1	385.9
							416.8	411.8	406.2	399.0	392.7	386.4
							412.2	409.3	403.7	398.2	391.4	385.5
291.2	318.4	410.7	447.3	449.6	442.9	423.8	414.1	408.0	403.3	402.9		
276.4												
258.7												
247.2												
241.3												

SHUTDOWN FLOODING (1.81 HOURS)



SHUTDOWN FLOODING (1.81 HOURS)

13 12 11 10 9 8 7 6 5 4 3 2 1

348.0 488.1 489.1 489.8 489.3 482.3 490.5 491.9 491.9

484.5 485.8 486.0 486.4 487.5 499.7 501.0 502.1 503.3 507.1 504.7 504.6 504.6

494.2 495.7 495.9 496.4 497.6 507.5 509.7 511.3 512.7 514.3 514.3 514.5 514.6

500.7 502.9 502.8 503.2 504.7

504.5 507.8 507.1 507.3 509.0 512.3 515.5 517.6 519.1 520.2 521.2 521.6 522.0

505.4 510.3 508.5 508.6 510.3

514.1 518.2 521.7 523.4 524.6 525.2 525.9 526.4

525.1 526.1 527.0 527.2 528.2 528.8

526.2 526.7 527.4 526.3 528.5 529.3

533.4 530.1 518.3 514.7 516.7 518.5 523.3 525.6 527.0 527.9 527.7

535.5

537.8

539.3

540.0 524.2 524.0 524.6 526.1

348.0 488.1 489.1 489.9 490.4 490.4 491.7 492.2 491.9

484.5 485.8 486.0 486.4 487.5 499.7 500.9 502.0 502.8 503.7 504.5 504.8 504.6

495.7 495.9 496.4 497.6 507.5 509.7 511.1 512.1 512.3 513.9 514.3 514.3

502.9 502.8 503.2 504.7 520.7 519.5 519.9 521.8

504.5 507.8 507.1 507.3 509.0 512.3 515.4 517.4 518.3 518.0

505.4 510.3 508.5 508.6 510.3 524.1 524.2 524.8 526.4

514.1 518.1 521.7 523.4 524.4

526.1 526.7 527.5 528.7

525.2 524.2 527.1 528.0 528.8 529.6

526.2 526.8 527.7 528.3 529.2 529.9

533.4 530.1 518.3 514.7 516.4 518.4 523.2 525.6 527.0 527.9 527.7

535.5

537.8

539.3

540.0

END OF SHUTDOWN (4.177 HOURS)

														103.1
													103.2	
												103.4		111.1
											104.0		111.3	
									100.0		105.3	112.5		113.1
										107.2	115.7		113.5	
					100.0				111.3	109.9	122.6	114.8		
							112.6	112.0		135.2	118.6			
		100.0			113.0	113.4			162.1	152.8	127.4			
				113.1	113.4			168.1	167.5		144.6			
111.1	112.5	113.2	112.7		157.7	161.0	164.6			208.3	185.9			
160.6	163.3	166.9	170.2	175.5	188.3	197.2	204.9	211.1	213.6					
203.5	204.0	207.2	212.7	219.3	226.1	233.6	241.0	248.1	255.7	264.1	268.4			
242.4	244.1	247.5	252.3	258.1	264.5	271.4	278.4	285.7	293.9	304.5	313.8			
											364.1	408.2	433.1	
275.6	278.0	281.5	286.0	291.4	297.3	303.6	310.3	317.3	324.9	333.3	338.3			
295.9	298.5	302.0	306.4	311.4	317.0	323.1	329.5	336.2	343.0	349.5	351.7			
299.5	302.1	305.7	310.0	315.0	320.6	326.6	332.9	339.5	346.2	352.0	353.2			
												414.0	435.9	

														103.1
													103.2	
												103.4		111.1
											104.0		111.3	
									100.0		105.3	112.5		113.1
										107.2	115.7		113.5	
					100.0				111.3	109.8	122.6	114.8		
							112.4	111.8		135.2	118.6			
		100.0			112.5	113.8			161.7	152.7	127.4			
				112.4	112.8			166.2	166.4		144.6			
110.5	111.6	112.2	111.8		154.6	158.3	162.3			207.3	186.1			
156.5	157.4	160.7	164.6	170.3	182.3	191.0	198.8	205.6	210.2					
184.8	184.5	187.6	192.9	199.9	207.5	215.5	223.2	230.7	239.7	258.2	290.3	322.3	398.4	429.9
282.6	308.4	326.6	341.3	353.4	363.7	372.6	[illegible]	388.0	395.1	402.1	408.5		408.9	433.4
													416.9	437.2 461.5 472.1
291.5	315.3	333.1	347.5	359.6	369.7	378.6	386.5	393.8	400.6	406.9	412.1		418.3	436.8
307.5	310.6	314.5	319.0	324.1	329.7	335.7	342.1	348.8	356.2	365.0	374.1	384.6	415.5	435.1
308.8	311.8	315.6	320.1	325.2	330.7	336.7	343.0	349.8	357.0	364.9	367.7			

END OF SHUTDOWN (4.177 HOURS)

```
100.0                          109.0 110.0 110.9 111.5 105.2       112.6 112.9 112.9
107.0 108.2 108.0  08.0 108.6 141.7 145.5 149.6 155.2 169.8       160.6 159.5 159.8
128.1 133.5 132.7 132.6 135.3 165.9 174.7 181.8 188.4 196.0       197.8 199.7 201.0
143.3 154.0 151.8 151.1 155.5
152.5 170.9 165.0 163.1 168.5 182.0 195.7 205.8 213.5 220.3       226.7 230.7 233.7
154.5 182.4 170.5 167.2 172.8
                               188.3 206.4 222.9 231.8 239.2       244.7 249.8 254.2

                                           238.6 243.9 249.9       253.4 260.5 265.4
                                           243.6 246.6 251.9       249.7 261.8 267.4
339.5 313.2 225.3 193.6 196.6 205.0 227.8 239.5 246.9 252.8 253.7
354.6
372.9
385.1                                                        240.4 240.3 245.6 257.3
391.2
```

```
100.0                          109.0 110.0 110.7 111.4 111.9       112.7 113.0 113.0
107.0 108.2 108.0 108.0 108.6 141.6 145.2 148.8 152.1 155.9       158.7 159.9 160.3
128.1 133.5 132.7 132.6 135.3 165.8 174.4 180.8 185.6 188.0       196.2 199.2 201.2
143.3 154.0 151.8 151.1 155.4                                224.9 220.5 224.5 237.5
152.5 170.9 165.0 163.1 168.5 181.9 195.4 205.0 210.8 210.0
154.5 182.4 170.5 167.2 172.7                                240.1 241.1 246.9 259.6
                               188.2 206.2 222.6 231.4 237.2
                                                             248.8 252.6 259.0 269.3
                                           238.7 244.2 250.3       257.9 264.3 270.6
                                           243.7 246.9 253.0       258.7 265.8 271.5
339.5 313.2 225.3 193.6 196.2 204.7 227.7 239.5 246.9 252.8 253.7
354.6
372.9
385.1
391.2
```

SUMMARY

The thermal analysis of the vessel shell considers heatup and cooldown transients and gamma heating. The results are used in Calculation CE-S-102-F.

TRANSIENTS

Heatup is at 100F per hour to 546F. Cooldown is at -100F per hour to 375F, flooding in a ten minute period during which the temperature drops to 330F, and then continuation of the -100F per hour rate. Transients having a small temperature range are considered as skin stresses, using the full ΔT, and are not tabulated in this analysis.

Gamma heating is a factor only at power, as it is essentially zero at standby. The energy absorption at the surface is given as 8100 Btu/hr-ft^3, and the average linear attenuation coefficient as 8.336 per foot through the vessel wall.

THERMAL MODEL

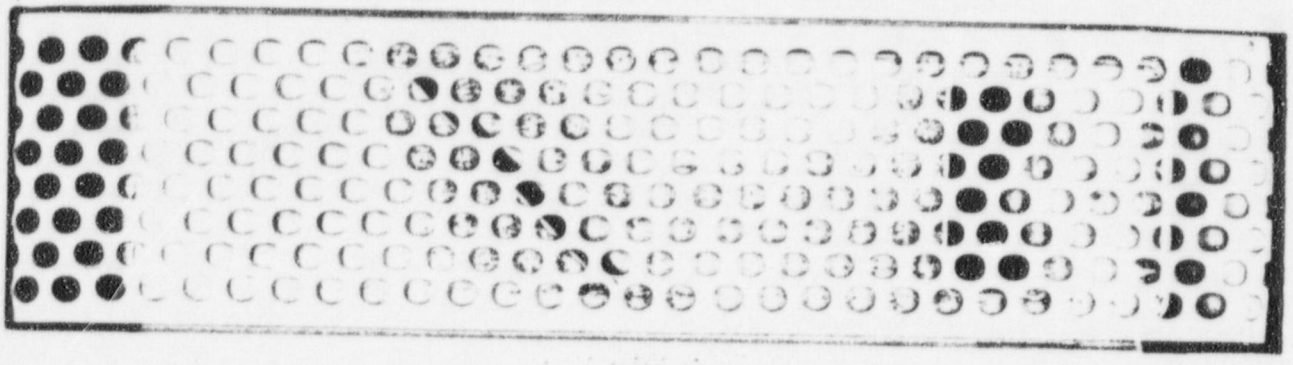
The vessel wall is considered to be a vertical infinite flat slab, 5-1/2 and 6-1/2 inches thick, and with 7/32 inch thick cladding. This assumption permits the use of one-dimensional models, and is conservative, as it neglects the axial heat flow between sections or at the water-steam interface.

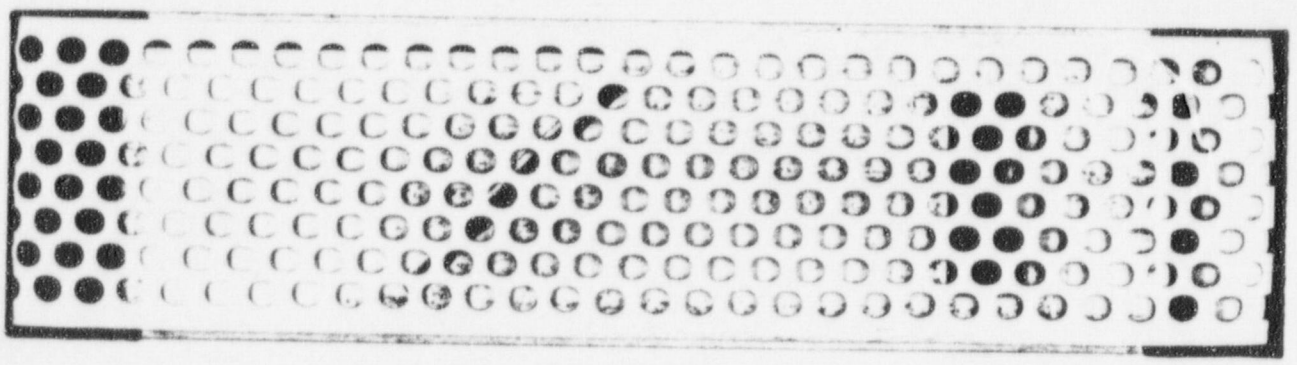
BOUNDARY CONDITIONS

In the heatup transient and for the gamma heating calculation, the film coefficient for heat transfer between the water and the wall is taken as 500 Btu/hr-ft^2-F, and the film coefficient for the surface that is condensing steam is taken as infinite. During cooldown, this surface is considered as insulated, while the film coefficient for surfaces in contact with water is taken as infinite. This is due to the wall being hotter than the water during periods of reducing pressure or when the flooding occurs so there will be boiling.

CALCULATIONS

At the end of the long heating and cooling transients, temperature of the wall will be changing at the same rate as the fluid and the heat flux at the wall and through the clad is given by $\frac{q}{A} = \frac{-\Delta T}{\Delta \tau} \rho\ c_p\ t$. The values of the heat flux and the film and clad temperature drops are given in Results.





The maximum radial gradient in the wall occurs at the end of flooding, when 330F water rises against the 546F wall. Considering the clad conductance as a film coefficient permits calculation of a Nusselt modulus and consequently determination, by using Fig. 2 of T-100F, of the maximum difference between the interface and the average wall temperatures.

$$Nu = \frac{ht}{k} = \left(\frac{k}{t}\right)_c \left(\frac{t}{k}\right)_b = \frac{10.8 \times 12}{.218} \times \frac{6.5}{12 \times 24} = 13.4$$

From Fig. 2, $\frac{T_s - \bar{T}}{\Delta T_{fluid}} = .62$, and with a ΔT_{fluid} equal to

546 - 330, or 216F, $\bar{T} - T_{IF} = 134F$.

TIF = Interface Temp

RESULTS

End of ± 100F Transient

Thickness of section, inches	5-1/2	6-1/2
Heat flux at interface, Btu/hr-ft^2	2750	3250
Heat flux at surface, Btu/hr-ft^2	2860	3360
$\bar{T} - T_{IF}$, F degrees	17.5	24.5
$T_{IF} - T_{surface}$, F degrees	4.6	5.5
$\bar{T} - T_{surface}$, F degrees	22.1	30.0
ΔT_{film}, F degrees	5.7	6.7
$T_{coolant} - \bar{T}$, F degrees (at end of 100F/hr heatup)	27.8	36.7
$\bar{T} - T_{fluid}$ due to gamma heating at core centerline, F degrees	6.4	
Max ΔT across water level, F degrees ($\bar{T}$ of wall above minus $\bar{T}$ of wall below)		141
Max radial ΔT, $\bar{T} - T_{IF}$, F degrees		134

546°F − 405 = 141°F